# Efficient Murine Norovirus Transport Across the Intestinal Epithelium Requires Microfold (M) Cells

by

Mariam Bernadette Gonzalez-Hernandez

A dissertation submitted in partial fulfillment
of the requirements for the degree of
Doctor of Philosophy
(Immunology)
in the University of Michigan
2014

Doctoral Committee:

Assistant Professor Christiane E. Wobus, Chair
Associate Professor David Aronoff
Professor Victor J. DiRita
Professor Juanita L. Merchant
Professor Bethany B. Moore

For everyone in my family, with love and appreciation.

# Acknowledgements

The journey to my doctoral degree could not have been accomplished if it wasn't for the people who have mentored me through this whole process. First, I would like to thank Dr. Richard J. Noel Jr. (Ponce School of Medicine, Puerto Rico) for introducing me to the world of biomedical research and virology during my high school and undergraduate degree. I am also grateful to Dr. Stephen Cooper (University of Michigan) for the opportunity to work in his lab at the University of Michigan, as part of the Summer Research Opportunity Program (SROP), and for influencing in my decision to become a Michigan alumni. Second, and foremost, I am eternally grateful to Dr. Christiane E. Wobus, for accepting me as her second graduate student in her career and for all her patience, scientific input and humanity. Words cannot describe how fortunate I was to find such a highly motivated, enthusiastic and understanding mentor. My time in the laboratory has been an outmost honor.

Special thanks go to all the members of the Wobus laboratory, past and present. It has been a great privilege, and amazing fun, to work with a team of diverse scientists with different perspectives. I have been fortunate to start with the first generation of scientists in the Wobus lab which include Stefan Taube, Jeffrey W. Perry and Heather Auble. I am grateful to you for all your help, support and laughter at the beginning of my

graduate career or at the end. Many thanks to all the undergraduates and rotating graduate students who I mentored for their patience and for putting up with me including: Hyun Soo, Charles Ko, Thomas Liu, Hillary Payne, Rachel Stephenson, Matthew Pauly, Lindsey Banks and Irina Zhang.

I need to thank all our collaborators, particularly Dr. Terrence Dermody (Vanderbilt), Jennifer Stencel-Baerenwald (Vanderbilt), Dr. Ifor R. Williams (Emory) and Dr. Nicholas Mantis (Wadsworth Center) for technical expertise, scientific insight, science templates and for their generous gifts important for my thesis project. Also, need to thank the Akira Ono laboratory and many of his lab members for great scientific input and for generously letting me use many of their equipment. Thank you.

My parents, Javier Gonzalez and Marta Hernandez, as well as my siblings, Maricarmen, Fonsi and Javi, many thanks for supporting me throughout this whole difficult process, not only scientifically but also emotionally. Love you dearly. Also, thanks go to my older sister Marta J. Gonzalez-Hernandez for her support, help, patience and for being my only family in Michigan helping me through any ups or downs. To my extended family, Pepo, Blanca and all the Rodriguez-Nieves family, you are the best family-in-law anyone could ask for. Thank you for all your support, patience and love.

Finally, I would like to thank my husband Jose A. Rodriguez-Nieves for his love and support. Remembering my first semester of graduate school and how much I struggled with classes, he was the one that tutored me and helped me get through with so much patience and dedication. Even through difficult times, he was always

supportive and I love him for that. Words cannot express my gratitude for his patience, support and love, even when things were looking grey.

# Table of Contents

# List of Tables

# List of Figures

# List of Appendices

# Abstract

Microfold (M) cells are known specialized intestinal epithelial cells that internalize particulate antigens and can aid in the establishment of immune responses to enteric pathogens. While certain enteric viruses have been observed within M cells, not much is understood about whether viruses in general use M cells to initiate a productive infection. Noroviruses (NoVs) are single-stranded RNA viruses that infect their host via the fecal-oral route. Murine NoV (MNV) infects intestinal macrophages and dendritic cells of its host and provides a tractable experimental system for understanding how an enteric virus interacts with the intestinal epithelium. This dissertation focuses in the mechanism of how MNV breaches the intestinal epithelial barrier to get in contact with its permissive cells for a productive infection. Using an *in vitro* transwell model of polarized intestinal epithelial cells, I demonstrated that MNV crosses the cell monolayer in the absence of viral replication or disruption of tight junctions. Additionally, this MNV transport was mediated by a subset of cells in the monolayer with functional M cell properties also termed as M-like cells. *In vivo*, replication of two divergent MNV strains was reduced in mice depleted of M cells and similar findings were made using reovirus, an enteric double-stranded RNA virus that infects intestinal epithelial cells. Finally, since residual MNV viral titers were still present, perhaps due to an incomplete depletion of M cells, two different genetically M cell deficient mouse models were used for MNV

infection studies: Rag2-/-γc-/- and RANK$^{fl/fl}$Villin-Cre mice. Results in both mouse models, show that oral MNV infection is greatly reduced when compared to controls and to our previous conditional M cell depletion model. Taken together, these results demonstrate that M cells are required for MNV pathogenesis. Similar findings were observed for reovirus. Interestingly, preliminary results suggest that, in the large intestine, alternate entry mechanisms (*e.g.* transepithelial dendritic cells or villous M cells) could take place for MNV infection in a virus-strain dependent way. Further examination into potential alternative MNV-strain dependent entry mechanisms still needs to be performed, but this dissertation has laid a framework for future studies.

# CHAPTER 1

## Introduction

### 1.1 *Caliciviridae* family

The family *Caliciviridae* consist of five well recognized genera all of which contain a single- stranded, poly-adenylated and positive-sense ribonucleic acid (RNA) genome in a protein capsid that has no lipid layer (80, 81, 290). They are divided in Lagoviruses, Vesiviruses, Sapoviruses, Noroviruses (NoVs) and Neboviruses. Recovirus, discovered in infected Rhesus monkeys is the newest proposed genus within the family (56). Overall, caliciviruses are known to be species-specific and only a few strains of these viruses can be cultured efficiently. Sapoviruses and noroviruses, for example, have only a porcine (85) or murine virus (120), respectively, that can grow in culture. However, due to the limitation of culturing the majority of the caliciviruses, research looking at molecular mechanisms involved in pathogenesis has been unsuccessful.

Noroviruses (NoVs) are one of the most characterized genus of the caliciviruses but with no anti-viral treatment available as of yet. They are highly stable in the environment, can infect at low viral doses, and can cause fast-spreading outbreaks due to high levels of viral particles that are being produced during infection. Caliciviruses

are considered an emerging pathogen threat and may also pose a national security concern, hence, the National Institute of Health has classified them as category B bio-defense agents (105). Originally, NoVs were isolated after an outbreak at an elementary school in Norwalk, Ohio (118). Currently, NoVs are divided into five genogroups (GI-GV), but a recent and new genogroup VI has been proposed. To date, the human NoVs (HuNoVs) are responsible for the majority of non-bacterial gastroenteritis worldwide (119). Humans can be infected with Genogroups I, II, and IV (80, 290). However, NoVs are highly widespread pathogens, as evidenced by infection in pigs, dogs, sheep, cattle, a lion cub and mice (120, 147, 149, 237, 272). Viruses from genogroup II can also infect swine (152), genogroup IV viruses were found in a dog and a lion (147, 149) and recently, viruses from the newly proposed genogroup VI were found to infect dogs (148, 158-160). On the other hand, genogroup III viruses were detected in sheep and cattle (282) and finally, genogroup V contains the only known viruses to date that infect mice (120) and rats (260). Symptoms after infection can show no signs of disease (*e.g.*, in wild-type mice), or can cause a severe acute gastroenteritis, as is known for HuNoV infection in individuals. Interestingly, the presence of NoVs in close relation to HuNoVs found in pigs (152, 272), the HuNoV replication in gnotobiotic (germfree) pigs (239) and even the replication of HuNoV in a mouse model (253), suggest that, NoVs may be able to cross species barriers. How these events occur, is an area of interest that is still yet to be defined. Nevertheless, this points to the likelihood of zoonotic transmission. Presently, no antiviral or FDA approved treatments to help prevent infection exist for HuNoVs, despite being a major public health concern. Hence, further research

examining all aspects of HuNoV biology will be a great asset to understand its pathogenesis and ways to avert it.

### 1.1.1 General Aspects of Human Norovirus (HuNoV)

HuNoVs, being the major cause of non-bacterial gastroenteritis worldwide, have resulted in an estimated 21 million cases of acute gastroenteritis, 70,000 hospitalizations and 800 deaths annually in the United States alone (86, 221). Since no viral decontamination protocol, as previously established by the World Health Organization (169), is efficient to clearly inactivate the virus, in case of a HuNoV outbreak, expensive and extensive decontamination procedures need to be performed. Consequently, HuNoV outbreaks can cause a serious economic burden worldwide. As of yet, the only effective way that helps control HuNoV spread are strict hygiene and taking extensive measures of decontamination. Therefore, understanding HuNoV pathogenesis through research is necessary to provide the public with potential antiviral treatments that can alleviate this problem.

Unfortunately, efforts in cultivating HuNoV in the laboratory have been unsuccessful for more than forty years (52). While a gnotobiotic pig model has been somewhat successful for HuNoV studies, this large animal model is expensive and limitations for conducting these experiments have narrowed its use (35). However, to understand the epidemiology and cellular-based mechanisms some progress has been made without the presence of a tissue culture system for HuNoV. Progress include the genome sequence of the prototype HuNoV, Norwalk virus (115), a RT-PCR protocol to

identify virus strains (269) and an immunoassay detection method for HuNoV (*i.e.*, Enzyme Linked Immunosorbent Assay, ELISA) (79, 124).

#### 1.1.1.2 HuNoV Genomic Organization

A schematic structure of the HuNoV genome, is shown in Figure 1.1. The genome is a positive-sense single-stranded RNA that is divided into three open reading frames (ORF), which are flanked by small untranslated regions at the 3' and 5' ends. Similar to other viruses (*e.g.,* polioviruses), a viral protein known as viral protein, genome-linked (VPg), is attached to the 5' end of the genome (197) and the 3' end contains a polyadenylated tail. Vpg can act as a primer during RNA synthesis and has a role in translation initiation by acting similar to 5' cap-binding proteins. Immediately after the VPg the first ORF is located and it is expressed as a polyprotein comprising the nonstructural genes: NS1/2 (p48 or N-Terminal protein), NS3 (nucleoside triphosphatase- like protein, NTPase), NS4 (p22 or 3A- like protein), NS5 (VPg), NS6 (viral protease, Pro), and NS7 (RNA- dependent RNA polymerase, RdRp). ORF2 located following ORF1, encodes for the major capsid protein VP1, which forms the viral capsid. Finally, ORF3 encodes the minor capsid protein VP2 that is hypothesized to stabilize the virus particle (120, 238).

#### 1.1.1.3 HuNoV Pathogenesis Studies

Currently, out of the three genogroups containing HuNoV, the one responsible for causing the majority of gastroenteritis outbreaks is genogroup II with its corresponding

genotype 4 (GII.4) (276). Within each genogroup there are different genotypes that refer to the classification of the virus based on the genetic material.

The study of HuNoV pathogenesis has been previously performed with human volunteers (116, 137). These studies estimate that 18 virus particles (257) or approximately 1320 virus genomic equivalents (7) are sufficient to cause an infection and symptoms can begin as early as 12 hours (137). The most common symptoms include: diarrhea, vomiting, mild fever, dizziness and dehydration. Although symptoms can resolve quickly within 24-72 hours after infection, virus shedding can persist for weeks to months even in immuno-competent individuals (116). On the contrary, immuno-compromised individuals, including organ transplant patients, can shed the virus and persistently feel symptoms for years (6, 207). Additionally, asymptomatically-infected individuals can shed virus for months and can potentially be the sources of new outbreaks (48). It has been calculated that the amount of viral shedding can be up to $10^{10}$ virus genomes per gram of stool (224). Hence, given a low infectious dose, one individual is capable of infecting a large population.

In order to study HuNoV, scientists have developed models to understand cellular based mechanisms of HuNoV entry and replication in humans. These models include a gnotobiotic pig model, virus- like particles (VLPs) and a HuNoV replicon system. VLPs are non-infectious HuNoV capsids without viral genetic material, and have been essential in understanding that histo-blood group antigens (HBGAs) are required for viral attachment (107, 228, 230, 244, 275, 286). The discovery of a HuNoV replicon system, which was developed from an eukaryotic expression plasmid which expresses the HuNoV complementary DNA without the viral capsid, has led to

understanding of the interferon response during genomic replication and helped for screening and testing antiviral drugs that could efficiently block replication (32, 33). Additionally, gnotobiotic pigs have been shown to be successfully infected with HuNoV (35). Chimpanzees are another model that was shown to be productively infected with HuNoV, although no signs of infection are observed (17). However, complicated issues with these model systems including the costs have been limiting. It wasn't until recently, that a small animal model for HuNoV was developed using Rag $2^{-/-}$ $\gamma c^{-/-}$ mice (which lack T lymphocyte, B lymphocyte and natural killer cells due to a deficiency in the common gamma chain cytokine receptor) (253). Although this new model gives promise of a new era for HuNoV studies, it does not show symptoms similar to its actual human host. Hence, studies still need to be performed to better understand the mechanisms involved in HuNoV pathogenesis. While several of these models have provided significant contributions to the norovirus research field, murine norovirus (MNV), with its research tools and reagents available that are non-existing for HuNoV studies, has allowed mechanistic studies that assist in unveiling many of the missing pieces of norovirus biology (120, 279).

### 1.1.2 Murine Norovirus (MNV): A Model System for Norovirus Studies

To date, murine norovirus (MNV) discovered in 2003, is the only norovirus that can replicate efficiently in a small animal model and in tissue culture. Initially, MNV was found at Washington University in St. Louis, in a mouse research colony that contained immunocompromised mice deficient in signal transducers and activators of transcription 1 (STAT-1) and in the recombination activating gene 2 (RAG 2) (120). Quickly after its

discovery, dendritic cells (DCs) and macrophages were identified to be the permissive cell types which MNV replicates (277). These findings led to the development of several tools to assist in studying norovirus biology: a tissue culture system (277), a small animal model (120) and a reverse genetics systems (5, 34, 273, 288). Thanks to these tools, scientists have made progress in understanding many of the aspects of norovirus biology, such as, how the virus attaches (254, 255), internalizes (72, 195, 196) and replicates (238, 277). Moreover, knowing that MNV can infect cells in culture and mice, which can be genetically manipulated, pathogenesis studies can be achieved.

Interestingly, mice infected with MNV do not show signs of sickness. This could explain why, until recent studies, this virus was never detected (120). MNV is wide-spread and has been found in mice research colonies worldwide (1, 102, 125, 127, 134), which in some cases resulted in difficulties in interpreting research results (125, 134). Studies show that mice with an acute infection can have fecal inconsistency, which is a mild form of diarrhea (172). Depending on the virus strain, infection can be resolved quickly within days or can persist for longer periods (*i.e.*, weeks and even months). In the case of the MNV-1 strain, once infected, mice develop a strong and protective adaptive immunity against the virus (30). However, mice that are immunocompromised, such as the STAT1 or RAG2 knockouts, have uncontrolled systemic MNV infection and in some cases, as it was shown for STAT1 mice at high doses of MNV, it may cause lethality (120).

#### 1.1.2.1 Characteristics Shared Between MNV and HuNoV

At the genome level, both MNV and HuNoV share similar features. Particularly,

the three ORFs have similarities in structure and sequence and are 65% identical at the nucleotide level (Figure1.1) (121). MNV-1 contains an additional fourth ORF, which expresses a virulence factor, but its mechanism of action is still unknown. Other features shared between HuNoV and MNV are that both infect via the oral route, replicate in the gastrointestinal (GI) tract, and are shed in the fecal content. Additionally, both cause infections that are acute or persist for longer periods with viral shedding for months (27, 70, 100, 101, 173, 233). While immunocompetent mice do not show overt signs of sickness with MNV, mice deficient in STAT1 or the interferon receptors display diarrhea, stomach distension and delay in emptying the stomach, which are surrogates for vomiting since mice lack the emetic reflex (120, 172). A study showed 15 distinct MNV strains (Figure 1.2) that have been isolated, forming one genogroup and one serogroup, but nowadays over 80 distinct MNV strains have been deposited in GenBank (NCBI). In the cases where it has been analyzed, these strains can display biological differences.

Both MNV and HuNoV have similarities in their respective viral capsids. The virus particle from each virus is made from 180 copies of the major structural protein, VP1, which in turn forms 90 dimers of the protruding (P) domain located in the surface of the capsid. The P domain has been suggested to play an important role in immune recognition and receptor interaction (248). The norovirus genome is encapsidated in an interior protein shell (S), or S domain, that prevents the genome from environmental destruction. The structure of the capsid and how stable the viral particles are in the environment have been shown in MNV and extrapolated to HuNoV (20, 26, 40, 75, 246,

247, 256). Additionally, HuNoV and MNV have carbohydrate binding motifs in similar regions of the P domain (226, 254).

#### 1.1.2.2 Differences Between MNV and HuNoV

While similarities between the two have been demonstrated, there are also several differences. One difference is that they bind to different host carbohydrate structures. Particularly, the histo-blood group antigens (HBGA) are the main carbohydrates HuNoV binds to, while MNV preferably binds to sialic acid, the ganglioside GD1a, and N-linked and O-linked cell surface glycoproteins (254). In addition, MNV does not cause the severe acute gastroenteritis, diarrhea or vomiting that is observed with HuNoV (120). The reason mice are unable to vomit is because they do not possess the emetic reflex required to do so (252), and a reason why immunocompetent mice with MNV infection do not experience diarrhea, could be due to differences in the physiology of the GI tract between mice and humans. Another difference is that no cell type that is permissive to HuNoV infection has been identified yet, while MNV was found to replicate in macrophages and DCs. Several attempts to infect macrophages and DCs from peripheral blood mononuclear cells with HuNoV have been performed, but have been unsuccessful (131). However, it is possible that HuNoV may in fact infect macrophages, since Kupffer cells (a specialized macrophage located in the liver) show HuNoV antigen-positive staining in HuNoV-infected mice (253). However, studies testing the ability to propagate the virus in culture for one or more specific cell types are still ongoing. Additionally, MNV possess a fourth ORF (ORF4), a virulence factor (156) not present in HuNoV. Understanding the differences between

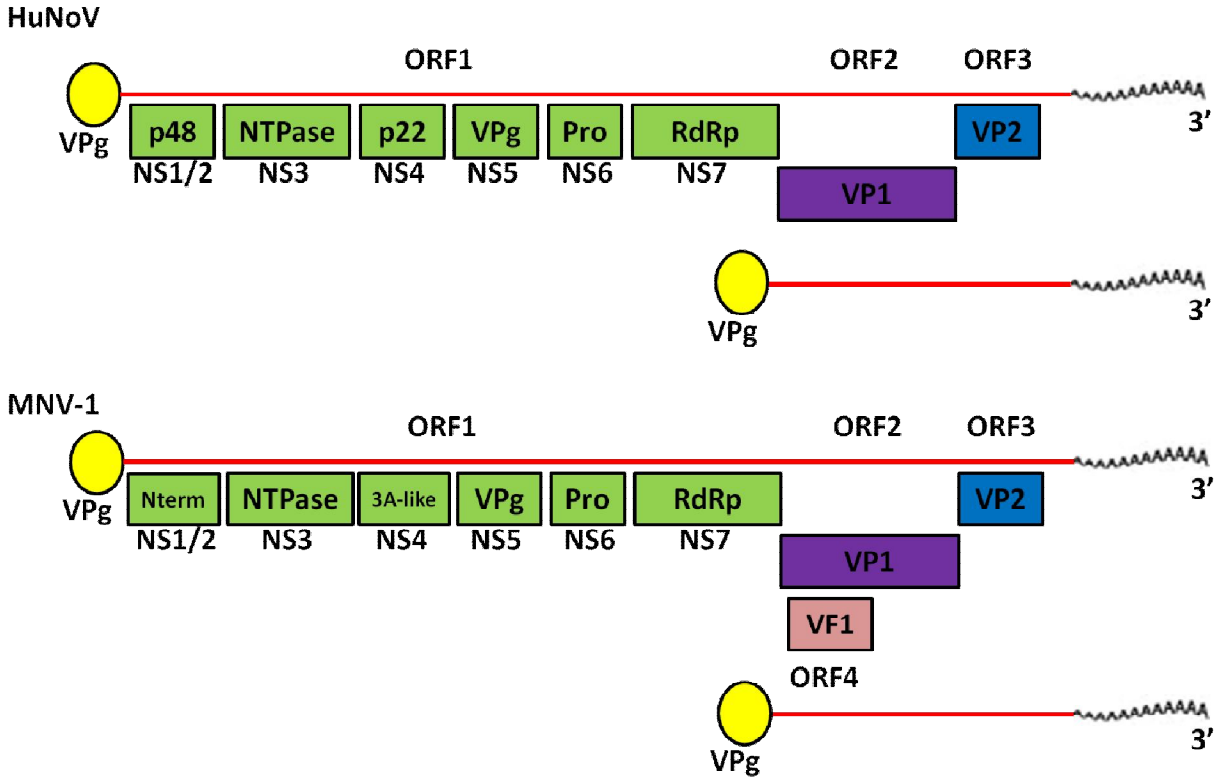


**Figure 1.1 Comparison of genomic organization between HuNoV (Norwalk) and MNV-1.** Schematic representation of the norovirus genomes (HuNoV and MNV-1). Both show four open reading frames (ORF). ORF1 contains the nonstructural proteins (green), ORF2 contains the major capsid protein (purple), ORF3 contains a minor capsid protein (blue). MNV-1 contains an additional ORF4 for a virulence factor 1 (pink). The subgenomic RNA is also shown below each genomic RNA.

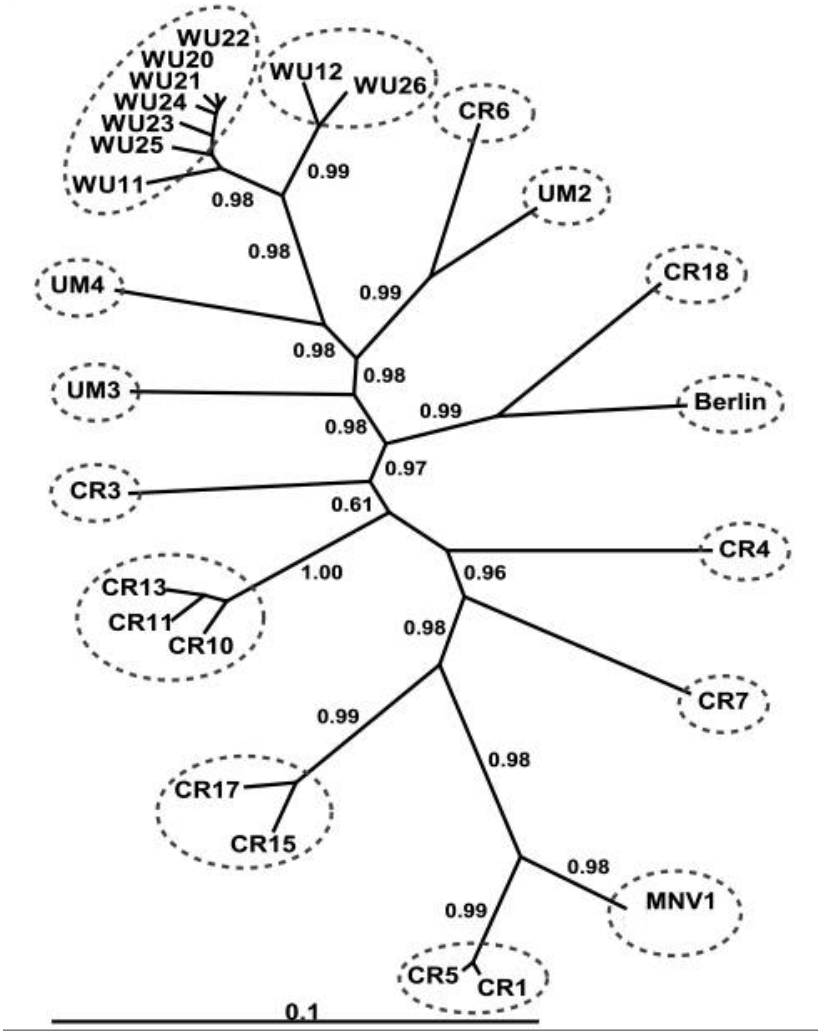


**Figure 1.2 Murine noroviruses phylogenetic analysis.** Circled are fifteen genetically distinct virus strains from 26 MNV genome sequences analyzed. Shown here is a consensus Bayesian phylogenetic tree that was based on full-length MNV genomes. Image from Thackray et. al. 2009.

each virus can help in developing newer systems to study their pathogenesis. Nonetheless, the insights obtained with MNV are indispensable for driving forward norovirus research.

Reasons to use MNV as a model system, revolve around the fact that there are multiple research tools and techniques available for this virus when compared to other noroviruses. As has previously been mentioned, it is thanks to the discovery of MNV that scientists have been able to develop several tools to understand its biology, using a reverse genetics system to manipulate the genome (5, 34, 273, 288), a tissue culture system to propagate the virus (278), and a small animal model to study the pathogenesis (120).

### 1.2 Norovirus Life Cycle

The NoV life cycle represents that of a typical positive-strand RNA virus life cycle. This life cycle can be divided into several steps: attachment, entry, uncoating, genome translation, replication, virus assembly and release (Figure 1.3). While it is not understood how all NoVs accomplish these steps, several mechanisms have been elucidated for HuNoV and MNV.

The first step is viral attachment/binding, in which an initial contact between the virus particle and the host cell is made. Particularly, attachment occurs between a viral component and a host cell component. Viral receptors can be classified as attachment or entry receptors and they can be host proteins, lipids, or carbohydrates. Attachment receptors, which can also be co-receptors, in many cases do not possess a strong interaction, but they can still assist in virus attachment to host cells (82). However, they

do not allow the virus to productively infect cells. Hence, entry receptor molecules are essential for a productive viral entry and infection. In the case of HuNoVs, carbohydrates used for attachment include *N*-acetylgalactosamine (GalNAc), *N*-acetylglucoseamine (GlcNAc), alpha-D-galactose (α-D-Gal), alpha-D-mannose/alpha-D-glucose (α-D-Man/α-D-Glc), α1,2-fucosylated carbohydrates, α2,3-sialylated carbohydrates, heparin and suramin, and galactosylceramides (GalCer) (8, 49, 53, 211, 244). Interestingly, in the early 2000s, mechanisms of HuNoV entry and infection into the host was mostly known based on observations from studies with volunteer individuals that linked the ABO blood type of individuals to susceptibility of infection (103, 104, 106, 229, 250). Moreover, observations confirmed that, *in vitro,* HuNoV VLPs can bind HBGA, which are carbohydrate chains present on the surface of many cells and are linked to lipids or proteins (144). Structural analysis of HuNoV VLPs bound to HBGAs, demonstrate that the P domain is the viral protein responsible for binding to carbohydrates (58, 88, 103, 202, 211, 247, 249-251). Additionally, the P domain alone is essential for binding HBGAs and disruption of the P domain obliterates this interaction (247). However, a study shows that binding to HBGAs is not sufficient to support viral entry into host cells for efficient replication and viral spread (84). Thus, it is hypothesized that a membranous protein is needed as a receptor for entry (84, 245). Similar to HuNoV P domains, the MNV P domain structure has been determined. Flexible loops in the MNV P domain were identified and are thought to allow for conformational changes in the viral capsid (122, 256). Moreover, reverse genetics analysis of the MNV-1 capsid demonstrate a binding region similar to the HBGA-binding sites of a HuNoV strain (254), which could reflect an important glycan-binding site, but

other additional binding sites likely exist. Interestingly, studies in the NoV field have discovered that both HuNoV and MNV use carbohydrates, such as sialic acid, as an important requirement during attachment (8, 211, 244, 254, 255).

MNV binding and attachment to the host cell requires carbohydrates in a strain-dependent manner, in particular, terminal sialic acid, the ganglioside GD1a, and N-linked and O-linked cell surface glycoproteins (254). However, just as it is observed with HuNoV, carbohydrates do not seem to be sufficient for MNV entry and infection into the host and, hence, it is hypothesized that a membrane protein is required as an entry receptor.

After successful attachment of the viral particle to the host cell, internalization is initiated by the interaction of the virus with its viral entry receptor(s). Non-enveloped viruses are internalized by different mechanisms depending on the virus, and do not possess the mechanism of its viral membranes fusing with host cell membranes that is observed for enveloped viruses. Once an interaction with the host entry receptor is made, the endocytic machinery further internalizes the viral particle. In general, this means that an invagination of the cellular membrane forms a vesicle-like structure known as an endosome that traffics into the cell to become an early/late endosome and finally a lysosome (87). During this process, the lumen of the endosome becomes acidified, by vacuolar ATPases (183). Some well-known forms of endocytosis are mediated by clathrin, caveolin, dynamin, lipid rafts/cholesterol. In addition, phagocytosis and macropinocytosis internalize larger or small particles, respectively. However, other less characterized forms of endocytosis are mediated by flotillin, ADP- ribosylation factor 6 (ARF6), GTPase regulator- associated with focal adhesion kinase-1 (GRAF1),

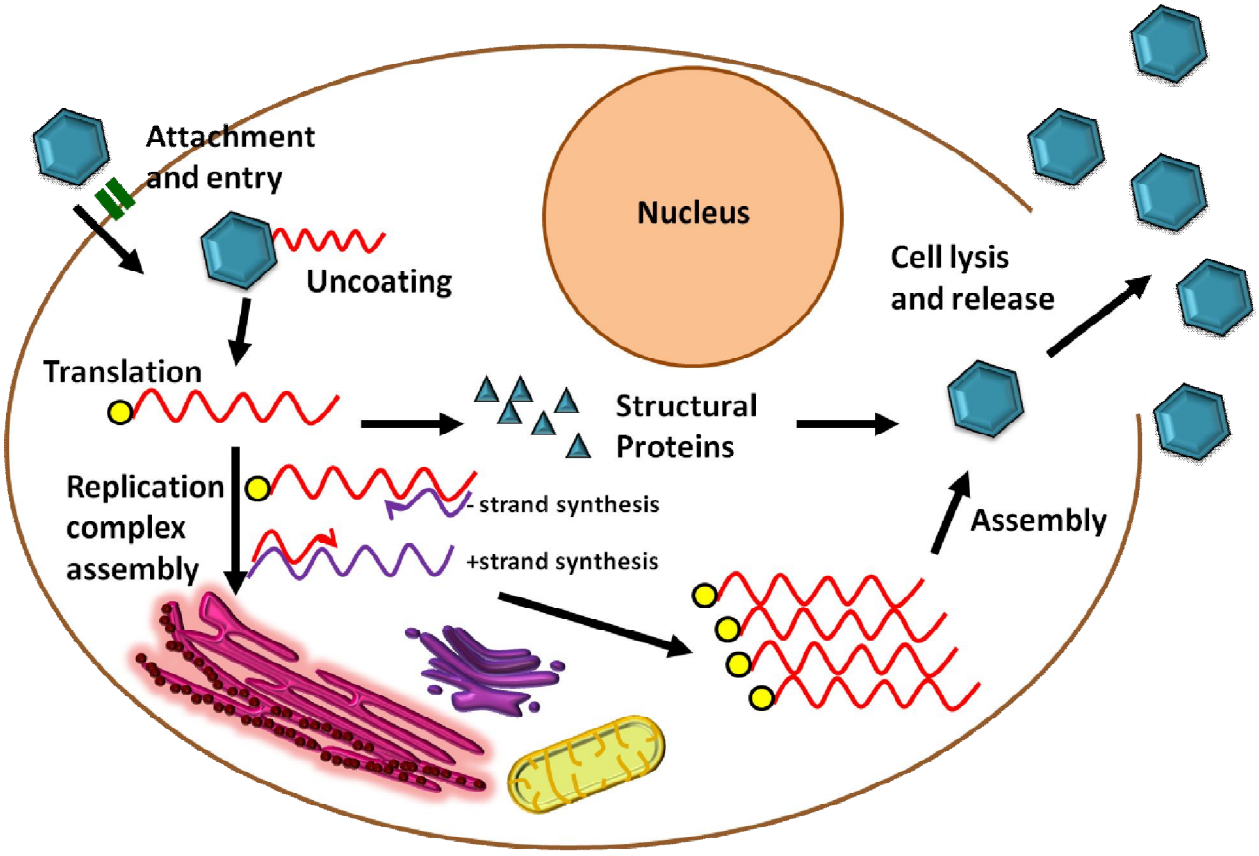


**Figure 1.3 Representative calicivirus life cycle.** Schematic of the life cycle of a positive-strand, non-enveloped RNA virus. Viral positive-sense RNA is shown in red and negative-sense RNA in purple. Yellow circles represent the virus protein genome-linked, VPg.

and interleukin 2 receptor (IL2R) (38). The mechanism of how HuNoV particles internalize into the host cell is still not clear. One study looking at glycosphingolipids present in giant unilamellar vesicles (GUVs) for GII HuNoV VLPs binding, demonstrated that these glycosphingolipids are mobile and cluster on the surface before inducing the formation of an invagination (212). Since many of the different forms of endocytosis have a similar initial step in which an invagination into the cell's lipid bilayer is formed (14, 15), it may be that these invaginations observed with HuNoV are in fact, the beginning of virus entry into the host cell. Hence, it is hypothesized that HuNoV enters the cells via one or more endocytic mechanisms (146). Interestingly, another study using a HuNoV replicon system, showed that host cholesterol is required during HuNoV replication (31). Studies with MNV have helped in understanding some of these questions and have found similarities in the requirement of cholesterol for entry and infection. Particularly, MNV entry to the host cells was found to require cholesterol and dynamin II in a matter independent of clathrin-mediated endocytosis, caveolin-mediated endocytosis, macropinocytosis, phagocytosis, flotillin or GRAF1 mechanisms (72, 196). Hence, using the MNV model has been helpful in understanding and acquiring a sense of how noroviruses can gain entry into cells.

Uncoating occurs through multistep processes that are triggered by virus-host-cell interactions. The protein shell, or capsid, contains the viral genome and protects it from environmental stresses, and only when time and important triggers have initiated, the genome will be released to the site of replication. Once viruses have disrupted or penetrated the endosomal or cellular membrane upon entry, replication in the cytosol or nucleus can begin. Uncoating can occur by either of two ways, and they involve the

acidification after maturing into late endosomes or lysosomes: 1) the virus capsid undergoes a conformational change triggered by environmental or host interactions that will eventually create a membrane pore in which the viral genome can exit and be transported to the replication site; or 2) during this conformational change the virus particle releases peptides that can distort the endosomal membrane integrity preventing continuous enclosing of the virus particle and the capsid is transported to the cytosol for another self-conformational change that will release the genome into either the cytosol or nucleus for further replication (93). Interestingly, while the internalization process for NoVs is still not clear, MNV-1 entry into permissive macrophage cells was shown to be independent of endosomal acidification (194). This suggested that other mechanisms of viral uncoating, *e.g.* viral receptor, may be playing a role. However, since the entry receptors for MNV or HuNoV are not known, studies looking at receptor-virus interactions have not been successful.

The next step of the life cycle involves the translation of the genome. NoVs can initiate translation with the help of a viral protein, VPg, that is linked to the genome at the 5' end (22, 46, 95, 120). For HuNoV and MNV-1, the VPg interacts directly with the host translational machinery (89, 258). The VPg recruits the 43S pre-initiation complex, that contains the eukaryotic factor 3 (eIF3), 40S ribosomal subunits, and initiator tRNA to mRNA (46, 47). Once translated, the viral genome contains a long poly-protein of nonstructural proteins in which the viral protease (3CL-protease or NS6) can cleave the polyprotein into the individual proteins.

After translation, host membranes undergo remodeling to generate membranous structures, otherwise known as virus replication factories or membranous web, that

carry membranes from ER and the Golgi apparatus (138, 277, 287). For MNV, it has been determined experimentally that replication occurs in these factories (110). Moreover, it was observed that some membrane structures during MNV replication contain double membrane characteristics, related to mitochondria (154). Based on these observations, it has been suggested that autophagy may play a role during viral replication. Autophagy is a catabolic mechanism that degrades components like organelles and cellular structures, to maintain cellular energy levels (126). Interestingly, certain autophagy proteins with a known function for autophagosome formation, were shown to be required for interferon (IFN) gamma (γ)-mediated host defense against MNV, but induction of autophagy was not required for antiviral properties of IFN-γ (109). However, whether autophagy is important during NoV replication in general is still not clear. The NoV replication machinery can be generally understood after studies with MNV were performed (277). First, the viral protein RdRp, can bind to the 3'end of the viral genome either by an interaction with the conserved three-dimensional structure of the 3' untranslated region and/or the VPg (80). Then, the RdRp begins to polymerize a matching anti-sense viral genome that once the VPg-linked 5' end is reached, the RdRp disassociates itself from the anti-sense genome. Next, the RdRp produces more positive-strand genomes using the matching anti-sense genome. Finally, after these additional positive-strand viral genomes are linked to the viral VPg by a covalent bond, they will then undergo translation or become packaged into new virus progeny. Additionally, sub-genomic transcripts with no ORF1 have been observed during MNV infection (77).

The final step of the viral life cycle involves packaging of the newly replicated

viral genome into the viral capsid for successful assembly of progeny. Once assembly of the virus is finalized, the progeny is released from the infected cell to infect a new cell and begin the viral life cycle all over again. Since non-enveloped viruses lack a lipid component to fuse with the cell membrane and exit the cell, they require the cell's membrane be destroyed or lysed. MNV (18) has been suggested to induce apoptosis late during the viral life cycle. However, concerns for this type of release have been brought up due to the observations in which unreleased membrane bound virus particles can be the result of apoptotic cells which fragment themselves into membrane blebs (220, 242). At the end, the newly synthesized and released progeny must find a new permissive cell so that, once found, the initiation of the whole viral life cycle can take place again. However, since not much is known about NoVs, future studies need to verify the mechanism of how assembly and release are accomplished.

### 1.3 Pathogen Interactions with the Intestinal Epithelial Barrier

Enteric pathogens such as bacteria, toxins and viruses that are transmitted through the fecal-oral route, need to conquer the GI tract's multilayer system of defense in order to productively replicate and propagate in the host. Pathogens have evolved mechanisms that make them competent enough to successfully do so. Particularly, when pathogens are able to breach the intestinal epithelium, they gain access to the interior of the host and cause infection that way. This infringement of the epithelial barrier can cause gastroenteritis, but many can even pose life-threatening consequences. For matters of this dissertation, some of the general aspects/functions of

the intestinal epithelium as well as how bacteria and viruses can traverse the intestinal epithelium for efficient infection will be discussed.

### 1.3.1 General Organization of the Intestinal Epithelium

The GI tract is divided into two major segments: the upper GI tract and the lower GI tract. The mouth, pharynx, esophagus and stomach, are the four components that make up the upper GI tract, while the small and large intestines belong to the lower GI tract. The small intestine is further divided into the duodenum, jejunum, proximal and distal ileum, and is the area were most of the digestion and absorption of nutrients from food contents take place (261). The large intestine, which contains the cecum, colon and rectum, is primarily responsible for the absorption of water from indigestible food content and to excrete the waste material from the body. Specific cell types, such as Paneth cells (261), are localized differentially within the intestines. Additionally, a gradient of bacterial microbiota is present from small quantities in the mucosal surfaces of the duodenum and jejunum, to higher quantities in the colon with high variation in bacterial species predominance across the length of the intestine (78, 261).

The intestinal mucosa, comprised of a layer of epithelial cells, lamina propria and a layer of smooth muscle (the muscularis mucosa) is organized into crypts and villi (261). The lamina propria supports the structure of intestinal villi, which in turn can increase the available surface area for absorption (261). In the small intestine, the crypt is generally occupied by stem cells, goblet cells, Paneth cells, undifferentiated secretory cells and enteroendocrine cells. The crypt is responsible for several cellular mechanisms including: ion and water secretion, cell renewal, endocrine-paracrine

secretions into the lamina propria and exocrine secretions into the crypt lumen (10, 225, 270). On the contrary, the villus is primarily responsible for nutrient absorption and is generally populated by absorptive enterocytes and goblet cells. A study showed that crypts are derived from a single progenitor cell (96), while the villus epithelium derives from multiple surrounding crypts in which its cells are arranged as vertical columns (Figure 1.4). These cells migrate up the villus when differentiating from a secretory to an absorptive enterocyte cell and are mainly correlated with the induction of nutrient transporters and brush border digestive enzymes (108). The absorptive enterocytes, which are the leading constituents of the villus epithelium, are tall columnar cells that contain an apical (luminal) surface with a lined dense brush border of microvilli (Figure 1.4). Enterocytes form a perijunctional actomyosin ring associated and involved with tight junction and adherens junction permeability, for barrier function (90, 141, 262, 263). These tight and adherens junctions, prevent combining molecules, by diffusion, of the apical and basolateral membrane. Moreover, after the absorptive enterocyte cells reach the villus tip, they undergo apoptosis without affecting cell-cell junctions or barrier functions (140, 208). The tight junction is a zone of close membrane contact from cell to cell. It is found in the upper compartment of the epithelial cells. A study using electron microscopy showed that the tight junction zone is composed of a network of strands and grooves (240), and the transmembrane proteins in these strands are claudin isoforms and occludin (68). *In vitro* studies have shown that occludin plays a major role in tight junction assembly and regulation (36, 66, 67, 135, 180, 235, 266, 283, 284). The claudins form the core of the tight junction and their distribution or expression throughout the GI tract varies (203). This explains observations in which certain

claudins are responsible for paracellular permeability of specific ions (199, 234) and how it varies in regions within the GI tract (199). Interestingly, pathogens can hijack claudins. *Clostridium perfringes*, for instance, has been shown to bind both claudin-3 and claudin-4 (65) resulting in withdrawal of claudins from the cell surface, loss of tight junctions and decreased transepithelial electrical resistance (TER), a measure of tight junction permeability.

Undifferentiated crypt enterocytes are thought to be an intermediate between the stem cell and the different types of epithelial cells. Unlike villus absorptive enterocytes, undifferentiated crypt enterocytes contain a less developed microvillus membrane with shorter and less dense microvilli (261). Additionally, undifferentiated crypt enterocytes are involved in the secretion of IgA into the intestinal lumen. They express the polymeric Ig receptor at the basolateral surface that binds IgA, previously secreted by plasma cells in the lamina propria (168) which ultimately undergoes proteolytic cleavage to release a portion of the receptor (or the secretory component) with the IgA (222). This receptor-IgA interaction initiates a transportation mechanism to the apical side, known as vesicular transcytosis (discussed later) (28).

Located within the villus and crypt epithelium are mucin-producing cells known as goblet cells. They are distributed throughout the small intestine and colon and are also derived from stem cells via undifferentiated crypt cells (157). In contrast to villus absorptive cells and undifferentiated crypt cells, they contain microvilli that is uneven with a tendency to be located in the junctional areas (261). The apical portion of the cell's cytoplasm is filled with granules packed with mucins (261). Studies have shown that mucin secretion by these goblet cells can drastically increase after *Escherichia coli*

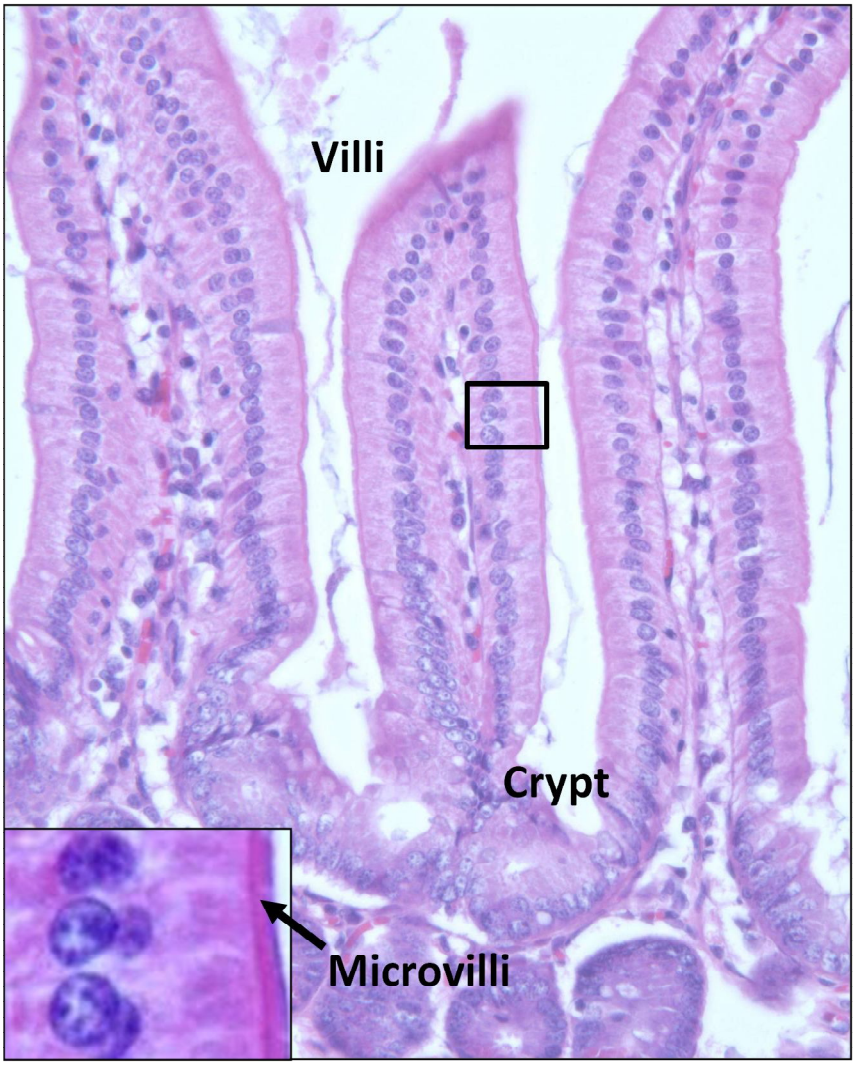


**Figure 1.4 Mouse small intestine.** Image of a section of the small intestine from a wild-type Balb/c mouse stained with hematoxylin and eosin stain (H&E stain). Represented in the image is the organization of the small intestinal mucosa into villi and crypts. The villus epithelium contains tall columnar cells (enterocytes) with a dense brush border of microvilli. Proliferation of the epithelium starts within the crypt. The enterocytes begin migrating up to the villus tip while maturing and turning into specialized cells for nutrient absorption.

(*E.coli*) and *Vibrio cholera* toxin infection, which may suggest a protective response against bacteria (132, 166). Mucins may allow for pathogenic bacteria to become confined and be removed by the mucous flow in the intestine. Additionally, carbohydrate binding sites present on mucins may play a role in luring pathogenic bacteria and preventing them from attaching to the epithelial cells' binding sites (50, 189). Several carbohydrate epitopes present on mucins that can serve as receptors for certain bacteria, such as enterotoxigenic *E. coli* (171) and *Salmonella typhimurium* (268) have already been described. Interestingly, mucins not only play a protective role against bacteria, but also against many viruses by inhibiting viral attachment and spread to host cells. For example, one study shows that porcine gastric mucins bound to HuNoV-like particles inhibit viral attachment to the Caco-2 intestinal epithelial cell line (259). Another study demonstrated that transmembrane mucin isolates significantly reduced herpes simplex virus type 1 (HSV-1) infection in epithelial cells, by blocking galectin-3-mediated viral entry (285). Additionally, scientists demonstrated that mucin 6 binds to DCs, via the dendritic cell-specific intercellular adhesion molecule-3 grabbing non integrin (DC-SIGN), and inhibits transfer of human immunodeficiency virus type-1 (HIV-1) to $CD4^+$ T lymphocytes (241). Hence, mucins can act as a first line of defense for bacterial and viral pathogens.

Enteroendocrine cells are another type of epithelial cells and are developed from the same stem cells as enterocytes, goblet cells and Paneth cells. They lack microvilli and they posses many secretory granules within their basal cytoplasm (261). Although this cell type is distributed throughout the intestinal mucosa, its function is not well understood. Interestingly, the number of enteroendocrine cells increases in diseases

such as ulcerative colitis (76, 261), thus, this could be the outcome of an adaptive response to injury (261).

Other cell types derived from the crypt stem cell that terminally differentiate are the Paneth cells (37). They possess secretory granules in their apical cytoplasm, similar to goblet cells, and their microvilli are dispersed. While their role in digestive function is not clear, it is thought that their primary role is in the production of antimicrobial peptides (261). Interestingly, antimicrobial peptides have been shown to possess antiviral properties. Particularly, defensins, which are a family of antimicrobial peptides, are known to have neutralizing activities that inactivate several viruses and inhibit infection. Some of these viruses include: herpes simplex virus (HSV) type 1/2, cytomegalovirus, vesicular stomatitis virus, influenza A virus, human adenovirus, human papillomavirus and human polyomavirus (13, 21, 45, 51).

### 1.3.2 Microfold Cells and their General Properties

Microfold (M) cells, also a cell type within the intestinal epithelium, are mainly present in the follicle-associated epithelium (FAE) within the GI tract (91, 184). These cells are uniquely specialized epithelial cells that are famously known for their antigen sampling mechanism. They are primarily found in high concentrations within aggregate lymphoid follicles known as Peyer's patches (PP) (177) (Figure 1.5), but can be found throughout the intestines as well, although rarely (128). In mice, PP are primarily located in the small intestine, cecum, colon and rectum (184, 187). In humans, they are found primarily in the ileum although isolated lymphoid follicles have been found in the large intestine (64, 181). M cells have very short, irregular and sparse microvilli and can

be distinguished via electron microscopy. They lack the brush border glycocalyx that is seen coating the microvilli of enterocytes (62, 153). Their basal membrane forms an intraepithelial cleft or pocket in which the apical and basal surfaces are close to each other, and where lymphocytes, DCs and macrophages migrate into. M cells are commonly known to provide an entry route into the intestinal mucosa for various antigens and microorganisms (175, 176, 179, 215, 217, 232). The mechanism by which many microorganisms can distinguish the FAE as a potential route of entry is not quite clear, but certain observations show differences in the composition and structure of the FAE from the whole epithelium and are suggestive of a potential role in increased pathogen-host interactions for entry (177). In congruency with this, enterocytes within the FAE express lower membrane-associated digestive hydrolases than do the enterocytes present in the villi (185, 219). Also, there is less mucus production in the FAE (184), less lysozyme- and defensin- producing Paneth cells (73) and deprivation of polymeric Ig receptor (191). However, while the FAE and M cells do not secret IgA, M cells have a receptor for IgA, as IgA has been found on the apical surface of PP M cells in animals and in humans (133, 142, 209, 280). Additionally, IgA can also bind non-specifically to certain pathogens (280) and it has been shown that exogenous IgA-antigen complexes that are taken up by M cells could achieve an induction of mucosal immunity (291). Differences in epithelial surface charges could also play a potential role in FAE attachment preference, since it was observed that, in mouse and rabbit PP, polystyrene microparticles are favorably attached to the FAE (62, 190). A study showed that virus-sized (120 nm) or bacterial-sized (1-microm) particles can attach differently to the apical surface of villus enterocytes, FAE enterocytes or M cells (143). This study

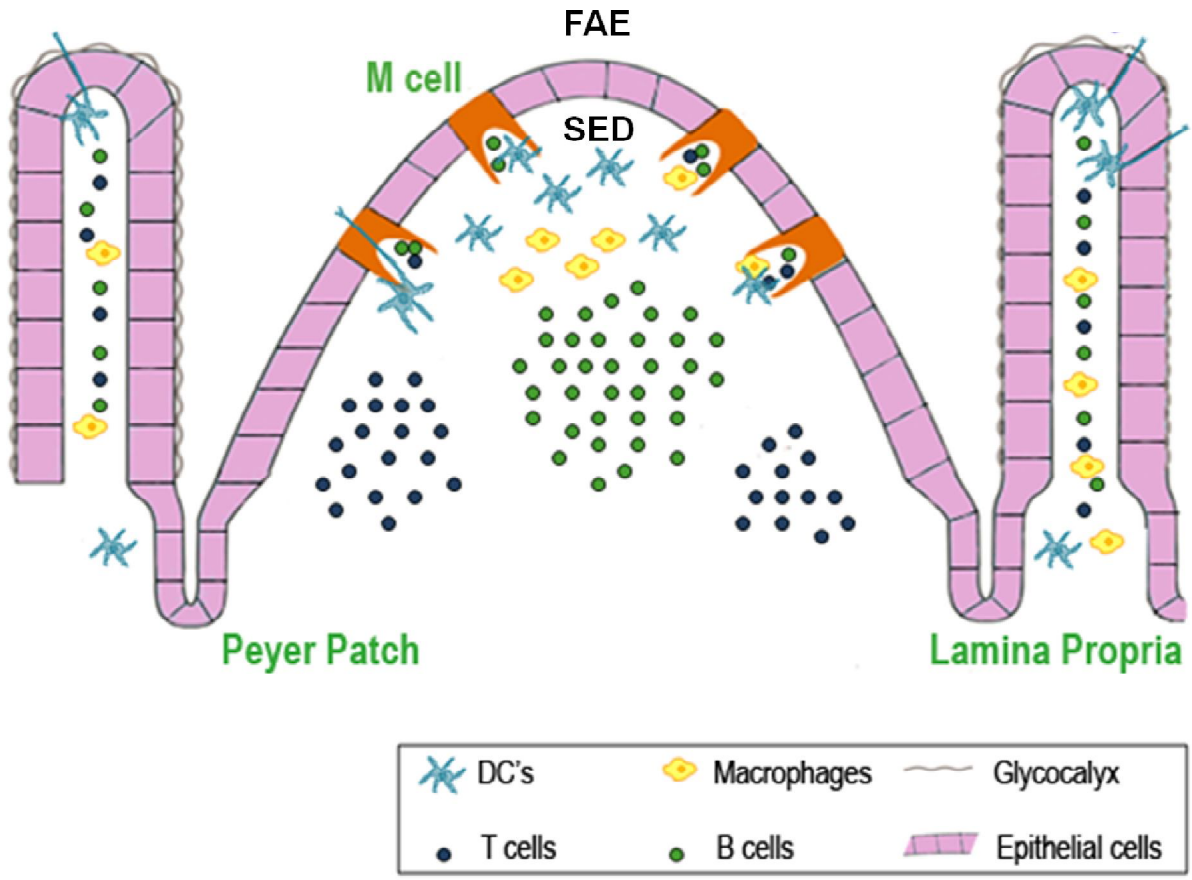


**Figure 1.5 Representation of a section of small intestine Peyer Patch and villa.** M cells are located within the follicle-associated epithelium (FAE) overlying Peyer's patches. DCs, macrophages and lymphocytes (T and B cells) are located within the sub-epithelial dome (SED) region or in the lamina propria.

further suggests that the thick brush border glycocalyx present on enterocytes but not on M cells, along with a thin glycoprotein coat present on M cells, can act as a size-selective barrier. Finally, carbohydrate structures in the FAE are different from the ones on villi (71, 73, 74, 227). M-cell-specific carbohydrates have been shown to be different between humans (74), mice (73) and rabbits (71, 114, 133). Hence, these and other factors not described here could play an important role for the microorganism's preference in attaching to different regions of the intestine.

Once antigens have successfully attached to M cells within the FAE region, they are taken up by endocytosis and moved across the epithelial barrier via a transepithelial vesicular transport mechanism (also known as transcytosis). Adherent macromolecules (24, 177, 178), ligand-coated particles (62, 177) and certain viruses, such as reovirus (130, 177), can enter via clathrin-mediated endocytosis. One study showed that *Salmonella typhimurium* entry and transport across an *in vitro* M cell model is caveolae-mediated (136). Additionally, transport of pathogens across M cells can be receptor mediated. Pattern recognition receptors present in the surface of M-like cells, such as TLR-4 and α5β1 integrin, have been shown to initiate transport of certain bacteria (264, 265). In addition, HIV-1 transport across M cells requires apical expression of the CXCR4, CCR5 and the glycosphingolipid galactosylceramide (59).

Hence, the M cell's transcytotic route is thought to be, in part, the mechanism by which antigens are routinely sampled along the mucosal surface.

#### 1.3.2.1 Transcytosis

Transcytosis is a widespread transport mechanism that a variety of cell types use. The most familiar case occurs in cell types that are polarized to form barriers between two different environments, that is, M cells and epithelial cells. They can move material from the apical to basolateral direction or vice-versa, depending on the cargo and the cellular context, without disrupting the barrier or the cell. However, osteoclasts (174, 213) and neurons (94) have also been reported to transport cargo in a similar fashion. Interestingly, a recent study demonstrated that goblet cells can also deliver soluble antigens that are less than 70 kilo Daltons in molecular weight, to underlying DCs (155). However, this phenomenon was termed goblet cell-associated antigen passages (GAPs) (128, 155). For the purpose of this dissertation, only transcytosis in the context of the specialized intestinal epithelial cells, *i.e.* M cells, will be discussed.

M cells are uniquely distinctive from all epithelial cells in that transcytosis is the prime mechanism for endocytosing particulate material. Once particles or microorganisms are taken up at the apical surface of the M cells, they are delivered to vesicles or endosomes that will end up moving towards the basal side to get in contact with the plasma membrane within the pocket and become released into the environment (177). Interestingly, pathogenic microorganisms that can cross via this transcytosis mechanism do not seem to undergo any decrease in their viability. Hence, many pathogens use this pathway to initiate infection in the host before a strong immune response takes place (176, 204).

### 1.3.3 Bacterial Pathogens Breach the Intestinal Epithelial Barrier to Cause Infection

Previously, electron microscopy studies showed that pathogens that cross the intestinal epithelial barrier via M cells are subsequently taken up by subepithelial phagocytes that were thought to be macrophages (188, 281). However, it is known that the cells located in the subepithelial dome (SED) region (Figure 1.5) are mainly DCs (123, 177). It has been shown that once DCs from this region take up antigens, they migrate to adjacent T-cell zones where presentation of antigens takes place (113, 231). Additionally, they can migrate to B-cell follicles or enter the T-cell zones of the draining lymph nodes (139, 177). While these DC movements are likely important to evoke a mucosal immune response against pathogens that is beneficial to the host (9, 206), it can also make it easier for certain pathogens to disseminate in the host and become systemic (151, 200).

*Shigella*, which is an enteroinvasive bacterial pathogen, causes intestinal cramps and bloody diarrhea in those who are infected. The reason for this occurrence involves a series of complex molecular events between epithelial cells and macrophages that result in loss of barrier function, activation and death of phagocytic cells, neutrophil influx and a severe inflammatory response (177). It has been shown, in rabbits and in rhesus macaque monkeys, that the initial site of *Shigella* entry into the host is the FAE (214, 215, 274). The mechanisms of how the bacteria invade and spread from cell-to-cell has been described *in vitro* (19, 214, 215). In addition, studies have shown that *Shigella* invades the epithelial cells through the basolateral side but not the apical side (170, 216). Once bacteria have crossed the epithelial barrier, it survives the attack from macrophages by activating caspase 1 for a rapid macrophage cell death by apoptosis

(97, 218). This and other events lead to an induction of the inflammatory response that can be destructive to the intestinal mucosa and the epithelial barrier (44, 57, 193, 198) .

Enteric *Yersinia enterocolitica* and *Yersinia pseudotuberculosis* have been shown to cross the intestinal epithelial barrier by adhering to M cells (83, 145). Invasin, which is an outer membrane protein, mediates this attachment via the host cell adhesion molecule β1 integrin as a receptor (111, 112). This was further confirmed after invasin-negative *Yersinia* mutants had lost their capacity to attach to M cells, colonize PP (41, 145, 192) and be transported across by M-like cell in an *in vitro* co-culture system (223). Once *Yersinia* species have crossed the FAE, they can inhibit phagocytosis from macrophages by secreting a set of proteins (Yop proteins) into the cell cytoplasm that disrupts the cytoskeleton (54) and eventually evokes apoptosis of the macrophage (162, 165, 210). This results in the pathogen remaining extracellular in the mucosa, mesenteric lymph nodes and, after some time, obliteration of the PP (177).

Similar to *Shigella* and *Yersinia*, *Salmonella Typhimurium* has been shown to select for M cells in the FAE as a route of entry (42, 117), but has also been found to enter via the villus epithelium (243, 267). Interestingly, in an *in vitro* model system of epithelial cell monolayers cocultured with DCs, *Salmonella* was observed in contact with DCs that reached through the epithelial tight junctions (205), and *in vivo*, the number of DC extensions increased after incubation with *Salmonella* (39). These studies suggest a role for transepithelial DCs in pathogen uptake. *Salmonella* that is intracellular has been shown to be cytotoxic to M cells leading to the disruption of the FAE and provoking very serious inflammatory lesions (117, 129). Once the bacteria has crossed the FAE, it is captured by SED DCs (99), it can survive inside live phagocyte cells (161) and infect

macrophages. Interestingly, a recent study demonstrated that *Salmonella enteritidis* can escape macrophage clearance by elevating intestinal epithelial micro RNA 128 (miR-128) levels, which in turn, diminished macrophage recruitment mediated by M-CSF cytokine signaling (289). Hence, the mechanism by which *Salmonella* survives the attack of macrophages may depend on the strain. Nevertheless, migration of the "infected" or antigen-presenting phagocytes to other sites of the host were shown to help mediate systemic dissemination (267). Hence, the efficiency in interaction with antigen-presenting cells has made attenuated *Salmonella* species an attractive vector for mucosal vaccines (236).

Other bacterial pathogens such as *Campylobacter jejuni* (271), *Mycobacterium paratuberculosis* (164) and *Mycobacterium bovis* (63) have also been shown to interact and cross the intestinal epithelium via M cells for invasion.

### 1.3.4 Viral Pathogens and the Intestine

Enteric viral pathogens, such as reovirus and poliovirus, have been suggested to use M cells as a route of viral entry after they were observed adhering to M cells (232, 281). For instance, reovirus, which can be transmitted by the oral and respiratory routes and causes respiratory and GI tract infections, not only binds to M cells in the respiratory airways (167), but can also bind selectively to M cells in PP (3, 12, 281) and in the colon (186). Proteolytic cleavage of the virus in the intestine has been shown to increase reovirus infectivity (11, 16) which is essential for M cell adherence (3). This adherence to M cells is mediated by the interaction with the virus' sigma 1 protein (92). Interestingly, the virus infects the epithelial cells from the basolateral side (12),

suggesting that reovirus M cell transport needs to occur first in order to get in contact with its receptor, the junctional adhesion molecule A (JAM-A), found in the basolateral surface of epithelial cells (4, 25). However, during this transport process, the possibility that reovirus can infect M cells is also likely to be the case since *in vivo* experiments have shown viral factories inside M cells (12).

Like reovirus, poliovirus infects humans via the oral route and can replicate in the PP before spreading elsewhere (201). This fact assisted in understanding the significance of developing mucosal immunity against the pathogen and, in fact, played a role for the establishment of a live attenuated poliovirus vaccine (182). Interestingly, when both poliovirus type 1 or the attenuated Sabin strain where incubated in PP explants from humans *in vitro*, viruses where visualized adhering to and being taken up by M cells (232). Hence, the capability of poliovirus to target M cells for crossing the epithelial barrier has proven a great interest for researching and developing vaccines. More so, poliovirus vectors have recently shown potential as mucosal vaccines for other pathogens (43).

There is evidence that suggests that M cells are involved in HIV-1 entry after mucosal explants in culture from mouse and rabbit, showed adherence of HIV-1 to M cells and transport of the virus to the M-cell pocket (2). Moreover, HIV-1 can be transmitted by the rectal mucosa (163), which is thought to be partly due to lymphoid follicles and M cells being present in this area (177, 181). Interestingly, *in vitro*, it has been shown that HIV-1 infection of intestinal epithelial cells can occur in culture with intestinal epithelial cell lines such as HT29 and Caco-2 cells, via the expression of the glycosphingolipid galactosylceramide in the cell membrane (55, 69). One study showed

that HIV-1 can infect and be transcytosed across undifferentiated and differentiated Caco-2 cells with M-like cell properties, only if the chemokine receptors CCR5 (R5 tropic) and CXCR4 (X4 tropic), along with the galactosylceramide were present in the cells (60). Thus, this study shows that transport of HIV-1 is receptor-mediated. However, while humans also contain galactosylceramide in their intestinal epithelium membrane (23, 98), no HIV-1 infection has been detected in the respective intestinal epithelial cells of infected individuals (61). It has been suggested that an explanation for this could be due to the intestinal enterocytes containing brush borders with thick glycocalyx that prevent the pathogen's access to the apical membrane (177). In addition, HIV-1 particles were unable to infiltrate the enterocyte's glycocalyx from mouse and rabbit PP, but were able to adhere to M-cells (2). Interestingly, a recent *in vitro* study showed that HIV-1 R5 tropic, but not X4 tropic, can selectively trigger DCs to migrate between intestinal epithelial cells for efficient sampling and transfer of infection to target cells (29). Hence, similarly to what has been showed with *Salmonella* (39, 205), exposure to a viral (29) or a bacterial stimuli, can lead to induction of transepithelial DC sampling. Therefore, besides M cells, transepithelial DCs can be another mechanism of pathogen uptake.

A study looking at the passage of human T-cell leukemia virus type 1 (HTLV) across the Caco-2 intestinal epithelial monolayer, showed that epithelial barrier integrity was not compromised when cells were cocultured with HTLV-1 infected T lymphocytes. Moreover, this study showed that HTLV-1 virions crossed the epithelial monolayer via a transcytosis mechanism that ended in the productive infection of DCs located below (150). Interestingly, the transcytosis process described in this study seems to be via the

enterocytes instead of M cells, and hence, future studies need to address whether M cells are infected at all and if they play a role in HTLV-1 transport.

While many of these studies that have been performed using *in vitro* or *ex vivo* techniques suggest M cells as a potential portal for virus infection, direct *in vivo* experimental evidence showing productive infection of the native host via these M cells is still not clear. Nevertheless, these studies have helped in understanding how viruses can use M cells for viral entry into the host. Thus, M cells can be targeted for the induction of mucosal immune responses against enteric viral pathogens, to aid in future development of mucosal oral vaccines.

## 1.4 Dissertation Aims

MNV, which efficiently infects cells in culture and in a small animal model, can help understand how this enteric virus overcomes the intestinal epithelial barrier to infect cells underneath it. Hence, information obtained with MNV might be applicable to HuNoV and could help develop strategies to limit infection. This dissertation aims to identify the mechanism or pathway by which MNV crosses the intestinal epithelial barrier *in vitro* and *in vivo*, and whether an unrelated enteric virus (*i.e.* reovirus) behaves similarly.

## 1.5 References

1. **Alvarez, L., A. M. Auld, G. M. del Fierro, P. Fung, D. A. Lawrence, E. F. McInnes, M. E. Quinn, L. Rasmussen, R. Stevenson, T. D. Utteridge, and B. A. Vassallo.** 2011. Prevalence of viral, bacterial and parasitological diseases in rats and mice used in research environments in Australasia over a 5-y period. Lab animal **40:**341+.

2. **Amerongen, H. M., R. Weltzin, C. M. Farnet, P. Michetti, W. A. Haseltine, and M. R. Neutra.** 1991. Transepithelial transport of HIV-1 by intestinal M cells: a mechanism for transmission of AIDS. J Acquir Immune Defic Syndr **4:**760-765.
3. **Amerongen, H. M., G. A. Wilson, B. N. Fields, and M. R. Neutra.** 1994. Proteolytic processing of reovirus is required for adherence to intestinal M cells. Journal of virology **68:**8428-8432.
4. **Antar, A. A., J. L. Konopka, J. A. Campbell, R. A. Henry, A. L. Perdigoto, B. D. Carter, A. Pozzi, T. W. Abel, and T. S. Dermody.** 2009. Junctional adhesion molecule-A is required for hematogenous dissemination of reovirus. Cell host & microbe **5:**59-71.
5. **Arias, A., D. Bailey, Y. Chaudhry, and I. Goodfellow.** 2012. Development of a reverse-genetics system for murine norovirus 3: long-term persistence occurs in the caecum and colon. The Journal of general virology **93:**1432-1441.
6. **Atmar, R. L., and M. K. Estes.** 2006. The epidemiologic and clinical importance of norovirus infection. Gastroenterology clinics of North America **35:**275-290.
7. **Atmar, R. L., A. R. Opekun, M. A. Gilger, M. K. Estes, S. E. Crawford, F. H. Neill, S. Ramani, H. Hill, J. Ferreira, and D. Y. Graham.** 2013. Determination of the Human Infectious Dose-50% for Norwalk Virus. The Journal of infectious diseases.
8. **Bally, M., G. E. Rydell, R. Zahn, W. Nasir, C. Eggeling, M. E. Breimer, L. Svensson, F. Hook, and G. Larson.** 2012. Norovirus GII.4 virus-like particles recognize galactosylceramides in domains of planar supported lipid bilayers. Angew Chem Int Ed Engl **51:**12020-12024.
9. **Banchereau, J., and R. M. Steinman.** 1998. Dendritic cells and the control of immunity. Nature **392:**245-252.
10. **Barret, K. E., and L. S. Bertelsen.** 2003. Physiological regulation of gastrointestinal ion transport, p. 241-266. *In* G. A. Hecht (ed.), Microbial Pathogenesis and the Intestinal Epithelial Cell. ASM Press, Washington, DC.
11. **Bass, D. M., D. Bodkin, R. Dambrauskas, J. S. Trier, B. N. Fields, and J. L. Wolf.** 1990. Intraluminal proteolytic activation plays an important role in replication of type 1 reovirus in the intestines of neonatal mice. Journal of virology **64:**1830-1833.
12. **Bass, D. M., J. S. Trier, R. Dambrauskas, and J. L. Wolf.** 1988. Reovirus type I infection of small intestinal epithelium in suckling mice and its effect on M cells. Laboratory investigation; a journal of technical methods and pathology **58:**226-235.
13. **Bastian, A., and H. Schafer.** 2001. Human alpha-defensin 1 (HNP-1) inhibits adenoviral infection in vitro. Regulatory peptides **101:**157-161.
14. **Baumgart, T., B. R. Capraro, C. Zhu, and S. L. Das.** 2011. Thermodynamics and mechanics of membrane curvature generation and sensing by proteins and lipids. Annu Rev Phys Chem **62:**483-506.
15. **Ben-Dov, N., and R. Korenstein.** 2012. Enhancement of cell membrane invaginations, vesiculation and uptake of macromolecules by protonation of the cell surface. PLoS ONE **7:**e35204.

16. **Bodkin, D. K., M. L. Nibert, and B. N. Fields.** 1989. Proteolytic digestion of reovirus in the intestinal lumens of neonatal mice. Journal of virology **63:**4676-4681.
17. **Bok, K., G. I. Parra, T. Mitra, E. Abente, C. K. Shaver, D. Boon, R. Engle, C. Yu, A. Z. Kapikian, S. V. Sosnovtsev, R. H. Purcell, and K. Y. Green.** 2011. Chimpanzees as an animal model for human norovirus infection and vaccine development. Proceedings of the National Academy of Sciences of the United States of America **108:**325-330.
18. **Bok, K., V. G. Prikhodko, K. Y. Green, and S. V. Sosnovtsev.** 2009. Apoptosis in Murine Norovirus-Infected RAW264.7 Cells Is Associated with Downregulation of Survivin. Journal of virology **83:**3647-3656.
19. **Bourdet-Sicard, R., C. Egile, P. J. Sansonetti, and G. Tran Van Nhieu.** 2000. Diversion of cytoskeletal processes by Shigella during invasion of epithelial cells. Microbes and infection / Institut Pasteur **2:**813-819.
20. **Bruggink, L. D., and J. A. Marshall.** 2009. Norovirus epidemics are linked to two distinct sets of controlling factors. International Journal of Infectious Diseases **13:**e125-e126.
21. **Buck, C. B., P. M. Day, C. D. Thompson, J. Lubkowski, W. Lu, D. R. Lowy, and J. T. Schiller.** 2006. Human alpha-defensins block papillomavirus infection. Proceedings of the National Academy of Sciences of the United States of America **103:**1516-1521.
22. **Burroughs, J. N., and F. Brown.** 1978. Presence of a Covalently Linked Protein on Calicivirus RNA. Journal of General Virology **41:**443-446.
23. **Butor, C., A. Couedel-Courteille, J. G. Guillet, and A. Venet.** 1996. Differential distribution of galactosylceramide, H antigen, and carcinoembryonic antigen in rhesus macaque digestive mucosa. J Histochem Cytochem **44:**1021-1031.
24. **Bye, W. A., C. H. Allan, and J. S. Trier.** 1984. Structure, distribution, and origin of M cells in Peyer's patches of mouse ileum. Gastroenterology **86:**789-801.
25. **Campbell, J. A., P. Schelling, J. D. Wetzel, E. M. Johnson, J. C. Forrest, G. A. Wilson, M. Aurrand-Lions, B. A. Imhof, T. Stehle, and T. S. Dermody.** 2005. Junctional adhesion molecule a serves as a receptor for prototype and field-isolate strains of mammalian reovirus. Journal of virology **79:**7967-7978.
26. **Cannon, J. L., E. Papafragkou, G. W. Park, J. Osborne, L. A. Jaykus, and J. Vinje.** 2006. Surrogates for the study of norovirus stability and inactivation in the environment: A comparison of murine norovirus and feline calicivirus. Journal of food protection **69:**2761-2765.
27. **Capizzi, T., G. Makari-Judson, R. Steingart, and W. Mertens.** 2011. Chronic diarrhea associated with persistent norovirus excretion in patients with chronic lymphocytic leukemia: report of two cases. BMC infectious diseases **11:**131.
28. **Casanova, J. E., P. P. Breitfeld, S. A. Ross, and K. E. Mostov.** 1990. Phosphorylation of the polymeric immunoglobulin receptor required for its efficient transcytosis. Science (New York, N.Y **248:**742-745.
29. **Cavarelli, M., C. Foglieni, M. Rescigno, and G. Scarlatti.** 2013. R5 HIV-1 envelope attracts dendritic cells to cross the human intestinal epithelium and sample luminal virions via engagement of the CCR5. EMBO molecular medicine **5:**776-794.

30. **Chachu, K. A., D. W. Strong, A. D. LoBue, C. E. Wobus, R. S. Baric, and H. W. Virgin IV.** 2008. Antibody is critical for the clearance of murine norovirus infection. Journal of virology **82:**6610-6617.
31. **Chang, K. O.** 2009. Role of cholesterol pathways in norovirus replication. Journal of virology **83:**8587-8595.
32. **Chang, K. O., and D. W. George.** 2007. Interferons and ribavirin effectively inhibit Norwalk virus replication in replicon-bearing cells. Journal of virology **81:**12111-12118.
33. **Chang, K. O., S. V. Sosnovtsev, G. Belliot, A. D. King, and K. Y. Green.** 2006. Stable expression of a Norwalk virus RNA replicon in a human hepatoma cell line. Virology **353:**463-473.
34. **Chaudhry, Y., M. A. Skinner, and I. G. Goodfellow.** 2007. Recovery of genetically defined murine norovirus in tissue culture by using a fowlpox virus expressing T7 RNA polymerase. The Journal of general virology **88:**2091-2100.
35. **Cheetham, S., M. Souza, T. Meulia, S. Grimes, M. G. Han, and L. J. Saif.** 2006. Pathogenesis of a genogroup II human norovirus in gnotobiotic pigs. Journal of virology **80:**10372-10381.
36. **Chen, Y., C. Merzdorf, D. L. Paul, and D. A. Goodenough.** 1997. COOH terminus of occludin is required for tight junction barrier function in early Xenopus embryos. The Journal of cell biology **138:**891-899.
37. **Cheng, H., J. Merzel, and C. P. Leblond.** 1969. Renewal of Paneth cells in the small intestine of the mouse. The American journal of anatomy **126:**507-525.
38. **Cheng, Z. J., R. D. Singh, D. L. Marks, and R. E. Pagano.** 2006. Membrane microdomains, caveolae, and caveolar endocytosis of sphingolipids. Molecular membrane biology **23:**101-110.
39. **Chieppa, M., M. Rescigno, A. Y. Huang, and R. N. Germain.** 2006. Dynamic imaging of dendritic cell extension into the small bowel lumen in response to epithelial cell TLR engagement. The Journal of experimental medicine **203:**2841-2852.
40. **Choi, J. M., A. M. Hutson, M. K. Estes, and B. V. Prasad.** 2008. Atomic resolution structural characterization of recognition of histo-blood group antigens by Norwalk virus. Proceedings of the National Academy of Sciences of the United States of America **105:**9175-9180.
41. **Clark, M. A., B. H. Hirst, and M. A. Jepson.** 1998. M-cell surface beta1 integrin expression and invasin-mediated targeting of Yersinia pseudotuberculosis to mouse Peyer's patch M cells. Infection and immunity **66:**1237-1243.
42. **Clark, M. A., M. A. Jepson, N. L. Simmons, and B. H. Hirst.** 1994. Preferential interaction of Salmonella typhimurium with mouse Peyer's patch M cells. Research in microbiology **145:**543-552.
43. **Crotty, S., C. J. Miller, B. L. Lohman, M. R. Neagu, L. Compton, D. Lu, F. X. Lu, L. Fritts, J. D. Lifson, and R. Andino.** 2001. Protection against simian immunodeficiency virus vaginal challenge by using Sabin poliovirus vectors. Journal of virology **75:**7435-7452.
44. **D'Hauteville, H., S. Khan, D. J. Maskell, A. Kussak, A. Weintraub, J. Mathison, R. J. Ulevitch, N. Wuscher, C. Parsot, and P. J. Sansonetti.** 2002. Two msbB genes encoding maximal acylation of lipid A are required for invasive

Shigella flexneri to mediate inflammatory rupture and destruction of the intestinal epithelium. J Immunol **168:**5240-5251.

45. **Daher, K. A., M. E. Selsted, and R. I. Lehrer.** 1986. Direct inactivation of viruses by human granulocyte defensins. Journal of virology **60:**1068-1074.
46. **Daughenbaugh, K. F., C. S. Fraser, J. W. Hershey, and M. E. Hardy.** 2003. The genome-linked protein VPg of the Norwalk virus binds eIF3, suggesting its role in translation initiation complex recruitment. The EMBO journal **22:**2852-2859.
47. **Daughenbaugh, K. F., C. E. Wobus, and M. E. Hardy.** 2006. VPg of murine norovirus binds translation initiation factors in infected cells. Virology journal **3:**33.
48. **de Wit, M. A., M. A. Widdowson, H. Vennema, E. de Bruin, T. Fernandes, and M. Koopmans.** 2007. Large outbreak of norovirus: the baker who should have known better. The Journal of infection **55:**188-193.
49. **Donaldson, E. F., L. C. Lindesmith, A. D. LoBue, and R. S. Baric.** 2010. Viral shape-shifting: norovirus evasion of the human immune system. Nature Reviews Microbiology **8:**231-241.
50. **Drumm, B., A. M. Roberton, and P. M. Sherman.** 1988. Inhibition of attachment of Escherichia coli RDEC-1 to intestinal microvillus membranes by rabbit ileal mucus and mucin in vitro. Infection and immunity **56:**2437-2442.
51. **Dugan, A. S., M. S. Maginnis, J. A. Jordan, M. L. Gasparovic, K. Manley, R. Page, G. Williams, E. Porter, B. A. O'Hara, and W. J. Atwood.** 2008. Human alpha-defensins inhibit BK virus infection by aggregating virions and blocking binding to host cells. The Journal of biological chemistry **283:**31125-31132.
52. **Duizer, E., K. J. Schwab, F. H. Neill, R. L. Atmar, M. P. Koopmans, and M. K. Estes.** 2004. Laboratory efforts to cultivate noroviruses. The Journal of general virology **85:**79-87.
53. **Esseili, M. A., Q. Wang, and L. J. Saif.** 2012. Binding of human GII.4 norovirus virus-like particles to carbohydrates of romaine lettuce leaf cell wall materials. Applied and environmental microbiology **78:**786-794.
54. **Fallman, M., C. Persson, and H. Wolf-Watz.** 1997. Yersinia proteins that target host cell signaling pathways. The Journal of clinical investigation **99:**1153-1157.
55. **Fantini, J., D. G. Cook, N. Nathanson, S. L. Spitalnik, and F. Gonzalez-Scarano.** 1993. Infection of colonic epithelial cell lines by type 1 human immunodeficiency virus is associated with cell surface expression of galactosylceramide, a potential alternative gp120 receptor. Proceedings of the National Academy of Sciences of the United States of America **90:**2700-2704.
56. **Farkas, T., K. Sestak, C. Wei, and X. Jiang.** 2008. Characterization of a rhesus monkey calicivirus representing a new genus of Caliciviridae. Journal of virology **82:**5408-5416.
57. **Fernandez, M. I., A. Thuizat, T. Pedron, M. Neutra, A. Phalipon, and P. J. Sansonetti.** 2003. A newborn mouse model for the study of intestinal pathogenesis of shigellosis. Cellular microbiology **5:**481-491.
58. **Fiege, B., C. Rademacher, J. Cartmell, P. I. Kitov, F. Parra, and T. Peters.** 2012. Molecular details of the recognition of blood group antigens by a human

norovirus as determined by STD NMR spectroscopy. Angew Chem Int Ed Engl **51:**928-932.

59. **Fotopoulos, G., A. Harari, P. Michetti, D. Trono, G. Pantaleo, and J.-P. Kraehenbuhl.** 2002. Transepithelial transport of HIV-1 by M cells is receptor-mediated. Proceedings of the National Academy of Sciences **99:**9410-9414.
60. **Fotopoulos, G., A. Harari, P. Michetti, D. Trono, G. Pantaleo, and J. P. Kraehenbuhl.** 2002. Transepithelial transport of HIV-1 by M cells is receptor-mediated. Proceedings of the National Academy of Sciences of the United States of America **99:**9410-9414.
61. **Fox, C. H., D. Kotler, A. Tierney, C. S. Wilson, and A. S. Fauci.** 1989. Detection of HIV-1 RNA in the lamina propria of patients with AIDS and gastrointestinal disease. The Journal of infectious diseases **159:**467-471.
62. **Frey, A., K. T. Giannasca, R. Weltzin, P. J. Giannasca, H. Reggio, W. I. Lencer, and M. R. Neutra.** 1996. Role of the glycocalyx in regulating access of microparticles to apical plasma membranes of intestinal epithelial cells: implications for microbial attachment and oral vaccine targeting. The Journal of experimental medicine **184:**1045-1059.
63. **Fujimura, Y.** 1986. Functional morphology of microfold cells (M cells) in Peyer's patches--phagocytosis and transport of BCG by M cells into rabbit Peyer's patches. Gastroenterologia Japonica **21:**325-335.
64. **Fujimura, Y., M. Hosobe, and T. Kihara.** 1992. Ultrastructural study of M cells from colonic lymphoid nodules obtained by colonoscopic biopsy. Dig Dis Sci **37:**1089-1098.
65. **Fujita, K., J. Katahira, Y. Horiguchi, N. Sonoda, M. Furuse, and S. Tsukita.** 2000. Clostridium perfringens enterotoxin binds to the second extracellular loop of claudin-3, a tight junction integral membrane protein. FEBS letters **476:**258-261.
66. **Furuse, M., K. Fujimoto, N. Sato, T. Hirase, S. Tsukita, and S. Tsukita.** 1996. Overexpression of occludin, a tight junction-associated integral membrane protein, induces the formation of intracellular multilamellar bodies bearing tight junction-like structures. Journal of cell science **109 ( Pt 2):**429-435.
67. **Furuse, M., T. Hirase, M. Itoh, A. Nagafuchi, S. Yonemura, S. Tsukita, and S. Tsukita.** 1993. Occludin: a novel integral membrane protein localizing at tight junctions. The Journal of cell biology **123:**1777-1788.
68. **Furuse, M., H. Sasaki, K. Fujimoto, and S. Tsukita.** 1998. A single gene product, claudin-1 or -2, reconstitutes tight junction strands and recruits occludin in fibroblasts. The Journal of cell biology **143:**391-401.
69. **Furuta, Y., K. Eriksson, B. Svennerholm, P. Fredman, P. Horal, S. Jeansson, A. Vahlne, J. Holmgren, and C. Czerkinsky.** 1994. Infection of vaginal and colonic epithelial cells by the human immunodeficiency virus type 1 is neutralized by antibodies raised against conserved epitopes in the envelope glycoprotein gp120. Proceedings of the National Academy of Sciences of the United States of America **91:**12559-12563.
70. **Gallimore, C. I., D. Lewis, C. Taylor, A. Cant, A. Gennery, and J. J. Gray.** 2004. Chronic excretion of a norovirus in a child with cartilage hair hypoplasia (CHH). J Clin Virol **30:**196-204.

71. **Gebert, A., and G. Hach.** 1993. Differential binding of lectins to M cells and enterocytes in the rabbit cecum. Gastroenterology **105:**1350-1361.
72. **Gerondopoulos, A., T. Jackson, P. Monaghan, N. Doyle, and L. O. Roberts.** 2010. Murine norovirus-1 cell entry is mediated through a non-clathrin-, non-caveolae-, dynamin- and cholesterol-dependent pathway. The Journal of general virology **91:**1428-1438.
73. **Giannasca, P. J., K. T. Giannasca, P. Falk, J. I. Gordon, and M. R. Neutra.** 1994. Regional differences in glycoconjugates of intestinal M cells in mice: potential targets for mucosal vaccines. The American journal of physiology **267:**G1108-1121.
74. **Giannasca, P. J., K. T. Giannasca, A. M. Leichtner, and M. R. Neutra.** 1999. Human intestinal M cells display the sialyl Lewis A antigen. Infection and immunity **67:**946-953.
75. **Girard, M., S. Ngazoa, K. Mattison, and J. Jean.** 2010. Attachment of Noroviruses to Stainless Steel and Their Inactivation, Using Household Disinfectants. Journal of Food Protection® **73:**400-404.
76. **Gledhill, A., P. A. Hall, J. P. Cruse, and D. J. Pollock.** 1986. Enteroendocrine cell hyperplasia, carcinoid tumours and adenocarcinoma in long-standing ulcerative colitis. Histopathology **10:**501-508.
77. **Goodfellow, I., Y. Chaudhry, I. Gioldasi, A. Gerondopoulos, A. Natoni, L. Labrie, J. F. Laliberte, and L. Roberts.** 2005. Calicivirus translation initiation requires an interaction between VPg and eIF 4 E. EMBO reports **6:**968-972.
78. **Gorbach, S. L., A. G. Plaut, L. Nahas, L. Weinstein, G. Spanknebel, and R. Levitan.** 1967. Studies of intestinal microflora. II. Microorganisms of the small intestine and their relations to oral and fecal flora. Gastroenterology **53:**856-867.
79. **Gray, J. J., E. Kohli, F. M. Ruggeri, H. Vennema, A. Sánchez-Fauquier, E. Schreier, C. I. Gallimore, M. Iturriza-Gomara, H. Giraudon, P. Pothier, I. Di Bartolo, N. Inglese, E. de Bruin, B. van der Veer, S. Moreno, V. Montero, M. C. de Llano, M. Höhne, and S. M. Diedrich.** 2007. European Multicenter Evaluation of Commercial Enzyme Immunoassays for Detecting Norovirus Antigen in Fecal Samples. Clinical and Vaccine Immunology **14:**1349-1355.
80. **Green, K. Y.** 2007. Caliciviridae, p. 949-980. *In* P. H. DM Knipe (ed.), Fields Virology, 5 ed, vol. 1. Lippincott Williams & Wilkins, Philadelphia.
81. **Green, K. Y., T. Ando, M. S. Balayan, T. Berke, I. N. Clarke, M. K. Estes, D. O. Matson, S. Nakata, J. D. Neill, M. J. Studdert, and H.-J. Thiel.** 2000. Taxonomy of the Caliciviruses. Journal of Infectious Diseases **181:**S322-S330.
82. **Grove, J., and M. Marsh.** 2011. The cell biology of receptor-mediated virus entry. The Journal of cell biology **195:**1071-1082.
83. **Grutzkau, A., C. Hanski, H. Hahn, and E. O. Riecken.** 1990. Involvement of M cells in the bacterial invasion of Peyer's patches: a common mechanism shared by Yersinia enterocolitica and other enteroinvasive bacteria. Gut **31:**1011-1015.
84. **Guix, S., M. Asanaka, K. Katayama, S. E. Crawford, F. H. Neill, R. L. Atmar, and M. K. Estes.** 2007. Norwalk virus RNA is infectious in mammalian cells. Journal of virology **81:**12238-12248.

85. **Guo, M., K. O. Chang, M. E. Hardy, Q. Zhang, A. V. Parwani, and L. J. Saif.** 1999. Molecular Characterization of a Porcine Enteric Calicivirus Genetically Related to Sapporo-Like Human Caliciviruses. Journal of virology **73:**9625-9631.
86. **Hall, A. J., A. T. Curns, L. C. McDonald, U. D. Parashar, and B. A. Lopman.** 2012. The roles of Clostridium difficile and norovirus among gastroenteritis-associated deaths in the United States, 1999-2007. Clin Infect Dis **55:**216-223.
87. **Hanover, J. A.** 1985. Transit of receptors for epidermal growth factor and transferrin through clathrin-coated pits. Analysis of the kinetics of receptor entry. The Journal of biological chemistry **260:**15938-15945.
88. **Hansman, G. S., C. Biertumpfel, I. Georgiev, J. S. McLellan, L. Chen, T. Zhou, K. Katayama, and P. D. Kwong.** 2011. Crystal structures of GII.10 and GII.12 norovirus protruding domains in complex with histo-blood group antigens reveal details for a potential site of vulnerability. Journal of virology **85:**6687-6701.
89. **Hardy, M. E., T. J. Crone, J. E. Brower, and K. Ettayebi.** 2002. Substrate specificity of the Norwalk virus 3C-like proteinase. Virus research **89:**29-39.
90. **Hecht, G., L. Pestic, G. Nikcevic, A. Koutsouris, J. Tripuraneni, D. D. Lorimer, G. Nowak, V. Guerriero, Jr., E. L. Elson, and P. D. Lanerolle.** 1996. Expression of the catalytic domain of myosin light chain kinase increases paracellular permeability. The American journal of physiology **271:**C1678-1684.
91. **Hein, W. R.** 1999. Organization of mucosal lymphoid tissue. Current topics in microbiology and immunology **236:**1-15.
92. **Helander, A., K. J. Silvey, N. J. Mantis, A. B. Hutchings, K. Chandran, W. T. Lucas, M. L. Nibert, and M. R. Neutra.** 2003. The viral sigma1 protein and glycoconjugates containing alpha2-3-linked sialic acid are involved in type 1 reovirus adherence to M cell apical surfaces. Journal of virology **77:**7964-7977.
93. **Helenius, A.** 2007. Virus entry and uncoating, p. 99-118. *In* D. M. Knipe, Howley, P. M. (ed.), Fields Virology, 5 ed, vol. 1. Wolters Kluwer, Philadelphia.
94. **Hemar, A., J. C. Olivo, E. Williamson, R. Saffrich, and C. G. Dotti.** 1997. Dendroaxonal transcytosis of transferrin in cultured hippocampal and sympathetic neurons. J Neurosci **17:**9026-9034.
95. **Herbert, T. P., I. Brierley, and T. D. Brown.** 1997. Identification of a protein linked to the genomic and subgenomic mRNAs of feline calicivirus and its role in translation. Journal of General Virology **78:**1033-1040.
96. **Hermiston, M. L., R. P. Green, and J. I. Gordon.** 1993. Chimeric-transgenic mice represent a powerful tool for studying how the proliferation and differentiation programs of intestinal epithelial cell lineages are regulated. Proceedings of the National Academy of Sciences of the United States of America **90:**8866-8870.
97. **Hilbi, H., J. E. Moss, D. Hersh, Y. Chen, J. Arondel, S. Banerjee, R. A. Flavell, J. Yuan, P. J. Sansonetti, and A. Zychlinsky.** 1998. Shigella-induced apoptosis is dependent on caspase-1 which binds to IpaB. The Journal of biological chemistry **273:**32895-32900.
98. **Holgersson, J., N. Stromberg, and M. E. Breimer.** 1988. Glycolipids of human large intestine: difference in glycolipid expression related to anatomical

localization, epithelial/non-epithelial tissue and the ABO, Le and Se phenotypes of the donors. Biochimie **70:**1565-1574.

99. **Hopkins, S. A., F. Niedergang, I. E. Corthesy-Theulaz, and J. P. Kraehenbuhl.** 2000. A recombinant Salmonella typhimurium vaccine strain is taken up and survives within murine Peyer's patch dendritic cells. Cellular microbiology **2:**59-68.
100. **Hsu, C. C., L. K. Riley, and R. S. Livingston.** 2007. Molecular characterization of three novel murine noroviruses. Virus Genes **34:**147-155.
101. **Hsu, C. C., L. K. Riley, H. M. Wills, and R. S. Livingston.** 2006. Persistent infection with and serologic cross-reactivity of three novel murine noroviruses. Comparative medicine **56:**247-251.
102. **Hsu, C. C., C. E. Wobus, E. K. Steffen, L. K. Riley, and R. S. Livingston.** 2005. Development of a microsphere-based serologic multiplexed fluorescent immunoassay and a reverse transcriptase PCR assay to detect murine norovirus 1 infection in mice. Clin Diagn Lab Immunol **12:**1145-1151.
103. **Huang, P., T. Farkas, S. Marionneau, W. Zhong, N. Ruvoen-Clouet, A. L. Morrow, M. Altaye, L. K. Pickering, D. S. Newburg, J. LePendu, and X. Jiang.** 2003. Noroviruses bind to human ABO, Lewis, and secretor histo-blood group antigens: identification of 4 distinct strain-specific patterns. The Journal of infectious diseases **188:**19-31.
104. **Huang, P., T. Farkas, W. Zhong, M. Tan, S. Thornton, A. L. Morrow, and X. Jiang.** 2005. Norovirus and histo-blood group antigens: demonstration of a wide spectrum of strain specificities and classification of two major binding groups among multiple binding patterns. Journal of virology **79:**6714-6722.
105. **Hutson, A. M., R. L. Atmar, and M. K. Estes.** 2004. Norovirus disease: changing epidemiology and host susceptibility factors. Trends in microbiology **12:**279-287.
106. **Hutson, A. M., R. L. Atmar, D. Y. Graham, and M. K. Estes.** 2002. Norwalk virus infection and disease is associated with ABO histo-blood group type. The Journal of infectious diseases **185:**1335-1337.
107. **Hutson, A. M., R. L. Atmar, D. M. Marcus, and M. K. Estes.** 2003. Norwalk virus-like particle hemagglutination by binding to h histo-blood group antigens. Journal of virology **77:**405-415.
108. **Hwang, E. S., B. A. Hirayama, and E. M. Wright.** 1991. Distribution of the SGLT1 Na+/glucose cotransporter and mRNA along the crypt-villus axis of rabbit small intestine. Biochemical and biophysical research communications **181:**1208-1217.
109. **Hwang, S., Nicole S. Maloney, Monique W. Bruinsma, G. Goel, E. Duan, L. Zhang, B. Shrestha, Michael S. Diamond, A. Dani, Stanislav V. Sosnovtsev, Kim Y. Green, C. Lopez-Otin, Ramnik J. Xavier, Larissa B. Thackray, and Herbert W. Virgin.** 2012. Nondegradative Role of Atg5-Atg12/ Atg16L1 Autophagy Protein Complex in Antiviral Activity of Interferon Gamma. Cell host & microbe **11:**397-409.
110. **Hyde, J. L., S. V. Sosnovtsev, K. Y. Green, C. Wobus, H. W. Virgin, and J. M. Mackenzie.** 2009. Mouse norovirus replication is associated with virus-induced

vesicle clusters originating from membranes derived from the secretory pathway. Journal of virology **83:**9709-9719.
111. **Isberg, R. R., and J. M. Leong.** 1990. Multiple beta 1 chain integrins are receptors for invasin, a protein that promotes bacterial penetration into mammalian cells. Cell **60:**861-871.
112. **Isberg, R. R., D. L. Voorhis, and S. Falkow.** 1987. Identification of invasin: a protein that allows enteric bacteria to penetrate cultured mammalian cells. Cell **50:**769-778.
113. **Iwasaki, A., and B. L. Kelsall.** 2000. Localization of distinct Peyer's patch dendritic cell subsets and their recruitment by chemokines macrophage inflammatory protein (MIP)-3alpha, MIP-3beta, and secondary lymphoid organ chemokine. The Journal of experimental medicine **191:**1381-1394.
114. **Jepson, M. A., M. A. Clark, N. L. Simmons, and B. H. Hirst.** 1993. Epithelial M cells in the rabbit caecal lymphoid patch display distinctive surface characteristics. Histochemistry **100:**441-447.
115. **Jiang, X., M. Wang, K. Wang, and M. K. Estes.** 1993. Sequence and genomic organization of Norwalk virus. Virology **195:**51-61.
116. **Johnson, P. C., J. J. Mathewson, H. L. DuPont, and H. B. Greenberg.** 1990. Multiple-challenge study of host susceptibility to Norwalk gastroenteritis in US adults. The Journal of infectious diseases **161:**18-21.
117. **Jones, B. D., N. Ghori, and S. Falkow.** 1994. Salmonella typhimurium initiates murine infection by penetrating and destroying the specialized epithelial M cells of the Peyer's patches. The Journal of experimental medicine **180:**15-23.
118. **Kapikian, A. Z., R. G. Wyatt, R. Dolin, T. S. Thornhill, A. R. Kalica, and R. M. Chanock.** 1972. Visualization by immune electron microscopy of a 27-nm particle associated with acute infectious nonbacterial gastroenteritis. Journal of virology **10:**1075–1081.
119. **Karst, S. M.** 2010. Pathogenesis of Noroviruses, Emerging RNA Viruses. Viruses **2:**748-781.
120. **Karst, S. M., C. E. Wobus, M. Lay, J. Davidson, and H. W. Virgin.** 2003. STAT1-dependent innate immunity to a Norwalk-like virus. Science (New York, N.Y **299:**1575-1578.
121. **Katayama, K., H. Shirato-Horikoshi, S. Kojima, T. Kageyama, T. Oka, F. Hoshino, S. Fukushi, M. Shinohara, K. Uchida, Y. Suzuki, T. Gojobori, and N. Takeda.** 2002. Phylogenetic analysis of the complete genome of 18 Norwalk-like viruses. Virology **299:**225-239.
122. **Katpally, U., N. R. Voss, T. Cavazza, S. Taube, J. R. Rubin, V. L. Young, J. Stuckey, V. K. Ward, H. W. t. Virgin, C. E. Wobus, and T. J. Smith.** 2010. High-resolution cryo-electron microscopy structures of murine norovirus 1 and rabbit hemorrhagic disease virus reveal marked flexibility in the receptor binding domains. Journal of virology **84:**5836-5841.
123. **Kelsall, B. L., and W. Strober.** 1996. Distinct populations of dendritic cells are present in the subepithelial dome and T cell regions of the murine Peyer's patch. The Journal of experimental medicine **183:**237-247.
124. **Khamrin, P., T. A. Nguyen, T. G. Phan, K. Satou, Y. Masuoka, S. Okitsu, N. Maneekarn, O. Nishio, and H. Ushijima.** 2008. Evaluation of

immunochromatography and commercial enzyme-linked immunosorbent assay for rapid detection of norovirus antigen in stool samples. Journal of virological methods **147:**360-363.

125. **Kim, J. R., S. H. Seok, D. J. Kim, M.-W. Baek, Y.-R. Na, J.-H. Han, T.-H. Kim, J.-H. Park, P. V. Turner, D. H. Chung, and B.-C. Kang.** 2011. Prevalence of Murine Norovirus Infection in Korean Laboratory Animal Facilities. The Journal of Veterinary Medical Science **73:**687-691.
126. **Kirkegaard, K.** 2009. Subversion of the cellular autophagy pathway by viruses. Current topics in microbiology and immunology **335:**323-333.
127. **Kitajima, M., T. Oka, Y. Tohya, H. Katayama, N. Takeda, and K. Katayama.** 2009. Development of a broadly reactive nested reverse transcription-PCR assay to detect murine noroviruses, and investigation of the prevalence of murine noroviruses in laboratory mice in Japan. Microbiol Immunol **53:**531-534.
128. **Knoop, K. A., M. J. Miller, and R. D. Newberry.** 2013. Transepithelial antigen delivery in the small intestine: different paths, different outcomes. Current opinion in gastroenterology **29:**112-118.
129. **Kohbata, S., H. Yokoyama, and E. Yabuuchi.** 1986. Cytopathogenic effect of Salmonella typhi GIFU 10007 on M cells of murine ileal Peyer's patches in ligated ileal loops: an ultrastructural study. Microbiol Immunol **30:**1225-1237.
130. **Kraehenbuhl, J. P., and M. R. Neutra.** 2000. Epithelial M cells: differentiation and function. Annu Rev Cell Dev Biol **16:**301-332.
131. **Lay, M. K., R. L. Atmar, S. Guix, U. Bharadwaj, H. He, F. H. Neill, K. J. Sastry, Q. Yao, and M. K. Estes.** 2010. Norwalk virus does not replicate in human macrophages or dendritic cells derived from the peripheral blood of susceptible humans. Virology **406:**1-11.
132. **Leitch, G. J.** 1988. Cholera enterotoxin-induced mucus secretion and increase in the mucus blanket of the rabbit ileum in vivo. Infection and immunity **56:**2871-2875.
133. **Lelouard, H., H. Reggio, P. Mangeat, M. Neutra, and P. Montcourrier.** 1999. Mucin-related epitopes distinguish M cells and enterocytes in rabbit appendix and Peyer's patches. Infection and immunity **67:**357-367.
134. **Lencioni, K. C., A. Seamons, P. M. Treuting, L. Maggio-Price, and T. Brabb.** 2008. Murine norovirus: an intercurrent variable in a mouse model of bacteria-induced inflammatory bowel disease. Comparative medicine **58:**522-533.
135. **Li, D., and R. J. Mrsny.** 2000. Oncogenic Raf-1 disrupts epithelial tight junctions via downregulation of occludin. The Journal of cell biology **148:**791-800.
136. **Lim, J. S., H. S. Na, H. C. Lee, H. E. Choy, S. C. Park, J. M. Han, and K. A. Cho.** 2009. Caveolae-mediated entry of Salmonella typhimurium in a human M-cell model. Biochemical and biophysical research communications **390:**1322-1327.
137. **Lindesmith, L., C. Moe, S. Marionneau, N. Ruvoen, X. Jiang, L. Lindblad, P. Stewart, J. LePendu, and R. Baric.** 2003. Human susceptibility and resistance to Norwalk virus infection. Nature medicine **9:**548-553.
138. **Love, D. N., and M. Sabine.** 1975. Electron microscopic observation of feline kidney cells infected with a feline calicivirus. Archives of virology **48:**213-228.

139. **MacPherson, G. G., and L. M. Liu.** 1999. Dendritic cells and Langerhans cells in the uptake of mucosal antigens. Current topics in microbiology and immunology **236:**33-53.
140. **Madara, J. L.** 1990. Maintenance of the macromolecular barrier at cell extrusion sites in intestinal epithelium: physiological rearrangement of tight junctions. The Journal of membrane biology **116:**177-184.
141. **Madara, J. L., J. Stafford, D. Barenberg, and S. Carlson.** 1988. Functional coupling of tight junctions and microfilaments in T84 monolayers. The American journal of physiology **254:**G416-423.
142. **Mantis, N. J., M. C. Cheung, K. R. Chintalacharuvu, J. Rey, B. Corthesy, and M. R. Neutra.** 2002. Selective adherence of IgA to murine Peyer's patch M cells: evidence for a novel IgA receptor. J Immunol **169:**1844-1851.
143. **Mantis, N. J., A. Frey, and M. R. Neutra.** 2000. Accessibility of glycolipid and oligosaccharide epitopes on rabbit villus and follicle-associated epithelium. Am J Physiol Gastrointest Liver Physiol **278:**G915-923.
144. **Marionneau, S., N. Ruvoen, B. Le Moullac-Vaidye, M. Clement, A. Cailleau-Thomas, G. Ruiz-Palacois, P. Huang, X. Jiang, and J. Le Pendu.** 2002. Norwalk virus binds to histo-blood group antigens present on gastroduodenal epithelial cells of secretor individuals. Gastroenterology **122:**1967-1977.
145. **Marra, A., and R. R. Isberg.** 1997. Invasin-dependent and invasin-independent pathways for translocation of Yersinia pseudotuberculosis across the Peyer's patch intestinal epithelium. Infection and immunity **65:**3412-3421.
146. **Marsh, M., and A. Helenius.** 2006. Virus entry: open sesame. Cell **124:**729-740.
147. **Martella, V., Campolo, M., Lorusso, E., Cavicchio, P., Camero, M., Bellacicco, A. L., Decaro, N., Elia, G., Greco, G., Corrente, M., Desario, C., Arista S., Banyai, K., Koopmans, M., Buonavoglia, C.** 2007. Norovirus in captive lion (Panthera leo). Emerging infectious diseases **13:**1071-1073.
148. **Martella, V., N. Decaro, E. Lorusso, A. Radogna, P. Moschidou, F. Amorisco, M. S. Lucente, C. Desario, V. Mari, G. Elia, K. Banyai, L. E. Carmichael, and C. Buonavoglia.** 2009. Genetic heterogeneity and recombination in canine noroviruses. Journal of virology **83:**11391-11396.
149. **Martella, V., E. Lorusso, N. Decaro, G. Elia, A. Radogna, M. D'Abramo, C. Desario, A. Cavalli, M. Corrente, M. Camero, C. A. Germinario, K. Banyai, B. Di Martino, F. Marsilio, L. E. Carmichael, and C. Buonavoglia.** 2008. Detection and molecular characterization of a canine norovirus. Emerging infectious diseases **14:**1306-1308.
150. **Martin-Latil, S., N. F. Gnädig, A. Mallet, M. Desdouits, F. Guivel-Benhassine, P. Jeannin, M.-C. Prevost, O. Schwartz, A. Gessain, S. Ozden, and P.-E. Ceccaldi.** 2012. Transcytosis of HTLV-1 across a tight human epithelial barrier and infection of subepithelial dendritic cells. Blood **120:**572-580.
151. **Masurier, C., B. Salomon, N. Guettari, C. Pioche, F. Lachapelle, M. Guigon, and D. Klatzmann.** 1998. Dendritic cells route human immunodeficiency virus to lymph nodes after vaginal or intravenous administration to mice. Journal of virology **72:**7822-7829.

152. **Mattison, K., A. Shukla, A. Cook, F. Pollari, R. Friendship, D. Kelton, S. Bidawid, and J. M. Farber.** 2007. Human noroviruses in swine and cattle. Emerging infectious diseases **13:**1184-1188.
153. **Maury, J., C. Nicoletti, L. Guzzo-Chambraud, and S. Maroux.** 1995. The filamentous brush border glycocalyx, a mucin-like marker of enterocyte hyper-polarization. Eur J Biochem **228:**323-331.
154. **McCartney, S. A., L. B. Thackray, L. Gitlin, S. Gilfillan, H. W. Virgin IV, and M. Colonna.** 2008. MDA-5 recognition of a murine norovirus. PLoS pathogens **4:**e1000108.
155. **McDole, J. R., L. W. Wheeler, K. G. McDonald, B. Wang, V. Konjufca, K. A. Knoop, R. D. Newberry, and M. J. Miller.** 2012. Goblet cells deliver luminal antigen to CD103+ dendritic cells in the small intestine. Nature **483:**345-349.
156. **McFadden, N., D. Bailey, G. Carrara, A. Benson, Y. Chaudhry, A. Shortland, J. Heeney, F. Yarovinsky, P. Simmonds, A. Macdonald, and I. Goodfellow.** 2011. Norovirus regulation of the innate immune response and apoptosis occurs via the product of the alternative open reading frame 4. PLoS pathogens **7:**e1002413.
157. **Merzel, J., and C. P. Leblond.** 1969. Origin and renewal of goblet cells in the epithelium of the mouse small intestine. The American journal of anatomy **124:**281-305.
158. **Mesquita, J. R., L. Barclay, M. S. Nascimento, and J. Vinje.** 2010. Novel norovirus in dogs with diarrhea. Emerging infectious diseases **16:**980-982.
159. **Mesquita, J. R., and M. S. Nascimento.** 2012. Gastroenteritis outbreak associated with faecal shedding of canine norovirus in a Portuguese kennel following introduction of imported dogs from Russia. Transboundary and emerging diseases **59:**456-459.
160. **Mesquita, J. R., and M. S. Nascimento.** 2012. Molecular epidemiology of canine norovirus in dogs from Portugal, 2007-2011. BMC veterinary research **8:**107.
161. **Miller, S. I.** 1991. PhoP/PhoQ: macrophage-specific modulators of Salmonella virulence? Mol Microbiol **5:**2073-2078.
162. **Mills, S. D., A. Boland, M. P. Sory, P. van der Smissen, C. Kerbourch, B. B. Finlay, and G. R. Cornelis.** 1997. Yersinia enterocolitica induces apoptosis in macrophages by a process requiring functional type III secretion and translocation mechanisms and involving YopP, presumably acting as an effector protein. Proceedings of the National Academy of Sciences of the United States of America **94:**12638-12643.
163. **Milman, G., and O. Sharma.** 1994. Mechanisms of HIV/SIV mucosal transmission. AIDS Res Hum Retroviruses **10:**1305-1312.
164. **Momotani, E., D. L. Whipple, A. B. Thiermann, and N. F. Cheville.** 1988. Role of M cells and macrophages in the entrance of Mycobacterium paratuberculosis into domes of ileal Peyer's patches in calves. Veterinary pathology **25:**131-137.
165. **Monack, D. M., J. Mecsas, N. Ghori, and S. Falkow.** 1997. Yersinia signals macrophages to undergo apoptosis and YopJ is necessary for this cell death. Proceedings of the National Academy of Sciences of the United States of America **94:**10385-10390.

166. **Moon, H. W., S. C. Whipp, and A. L. Baetz.** 1971. Comparative effects of enterotoxins from Escherichia coli and Vibrio cholerae on rabbit and swine small intestine. Laboratory investigation; a journal of technical methods and pathology **25:**133-140.
167. **Morin, M. J., A. Warner, and B. N. Fields.** 1994. A pathway for entry of reoviruses into the host through M cells of the respiratory tract. The Journal of experimental medicine **180:**1523-1527.
168. **Mostov, K. E.** 1994. Transepithelial transport of immunoglobulins. Annu Rev Immunol **12:**63-84.
169. **Mouchtouri, V. A.** 2010. State of the art: public health and passenger ships. International maritime health **61:**49-98.
170. **Mounier, J., T. Vasselon, R. Hellio, M. Lesourd, and P. J. Sansonetti.** 1992. Shigella flexneri enters human colonic Caco-2 epithelial cells through the basolateral pole. Infection and immunity **60:**237-248.
171. **Mouricout, M. A., and R. A. Julien.** 1987. Pilus-mediated binding of bovine enterotoxigenic Escherichia coli to calf small intestinal mucins. Infection and immunity **55:**1216-1223.
172. **Mumphrey, S. M., H. Changotra, T. N. Moore, E. R. Heimann-Nichols, C. E. Wobus, M. J. Reilly, M. Moghadamfalahi, D. Shukla, and S. M. Karst.** 2007. Murine norovirus 1 infection is associated with histopathological changes in immunocompetent hosts, but clinical disease is prevented by STAT1-dependent interferon responses. Journal of virology **81:**3251-3263.
173. **Murata, T., N. Katsushima, K. Mizuta, Y. Muraki, S. Hongo, and Y. Matsuzaki.** 2007. Prolonged norovirus shedding in infants <or=6 months of age with gastroenteritis. The Pediatric infectious disease journal **26:**46-49.
174. **Nesbitt, S. A., and M. A. Horton.** 1997. Trafficking of matrix collagens through bone-resorbing osteoclasts. Science (New York, N.Y **276:**266-269.
175. **Neutra, M. R., A. Frey, and J. P. Kraehenbuhl.** 1996. Epithelial M cells: gateways for mucosal infection and immunization. Cell **86:**345-348.
176. **Neutra, M. R., N. J. Mantis, A. Frey, and P. J. Giannasca.** 1999. The composition and function of M cell apical membranes: implications for microbial pathogenesis. Seminars in immunology **11:**171-181.
177. **Neutra, M. R., P. Sansonetti, and J.P. Kraehenbuhl.** 2003. Role of intestinal M cells in microbial pathogenesis, p. 23-42. *In* G. A. Hecht (ed.), Microbial Pathogenesis and the Intestinal Epithelial Cell. ASM Press, Washington, DC.
178. **Neutra, M. R., T. L. Phillips, E. L. Mayer, and D. J. Fishkind.** 1987. Transport of membrane-bound macromolecules by M cells in follicle-associated epithelium of rabbit Peyer's patch. Cell and tissue research **247:**537-546.
179. **Nibert, M. L.** 1998. Structure of mammalian orthoreovirus particles. Current topics in microbiology and immunology **233:**1-30.
180. **Nusrat, A., J. A. Chen, C. S. Foley, T. W. Liang, J. Tom, M. Cromwell, C. Quan, and R. J. Mrsny.** 2000. The coiled-coil domain of occludin can act to organize structural and functional elements of the epithelial tight junction. The Journal of biological chemistry **275:**29816-29822.
181. **O'Leary, A. D., and E. C. Sweeney.** 1986. Lymphoglandular complexes of the colon: structure and distribution. Histopathology **10:**267-283.

182. **Ogra, P. L., and D. T. Karzon.** 1969. Distribution of poliovirus antibody in serum, nasopharynx and alimentary tract following segmental immunization of lower alimentary tract with poliovaccine. J Immunol **102:**1423-1430.
183. **Owen, D. J., and J. P. Luzio.** 2000. Structural insights into clathrin-mediated endocytosis. Current opinion in cell biology **12:**467-474.
184. **Owen, R. L.** 1999. Uptake and transport of intestinal macromolecules and microorganisms by M cells in Peyer's patches--a personal and historical perspective. Seminars in immunology **11:**157-163.
185. **Owen, R. L., and D. K. Bhalla.** 1983. Cytochemical analysis of alkaline phosphatase and esterase activities and of lectin-binding and anionic sites in rat and mouse Peyer's patch M cells. The American journal of anatomy **168:**199-212.
186. **Owen, R. L., D. M. Bass, and A. J. Piazza.** 1990. Colonic lymphoid patches. A portal of entry in mice for type I reovirus administered anally. Gastroenterology **98:**A468.
187. **Owen, R. L., A. J. Piazza, and T. H. Ermak.** 1991. Ultrastructural and cytoarchitectural features of lymphoreticular organs in the colon and rectum of adult BALB/c mice. The American journal of anatomy **190:**10-18.
188. **Owen, R. L., N. F. Pierce, R. T. Apple, and W. C. Cray, Jr.** 1986. M cell transport of Vibrio cholerae from the intestinal lumen into Peyer's patches: a mechanism for antigen sampling and for microbial transepithelial migration. The Journal of infectious diseases **153:**1108-1118.
189. **Paerregaard, A., F. Espersen, O. M. Jensen, and M. Skurnik.** 1991. Interactions between Yersinia enterocolitica and rabbit ileal mucus: growth, adhesion, penetration, and subsequent changes in surface hydrophobicity and ability to adhere to ileal brush border membrane vesicles. Infection and immunity **59:**253-260.
190. **Pappo, J., and T. H. Ermak.** 1989. Uptake and translocation of fluorescent latex particles by rabbit Peyer's patch follicle epithelium: a quantitative model for M cell uptake. Clin Exp Immunol **76:**144-148.
191. **Pappo, J., and R. L. Owen.** 1988. Absence of secretory component expression by epithelial cells overlying rabbit gut-associated lymphoid tissue. Gastroenterology **95:**1173-1177.
192. **Pepe, J. C., and V. L. Miller.** 1993. Yersinia enterocolitica invasin: a primary role in the initiation of infection. Proceedings of the National Academy of Sciences of the United States of America **90:**6473-6477.
193. **Perdomo, O. J., J. M. Cavaillon, M. Huerre, H. Ohayon, P. Gounon, and P. J. Sansonetti.** 1994. Acute inflammation causes epithelial invasion and mucosal destruction in experimental shigellosis. The Journal of experimental medicine **180:**1307-1319.
194. **Perry, J. W., S. Taube, and C. E. Wobus.** 2009. Murine norovirus-1 entry into permissive macrophages and dendritic cells is pH-independent. Virus research **143:**125-129.
195. **Perry, J. W., Taube, S., Wobus, C. E.** 2009. Murine Norovirus-1 entry into permissive macrophages and dendritic cells is pH-independent Virus research **143:**125-129.

196. **Perry, J. W., and C. E. Wobus.** 2010. Endocytosis of murine norovirus 1 into murine macrophages is dependent on dynamin II and cholesterol. Journal of virology **84:**6163-6176.
197. **Pettersson, R. F., V. Ambros, and D. Baltimore.** 1978. Identification of a protein linked to nascent poliovirus RNA and to the polyuridylic acid of negative-strand RNA. Journal of virology **27:**357-365.
198. **Phalipon, A., and P. J. Sansonetti.** 2003. Shigellosis: innate mechanisms of inflammatory destruction of the intestinal epithelium, adaptive immune response, and vaccine development. Crit Rev Immunol **23:**371-401.
199. **Powell, D. W.** 1981. Barrier function of epithelia. The American journal of physiology **241:**G275-288.
200. **Pron, B., C. Boumaila, F. Jaubert, P. Berche, G. Milon, F. Geissmann, and J. L. Gaillard.** 2001. Dendritic cells are early cellular targets of Listeria monocytogenes after intestinal delivery and are involved in bacterial spread in the host. Cellular microbiology **3:**331-340.
201. **Racaniello, V. R., and R. Ren.** 1996. Poliovirus biology and pathogenesis. Current topics in microbiology and immunology **206:**305-325.
202. **Rademacher, C., J. Guiard, P. I. Kitov, B. Fiege, K. P. Dalton, F. Parra, D. R. Bundle, and T. Peters.** 2011. Targeting norovirus infection-multivalent entry inhibitor design based on NMR experiments. Chemistry **17:**7442-7453.
203. **Rahner, C., L. L. Mitic, and J. M. Anderson.** 2001. Heterogeneity in expression and subcellular localization of claudins 2, 3, 4, and 5 in the rat liver, pancreas, and gut. Gastroenterology **120:**411-422.
204. **Raupach, B., J. Mecsas, U. Heczko, S. Falkow, and B. B. Finlay.** 1999. Bacterial epithelial cell cross talk. Current topics in microbiology and immunology **236:**137-161.
205. **Rescigno, M., M. Urbano, B. Valzasina, M. Francolini, G. Rotta, R. Bonasio, F. Granucci, J. P. Kraehenbuhl, and P. Ricciardi-Castagnoli.** 2001. Dendritic cells express tight junction proteins and penetrate gut epithelial monolayers to sample bacteria. Nature immunology **2:**361-367.
206. **Rissoan, M. C., V. Soumelis, N. Kadowaki, G. Grouard, F. Briere, R. de Waal Malefyt, and Y. J. Liu.** 1999. Reciprocal control of T helper cell and dendritic cell differentiation. Science (New York, N.Y **283:**1183-1186.
207. **Rockx, B. H., M. de Wit, H. Vennema, J. Vinje, E. De Bruin, v. D. Y., and M. Koopmans.** 2002. Natural History of Human Calicivirus Infection: A Prospective Cohort Study. Clin Infect Dis **35:**246-253.
208. **Rosenblatt, J., M. C. Raff, and L. P. Cramer.** 2001. An epithelial cell destined for apoptosis signals its neighbors to extrude it by an actin- and myosin-dependent mechanism. Curr Biol **11:**1847-1857.
209. **Roy, M. J., and M. Varvayanis.** 1987. Development of dome epithelium in gut-associated lymphoid tissues: association of IgA with M cells. Cell and tissue research **248:**645-651.
210. **Ruckdeschel, K., A. Roggenkamp, V. Lafont, P. Mangeat, J. Heesemann, and B. Rouot.** 1997. Interaction of Yersinia enterocolitica with macrophages leads to macrophage cell death through apoptosis. Infection and immunity **65:**4813-4821.

211. **Rydell, G. E., J. Nilsson, J. Rodriguez-Diaz, N. Ruvoen-Clouet, L. Svensson, J. Le Pendu, and G. Larson.** 2009. Human noroviruses recognize sialyl Lewis x neoglycoprotein. Glycobiology **19:**309-320.
212. **Rydell, G. E., L. Svensson, G. Larson, L. Johannes, and W. Romer.** 2013. Human GII.4 norovirus VLP induces membrane invaginations on giant unilamellar vesicles containing secretor gene dependent alpha1,2-fucosylated glycosphingolipids. Biochimica et biophysica acta **1828:**1840-1845.
213. **Salo, J., P. Lehenkari, M. Mulari, K. Metsikko, and H. K. Vaananen.** 1997. Removal of osteoclast bone resorption products by transcytosis. Science (New York, N.Y **276:**270-273.
214. **Sansonetti, P. J.** 1991. Genetic and molecular basis of epithelial cell invasion by Shigella species. Reviews of infectious diseases **13 Suppl 4:**S285-292.
215. **Sansonetti, P. J., J. Arondel, J. R. Cantey, M. C. Prevost, and M. Huerre.** 1996. Infection of rabbit Peyer's patches by Shigella flexneri: effect of adhesive or invasive bacterial phenotypes on follicle-associated epithelium. Infection and immunity **64:**2752-2764.
216. **Sansonetti, P. J., J. Mounier, M. C. Prevost, and R. M. Mege.** 1994. Cadherin expression is required for the spread of Shigella flexneri between epithelial cells. Cell **76:**829-839.
217. **Sansonetti, P. J., and A. Phalipon.** 1999. M cells as ports of entry for enteroinvasive pathogens: mechanisms of interaction, consequences for the disease process. Seminars in immunology **11:**193-203.
218. **Sansonetti, P. J., A. Phalipon, J. Arondel, K. Thirumalai, S. Banerjee, S. Akira, K. Takeda, and A. Zychlinsky.** 2000. Caspase-1 activation of IL-1beta and IL-18 are essential for Shigella flexneri-induced inflammation. Immunity **12:**581-590.
219. **Savidge, T. C., and M. W. Smith.** 1995. Evidence that membranous (M) cell genesis is immuno-regulated. Advances in experimental medicine and biology **371A:**239-241.
220. **Savill, J., I. Dransfield, C. Gregory, and C. Haslett.** 2002. A blast from the past: clearance of apoptotic cells regulates immune responses. Nat Rev Immunol **2:**965-975.
221. **Scallan, E., R. M. Hoekstra, F. J. Angulo, R. V. Tauxe, W. M-A., S. L. Roy, J. L. Jones, and P. M. Griffin.** 2011. Foodborne illness acquired in the United States - major pathogens. Emerging infectious diseases **17:**7-15.
222. **Schaerer, E., M. R. Neutra, and J. P. Kraehenbuhl.** 1991. Molecular and cellular mechanisms involved in transepithelial transport. The Journal of membrane biology **123:**93-103.
223. **Schulte, R., S. Kerneis, S. Klinke, H. Bartels, S. Preger, J. P. Kraehenbuhl, E. Pringault, and I. B. Autenrieth.** 2000. Translocation of Yersinia entrocolitica across reconstituted intestinal epithelial monolayers is triggered by Yersinia invasin binding to beta1 integrins apically expressed on M-like cells. Cellular microbiology **2:**173-185.
224. **Scipioni, A., I. Bourgot, A. Mauroy, D. Ziant, C. Saegerman, G. Daube, and E. Thiry.** 2008. Detection and quantification of human and bovine noroviruses by

a TaqMan RT-PCR assay with a control for inhibition. Molecular and Cellular Probes **22:**215-222.

225. **Selsted, A. J. O. a. M. E.** 2003. Antimicrobial peptide effectors of small intestinal innate immunity, p. 191-221. *In* G. A. Hecht (ed.), Microbial Pathogenesis and the Intestinal Epithelial Cell. ASM Press, Washington, DC.
226. **Shanker, S., J. M. Choi, B. Sankaran, R. L. Atmar, M. K. Estes, and B. V. Prasad.** 2011. Structural analysis of histo-blood group antigen binding specificity in a norovirus GII.4 epidemic variant: implications for epochal evolution. Journal of virology **85:**8635-8645.
227. **Sharma, R., E. J. van Damme, W. J. Peumans, P. Sarsfield, and U. Schumacher.** 1996. Lectin binding reveals divergent carbohydrate expression in human and mouse Peyer's patches. Histochemistry and cell biology **105:**459-465.
228. **Shirato-Horikoshi, H., S. Ogawa, T. Wakita, N. Takeda, and G. S. Hansman.** 2007. Binding activity of norovirus and sapovirus to histo-blood group antigens. Archives of virology **152:**457-461.
229. **Shirato, H.** 2011. Norovirus and histo-blood group antigens. Japanese journal of infectious diseases **64:**95-103.
230. **Shirato, H., S. Ogawa, H. Ito, T. Sato, A. Kameyama, H. Narimatsu, Z. Xiaofan, T. Miyamura, T. Wakita, K. Ishii, and N. Takeda.** 2008. Noroviruses distinguish between type 1 and type 2 histo-blood group antigens for binding. Journal of virology.
231. **Shreedhar, V. K., B. L. Kelsall, and M. R. Neutra.** 2003. Cholera toxin induces migration of dendritic cells from the subepithelial dome region to T- and B-cell areas of Peyer's patches. Infection and immunity **71:**504-509.
232. **Sicinski, P., J. Rowinski, J. B. Warchol, Z. Jarzabek, W. Gut, B. Szczygiel, K. Bielecki, and G. Koch.** 1990. Poliovirus type 1 enters the human host through intestinal M cells. Gastroenterology **98:**56-58.
233. **Siebenga, J. J., M. F. Beersma, H. Vennema, P. van Biezen, N. J. Hartwig, and M. Koopmans.** 2008. High Prevalence of Prolonged Norovirus Shedding and Illness among Hospitalized Patients: A Model for In Vivo Molecular Evolution. The Journal of infectious diseases **198:**994-1001.
234. **Simon, D. B., Y. Lu, K. A. Choate, H. Velazquez, E. Al-Sabban, M. Praga, G. Casari, A. Bettinelli, G. Colussi, J. Rodriguez-Soriano, D. McCredie, D. Milford, S. Sanjad, and R. P. Lifton.** 1999. Paracellin-1, a renal tight junction protein required for paracellular Mg2+ resorption. Science (New York, N.Y **285:**103-106.
235. **Simonovic, I., J. Rosenberg, A. Koutsouris, and G. Hecht.** 2000. Enteropathogenic Escherichia coli dephosphorylates and dissociates occludin from intestinal epithelial tight junctions. Cellular microbiology **2:**305-315.
236. **Sirard, J. C., F. Niedergang, and J. P. Kraehenbuhl.** 1999. Live attenuated Salmonella: a paradigm of mucosal vaccines. Immunological reviews **171:**5-26.
237. **Smiley, J. R., A. E. Hoet, M. Tråvén, H. Tsunemitsu, and L. J. Saif.** 2003. Reverse Transcription-PCR Assays for Detection of Bovine Enteric Caliciviruses (BEC) and Analysis of the Genetic Relationships among BEC and Human Caliciviruses. Journal of clinical microbiology **41:**3089-3099.

238. **Sosnovtsev, S. V., G. Belliot, K. O. Chang, V. G. Prikhodko, L. B. Thackray, C. E. Wobus, S. M. Karst, H. W. Virgin, and K. Y. Green.** 2006. Cleavage map and proteolytic processing of the murine norovirus nonstructural polyprotein in infected cells. Journal of virology **80:**7816-7831.
239. **Souza, M., M. S. Azevedo, K. Jung, S. Cheetham, and L. J. Saif.** 2008. Pathogenesis and immune responses in gnotobiotic calves after infection with the genogroup II.4-HS66 strain of human norovirus. Journal of virology **82:**1777-1786.
240. **Staehelin, L. A., T. M. Mukherjee, and A. W. Williams.** 1969. Freeze-etch appearance of the tight junctions in the epithelium of small and large intestine of mice. Protoplasma **67:**165-184.
241. **Stax, M. J., T. van Montfort, R. R. Sprenger, M. Melchers, R. W. Sanders, E. van Leeuwen, S. Repping, G. Pollakis, D. Speijer, and W. A. Paxton.** 2009. Mucin 6 in seminal plasma binds DC-SIGN and potently blocks dendritic cell mediated transfer of HIV-1 to CD4+ T-lymphocytes. Virology **391:**203-211.
242. **Strasser, A., L. O'Connor, and V. M. Dixit.** 2000. APOPTOSIS SIGNALING. Annual review of biochemistry **69:**217-245.
243. **Takeuchi, A.** 1967. Electron microscope studies of experimental Salmonella infection. I. Penetration into the intestinal epithelium by Salmonella typhimurium. Am J Pathol **50:**109-136.
244. **Tamura, M., K. Natori, M. Kobayashi, T. Miyamura, and N. Takeda.** 2004. Genogroup II noroviruses efficiently bind to heparan sulfate proteoglycan associated with the cellular membrane. Journal of virology **78:**3817-3826.
245. **Tan, M., and X. Jiang.** 2010. Virus-Host Interaction and Cellular Receptors of Caliciviruses, p. 111-130. *In* G. S. Hansman, X. J. Jiang, and K. Y. Green (ed.), Caliciviruses: Molecular and Cellular Virology. Caister Academic Press, Norfolk, UK.
246. **Tan, M., P. Fang, T. Chachiyo, M. Xia, P. Huang, Z. Fang, W. Jiang, and X. Jiang.** 2008. Noroviral P particle: structure, function and applications in virus-host interaction. Virology **382:**115-123.
247. **Tan, M., R. S. Hegde, and X. Jiang.** 2004. The P domain of norovirus capsid protein forms dimer and binds to histo-blood group antigen receptors. Journal of virology **78:**6233-6242.
248. **Tan, M., R. S. Hegde, and X. Jiang.** 2004. The P Domain of Norovirus Capsid Protein Forms Dimer and Binds to Histo-Blood Group Antigen Receptors. Journal of virology **78:**6233-6242.
249. **Tan, M., P. Huang, J. Meller, W. Zhong, T. Farkas, and X. Jiang.** 2003. Mutations within the P2 domain of norovirus capsid affect binding to human histo-blood group antigens: evidence for a binding pocket. Journal of virology **77:**12562-12571.
250. **Tan, M., and X. Jiang.** 2005. Norovirus and its histo-blood group antigen receptors: an answer to a historical puzzle. Trends in microbiology **13:**285-293.
251. **Tan, M., and X. Jiang.** 2005. The p domain of norovirus capsid protein forms a subviral particle that binds to histo-blood group antigen receptors. Journal of virology **79:**14017-14030.

252. **Tatsuo, F., and Y. Katsushi.** 1980. The α-naphthoxyacetic acid-elicited retching involves dopaminergic inhibition in mice. Pharmacology Biochemistry and Behavior **12:**735-738.
253. **Taube, S., A. O. Kolawole, M. Hohne, J. E. Wilkinson, S. A. Handley, J. W. Perry, L. B. Thackray, R. Akkina, and C. E. Wobus.** 2013. A mouse model for human norovirus. MBio **4**.
254. **Taube, S., J. W. Perry, E. McGreevy, K. Yetming, C. Perkins, K. Henderson, and C. E. Wobus.** 2012. Murine Noroviruses (MNV) bind glycolipid and glycoprotein attachment receptors in a strain- dependent manner. Journal of virology **doi:10.1128/JVI.06854-11**.
255. **Taube, S., J. W. Perry, K. Yetming, S. P. Patel, H. Auble, L. Shu, H. F. Nawar, C. H. Lee, T. D. Connell, J. A. Shayman, and C. E. Wobus.** 2009. Ganglioside-linked terminal sialic acid moieties on murine macrophages function as attachment receptors for Murine Noroviruses (MNV). Journal of virology **83:**4092-4101.
256. **Taube, S., J. R. Rubin, U. Katpally, T. J. Smith, A. Kendall, J. A. Stuckey, and C. E. Wobus.** 2010. High-resolution x-ray structure and functional analysis of the murine norovirus 1 capsid protein protruding domain. Journal of virology **84:**5695-5705.
257. **Teunis, P. F., C. L. Moe, P. Liu, S. E. Miller, L. Lindesmith, R. S. Baric, J. Le Pendu, and R. L. Calderon.** 2008. Norwalk virus: how infectious is it? Journal of medical virology **80:**1468-1476.
258. **Thackray, L. B., C. E. Wobus, K. A. Chachu, B. Liu, E. R. Alegre, K. S. Henderson, S. T. Kelley, and H. W. t. Virgin.** 2007. Murine noroviruses comprising a single genogroup exhibit biological diversity despite limited sequence divergence. Journal of virology **81:**10460-10473.
259. **Tian, P., M. Brandl, and R. Mandrell.** 2005. Porcine gastric mucin binds to recombinant norovirus particles and competitively inhibits their binding to histo-blood group antigens and Caco-2 cells. Lett Appl Microbiol **41:**315-320.
260. **Tse, H., W. M. Chan, C. S. Lam, S. K. Lau, P. C. Woo, and K. Y. Yuen.** 2012. Complete genome sequences of novel rat noroviruses in Hong Kong. Journal of virology **86:**12435-12436.
261. **Turner, J. R.** 2003. Functional morphology of the intestinal mucosae: from crypts to tips, p. 1-22. *In* G. A. Hecht (ed.), Microbial Pathogenesis and the Intestinal Epithelial Cell. ASM Press, Washington, DC.
262. **Turner, J. R.** 2000. 'Putting the squeeze' on the tight junction: understanding cytoskeletal regulation. Seminars in cell & developmental biology **11:**301-308.
263. **Turner, J. R., B. K. Rill, S. L. Carlson, D. Carnes, R. Kerner, R. J. Mrsny, and J. L. Madara.** 1997. Physiological regulation of epithelial tight junctions is associated with myosin light-chain phosphorylation. The American journal of physiology **273:**C1378-1385.
264. **Tyrer, P., A. R. Foxwell, A. W. Cripps, M. A. Apicella, and J. M. Kyd.** 2006. Microbial pattern recognition receptors mediate M-cell uptake of a gram-negative bacterium. Infection and immunity **74:**625-631.
265. **Tyrer, P. C., A. Ruth Foxwell, J. M. Kyd, D. C. Otczyk, and A. W. Cripps.** 2007. Receptor mediated targeting of M-cells. Vaccine **25:**3204-3209.

266. **Van Itallie, C. M., and J. M. Anderson.** 1997. Occludin confers adhesiveness when expressed in fibroblasts. Journal of cell science **110 ( Pt 9):**1113-1121.
267. **Vazquez-Torres, A., J. Jones-Carson, A. J. Baumler, S. Falkow, R. Valdivia, W. Brown, M. Le, R. Berggren, W. T. Parks, and F. C. Fang.** 1999. Extraintestinal dissemination of Salmonella by CD18-expressing phagocytes. Nature **401:**804-808.
268. **Vimal, D. B., M. Khullar, S. Gupta, and N. K. Ganguly.** 2000. Intestinal mucins: the binding sites for Salmonella typhimurium. Mol Cell Biochem **204:**107-117.
269. **Vinjé, J., R. A. Hamidjaja, and M. D. Sobsey.** 2004. Development and application of a capsid VP1 (region D) based reverse transcription PCR assay for genotyping of genogroup I and II noroviruses. Journal of virological methods **116:**109-117.
270. **Viswanathan, V. K., and G. Hecht.** 2003. Epithelial response to enteric pathogens: activation of chloride secretory pathways, p. 267-284. *In* G. A. Hecht (ed.), Microbial Pathogenesis and the Intestinal Epithelial Cell. ASM Press, Washington, DC.
271. **Walker, R. I., E. A. Schmauder-Chock, J. L. Parker, and D. Burr.** 1988. Selective association and transport of Campylobacter jejuni through M cells of rabbit Peyer's patches. Can J Microbiol **34:**1142-1147.
272. **Wang, Q. H., M. G. Han, S. Cheetham, M. Souza, J. A. Funk, and L. J. Saif.** 2005. Porcine noroviruses related to human noroviruses. Emerging infectious diseases **11:**1874-1881.
273. **Ward, V. K., C. J. McCormick, I. N. Clarke, O. Salim, C. E. Wobus, L. B. Thackray, H. W. Virgin IV, and P. R. Lambden.** 2007. Recovery of infectious murine norovirus using pol II-driven expression of full-length cDNA. Proceedings of the National Academy of Sciences of the United States of America **104:**11050-11055.
274. **Wassef, J. S., D. F. Keren, and J. L. Mailloux.** 1989. Role of M cells in initial antigen uptake and in ulcer formation in the rabbit intestinal loop model of shigellosis. Infection and immunity **57:**858-863.
275. **White, L. J., J. M. Ball, M. E. Hardy, T. N. Tanaka, N. Kitamoto, and M. K. Estes.** 1996. Attachment and entry of recombinant Norwalk virus capsids to cultured human and animal cell lines. Journal of virology **70:**6589-6597.
276. **Widdowson, M. A., S. S. Monroe, and R. I. Glass.** 2005. Are noroviruses emerging? Emerging infectious diseases **11:**735-737.
277. **Wobus, C. E., S. M. Karst, L. B. Thackray, K. O. Chang, S. V. Sosnovtsev, G. Belliot, A. Krug, J. M. Mackenzie, K. Y. Green, and H. W. Virgin.** 2004. Replication of Norovirus in cell culture reveals a tropism for dendritic cells and macrophages. PLoS Biol **2:**e432.
278. **Wobus, C. E., L. B. Thackray, and H. W. Virgin.** 2006. Murine Norovirus: a Model System To Study Norovirus Biology and Pathogenesis. Journal of virology **80:**5104-5112.
279. **Wobus, C. E., L. B. Thackray, and H. W. t. Virgin.** 2006. Murine norovirus: a model system to study norovirus biology and pathogenesis. Journal of virology **80:**5104-5112.

280. **Wold, A. E., J. Mestecky, M. Tomana, A. Kobata, H. Ohbayashi, T. Endo, and C. S. Eden.** 1990. Secretory immunoglobulin A carries oligosaccharide receptors for Escherichia coli type 1 fimbrial lectin. Infection and immunity **58:**3073-3077.
281. **Wolf, J. L., D. H. Rubin, R. Finberg, R. S. Kauffman, A. H. Sharpe, J. S. Trier, and B. N. Fields.** 1981. Intestinal M cells: a pathway for entry of reovirus into the host. Science (New York, N.Y **212:**471-472.
282. **Wolf, S., W. Williamson, J. Hewitt, S. Lin, M. Rivera-Aban, A. Ball, P. Scholes, M. Savill, and G. E. Greening.** 2009. Molecular detection of norovirus in sheep and pigs in New Zealand farms. Veterinary microbiology **133:**184-189.
283. **Wong, V.** 1997. Phosphorylation of occludin correlates with occludin localization and function at the tight junction. The American journal of physiology **273:**C1859-1867.
284. **Wong, V., and B. M. Gumbiner.** 1997. A synthetic peptide corresponding to the extracellular domain of occludin perturbs the tight junction permeability barrier. The Journal of cell biology **136:**399-409.
285. **Woodward, A. M., J. Mauris, and P. Argueso.** 2013. Binding of transmembrane mucins to galectin-3 limits herpesvirus 1 infection of human corneal keratinocytes. Journal of virology **87:**5841-5847.
286. **Xia, M., T. Farkas, and X. Jiang.** 2007. Norovirus capsid protein expressed in yeast forms virus-like particles and stimulates systemic and mucosal immunity in mice following an oral administration of raw yeast extracts. Journal of medical virology **79:**74-83.
287. **Yokota, A., H. Takeuchi, N. Maeda, Y. Ohoka, C. Kato, S. Y. Song, and M. Iwata.** 2009. GM-CSF and IL-4 synergistically trigger dendritic cells to acquire retinoic acid-producing capacity. Int Immunol **21:**361-377.
288. **Yunus, M. A., L. M. Chung, Y. Chaudhry, D. Bailey, and I. Goodfellow.** 2010. Development of an optimized RNA-based murine norovirus reverse genetics system. Journal of virological methods **169:**112-118.
289. **Zhang, T., J. Yu, Y. Zhang, L. Li, Y. Chen, D. Li, F. Liu, C. Y. Zhang, H. Gu, and K. Zen.** 2014. Salmonella enterica serovar Enteritidis modulates intestinal epithelial miR-128 levels to decrease macrophage recruitment via M-CSF. The Journal of infectious diseases.
290. **Zheng, D., T. Ando, R. Fankhauser, R. Beard, R. Glass, and S. Monroe.** 2006. Norovirus classification and proposed strain nomenclature. Virology **346:**312-323.
291. **Zhou, F., J. P. Kraehenbuhl, and M. R. Neutra.** 1995. Mucosal IgA response to rectally administered antigen formulated in IgA-coated liposomes. Vaccine **13:**637-644.

# CHAPTER 2

## Murine Norovirus Transcytosis Across an *In Vitro* Polarized Intestinal Epithelial Cell Line is Mediated by M-like Cells

The work presented in this chapter was recently published in the Journal of Virology, Volume 87, Issue 23, pages 12685 to 12693; 2013.

### 2.1 Abstract

Noroviruses (NoVs) are the causative agent of the vast majority of non-bacterial gastroenteritis worldwide. Due to the inability to culture human NoVs, and the inability to orally infect a small animal model, little is known about the initial steps of viral entry. One particular step that is not understood is how NoVs breach the intestinal epithelial barrier. Murine NoV (MNV) is the only NoV that can be propagated *in vitro* by infecting murine macrophages and dendritic cells, making this virus an attractive model for studies of different aspects of NoV biology. Polarized murine intestinal epithelial $mIC_{cl2}$ cells were used to investigate how MNV interacts with and crosses the intestinal epithelium. In this *in vitro* model of the follicular-associated epithelium (FAE), MNV is transported across the polarized cell monolayer in the absence of viral replication or disruption of tight junctions by a distinct epithelial cell with microfold (M) cell properties. In addition to transporting MNV, these M-like cells also transcytose microbeads and express an IgA receptor. Interestingly, B myeloma cells cultured in the basolateral

compartment underlying the epithelial monolayer did not alter the number of M-like cells but increased their transcytotic activity. Our data demonstrate that MNV can cross an intact intestinal epithelial monolayer *in vitro* by hijacking the M-like cells' intrinsic transcytotic pathway and suggest a potential mechanism for MNV entry into the host.

## 2.2 Introduction

Human noroviruses (HuNoVs) are genetically diverse, environmentally stable, highly infectious viruses that infect their host via the fecal-oral route and aerosolization (16, 18). They are the causative agents of most nonbacterial infectious gastroenteritis worldwide (6, 30, 54). HuNoV infections spread rapidly and outbreaks often take place in closed or semi-closed settings where communities gather (e.g., nursing homes, schools, hospitals, restaurants and cruise ships) (3, 36, 40). Annually, HuNoVs cause an estimate of 21 million cases of acute gastroenteritis and 800 deaths in the United States alone (17, 45). Despite being a major public health concern, the inability to culture HuNoVs *in vitro* (11, 19) and lack of a small animal model for oral infection (48) has limited our progress in understanding NoV biology. Nevertheless, the discovery of the first murine-specific NoV, MNV, which is highly homologous to its human counterpart and can efficiently replicate in cell culture and in a small animal, provides the means to study NoV biology in detail (26, 55, 56).

The early events during viral infection are essential for a productive replication in the host but little is known about this step during NoV infection. Particularly, how NoVs cross the epithelial barrier to reach their susceptible target cells remains unclear. Since MNV efficiently replicates in macrophages and dendritic cells *in vitro* (55) and in mice

(26), the goal of this study was to understand how MNV interacts with the intestinal epithelium. MNV strains have high sequence similarity (> 75%), but differ in their biological phenotypes (46, 51). For example, the fecally isolated MNV strains S99 and CR3 persist in wild-type mice for at least 35 days (37, 51). In contrast, MNV-1 causes acute infections in mice, and virus is not detectable in fecal contents after 7 days post infection (dpi) (51). Persistence and colonic tropism mapped to a single amino acid residue within the non-structural protein NS1/2 (39). Further differences between virus strains are observed in culture with respect to carbohydrate interaction. MNV-1 and S99 binding to murine macrophages is dependent on terminal sialic acid residues of the ganglioside GD1a, N-linked, or O-linked glycoproteins, while CR3 binding only requires N-linked glycoproteins (49, 50). Although multiple studies have elucidated aspects of the multi-step process by which MNV enters permissive macrophages (14, 43, 44, 49, 50), how the virus crosses the intestinal epithelial barrier to reach susceptible macrophages and dendritic cells in the first place is unknown.

The intestinal tract comprises multiple types of intestinal cells including epithelial cells and microfold (M) cells. M cells are specialized epithelial cells usually associated with the follicle-associated epithelium (FAE) overlying the Peyer's patches where mucosal-associated lymphoid tissues are organized. These cells routinely sample diverse antigens along the entire mucosal surface for immune surveillance, including microorganisms and inert particles (i.e., latex beads) (9, 31, 38). Over the years, researchers have taken advantage of established *in vitro* FAE models for gaining a better understanding of the mechanisms required for enteric pathogen entry into or across the intestinal epithelium. A fraction of the *in vitro* polarized intestinal epithelial

cells acquires characteristics that resemble those of M cells (i.e., uptake of particulate antigens) and show increased uptake of fluorescently labeled polystyrene latex beads after co-culture with B cells or Peyer's patch-derived lymphocytes (2, 12, 29). Thus, pathogen interaction with M-like cells can also be studied in these polarized intestinal epithelial monolayers (2, 4, 5, 12, 29). For example, poliovirus translocates from the apical to the basolateral compartment in a temperature-dependent manner when polarized Caco-2 cell monolayers are co-cultured with Peyer's patch lymphocytes to induce M-like cells (42). Another study demonstrated that a human immunodeficiency virus 1 (HIV-1) strain tropic for the chemokine receptor CXCR4 (but not for CCR5) infects and is transported across polarized Caco-2 monolayers co-cultured with B cells in a receptor-dependent manner (13). In addition, human T-cell leukemia virus type 1 (HTLV-1) crosses polarized Caco-2 cell monolayers without disruption of tight junctions or infection of the epithelium to productively infect dendritic cells in the basolateral compartment (25).

The current study focused on the interaction of the murine enteric virus MNV with polarized murine intestinal epithelial cells ($mIC_{cl2}$) as an *in vitro* FAE model system to determine whether MNV invades and/or crosses a polarized intestinal epithelium. The $mIC_{cl2}$ cell line, when grown on permeable filters, forms polarized cells with tight junctions and conserves main features of small intestine crypt cells (2, 12). Herein, we demonstrate that MNV traffics across the polarized cell monolayer using M-like cells without replicating or disrupting tight junctions. Addition of B myeloma cells in the cultures did not alter the numbers of M-like cells but instead increased the transcytotic

activity of M-like cells. These results suggest that M cells may be a gateway for MNV invasion of the host.

### 2.3 Material and Methods

**Cell culture.** The $mIC_{cl2}$ cells were generously provided by Dr. A. Vandewalle, INSERM, Paris, France (2). Cells were maintained in 75-$cm^2$ flasks (Falcon; BD Labware) as described (2) and used from passages ~70 to 90. The Ag8.653 cell line was generously provided by Dr. S. Lundy, University of Michigan, Ann Arbor, USA, and was maintained as described (27). The murine macrophage RAW 264.7 cell line was maintained as described and used for plaque assays (55).

**Virus stocks and plaque assays.** The plaque-purified MNV-1 clone (GV/MNV1/2002/USA) MNV-1.CW3 and the fecal isolates CR3 (GV/CR3/2005/USA) and S99 (GV/S99/Berlin/2006/DE) were used at passage 6 for all experiments (37, 51). Viral titers were quantified by plaque assay after visualizing plaques by staining cells with a 0.01% neutral red solution in PBS for 1-3 h as previously described (15, 55).

**Transcytosis experiments.** $mIC_{cl2}$ cells were plated at a density of $10^6$ cells/well on a polyester membrane filter of a 12-well transwell permeable support (3 µm pore size; Costar). Cells were cultured for 10-14 days as described (2, 12) until TER was > 250 Ω x $cm^2$ using a voltohmmeter device (World Precision Instruments,FL) (Figure 2.1A). For co-cultures, the mouse myeloma B cell line Ag8.653 (ATCC; Manassas, VA) was added at $10^6$ cells/well on the bottom of the transwell in $mIC_{cl2}$ media on day 10 of the $mIC_{cl2}$ culture. In this experimental set-up, Ag8.653 did not come into direct contact with polarized $mIC_{cl2}$ monolayers during culture and monolayers were transferred to new

wells before performing experiments (Figure 2.2A). For transcytosis experiments, monolayers were washed three times with PBS before adding MNV-1, S99 or CR3 to the apical side for indicated time points. All compartments (apical medium, membrane with cells, and basolateral medium) were harvested and freeze-thawed once. Viral titers were determined by plaque assay.

To measure viral replication, a neutral red (NR) light-sensitive virus was generated and used as described previously (44). Briefly, polarized mICcl2 monolayers co-cultured with B myeloma cells were incubated with (NR) light-sensitive MNV-1 in the dark for 4 and 24 h before harvesting all compartments (apical medium, membrane with cells, and basolateral medium) in the dark. Samples were freeze-thawed once and duplicate plaque assays were performed either in the dark or in the light following a 10 min light exposure to measure replicated virus or total.

To test for tight junction integrity, lucifer yellow dye (Life Technologies) with a molecular weight of 457.24 Daltons was used as described previously (5). In the case of $mIC_{cl2}$ co-cultures, the transwell insert was transferred to a new 12 well plate without B myeloma cells before performing the assay.

To measure the transcytotic activity of polarized monolayers cultured with or without Ag8.653 cells, monolayers were transferred to a new well and incubated with $2.5 \times 10^{10}$ beads/mL of 200 nm fluorescently green polystyrene latex nanoparticles (Fluoresbrite, YG; Polysciences) for 0, 0.5, 1, 2, 4, and 8 h. The basolateral medium was collected for each time-point, and fluorescence was measured by flow cytometry as described previously (33).

To measure the temperature dependence, polarized $mIC_{cl2}$ monolayers cultured

with or without Ag8.653 B myeloma cells were incubated with MNV-1 for 0, 15, 30, 45 and 60 min at 4°C and viral titers were measured by plaque assay.

**Immunofluorescence analysis.** Immuno-staining of the tight junction-associated protein ZO-1 was performed on 0.1% saponin-permeabilized $mIC_{cl2}$ cells as described previously (5). To enumerate M-like cells in polarized $mIC_{cl2}$ monolayers, 200 nm fluorescent polystyrene latex nanoparticles (*i.e.*, microbeads) (Fluoresbrite; Polysciences) and IgA isolated from human colostrum (0.5 mg/ml, Sigma) were incubated on the apical side of the monolayer at 37°C for 30 min. Following a PBS wash, cells were fixed in 4% paraformaldehyde in PBS for 15 min and permeabilized with 0.1% Triton X-100 for 15 min. Monolayers were washed and incubated for 1 h with a 1:500 anti-human IgA FITC-conjugated antibody (Sigma, F-9637) in PBS containing 1 µg/mL DAPI at room temperature. After three washes with PBS, membranes were dissected from transwells, mounted with ProLong Gold antifade reagent containing DAPI (Invitrogen, Grand Island, NY) and processed for confocal microscopy as detailed previously (5).

To visualize MNV-1 within polarized $mIC_{cl2}$ monolayers, MNV-1 at an MOI of 100 PFU/cell was added to the transwells' apical surface together with 200 nm fluorescently labeled polystyrene latex nanoparticles at 37°C for 30 min. Cells were fixed and permeabilized as described above. Cells were blocked with 10% (v/v) of FBS and 1% (v/v) of normal goat serum (NGS; Gibco) in PBS for 30-60 min. MNV-1 was detected by staining with the mouse monoclonal antibody A6.2 recognizing the MNV-1 capsid (55) (0.5 µg/mL in PBS containing 1 µg/mL DAPI) at room temperature for 1 h, followed by another 1 h incubation with a 1:500 dilution of an Alexa 488-labeled secondary goat

anti-mouse antibody (Invitrogen) in PBS containing DAPI. Membranes were then dissected from transwells, mounted and processed for laser scanning confocal microscopy and Z-stacks of 0.5-1.0 µm slides were obtained using the LSM software on a Zeiss confocal microscope. Immunofluorescence images were quantified from three to six regions of the monolayer each from three to four independent experiments using the scoring system of intensities by the Metamorph Premier v6.3 image analysis software (Molecular Devices; Downington, PA).

To visualize the transport of microbeads in each culture, monolayers were incubated for 30 min at 4°C as well as 2 h or 4 h at 37°C, immunostained for ZO-1 and processed for confocal imaging as mentioned above.

**Statistical analysis.** Data are presented as mean ± standard error (SEM). Statistical analysis was performed using Prism software version 5.01 (GraphPad Software, CA). The two-tailed Student's *t* test was used to determine statistical significance.

## 2.4 Results

### MNV does not disrupt the integrity of an *in vitro* polarized intestinal epithelium.

To determine how NoVs overcome the intestinal epithelial barrier, we first investigated the effect of MNV on tight junction integrity in an *in vitro* model of the polarized intestinal epithelium (Figure 2.1A). Towards that end, three MNV strains MNV-1, S99, or CR3 were added to the apical surface of polarized murine intestinal epithelial $mIC_{cl2}$ cell monolayers in a transwell system for 4 hours (h) (Figure 2.1A). Transepithelial resistance (TER), an indicator of tight junction integrity, was greater than 300 Ohms x $cm^2$ and remained unaffected by incubation with any MNV strain even at a

multiplicity of infection (MOI) of 50 PFU/cell compared with mock-treated monolayers (Figure 2.1B), suggesting that the integrity of the epithelial barrier is not affected by incubation with MNV. In addition, MNV-1 did not alter localization of the tight junction-associated protein ZO-1 compared with a mock-treated control (Figures 2.1C, D). As a control, monolayers were treated with methyl-beta-cyclodextrin (MBCD), a drug that at high doses disrupts tight junctions (32), and relocalization of ZO-1 staining to the cytoplasm was readily observed (Figure 2.1E). Finally, lucifer yellow, a tight junction- and membrane-impermeable fluorescent dye (5), was added apically and fluorescence was quantified in the basolateral compartment. No passive diffusion of the dye was observed after incubating monolayers with the three MNV strains or a mock-treated control (Figure 2.1F). This was in contrast to wells without epithelial cells or monolayers treated with 20 mM MBCD, where lucifer yellow diffused into the basolateral compartment (Figure 2.1F). Taken together, these data indicate that incubation with MNV does not disrupt tight junctions of an *in vitro* polarized intestinal epithelial monolayer.

**Transcytosis of MNV is increased following co-cultures with B myeloma cells.**

Previous studies of pathogen interactions with polarized intestinal epithelial monolayers used co-cultures of freshly isolated murine Peyer's patch lymphocytes or human Raji B lymphoblast-like cells with polarized human colonic Caco-2 or mouse small intestinal $mIC_{cl2}$ cells (2, 12, 29). Thus, to investigate whether MNV replicated in murine intestinal epithelial cells or crossed a polarized intestinal epithelial monolayer, polarized $mIC_{cl2}$ monolayers were cultured in the absence or presence of BALB/c Peyer's patch lymphocytes or Ag8.653 murine B myeloma cells in the basolateral

A

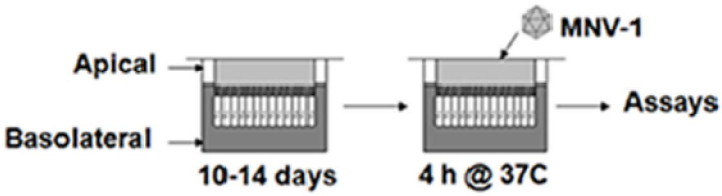
MNV-1
Apical
Basolateral
Assays
10-14 days
4 h @ 37C

C

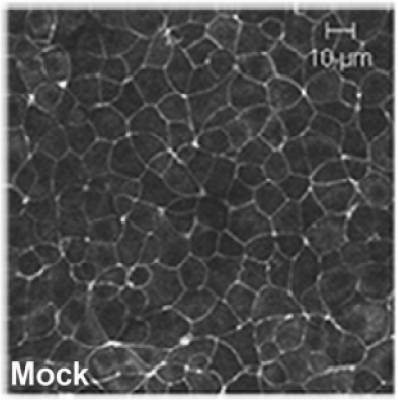
10 µm
Mock

B

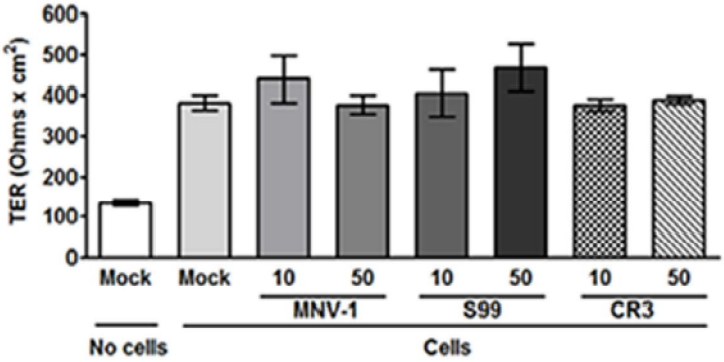
TER (Ohms x cm²)
600
500
400
300
200
100
0
Mock
Mock
10
50
10
50
10
50
MNV-1
S99
CR3
No cells
Cells

D

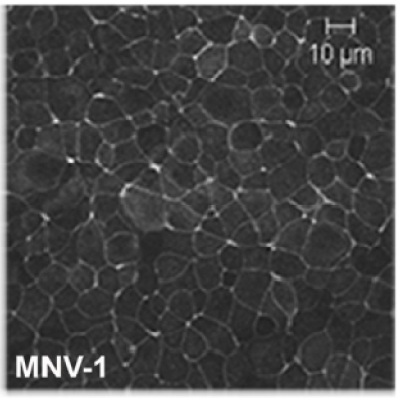
10 µm
MNV-1

F

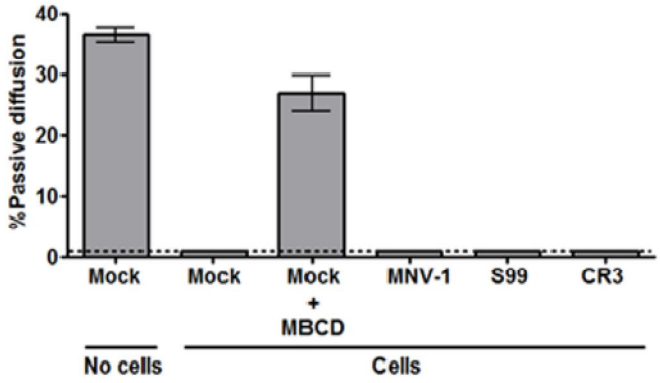
%Passive diffusion
40
30
20
10
0
Mock
Mock
Mock
+
MBCD
MNV-1
S99
CR3
No cells
Cells

E

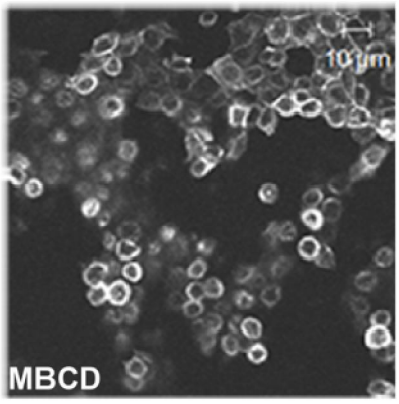
10 µm
MBCD

**Figure 2.1. MNV-1 does not affect epithelial integrity.** (A) Schematic of the *in vitro* intestinal epithelial cell studies. Murine intestinal epithelial cells ($mIC_{cl2}$) were plated in a transwell and allowed to polarize for 10-14 days before addition of MNV-1 to the apical surface at 37°C for 4 h to perform follow-up assays. (B) MNV-1, S99 or CR3 were added to the apical surface of polarized monolayers at an MOI of 10 or 50 PFU/cell for 4 h and compared to a mock lysate and a no-cell control. Transepithelial electrical resistance (TER) was measured after incubation for 4 h. (C-E) Representative ZO-1 immunostaining of polarized monolayers following 4 h of incubation with mock lysate (C) or MNV-1 (MOI 10 PFU/cell) (D) or after 20 mM methyl-beta-cyclodextrin (MBCD) (E) treatment for 1 h by confocal microscopy. (F) Polarized monolayers were incubated with the indicated combinations of MNV-1 (MOI 10 PFU/cell), 20 mM MBCD, and mock lysate. Following a 4 h incubation period, lucifer yellow dye was added to the apical side for 15 min, and absorbance was measured in the basolateral media. The dotted line represents the limit of detection. Data are expressed as mean ± SEM for three independent experiments in duplicates.

compartment (Figures 2.1A and 2.2A). MNV-1 (MOI 10 PFU/cell) was added to the apical surface of these monolayers and incubated for defined intervals. Infectious particles in the apical and basolateral compartments and the membrane (i.e., cell-associated virus) were then quantified by plaque assay. Three to four logs of MNV-1 were transported across the monolayer alone or following co-culture with either Peyer's patch lymphocytes or Ag8.653 cells (Table 2.1, Figures 2.2B and data not shown). Since $mIC_{cl2}$ monolayers co-cultured with Ag8.653 cells were more stable and reproducibly increased MNV-1 transcytosis, the $mIC_{cl2}$ - Ag8.653 system was adopted for the remainder of the studies. MNV-1 titers initially increased quickly in the basolateral compartment but stabilized around 4 h, indicating that transport through the monolayer occurred in a saturable manner (Figure 2.2B). Virus that crossed the epithelial barrier remained infectious and was capable of infecting the murine macrophage cell line RAW 264.7 used for plaque assay. No significant increase in total MNV-1 titers occurred over 24 h in $mIC_{cl2}$ monolayers cultured with Ag8.653 cells or in Ag8.653 cells alone (Figure 2.2B and data not shown), while increases are seen within 12 h in permissive macrophages and dendritic cells (55). To further verify the lack of MNV replication, a neutral red (NR) light-sensitive MNV-1 was used to distinguish input virus from replicated virus (44). Neutral red is a photo-activated dye, which is passively incorporated into viral particles. When particles are exposed to white light, the dye cross-links the viral genome and the capsid protein rendering the virus non-infectious (7). Monolayers were incubated with the NR light-sensitive MNV-1 for 4 and 24 h. Viral titers in the basolateral compartment were measured in the dark (i.e. total virus) or following light exposure (i.e. replicated virus) and were below the limit of detection after

light-exposure despite detecting several logs of total virus (Figure 2.2C). Taken together, these data demonstrate that MNV-1 does not replicate in $mIC_{cl2}$ or in Ag8.653 cells. As observed before, TER was not altered by MNV-1 addition, demonstrating that tight junctions remained intact and suggesting that MNV-1 was trafficked intracellularly (Figure 2.2D).

Transcytosis is a form of intracellular transport in polarized cells, which is inhibited at 4°C (20, 42). To determine whether MNV-1 transport across polarized monolayers was temperature-dependent, MNV-1 was incubated with the apical side of the monolayer at 4°C for 0, 15, 30, 45, and 60 min (Figures 2.2E and F). Tight junction integrity was monitored by measuring passive diffusion of lucifer yellow (Figure 2.2F). No significant amount of virus was detected in the basolateral compartment at time points when tight junction integrity was intact (i.e., 0 – 45 min) (Figures 2.2E and F). Taken together, these data demonstrate that MNV-1 transport across polarized monolayers occurs intracellularly by a temperature-dependent mechanism, suggestive of transcytosis.

To determine whether MNV strains with different persistence phenotypes are transported similarly across this polarized intestinal epithelial monolayer, MNV-1 or S99 were added to the apical side of the cells and incubated for 4 h (Figure 2.3). Viral titers in each compartment were quantified by plaque assay. Transport of both MNV strains to the basolateral compartment was observed but this was significantly increased in the co-cultures compared with $mIC_{cl2}$ cells alone (Figure 2.3 and Table 2.1). Tight junction integrity remained unaffected throughout the experiment based on monitoring TER (Figures 2.3B and D). Taken together, these data indicate that MNV traffics

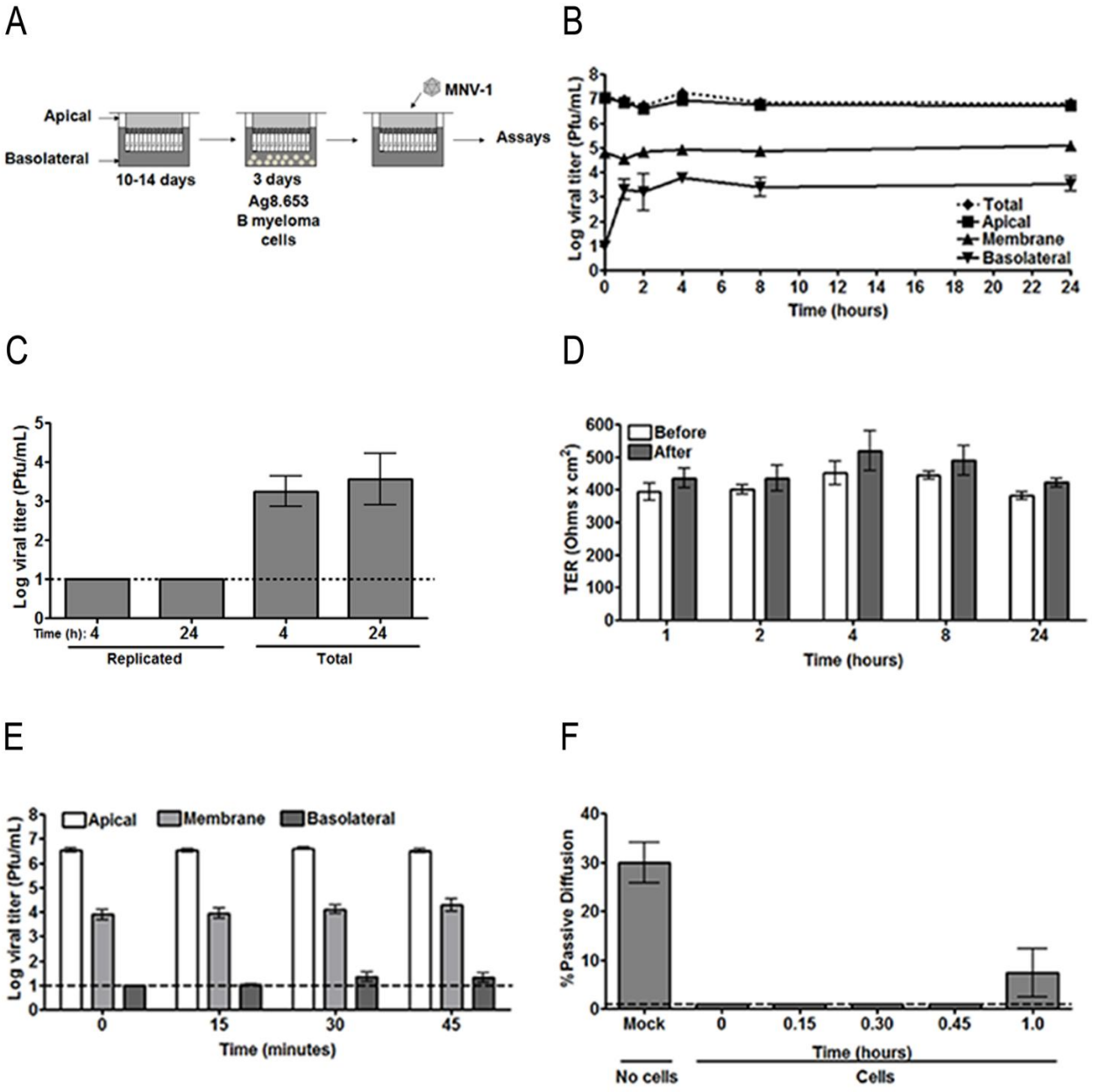


**Figure 2.2. MNV-1 crosses a polarized intestinal epithelial monolayer in a saturable, temperature-dependent manner.** (A) Murine intestinal epithelial cells ($mIC_{cl2}$) were placed in a transwell and allowed to differentiate for 10-14 days before addition of Ag8.653 B myeloma cells in the bottom of the transwell. After 3 days of co-culture, the transwell was moved to a new well before adding MNV-1 to the apical surface at 37°C for 4 h to perform follow-up assays. (B) MNV-1 is transcytosed across intestinal epithelial monolayers in a saturable manner, remains infectious, and does not

replicate in these cells. MNV-1 (MOI 10 PFU/cell) was added to the apical side of polarized monolayers and incubated at 37°C for the times shown. Viral titers in each compartment were quantified by plaque assay. (C) MNV-1 does not replicate in polarized intestinal monolayers. Neutral red (NR) containing light-sensitive MNV-1 was added to the apical side of co-cultured polarized monolayers and incubated at 37°C for the times shown. Viral titers in the basolateral compartment were quantified by plaque assay in the dark to measure total virus or exposed to light to measure replicated virus. (D) TER's from cultures with B myeloma cells (Ag8.653) were measured before and after MNV-1 addition at indicated time points. (E) Polarized $mIC_{cl2}$ monolayers following co-culture with B myeloma cells (Ag8.653) were incubated with MNV-1 at 4°C for the indicated times. Viral titers in each compartment were quantified by plaque assay. (F) Polarized monolayers were incubated at 4°C for the indicated times before adding lucifer yellow to the apical side for 15 min and measuring absorbance in the basolateral media. The dotted lines represent the limit of detection for each assay. Data are expressed as mean ± SEM for at least three independent experiments from duplicate wells.

**Table 2.1: Percent of MNV-1 and S99 transcytosed to the basolateral compartment after 4 h**

| **Samples** | **% MNV-1 Transcytosis[a] +/- SEM[b]** | **% S99 Transcytosis[a] +/- SEM[b]** |
|---|---|---|
| $mIC_{cl2}$ alone | 0.003 +/- 0.001 | 0.002 +/- 0.001 |
| Co-cultures | 0.076 +/- 0.040 *p*=0.0501[c] | 0.023 +/- 0.007 **p*=0.0257[c] |

[a]Percentages were calculated based on viral titers with the equation: (basolateral/[apical+membrane+basolateral])x100.
[b]SEM = Standard error of the mean.
[c]P values compare co-cultures with $mIC_{cl2}$ alone

intracellularly through the $mIC_{cl2}$ monolayer to reach the basolateral compartment, and this process is enhanced following co-culture with Ag8.653 cells.

**M-like cell numbers are similar in $mIC_{cl2}$ monolayers but co-cultured monolayers transcytose more efficiently.**

The previously described presence of M-like cells in polarized monolayers following co-culture (2, 12, 29, 35), prompted us to test whether the increase in MNV transcytosis following Ag8.653 co-culture is due to an increase in M-like cell numbers within the $mIC_{cl2}$ monolayer. M cells are known to selectively bind and endocytose IgA or secretory IgA in its natural form or by adding it exogenously into mice PPs (34). Also, M cells have the innate ability to take up fluorescently labeled beads (23). Therefore, cells cultured in the absence or presence of Ag8.653 B myeloma cells were analyzed for these two M cell-associated properties, i.e., the ability to bind exogenous IgA, and to take up fluorescently labeled beads (microbeads). Monolayers were incubated with fluorescently-labeled microbeads or IgA isolated from human colostrum followed by a fluorescently-labeled anti-IgA secondary antibody and analyzed by confocal microscopy (Figures 2.4A-F). The number of cells positive for IgA and microbeads alone or positive for both was not significantly different between cultures with or without B myeloma cells (Figure 2.4G). Approximately 2% of total cells were single positive for either IgA and microbeads, while ~10% of total cells in each monolayer were double positive for both (Figure 2.4G). These results suggest that IgA- and microbead-positive cells are present within polarized $mIC_{cl2}$ monolayers and that addition of B myeloma cells to the basolateral compartment does not increase the number of these cells in the monolayer. Taken together, the data demonstrate that the increase in MNV transcytosis following

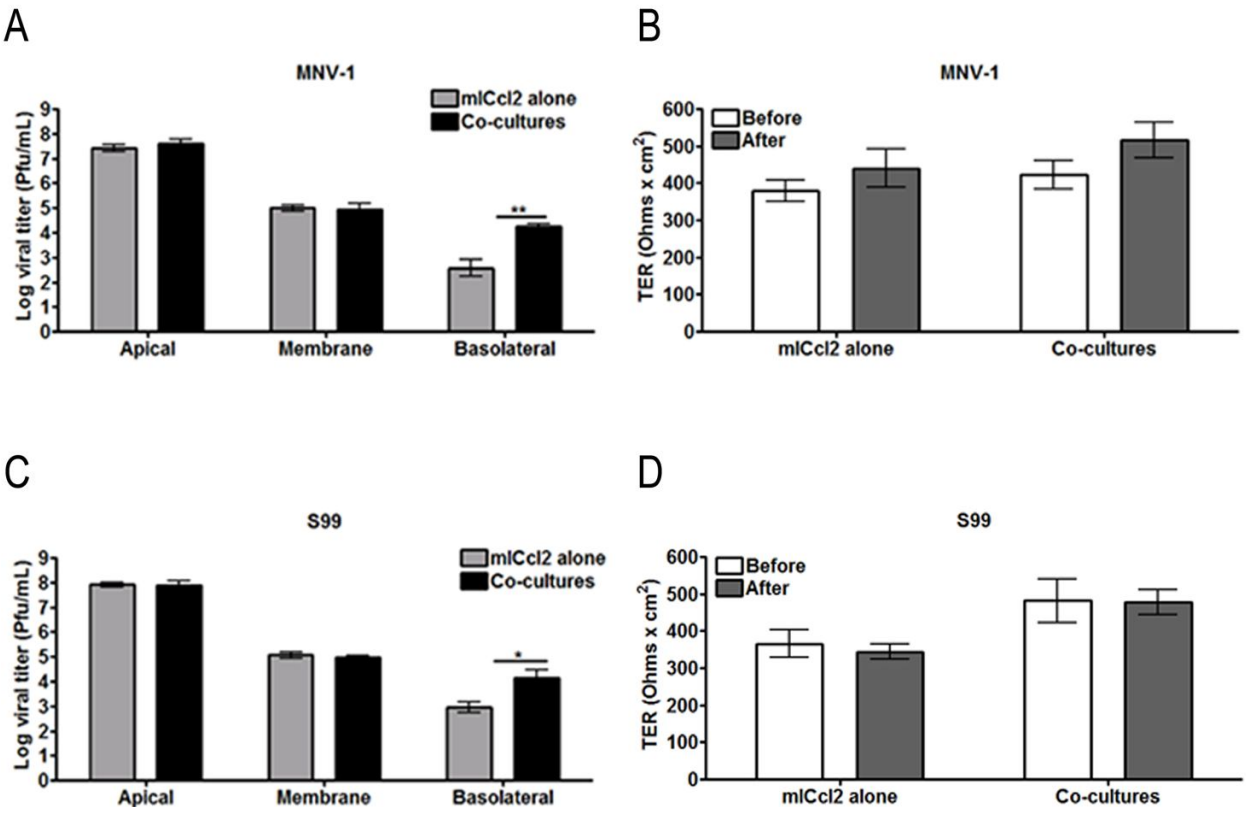


**Figure 2.3. Co-culture with B myeloma cells increases MNV transcytosis.** Co-cultures were established as outlined in Figure 2.2A. (A and C) Co-cultures increased viral titers in the basolateral side. Cultures in the presence or absence of B myeloma cells were incubated with either MNV-1 (A) or S99 (C) (MOI 10 PFU/cell) at 37°C for 4 h. Viral titers were quantified by plaque assay. (B and D) TER's were measured in the presence or absence of B myeloma cells (Ag8.653) before and 4 h after MNV-1 (B) or S99 (D) incubation. Results represent duplicates of at least three independent experiments. Data are expressed as mean ± SEM. * $p < 0.05$, ** $p < 0.01$.

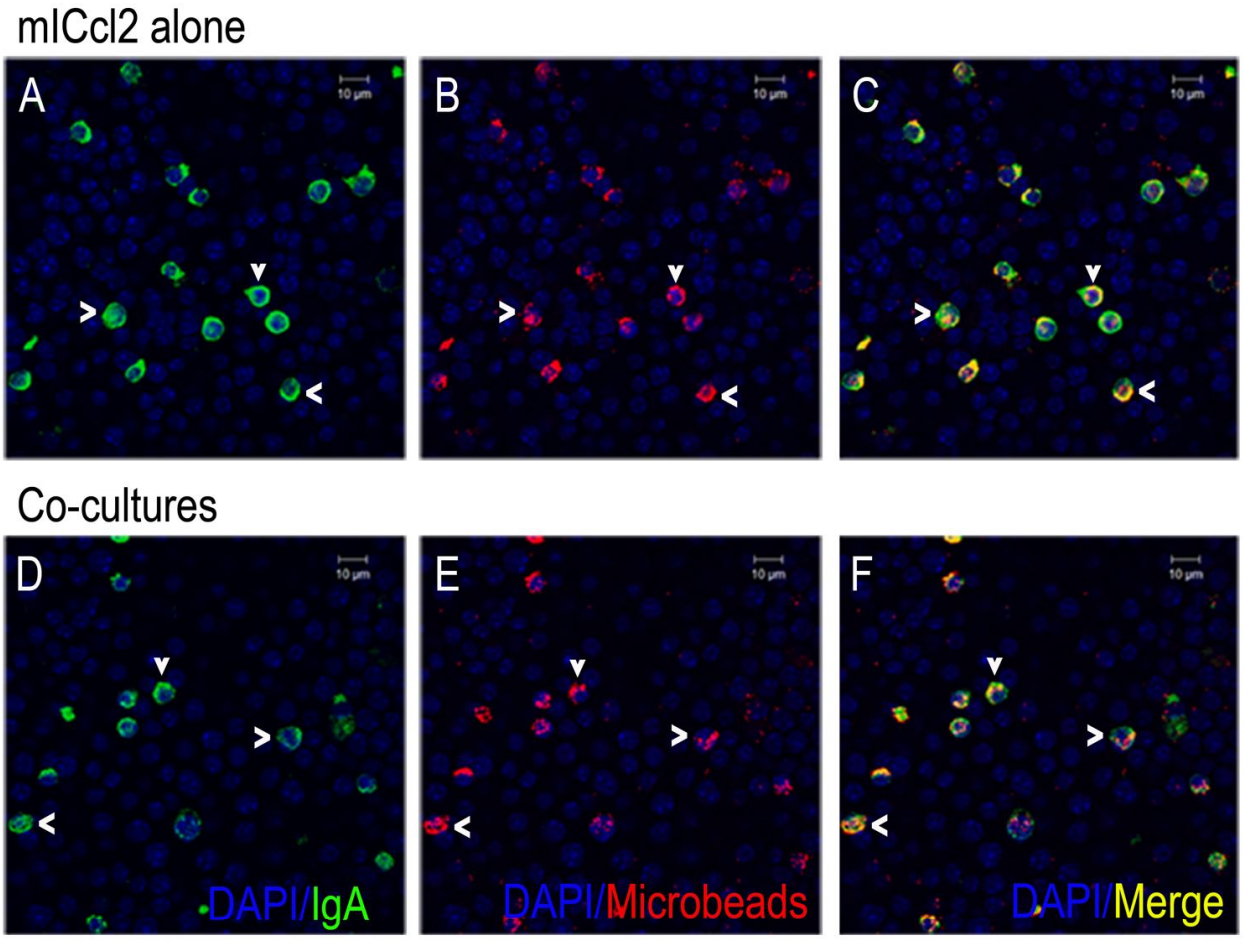
mICcl2 alone
A
B
C
10 µm
Co-cultures
D
E
F
DAPI/IgA
DAPI/Microbeads
DAPI/Merge

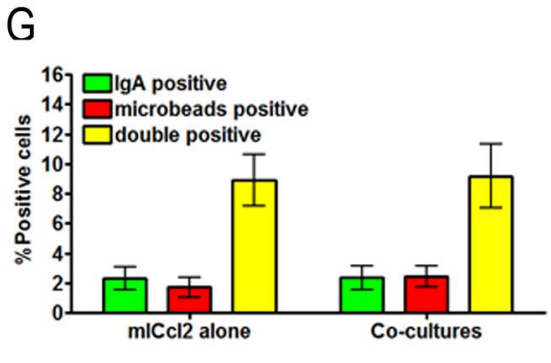
G
% Positive cells
IgA positive
microbeads positive
double positive
mICcl2 alone
Co-cultures

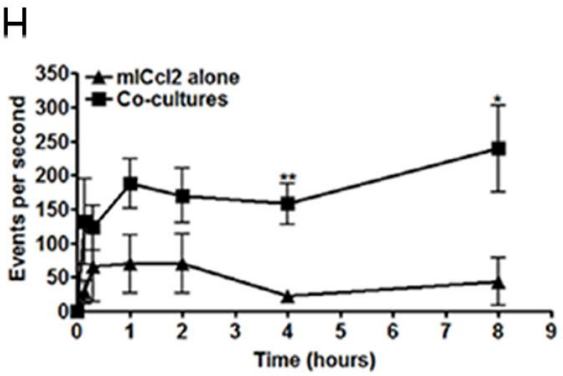
H
Events per second
mICcl2 alone
Co-cultures
Time (hours)

**Figure 2.4. Polarized $mIC_{cl2}$ monolayers alone or from co-cultures have similar numbers of M-like cells but increased transcytosis of particles.** (A-F) Representative confocal images of cell monolayers from cultures without ($mIC_{cl2}$ alone) or with B myeloma cells (co-cultures) stained for IgA (green) and microbeads (red), as well as the merge of both. DAPI was used to stain the nuclei. White arrows indicate individual double-positive cells. A 10 µm scale bar is shown in the upper right corner of each image. (G) Quantification of images. Images from three-to-four independent experiments each of three-to-six fields of view within independent monolayers were quantified using Metamorph. (H) Microbeads were added to the apical side of the cultures for the times shown, and basolateral media was analyzed by flow cytometry. Results represent duplicates of at least nine independent experiments. Data are expressed as mean ± SEM. * $p < 0.05$, ** $p < 0.01$.

co-culture with Ag8.653 is not due to an increase in M-like cell numbers within the $mIC_{cl2}$ monolayer.

An alternative hypothesis to changes in cell numbers that could lead to an increase in virus titers in the basolateral compartment following co-culture is through an increase in the rate of particle transport. To investigate this possibility and verify that mono- and co-cultured polarized monolayers could transcytose particulate antigens, microbead uptake was measured over time in both monolayers cultured with or without Ag8.653 cells by first quantifying microbeads in the basolateral compartment by flow cytometry (Figure 2.4H). Microbeads were being transcytosed under both conditions. However, co-cultures showed significantly increased numbers of microbeads in the basolateral chamber compared to $mIC_{cl2}$ cells alone.

The transport of fluorescent microbeads across polarized monolayers cultured with or without Ag8.653 B myeloma cells was further verified by confocal microscopy (Figures 2.5 and 2.6). As anticipated, microbeads incubated with the apical side for 30 min at 4°C remained near the apical surface of the cells under both culturing conditions (Figures 2.5A and 2.6A) because transcytosis is inhibited at this temperature. In contrast, microbeads were located near the transwell membrane in the basolateral portion of cells after a 2-4 h incubation at 37°C (Figures 2.5B-C and 2.6B-C).

Taken together, these data demonstrate that a fraction of $mIC_{cl2}$ enterocytes exhibit M-like cell properties (i.e., the ability to transport microbeads) in polarized monolayers cultured with or without Ag8.653 B myeloma cells. Microbead transport *per se* is independent of the presence of Ag8.653 B myeloma cells, but the process is enhanced by co-culturing with the Ag8.653 B cells.

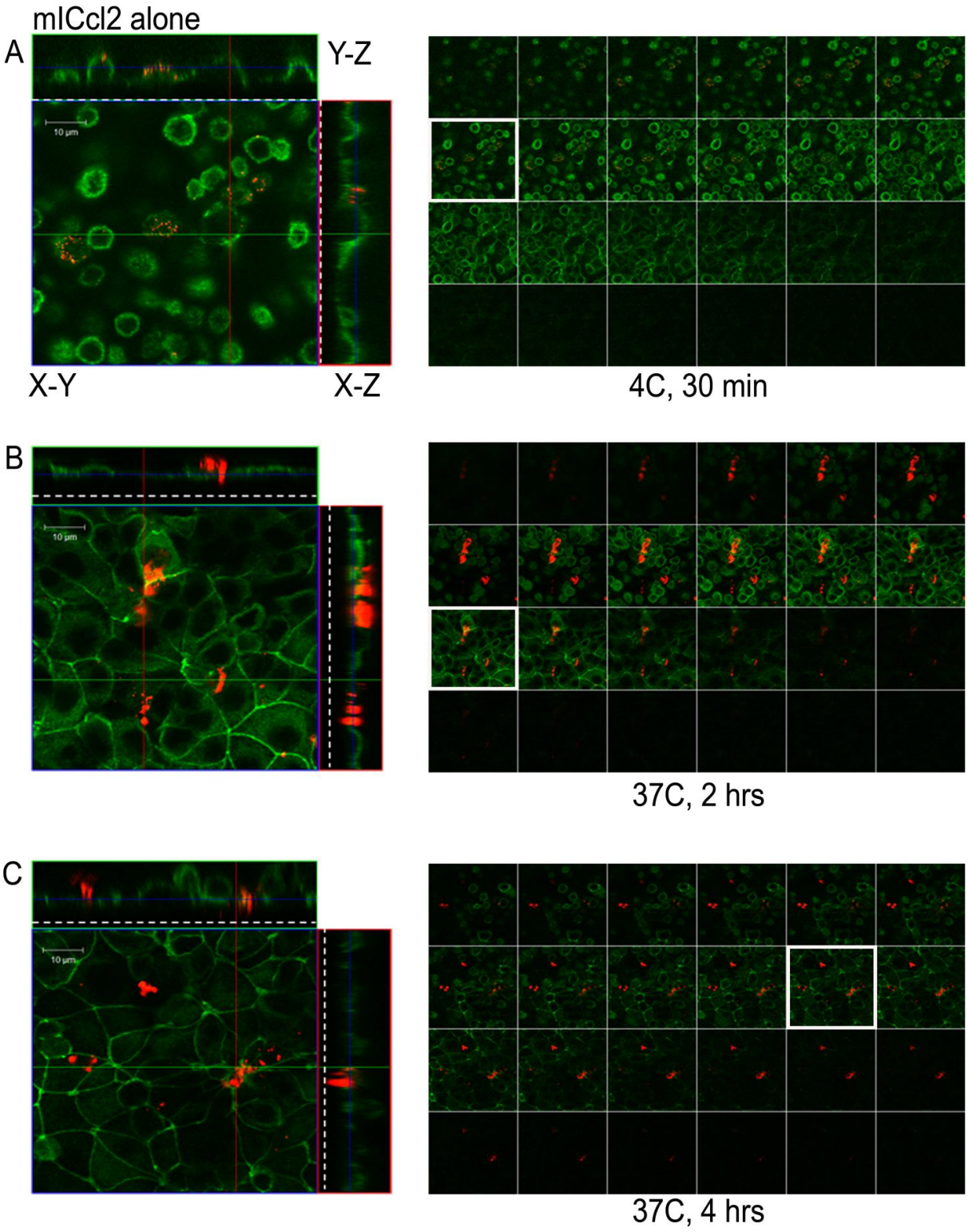
mICcl2 alone
A
Y-Z
10 µm
X-Y
X-Z
4C, 30 min
B
10 µm
37C, 2 hrs
C
10 µm
37C, 4 hrs

**Figure 2.5. Polarized mIC$_{cl2}$ monolayers alone transcytose microbeads in a time- and temperature-dependent manner**. Polarized mIC$_{cl2}$ monolayers were incubated with microbeads (in red) for 30 min at 4°C (A), as well as 2 h (B) or 4 h (C) at 37°C. ZO-1 (in green) was used to identify tight junctions. Dashed lines in the Y-Z and X-Z projections correspond to the relative location of the membrane in the transwell insert. Representative Z-stack images of 0.5 µm slices are shown on the left, while the corresponding Z-stack sections are shown on the right. A white square indicates the X-Y view shown on the left. In each gallery of images the first image is near the apical (top) side, while the last image is near the bottom (membrane) side.

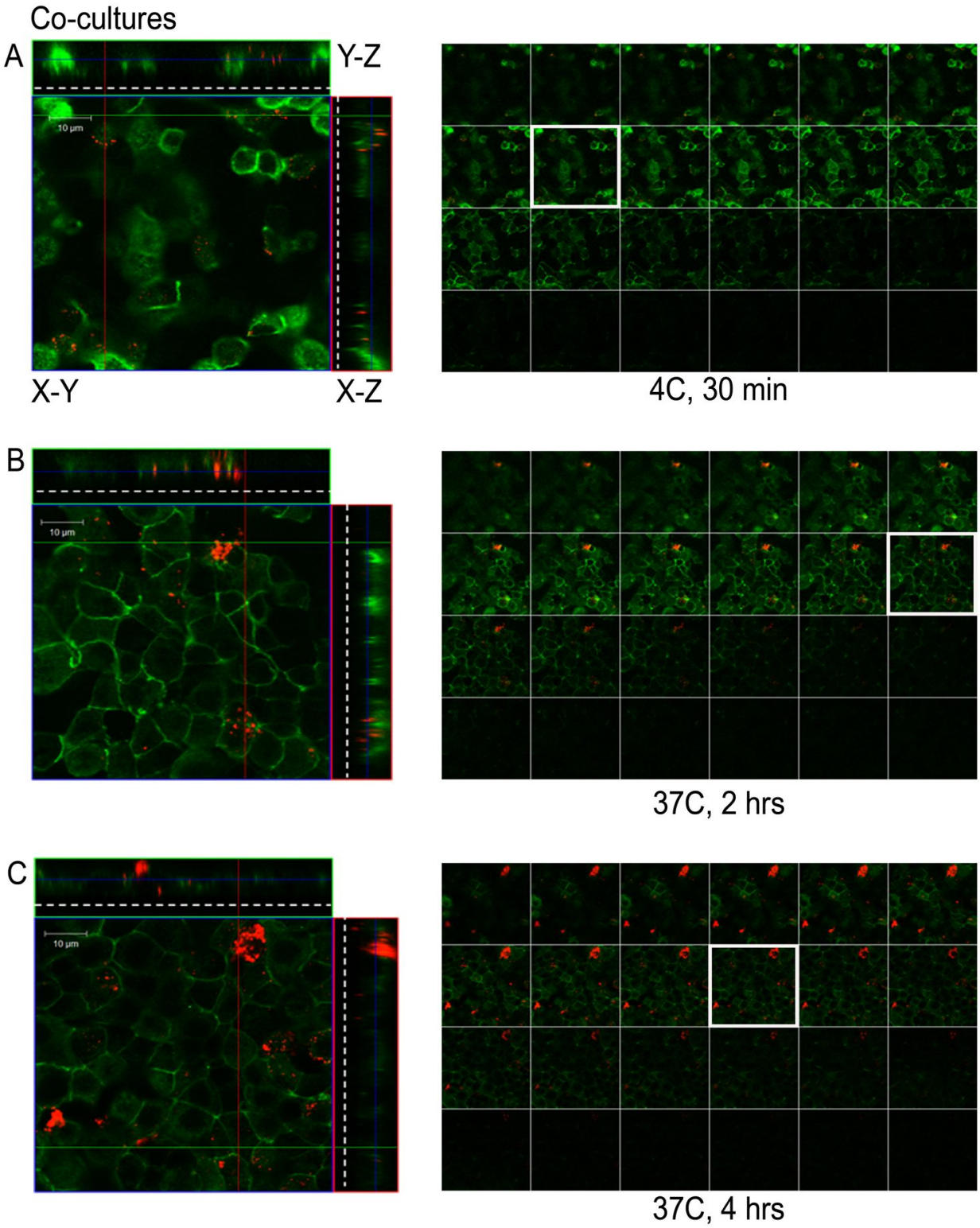
Co-cultures
A
Y-Z
10 µm
X-Y
X-Z
4C, 30 min
B
10 µm
37C, 2 hrs
C
10 µm
37C, 4 hrs

**Figure 2.6. Polarized mIC$_{cl2}$ monolayers following co-cultures with Ag8.653 B myeloma cells transcytose microbeads in a time- and temperature-dependent manner**. Polarized mIC$_{cl2}$ monolayers co-cultured with Ag8.653 cells were incubated with microbeads (in red) for 30 min at 4°C (A), as well as 2 h (B) or 4 h (C) at 37°C as well as with ZO-1 (in green) similarly as Figure 2.5. Dashed lines in the Y-Z and X-Z projections correspond to the relative location of the membrane in the transwell insert. Representative Z-stack images of 0.5 µm slices are shown on the left, while the corresponding Z-stack sections are shown on the right. A white square indicates the X-Y view shown on the left. In each gallery of images, the first image is near the apical (top) side, while the last section is near the bottom (membrane) side.

**MNV transcytosis is specifically mediated by M-like cells.**

To determine whether MNV is transcytosed by M-like cells, $mIC_{cl2}$ cell monolayers co-cultured with Ag8.653 B myeloma cells were incubated with fluorescently-labeled microbeads and either MNV-1 or mock lysate for 30 min at 37$^{o}$C, and analyzed by confocal microscopy (Figure 2.7). Virus was observed through the length of the cell alongside microbeads (Figures 2.7A-C). As anticipated, mock-inoculated cells stained positive only for microbeads (Figures 2.7D-F). Quantification of the immunofluorescence images indicated that the majority of immune-stained cells or approximately 10% of all cells were positive for both microbeads and MNV-1 (Figure 2.7G). In contrast, only a few cells (~2% of total cells) were positive for microbeads or MNV-1 alone (Figure 2.7G). Thus, MNV transcytosis is primarily mediated by microbead-positive, M-like cells present in the monolayer.

## 2.5 Discussion

Many enteric viral pathogens have evolved strategies to infect their host by hijacking or circumventing intestinal host defenses. Studies understanding the initial step of enteric virus infection, i.e., of overcoming the intestinal epithelial barrier, can identify potential targets for intervention. In the case of NoVs, not much is known about how NoVs initiate a productive infection in the host. Herein, we used the murine enteric virus MNV and a murine intestinal epithelial cell line to point to M-like cells as a cell type mediating MNV transport across the intestinal epithelium in the absence of viral replication.

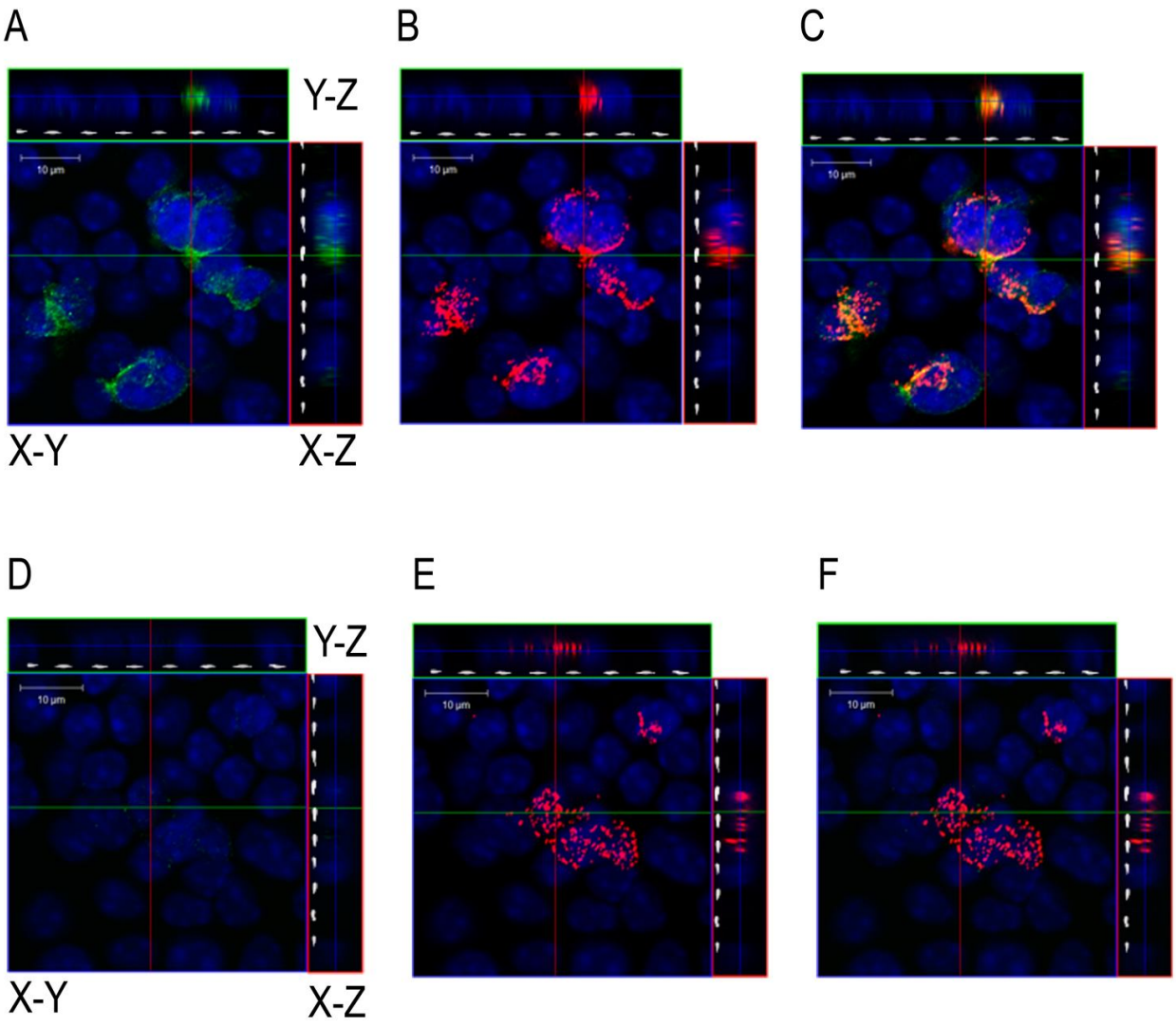
A
B
C
Y-Z
10 µm
X-Y
X-Z
D
E
F
Y-Z
10 µm
X-Y
X-Z
G
% Positive cells
14
12
10
8
6
4
2
0
*
*
MNV-1
Microbeads
Co-localization

**Figure 2.7. MNV-1 transcytosis is mediated by M-like cells.** Co-cultures of $mIC_{cl2}$ and B myeloma cells were incubated for 30 min with microbeads and MNV-1 (MOI 100 PFU/cell) or mock lysate and processed for confocal microscopy. (A-C) Representative Z-stack image of 1.0 µm slices showing staining of MNV-1 (green, A), microbeads (red, B), and the merge (yellow, C). DAPI was used to stain the nuclei. A 10 µm scale bar is shown in the upper left corner of each image. (D-F) Representative Z-stack image of 0.5 µm slices incubated with mock lysate and microbeads. (A and D) The dashed line on the Y-Z and X-Z projections indicates the relative location of the membrane from the transwell insert. (G) Quantification of confocal images. Three to six different regions in the monolayer were quantified using Metamorph from three independent experiments. Data are expressed as mean ± SEM. * $p < 0.05$.

Our data demonstrated that MNV does not disrupt the epithelial integrity of polarized intestinal epithelial cells *in vitro* for at least 24 h as measured by staining for ZO-1, monitoring TER, and passive diffusion of lucifer yellow dye (see Figure 2.1). In contrast, symptomatic human norovirus infections exhibit reduced expression of tight junction proteins, increased epithelial cell apoptosis, and decreased TER resulting in epithelial barrier dysfunction in duodenal biopsies from infected individuals (52). The inability of MNV to replicate in intestinal epithelial cells and to disrupt tight junctions in this *in vitro* model may also explain why MNV-infected wild-type mice show no overt symptoms of diarrhea (51, 56).

In addition, MNV remained infectious after being transcytosed by M-like cells to the basolateral compartment of *in vitro* polarized intestinal epithelial monolayers. This process was enhanced by co-cultures with Ag8.653 B myeloma cells, although MNV did not replicate in these cells (Figures 2.2, 2.4 and data not shown). Similar findings were made with HTLV-1, which show that HTLV-1 remains infectious following transcytosis across a polarized Caco-2 monolayer but does not replicate in these cells (25). The average percentage of MNV transcytosis across polarized monolayers was less than 0.1%. While this may reflect an inefficiency of the *in vitro* system, others have reported a similar level of transcytosis for poliovirus (~ 0.2%) across polarized Caco-2 monolayers (42). For enteric bacteria, transcytosis frequency is more variable with values between 0.1 - 10% (28, 29). While MNV-1 co-localized with the majority of microbead-positive M-like cells present in the monolayer, some microbead-positive cells without MNV-1 were also observed (Figure 2.7G). This result suggested that some of the M-like cells do not internalize virus. Furthermore, the observation of cells single-

positive for MNV-1 suggested that microbeads may not label all M-like cells in the monolayer or that a small percentage of MNV-1 may be transcytosed by epithelial cells. We favor the former hypothesis that MNV-1 is taken up by M-like cells not stained by microbeads because of reports that, *in vivo,* certain immune stimuli or a *Salmonella typhimurium* virulence factor can cause phenotypic transdifferentiation and lead to the generation of new M cell subsets without cell division (41, 47, 53). In this scenario, microbead staining would not occur in all stages of M-like cell differentiation and other markers may be required to identify those M-like cells.

Using IgA binding and microbead uptake as properties of M-like cells, we demonstrated that the presence of Ag8.653 B myeloma cells in *in vitro* polarized intestinal epithelial cell monolayers did not significantly alter M-like cell numbers compared to $mIC_{cl2}$ cultures without Ag8.653 B myeloma cells. Instead, co-culture with Ag8.653 cells increased the transport of particulate antigens across the monolayer (Figures 2.4) despite the lack of direct contact between Ag8.653 B myeloma cells and the intestinal epithelial cells. One potential explanation for the different levels of transcytosis might lie in the maturation state of the M-like cells in each culture condition, which may be influenced by secreted factors from Ag8.653 B myeloma cells. In support of this hypothesis are findings that transcytosis is an acquired property of M cells as they mature (8, 24) and that secreted factors influence this process (21, 33). For example, macrophage migration inhibitory factor (MIF) secreted by Raji B cells induces M-like cell conversion in *in vitro* polarized Caco-2 cell monolayers, and MIF-deficient mice fail to upregulate M cell-mediated antigen sampling upon bacterial challenge (33). Furthermore, CD137 (a TNF-superfamily receptor member, TNFRSF9) is highly induced

in intestinal epithelial monolayers and CD137-deficient mice show abnormal M cell differentiation and defects in particle transcytosis (21). In addition, M cell differentiation is regulated by the ETS transcription factor Spi-B (10, 24) and ectopic expression of *SPIB* and *EHF* (another ETS transcription factor) partially substituted Raji B-cell stimulated signals in differentiated TC7 cells (a Caco-2 cell subclone) (1). Interestingly, when we co-cultured $mIC_{cl2}$ monolayers in conditioned media from the Ag8.653 B myeloma cells instead of Ag8.653 cells themselves, a trend (although not statistically significant) of increased MNV-1 transcytosis was observed when compared to $mIC_{cl2}$ cells cultured without conditioned media (data not shown). Thus, one potential way that co-culturing with Ag8.653 cells increases M-like cell transcytosis is via the secretion of cytokines that can lead to TNF/lymphotoxin signaling and/or the expression of ETS transcription factors. Further studies are needed to test this model and identify secreted factors important in this context.

Taken together, our work demonstrates that M-like cells mediate MNV transport across polarized murine intestinal epithelial monolayers but do not support viral replication. This suggests that M cells are a likely gateway for MNV entry into the host. Support for the importance of M cells *in vivo* during the establishment of a productive MNV infection comes from the observation that mice depleted of M cells have significantly lower MNV titers compared to isotype control depleted mice (Gonzalez-Hernandez et al., submitted). Our study further demonstrates that MNV transcytosis is saturable in this *in vitro* murine intestinal epithelial model, indicating the presence of a receptor, and that addition of B myeloma cells increases the transcytotic activity of the polarized monolayer. Establishment of this *in vitro* murine FAE model provides a

foundation for future studies to identify an M cell receptor for MNV, and may reveal critical targets for the development of effective norovirus vaccines because targeting M cells is one approach to elicit effective mucosal immune responses (22).

## 2.6 References


1. **Asai, T., and S. L. Morrison.** 2013. The SRC family tyrosine kinase HCK and the ETS family transcription factors SPIB and EHF regulate transcytosis across a human follicle-associated epithelium model. The Journal of biological chemistry **288:**10395-10405.
2. **Bens, M., A. Bogdanova, F. Cluzeaud, L. Miquerol, S. Kerneis, J. P. Kraehenbuhl, A. Kahn, E. Pringault, and A. Vandewalle.** 1996. Transimmortalized mouse intestinal cells (m-ICc12) that maintain a crypt phenotype. The American journal of physiology **270:**C1666-1674.
3. **Bernard, H., M. Hohne, S. Niendorf, D. Altmann, and K. Stark.** 2013. Epidemiology of norovirus gastroenteritis in Germany 2001-2009: eight seasons of routine surveillance. Epidemiol Infect**:**1-12.
4. **Blanco, L. P., and V. J. Dirita.** 2006. Antibodies enhance interaction of Vibrio cholerae with intestinal M-like cells. Infection and immunity **74:**6957-6964.
5. **Blanco, L. P., and V. J. DiRita.** 2006. Bacterial-associated cholera toxin and GM1 binding are required for transcytosis of classical biotype Vibrio cholerae through an in vitro M cell model system. Cellular microbiology **8:**982-998.
6. **Blanton, L. H., S. M. Adams, R. S. Beard, G. Wei, S. N. Bulens, M. A. Widdowson, R. I. Glass, and S. S. Monroe.** 2006. Molecular and epidemiologic trends of caliciviruses associated with outbreaks of acute gastroenteritis in the United States, 2000-2004. The Journal of infectious diseases **193:**413-421.
7. **Brandenburg, B., L. Y. Lee, M. Lakadamyali, M. J. Rust, X. Zhuang, and J. M. Hogle.** 2007. Imaging Poliovirus Entry in Live Cells. PLoS Biol **5:**e183.
8. **Clarke, I. N., M. K. Estes, K. Y. Green, G. S. Hansman, N. J. Knowles, M. K. Koopmans, D. O. Matson, G. Meyers, J. D. Neill, A. Radford, A. W. Smith, M. J. Studdert, H.-J. Thiel, and J. Vinjé.** 2012. Caliciviridae, p. 977-986. *In* A. M. King AMQ, Carstens EB, Lefkowitz EJ (ed.), Virus Taxonomy: Classification and Nomenclature of Viruses: Ninth Report of the International Committee on Taxonomy of Viruses. Elsevier, San Diego.
9. **Corr, S. C., C. C. Gahan, and C. Hill.** 2008. M-cells: origin, morphology and role in mucosal immunity and microbial pathogenesis. FEMS Immunol Med Microbiol **52:**2-12.
10. **de Lau, W., P. Kujala, K. Schneeberger, S. Middendorp, V. S. Li, N. Barker, A. Martens, F. Hofhuis, R. P. DeKoter, P. J. Peters, E. Nieuwenhuis, and H. Clevers.** 2012. Peyer's patch M cells derived from Lgr5(+) stem cells require

SpiB and are induced by RankL in cultured "miniguts". Molecular and cellular biology **32:**3639-3647.

11. **Duizer, E., K. J. Schwab, F. H. Neill, R. L. Atmar, M. P. Koopmans, and M. K. Estes.** 2004. Laboratory efforts to cultivate noroviruses. The Journal of general virology **85:**79-87.
12. **El Bahi, S., E. Caliot, M. Bens, A. Bogdanova, S. Kerneis, A. Kahn, A. Vandewalle, and E. Pringault.** 2002. Lymphoepithelial interactions trigger specific regulation of gene expression in the M cell-containing follicle-associated epithelium of Peyer's patches. J Immunol **168:**3713-3720.
13. **Fotopoulos, G., A. Harari, P. Michetti, D. Trono, G. Pantaleo, and J. P. Kraehenbuhl.** 2002. Transepithelial transport of HIV-1 by M cells is receptor-mediated. Proceedings of the National Academy of Sciences of the United States of America **99:**9410-9414.
14. **Gerondopoulos, A., T. Jackson, P. Monaghan, N. Doyle, and L. O. Roberts.** 2010. Murine norovirus-1 cell entry is mediated through a non-clathrin-, non-caveolae-, dynamin- and cholesterol-dependent pathway. The Journal of general virology **91:**1428-1438.
15. **Gonzalez-Hernandez, M. B., J. Bragazzi Cunha, and C. E. Wobus.** 2012. Plaque assay for murine norovirus. J Vis Exp**:**e4297.
16. **Green, K. Y.** 2007. Caliciviridae, p. 949-980. *In* P. H. DM Knipe (ed.), Fields Virology, 5 ed, vol. 1. Lippincott Williams & Wilkins, Philadelphia.
17. **Hall, A. J., A. T. Curns, L. C. McDonald, U. D. Parashar, and B. A. Lopman.** 2012. The roles of Clostridium difficile and norovirus among gastroenteritis-associated deaths in the United States, 1999-2007. Clin Infect Dis **55:**216-223.
18. **Hansman, G. S., X. J. Jiang, and K. Y. Green.** 2010. Caliciviruses Molecular and Cellular Virology, 1 ed, vol. 1. Caister Academic Press, Norfolk, UK.
19. **Herbst-Kralovetz, M. M., A. L. Radtke, M. K. Lay, B. E. Hjelm, A. N. Bolick, S. S. Sarker, R. L. Atmar, D. H. Kingsley, C. J. Arntzen, M. K. Estes, and C. A. Nickerson.** 2013. Lack of norovirus replication and histo-blood group antigen expression in 3-dimensional intestinal epithelial cells. Emerging infectious diseases **19:**431-438.
20. **Hocini, H., P. Becquart, H. Bouhlal, N. Chomont, P. Ancuta, M. D. Kazatchkine, and L. Belec.** 2001. Active and selective transcytosis of cell-free human immunodeficiency virus through a tight polarized monolayer of human endometrial cells. Journal of virology **75:**5370-5374.
21. **Hsieh, E. H., X. Fernandez, J. Wang, M. Hamer, S. Calvillo, M. Croft, B. S. Kwon, and D. D. Lo.** 2010. CD137 is required for M cell functional maturation but not lineage commitment. Am J Pathol **177:**666-676.
22. **Jepson, M. A., M. A. Clark, and B. H. Hirst.** 2004. M cell targeting by lectins: a strategy for mucosal vaccination and drug delivery. Advanced drug delivery reviews **56:**511-525.
23. **Jepson, M. A., N. L. Simmons, T. C. Savidge, P. S. James, and B. H. Hirst.** 1993. Selective binding and transcytosis of latex microspheres by rabbit intestinal M cells. Cell and tissue research **271:**399-405.
24. **Kanaya, T., K. Hase, D. Takahashi, S. Fukuda, K. Hoshino, I. Sasaki, H. Hemmi, K. A. Knoop, N. Kumar, M. Sato, T. Katsuno, O. Yokosuka, K.**

**Toyooka, K. Nakai, A. Sakamoto, Y. Kitahara, T. Jinnohara, S. J. McSorley, T. Kaisho, I. R. Williams, and H. Ohno.** 2012. The Ets transcription factor Spi-B is essential for the differentiation of intestinal microfold cells. Nature immunology.

25. **Kapikian, A. Z., R. G. Wyatt, R. Dolin, T. S. Thornhill, A. R. Kalica, and R. M. Chanock.** 1972. Visualization by immune electron microscopy of a 27-nm particle associated with acute infectious nonbacterial gastroenteritis. Journal of virology **10:**1075–1081.
26. **Karst, S. M., C. E. Wobus, M. Lay, J. Davidson, and H. W. Virgin IV.** 2003. STAT1-dependent innate immunity to a Norwalk-like virus. Science (New York, N.Y **299:**1575-1578.
27. **Kearney, J. F., A. Radbruch, B. Liesegang, and K. Rajewsky.** 1979. A new mouse myeloma cell line that has lost immunoglobulin expression but permits the construction of antibody-secreting hybrid cell lines. J Immunol **123:**1548-1550.
28. **Kerneis, S., A. Bogdanova, J. P. Kraehenbuhl, and E. Pringault.** 1997. Conversion by Peyer's patch lymphocytes of human enterocytes into M cells that transport bacteria. Science (New York, N.Y **277:**949-952.
29. **Kerneis, S., E. Caliot, H. Stubbe, A. Bogdanova, J. Kraehenbuhl, and E. Pringault.** 2000. Molecular studies of the intestinal mucosal barrier physiopathology using cocultures of epithelial and immune cells: a technical update. Microbes and infection / Institut Pasteur **2:**1119-1124.
30. **Koopmans, M., J. Vinje, E. Duizer, M. de Wit, and Y. van Duijnhoven.** 2001. Molecular epidemiology of human enteric caliciviruses in The Netherlands. Novartis Foundation symposium **238:**197-214; discussion 214-198.
31. **Kraehenbuhl, J. P., and M. R. Neutra.** 2000. Epithelial M cells: differentiation and function. Annu Rev Cell Dev Biol **16:**301-332.
32. **Lambert, D., C. A. O'Neill, and P. J. Padfield.** 2007. Methyl-beta-cyclodextrin increases permeability of Caco-2 cell monolayers by displacing specific claudins from cholesterol rich domains associated with tight junctions. Cell Physiol Biochem **20:**495-506.
33. **Man, A. L., F. Lodi, E. Bertelli, M. Regoli, C. Pin, F. Mulholland, A. R. Satoskar, M. J. Taussig, and C. Nicoletti.** 2008. Macrophage migration inhibitory factor plays a role in the regulation of microfold (M) cell-mediated transport in the gut. J Immunol **181:**5673-5680.
34. **Mantis, N. J., M. C. Cheung, K. R. Chintalacharuvu, J. Rey, B. Corthesy, and M. R. Neutra.** 2002. Selective adherence of IgA to murine Peyer's patch M cells: evidence for a novel IgA receptor. J Immunol **169:**1844-1851.
35. **Masuda, K., A. Kajikawa, and S. Igimi.** 2011. Establishment and Evaluation of an *in vitro* M Cell Model using B2BBe1 Cells and Raji Cells. Bioscience Microflora **30:**37-44.
36. **Matthews, J. E., B. W. Dickey, R. D. Miller, J. R. Felzer, B. P. Dawson, A. S. Lee, J. J. Rocks, J. Kiel, J. S. Montes, C. L. Moe, J. N. Eisenberg, and J. S. Leon.** 2012. The epidemiology of published norovirus outbreaks: a review of risk factors associated with attack rate and genogroup. Epidemiol Infect **140:**1161-1172.

37. **Muller, B., U. Klemm, A. Mas Marques, and E. Schreier.** 2007. Genetic diversity and recombination of murine noroviruses in immunocompromised mice. Archives of virology **152:**1709-1719.
38. **Neutra, M. R., N. J. Mantis, A. Frey, and P. J. Giannasca.** 1999. The composition and function of M cell apical membranes: implications for microbial pathogenesis. Seminars in immunology **11:**171-181.
39. **Nice, T. J., D. W. Strong, B. T. McCune, C. S. Pohl, and H. W. Virgin.** 2013. A single-amino-acid change in murine norovirus NS1/2 is sufficient for colonic tropism and persistence. Journal of virology **87:**327-334.
40. **Noda, M., S. Fukuda, and O. Nishio.** 2008. Statistical analysis of attack rate in norovirus foodborne outbreaks. Int J Food Microbiol **122:**216-220.
41. **Ohno, H., T. Kanaya, and I. R. Williams.** 2012. M cell differentiation: distinct lineage or phenotypic transition? Salmonella provides answers. Cell host & microbe **12:**607-609.
42. **Ouzilou, L., E. Caliot, I. Pelletier, M. C. Prevost, E. Pringault, and F. Colbere-Garapin.** 2002. Poliovirus transcytosis through M-like cells. The Journal of general virology **83:**2177-2182.
43. **Perry, J. W., S. Taube, and C. E. Wobus.** 2009. Murine norovirus-1 entry into permissive macrophages and dendritic cells is pH-independent. Virus research **143:**125-129.
44. **Perry, J. W., and C. E. Wobus.** 2010. Endocytosis of murine norovirus 1 into murine macrophages is dependent on dynamin II and cholesterol. Journal of virology **84:**6163-6176.
45. **Scallan, E., R. M. Hoekstra, F. J. Angulo, R. V. Tauxe, M. A. Widdowson, S. L. Roy, J. L. Jones, and P. M. Griffin.** 2011. Foodborne illness acquired in the United States--major pathogens. Emerging infectious diseases **17:**7-15.
46. **Smith, D. B., N. McFadden, R. J. Blundell, A. Meredith, and P. Simmonds.** 2012. Diversity of murine norovirus in wild-rodent populations: species-specific associations suggest an ancient divergence. The Journal of general virology **93:**259-266.
47. **Tahoun, A., S. Mahajan, E. Paxton, G. Malterer, D. S. Donaldson, D. Wang, A. Tan, T. L. Gillespie, M. O'Shea, A. J. Roe, D. J. Shaw, D. L. Gally, A. Lengeling, N. A. Mabbott, J. Haas, and A. Mahajan.** 2012. Salmonella transforms follicle-associated epithelial cells into m cells to promote intestinal invasion. Cell host & microbe **12:**645-656.
48. **Taube, S., A. O. Kolawole, M. Hoehne, J. E. Wilkinson, S. A. Hanley, J. W. Perry, L. B. Thackray, R. Akkina, and C. E. Wobus.** 2013. **A mouse model for Human Norovirus**. MBio **in press**.
49. **Taube, S., J. W. Perry, E. McGreevy, K. Yetming, C. Perkins, K. Henderson, and C. E. Wobus.** 2012. Murine noroviruses bind glycolipid and glycoprotein attachment receptors in a strain-dependent manner. Journal of virology **86:**5584-5593.
50. **Taube, S., J. W. Perry, K. Yetming, S. P. Patel, H. Auble, L. Shu, H. F. Nawar, C. H. Lee, T. D. Connell, J. A. Shayman, and C. E. Wobus.** 2009. Ganglioside-linked terminal sialic acid moieties on murine macrophages function as attachment receptors for murine noroviruses. Journal of virology **83:**4092-4101.

51. **Thackray, L. B., C. E. Wobus, K. A. Chachu, B. Liu, E. R. Alegre, K. S. Henderson, S. T. Kelley, and H. W. Virgin IV.** 2007. Murine noroviruses comprising a single genogroup exhibit biological diversity despite limited sequence divergence. Journal of virology **81:**10460-10473.
52. **Troeger, H., C. Loddenkemper, T. Schneider, E. Schreier, H. J. Epple, M. Zeitz, M. Fromm, and J. D. Schulzke.** 2009. Structural and functional changes of the duodenum in human norovirus infection. Gut **58:**1070-1077.
53. **Wang, J., V. Gusti, A. Saraswati, and D. D. Lo.** 2011. Convergent and divergent development among M cell lineages in mouse mucosal epithelium. J Immunol **187:**5277-5285.
54. **Widdowson, M. A., S. S. Monroe, and R. I. Glass.** 2005. Are noroviruses emerging? Emerging infectious diseases **11:**735-737.
55. **Wobus, C. E., S. M. Karst, L. B. Thackray, K. O. Chang, S. V. Sosnovtsev, G. Belliot, A. Krug, J. M. Mackenzie, K. Y. Green, and H. W. Virgin.** 2004. Replication of Norovirus in cell culture reveals a tropism for dendritic cells and macrophages. PLoS Biol **2:**e432.
56. **Wobus, C. E., L. B. Thackray, and H. W. Virgin IV.** 2006. Murine norovirus: a model system to study norovirus biology and pathogenesis. Journal of virology **80:**5104-5112.

# CHAPTER 3

## Efficient Norovirus and Reovirus Replication in the Mouse Intestine Requires Microfold (M) cells

The work presented in this chapter was recently submitted for publication.

### 3.1 Abstract

Microfold (M) cells are specialized intestinal epithelial cells that internalize particulate antigens and aid in the establishment of immune responses to enteric pathogens. M cells have also been suggested as a portal for pathogen entry into the host. While virus particles have been observed in M cells, it is not known whether viruses use M cells to initiate a productive infection. Noroviruses (NoVs) are single-stranded RNA viruses that infect host organisms via the fecal-oral route. Murine NoV (MNV) infects intestinal macrophages and dendritic cells and provides a tractable experimental system for understanding how an enteric virus overcomes the intestinal epithelial barrier to infect underlying target cells. We found that replication of two divergent MNV strains was reduced in mice depleted of M cells. Reoviruses are double-stranded RNA viruses that infect hosts via respiratory or enteric routes. In contrast to MNV, reovirus infects enterocytes in the intestine. Despite differences in cell tropism, reovirus infection was also reduced in M cell-depleted mice. These data demonstrate

that M cells are required for the pathogenesis of two unrelated enteric viruses that replicate in different cell types within the intestine.

### 3.2 Introduction

The gastrointestinal (GI) tract, being the largest mucosal surface in the body, forms a barrier between the interior and exterior milieu. Although multiple protective mechanisms are present, enteric viruses have evolved strategies to overcome this barrier and infect the host. Some enteric viruses enter the host by directly infecting enterocytes, *e.g.*, rotavirus.(45) Alternatively, microfold (M) cells have been proposed as a route of viral entry after visualization of selective uptake of poliovirus and reovirus particles by Peyer's patch (PP) M cells.(43, 56) However, direct evidence demonstrating that M cells are required for the establishment of a productive virus infection is lacking.

M cells are specialized epithelial cells that are mostly located in the follicle-associated epithelium (FAE) of organized lymphoid tissues like PPs. However, M cells also are found in intestinal villi, although villous M cells are less abundant than PP M cells.(29) M cells selectively bind and endocytose IgA(33) and selectively express GPI-anchored glycoprotein 2 (GP2).(22) Mouse M cells also react with the *Ulex europaeus* agglutinin-I (UEA-I) lectin, which recognizes α1,2 fucose.(13) M cells arise from individual stem cells in the crypt.(41) Development of M cells depends on the receptor activator of NF-κB ligand (RANKL), which is expressed by subepithelial stromal cells in the PP domes.(28) Antibody-mediated neutralization of RANKL in wild-type mice eliminates most PP M cells, while systemic administration of RANKL to RANKL-deficient mice restores PP M cells and induces differentiation of villous M cells.(28) M cells

function to sample antigens in the intestinal lumen for immune surveillance, including microorganisms and inert particles (e.g., latex beads).(14, 31, 35) For example, the bacterial pathogens *Listeria monocytogenes, Salmonella typhimurium, Shigella flexneri*, and *Yersinia enterocolitica* exploit M cells to invade the host and establish infections.(4, 24, 26, 40) In the case of *S. typhimurium*, selective M cell uptake is mediated by a specific ligand-receptor interaction between FimH, a component of type I pili on the bacterial outer membrane, and GP2, a protein specifically expressed on M cells.(22) Binding of secretory IgA to its receptor on M cells is important to facilitate the sampling of commensal bacteria.(39) Remarkably, deletion of M cells in mice by RANKL antibody treatment inhibits prion accumulation and subsequent neuroinvasion,(15) suggesting that M cells are sites of prion uptake. While collectively these studies provide evidence that M cells contribute to the pathogenesis of bacterial and prion diseases, the role of M cells in the initiation of productive virus infection is less clear.

Noroviruses (NoVs) are nonenveloped, highly stable, positive-sense RNA viruses that infect hosts via the fecal-oral route.(21) Little is known about NoV pathogenesis including the early events during infection of the intestine. Murine noroviruses (MNVs) efficiently replicate in macrophages and dendritic cells in cell culture(54) and in mice,(27, 34, 52) providing a tractable experimental system for understanding how an enteric virus overcomes the intestinal epithelial barrier to reach its target cells in the intestinal lamina propria. Despite the high sequence similarity of MNV strains (> 75%), they differ in biological phenotypes.(44, 48) For example, the MNV strain CR3, which was isolated from the feces of mice, persists in wild-type mice for at least 35 days (d), while MNV-1 establishes acute infections, and virus is not detectable in fecal contents 7

d post-inoculation (dpi).(46, 48) Studies using an *in vitro* model of the FAE demonstrated that MNV is transported across a polarized intestinal epithelial monolayer using M-like cells.(20) However, how MNV crosses the intestinal epithelial barrier *in vivo* to reach the underlying permissive macrophages and dendritic cells is not known.

Mammalian reoviruses are another widely used model for studies of viral pathogenesis.(18) Reoviruses are nonenveloped, segmented, double-stranded RNA viruses that cause disease in the very young but do not produce symptoms in adults.(42) Reoviruses are classified into three serotypes represented by the prototype strains, type 1 Lang (T1L), type 2 Jones (T2J), and type 3 Dearing (T3D). While T1L and T3D differ in pathways of virus spread (hematogenous vs. neural, respectively),(51) the primary site of replication for both strains in perorally inoculated newborn mice are intestinal enterocytes at the villus tips.(3) T1L binds to α2-3-linked sialic acid-containing glycans on the apical surface of M cells via the attachment protein σ1.(23, 55) Visualization of virus particles by transmission electron microscopy during the first hours of infection suggests that following binding to the apical surface of M cells, reovirus is internalized into and replicates in M cells, prior to infecting enterocytes from the basolateral surface.(8) However, it is not apparent whether reovirus can establish productive infection in the host in the absence of M cells, for example via apical infection of enterocytes.

In this study, we used an M-cell depletion protocol to investigate whether M cells are required for infection by MNV and reovirus, which replicate in different cell types (macrophages and dendritic cells vs. enterocytes) in the murine intestine. Using a light-sensitive MNV to distinguish between input and replicated virus, we found that two MNV

strains have different replication kinetics and both depend on M cells for efficient intestinal infection. Despite the differences in cell tropism, reovirus infection of the murine intestine also depends on M cells. Thus, intestinal M cells are used as a portal of entry for two unrelated enteric viruses to initiate productive infection in the murine host.

### 3.2 Material and Methods

**Mice.** Wild-type BALB/c (#000651) and 129S6/SvEv STAT1-/- (#2045) mice were purchased from Jackson Laboratory (Bar Harbor, ME) and Taconic Farms (Hudson, NY), respectively. Six- to eight-week-old mice were used for MNV studies, and three- to four-week-old mice were used for reovirus studies. To deplete M cells *in vivo*, Balb/c mice were inoculated intraperitoneally with 250 µg of IK22-5 rat anti-mouse RANKL monoclonal antibody every 2 d for a total of four doses prior to infection as described.(28) A parallel group of mice were similarly treated with a rat isotype-control IgG (Sigma) or left untreated. All mice used in the study were tested for anti-MNV antibodies by ELISA as described(54) and found to be seronegative.

**Virus stocks and plaque assays.** The plaque-purified MNV-1 clone (GV/MNV1/2002/USA) MNV-1.CW3 and the fecally isolated MNV strain CR3 (GV/*CR3*/2005/USA) were used at passage 6 for all experiments.(48) Viral titers were quantified by plaque assay after visualizing plaques by staining cells with a 0.01% neutral red solution in PBS for 1-3 h as described.(19, 54) Reovirus T1L stocks were prepared using reverse genetics.(11, 30) Viral titers were quantified by plaque assay as described.(6)

**Infection of mice with neutral red-containing MNV.** NR-containing MNV stocks were generated as described.(38) All NR virus preparations displayed 100- to 1000-fold reductions in viral titers upon light exposure. Mice were inoculated perorally with $10^5$ PFU MNV (NR), and tissues were aseptically removed using a red safety light 12 (MNV-1) or 18 (CR3) hpi. Regions of the GI tract including the stomach (ST), jejunum/duodenum (J/D), proximal ileum (PI), distal ileum (DI), cecum (CE), and colon (CO) were harvested, and one fecal pellet (FE) was collected. Tissue samples were flash-frozen in a dry ice/ethanol bath and stored at -80°C. Tissues were homogenized in 1 ml of medium with 1.0-mm-diameter zirconia-silica beads (BioSpec Products) using a MagNALyser (Roche Applied Sciences, Hague Road, IN). Plaque assays were performed in duplicate, one in the dark and the other following a 10 min light exposure. Viral plaques were enumerated 48 h later.

**Infection of mice with reovirus.** Three- to four-week-old Balb/c mice were inoculated with $10^6$ PFU of reovirus T1L by oral gavage. Tissue samples were collected 24 hpi and processed as described for MNV with the exception that tissues were homogenized in PBS with $MgCl_2$ and $CaCl_2$. Viral titers were determined by plaque assay using L929 cells.(3)

**Immunostaining of whole-mounts, cryosections, and paraffin embedded tissue.** For whole-mounts, PP were harvested from untreated, IgG isotype control-treated, and anti-RANKL-treated mice at various intervals post-inoculation and vortexed in 1 ml PBS containing 0.05% Tween-20 for 30 seconds. After vortexing, PPs were washed once with PBS, fixed in 4% paraformaldehyde in PBS for 15 min, and permeabilized with 0.1% Triton X-100 for 15 min. PPs were blocked with 10% (v/v) of FBS and 1% (v/v) of

normal goat serum (NGS; Gibco) in PBS for 30 to 60 min. GP2 staining was performed by incubating PPs with a primary rat anti-mouse glycoprotein 2/GP2 (MBL, Woburn, MA) antibody in PBS containing 1 µg/ml DAPI for 1 h, followed by three consecutive PBS washes. PPs were incubated with FITC-conjugated secondary rat anti-IgG antibody (eBioscences, San Diego, CA) for 1 h, along with rhodamin-conjugated *Ulex europeaus* agglutinin I (UEA-1; Vector Laboratories, Burlingame, CA). PPs were washed three times with PBS and mounted with ProLong Gold antifade reagent containing DAPI (Invitrogen, Grand Island, NY) between two coverslips separated by double-stick tape or clay. Images were captured by laser scanning confocal microscopy using the LSM software with a Zeiss confocal microscope. Immunofluorescence images were quantified from 5 to 6 individual PPs using the scoring system of intensities by the Metamorph Premier v6.3 image analysis software (Molecular Devices; Downington, PA).

For cryosections, PPs were harvested from Balb/c or STAT1-/- mice orally infected with MNV ($6 \times 10^7$ pfu/mouse). Tissues were processed as described for whole-mounts. M cells were detected with primary rat anti-mouse glycoprotein 2/GP2 antibody (MBL, Woburn, MA), and MNV was detected with a rabbit polyclonal antibody raised against the MNV non-structural protein N-term(5) generously provided by Dr. Vernon Ward (Otago University, Dunedin, New Zealand). Images were captured using an Olympus BX60 upright microscope.

For paraffin embedded sections from reovirus-infected mice, PPs were harvested from isotype control-treated or anti-RANKL-treated mice, fixed with 10% formalin and embedded in paraffin. Tissues were then sectioned, deparaffinized and immunostained

as described above for whole-mounts using a primary rat anti-mouse glycoprotein 2/GP2 antibody (MBL, Woburn, MA) and anti-reovirus immunoglobulin G (IgG) fractions of rabbit antisera raised against T1L and T3D reovirus(53) purified by protein A Sepharose.(6) Images were captured using an Olympus BX60 upright microscope.

**Statistical analysis.** Data are presented as mean ± standard error of the mean (SEM). Statistical analysis was performed using Prism software version 5.01 (GraphPad Software, CA). The two-tailed Student's *t* test was used to determine statistical significance.

### 3.4 Results

**MNV strains have different replication kinetics.**

Analysis of early events in the virus-host encounter benefits from the ability to distinguish between input and replicated virus. For this purpose, we adapted the light-sensitive, neutral red (NR)-containing MNV(38) for *in vivo* studies. The basic premise of this technology is that the input NR-labeled virions are inactivated upon exposure to light, whereas the progeny virions (virions produced after replication) are no longer labeled with NR and thus become light-insensitive. As proof of concept, BALB/c mice were inoculated perorally with MNV-1 (NR), and the intestine was harvested 3 or 72 hours post-infection (hpi) as representative time points that do not or do permit replication, respectively. As anticipated, progeny virus at or below the limit of detection was observed in the distal ileum and colon at 3 hpi, while a significant amount of input virus was observed in the colon at this timepoint (Figure 3.1a). In contrast, newly replicated virus was observed at 72 hpi in the distal ileum, the primary site of MNV-1

replication,(48) but not in the colon (Figure 3.1a). Therefore, NR-containing MNV enables the study of early events during pathogenesis and allows input virus to be distinguished from newly formed virus.

To identify an early time point at which lab-adapted MNV strain MNV-1 and persistent MNV strain CR3 undergo the first round of viral replication, BALB/c mice were inoculated perorally with NR-containing MNV-1 or CR3, and viral titers in the intestine were quantified by plaque assay at 12, 24, or 72 hpi (Figures 3.1b-d). Maximum levels of newly replicated virus from mice infected with MNV-1 (NR) were detected in the small intestine (jejunum/duodenum, proximal ileum, distal ileum) or large intestine (cecum) at 12 hpi. In contrast, CR3 (NR) replicated mostly in the cecum at 12 hpi, while maximum levels of replicated virus throughout the entire GI tract were reached at 72 hpi. These data confirmed previous reports from experiments using C57BL/6 mice that CR3 but not MNV-1 replicates in the colon(46) and demonstrated that CR3 has slower replication kinetics than MNV-1 *in vivo*. More importantly, these data demonstrate that this light-sensitive virus is a powerful tool to investigate early events in viral pathogenesis.

**MNV requires M cells for productive infection.**

To determine whether M cells are required to initiate a productive MNV infection *in vivo*, BALB/c mice were selectively depleted of M cells using an antibody against RANKL (anti-RANKL) administered intraperitoneally (i.p.) every 2 d for a total of four doses as described (Figure 3.2a)(28) and infected with either MNV-1 or CR3. This M cell depletion protocol does not alter the presence and distribution of F4/80+ and CD11c+ cells in the intestine, gastrointestinal lymphoid follicles, and spleen, most likely

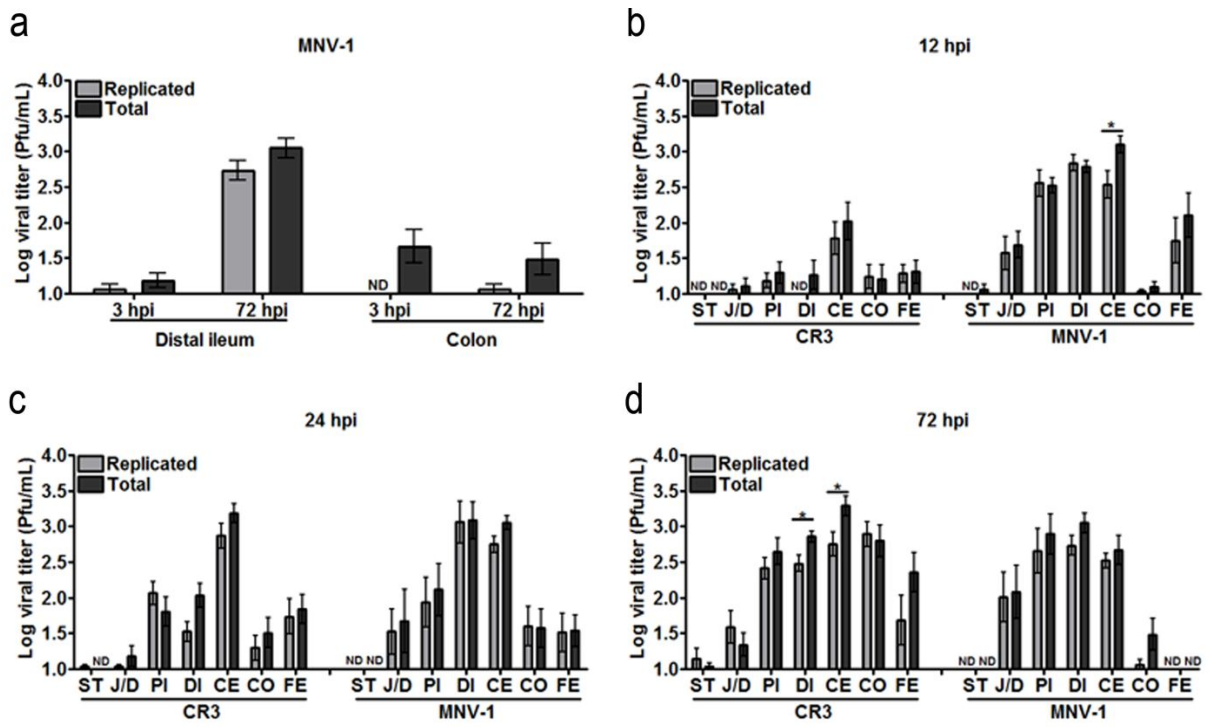


**Figure 3.1. The neutral red assay distinguishes between input and replicated MNV.** (**a**) BALB/c mice (7-to-8 weeks old) were inoculated perorally with $10^5$ PFU of a neutral red-containing MNV-1. Distal ileum and colon were harvested at the times shown. Viral titers were determined by plaque assay in the light (replicated) or dark (total). (**b-d**) MNV strains differ in replication kinetics. BALB/c mice were inoculated perorally with $10^5$ PFU of either MNV-1 or CR3 containing neutral red. The GI tract was dissected 12, 24, or 72 h later, and viral titers determined by plaque assay as for (**a**). Data are expressed as mean ± SEM for three independent experiments. *, $P < 0.05$; ND = not detectable; ST = stomach; J/D = jejunum/duodenum; PI = proximal ileum; DI = distal ileum; CE = cecum; CO = colon; FE = feces.

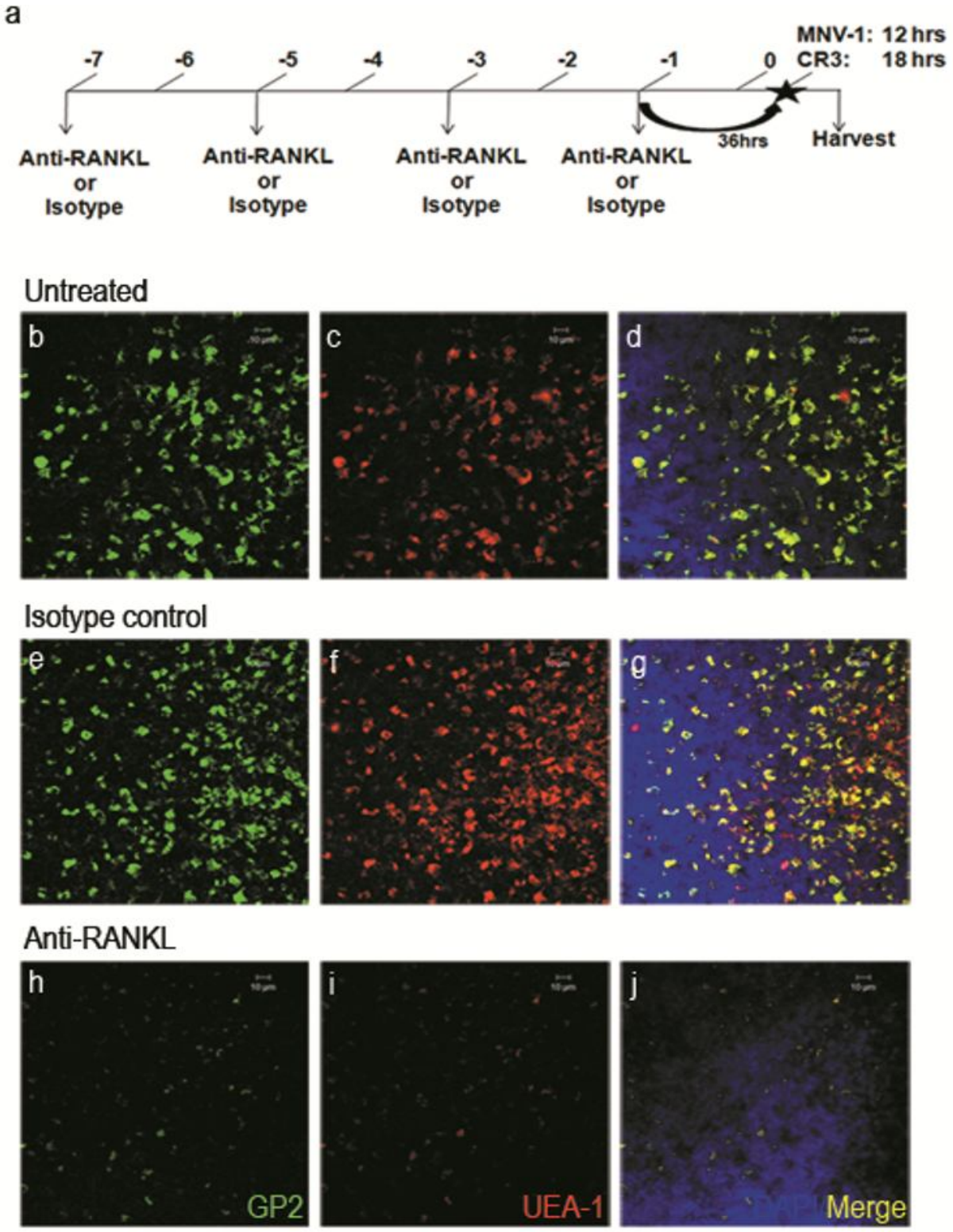
a
MNV-1: 12 hrs
CR3: 18 hrs
-7
-6
-5
-4
-3
-2
-1
0
36hrs
Harvest
Anti-RANKL or Isotype
Anti-RANKL or Isotype
Anti-RANKL or Isotype
Anti-RANKL or Isotype
Untreated
b
c
d
Isotype control
e
f
g
Anti-RANKL
h
i
j
GP2
UEA-1
Merge

**Figure 3.2. Whole-mount staining of Peyer's patches shows decreased numbers of M cells in anti-RANKL-treated mice.** (**a**) Schematic of the experimental design for M cell depletions. BALB/c mice were inoculated i.p. with anti-RANKL or isotype control antibody every other day for a total of four doses, infected with either MNV-1 (NR) or CR3 (NR) 36 h later, and regions of the GI tract were harvested 12 hpi for MNV-1 and 18 hpi for CR3. (**b-j**) Representative confocal microscopic images of Peyer's patches stained with M cell markers GP2 (green) and UEA-1 (red) from untreated (**b-d**), isotype-control-treated (**e-g**), and anti-RANKL-treated (**h-j**) mice. DAPI was used to stain the nuclei. A 10 µm scale bar is shown in the upper right corner of each image.

because macrophages and DCs at these sites express negligible levels of RANK.(15) As depletion controls, mice were administered an IgG isotype control antibody or left untreated. At 36 h following the last dose, mice were inoculated perorally with MNV-1 (NR) or CR3 (NR). The GI tract was excised at 12 hpi for MNV-1 (NR) or 18 hpi for CR3 (NR), and viral titers were determined by plaque assay. An early time point was chosen for each virus to capture the first round of viral replication, because we reasoned that if MNV enters via M cells, reducing the number of M cells should reduce the number of virus particles capable of reaching the underlying target cells (i.e., macrophages and dendritic cells). To verify that M cells were successfully depleted, PPs were harvested from each mouse, fixed, and prepared for whole-mount staining using two M-cell markers, GP2 and UEA-1 (Figures 3.2b-j). Both M cell markers showed significantly reduced staining in the PPs of anti-RANKL-treated mice (Figures 3.2h-j and Figure 3.3) compared with isotype-control-treated animals (Figures 3.2e-g and Figure 3.3) or untreated mice (Figures 3.2b-d and Figure 3.3). Total MNV-1 titers were significantly decreased in the distal ileum and feces of mice treated with anti-RANKL compared with control animals, while replicated MNV-1 titers also were decreased in the cecum (Figures 3.4a and b). Anti-RANKL-treated mice perorally inoculated with CR3 (NR) produced significantly decreased total and replicated viral titers in the cecum and feces but not the jejunum/duodenum, proximal ileum, or distal ileum compared with control animals (Figures 3.4c and d). These data suggest that M cells are required for efficient MNV entry into and early replication in the mouse intestine. To test if MNV infects M cells, immunostaining of the M cell marker GP2 and the viral protein N-term, which is only expressed during active replication, was performed in PPs sections from MNV-

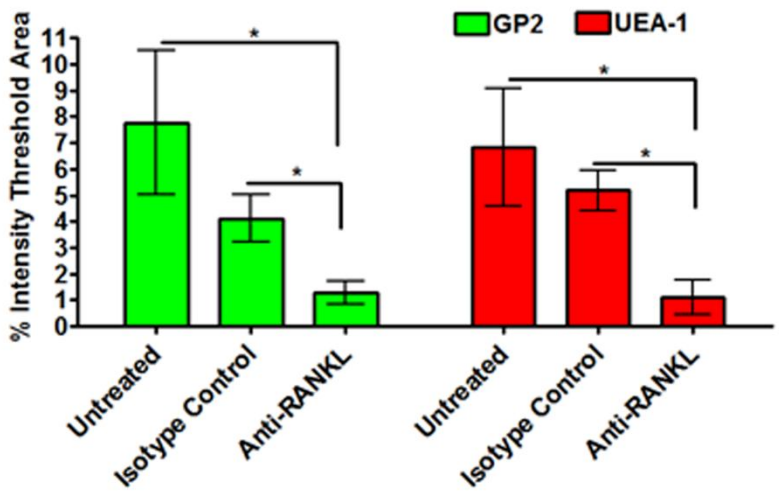


**Figure 3.3. Quantification of whole-mount staining of Peyer's patches for mouse depletion studies.** BALB/c mice (7-to-8 weeks old) were inoculated i.p. with anti-RANKL or isotype control antibody every other day for a total of four doses or left untreated. One Peyer's patch per mouse from a total of 5-to-6 mice per group was harvested and stained with M cell markers GP2 and UEA-1. Immunofluorescence staining was quantified using the scoring system of intensities by the Metamorph Premier v6.3 image analysis software. Data are expressed as mean ± SEM for three independent experiments. *, $P < 0.05$

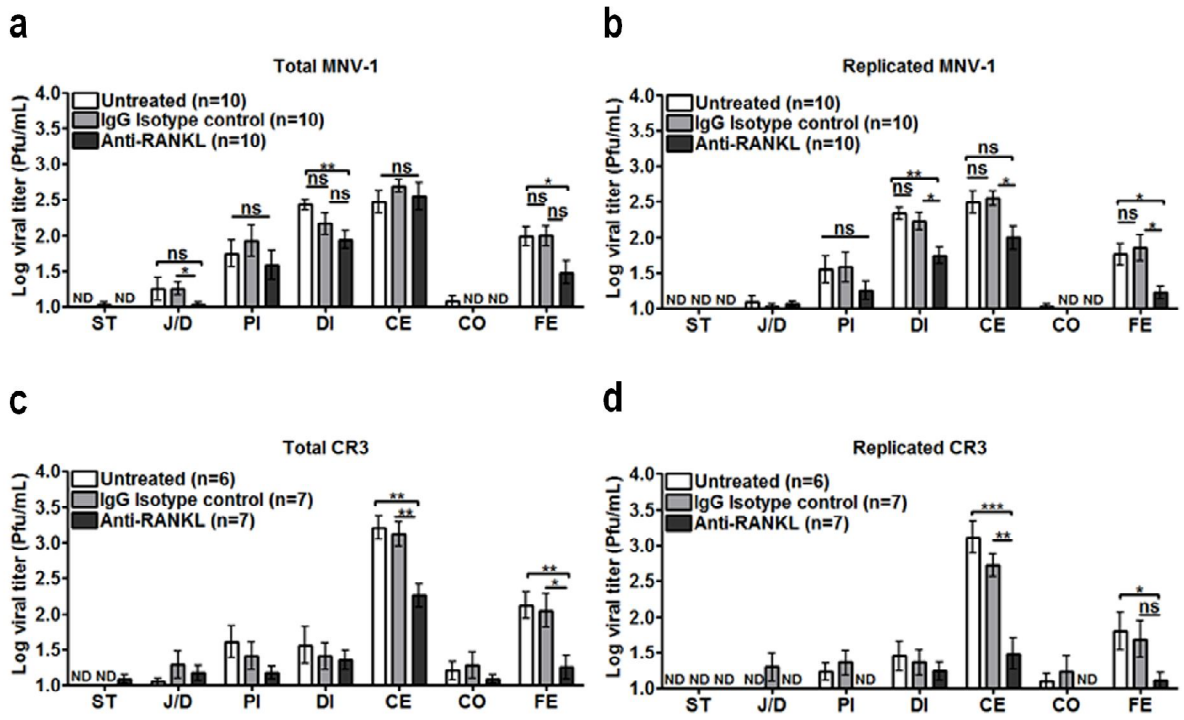


**Figure 3.4. MNV infection is reduced in the GI tract following M cell depletion.** (**a-d**) BALB/c mice (7-to-8 weeks old) were inoculated i.p. with anti-RANKL or isotype control antibody every other day for a total of four doses or left untreated. The number of mice analyzed in each group is indicated in parentheses. Viral titers were quantified by plaque assay in the dark (total, **a** and **c**) or in the light (replicated, **b** and **d**). Data are expressed as mean ± SEM for two-to-three independent experiments. *, $P < 0.05$; **, $P < 0.01$; ***, $P < 0.001$; ns = not significant; ND = not detectable; ST = stomach; J/D = jejunum/duodenum; PI = proximal ileum; DI = distal ileum; CE = cecum; CO = colon; FE = feces.

infected wild-type mice and STAT1-/- mice (which are mice highly susceptible to MNV infection (27, 34)). Our results show that MNV replicates in cells located in the subepithelial dome underneath the FAE in highly susceptible STAT1-/- mice, but not in M cells (Figure 3.7). Taken together, our data suggest that while MNV does not infect M cells, it requires M cells for efficient MNV entry and replication in the mouse intestine.

**Reovirus requires M cells for a productive infection in mice.**

To determine whether an unrelated virus that replicates in a different cell type within the intestine compared with MNV also traverses the intestinal mucosal barrier using M cells, we tested the effect of M cell depletion on reovirus infection. M cells weredepleted from mice prior to peroral inoculation with reovirus strain T1L, and viral titers were determined by plaque assay at 24 hpi. Mice treated with anti-RANKL had no detectable reovirus titers in the jejunum/duodenum, proximal ileum, cecum, and colon compared with isotype control-treated or untreated animals (Figure 3.5). In addition, significantly lower titers were produced in the distal ileum and feces (Figure 3.5). Taken together, these data demonstrate that like MNV, reovirus requires M cells to establish a productive infection in the murine host.

## 2.5 Discussion

The initial steps of virus entry into an infected animal can dictate host range and pathogenesis and offer a point of potential intervention. However, little is known about how enteric viruses cross the intestinal barrier and initiate a productive infection. Virus particles have been observed within M cells, implicating this cell type as a portal of entry into the host, but whether these particles actually initiate a productive infection in

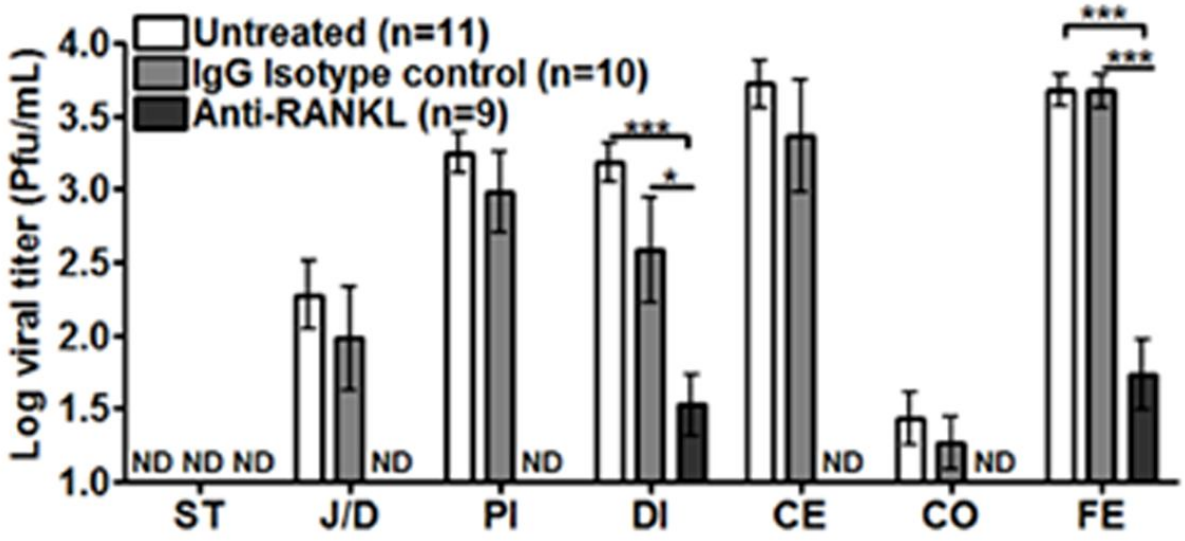


**Figure 3.5. Reovirus infection is reduced in the GI tract following M cell depletion.** BALB/c mice (3-to-4 weeks old) were depleted of M cells as described in Figure 3.1, inoculated perorally with T1L reovirus 24 h later, and regions of the GI tract were harvested 24 hpi. The number of mice analyzed in each group is indicated in parentheses. Viral titers were quantified by plaque assay. Data are expressed as mean ± SEM for two independent experiments. *, $P < 0.05$; ***, $P < 0.001$; ND = not detectable; ST = stomach; J/D = jejunum/duodenum; PI = proximal ileum; DI = distal ileum; CE = cecum; CO = colon; FE = feces.

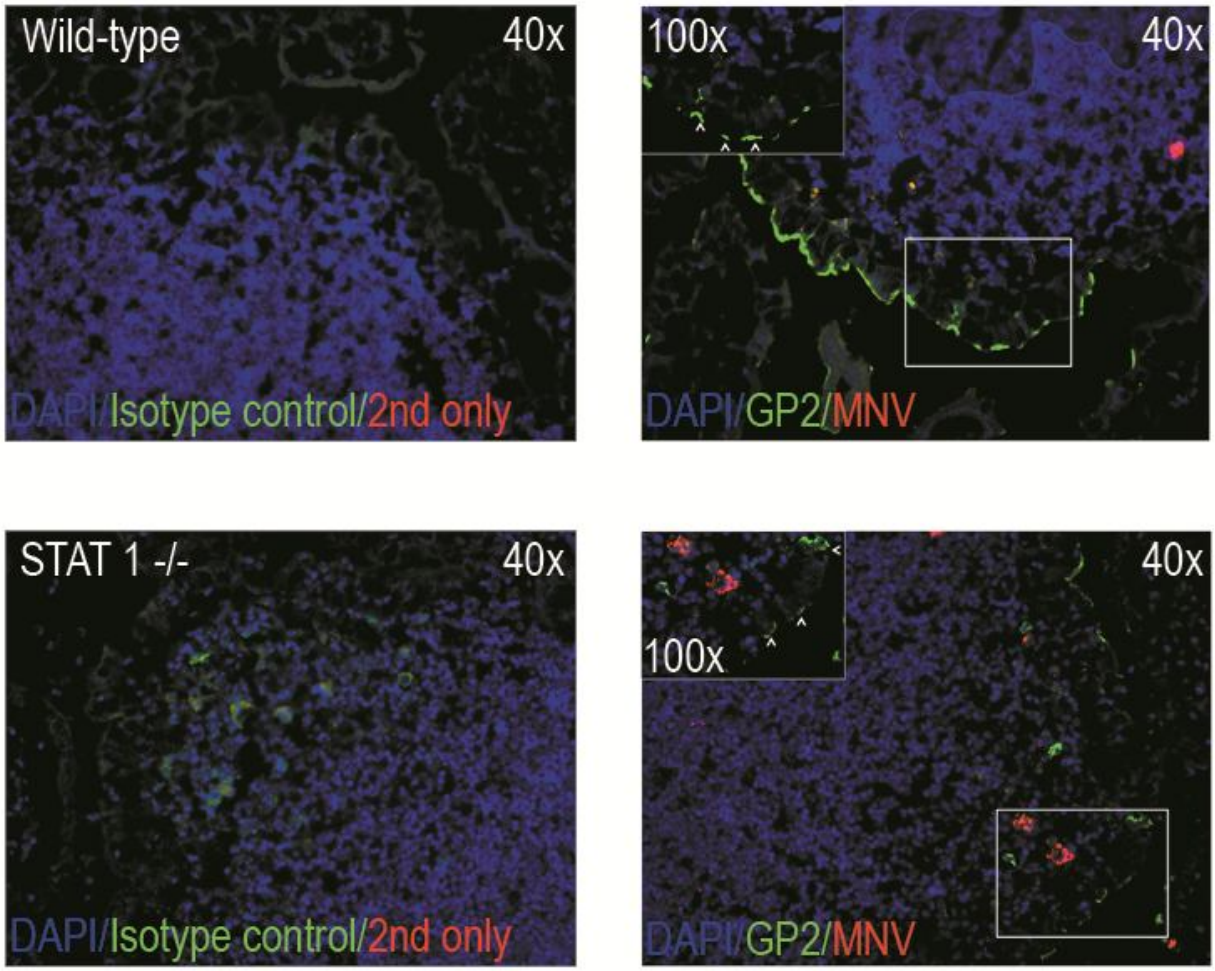


**Figure 3.6. MNV does not replicate in M cells.** Balb/c and STAT1-/- mice were infected with MNV, and Peyer's patches were harvested 24 hpi for cryosectioning and immunostaining. MNV replication was detected using an antibody against the nonstructural protein N-term (red), and M cells were detected using an anti-GP2 antibody (green).

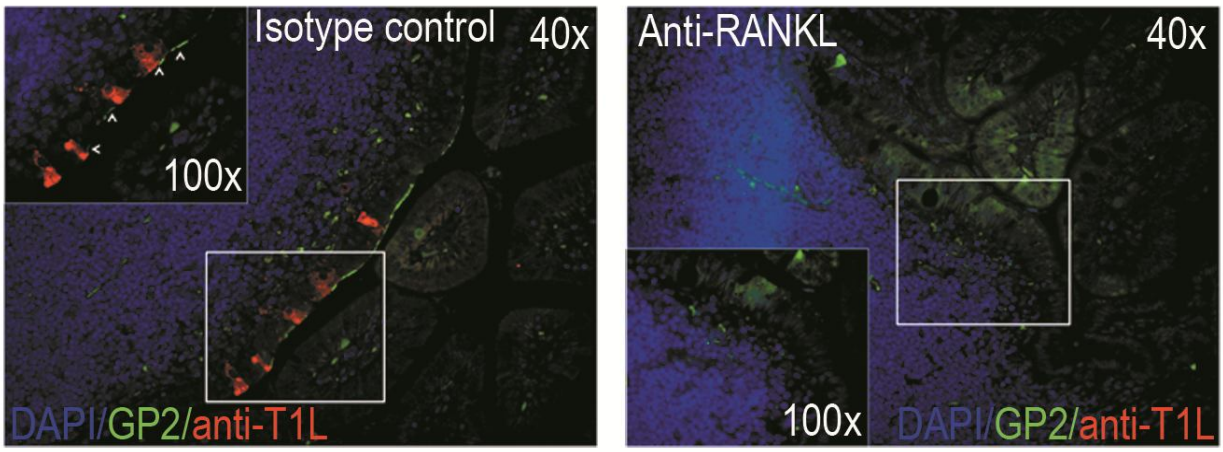


**Figure 3.7. Reovirus replicates in enterocytes adjacent to M cells of control mice but not in M cell-depleted mice.** Isotype control-treated or anti-RANKL-treated Balb/c mice were infected with reovirus for 24 h. Peyer's patches were harvested for paraffin embedding and immunostaining. Reovirus replication was detected using an antibody raised against reovirus T1L and T3D (red), and M cells were detected using an anti-GP2 antibody (green).

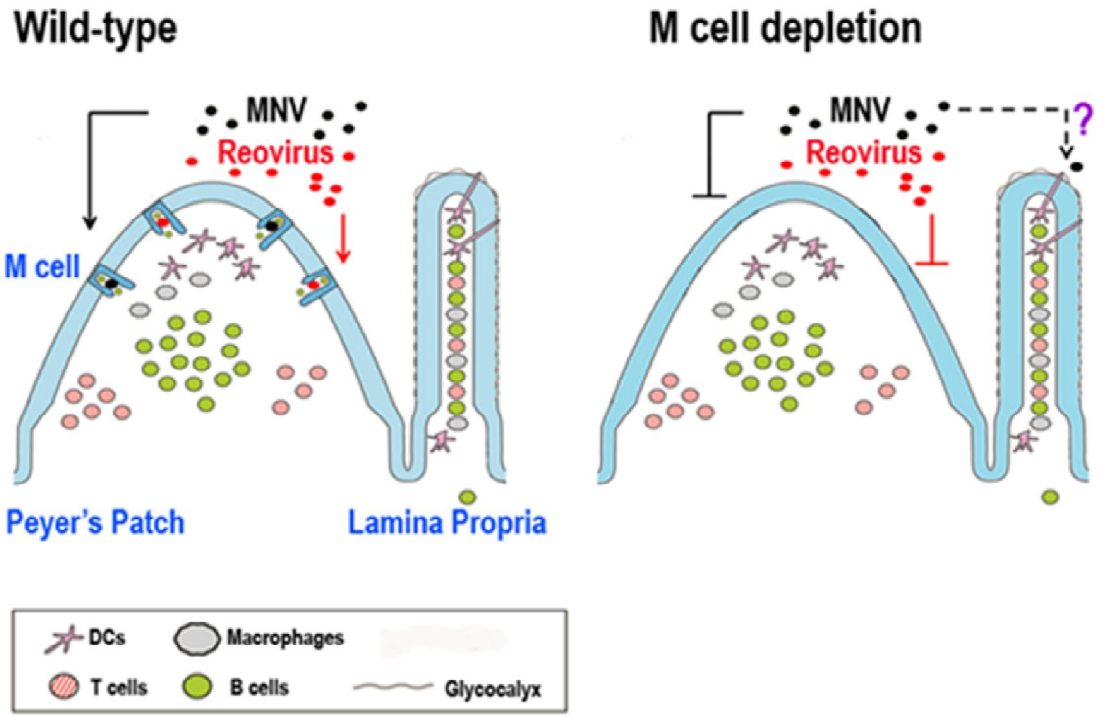


**Figure 3.8. Proposed mechanisms of MNV and reovirus entry into the intestinal mucosa.** MNV (black circles) and reovirus (red circles) in the intestinal lumen initially interact with M cells within the follicle-associated epithelium (FAE) overlying Peyer's patches (PP) to establish a productive infection in untreated animals. However, in mice depleted of M cells, reovirus infection in the gastrointestinal tract is substantially diminished, while MNV infection is only partially reduced. It is possible that trans-epithelial dendritic cell processes provide an alternative route of entry for MNV.

addition to contributing to the development of antiviral immune responses is not clear. The M cell depletion studies presented here collectively point to the importance of M cells in the pathogenesis of enteric viruses that replicate within intestinal epithelial cells (reovirus) or intestinal mononuclear phagocytes (MNV) (Figure 3.8).

Adapting the use of neutral red-labeled MNV for pathogenesis studies enabled us to determine that the MNV strain CR3 has slower replication kinetics in the GI tract than does strain MNV-1 (Figure 3.1). CR3 causes a persistent infection in mice and shares the viral determinant for persistence (Glu94 in the N-terminal protein) identified in CR6, while MNV-1 causes an acute infection.(27, 36, 48) A similar correlation between replication kinetics and persistence was observed for lymphocytic choriomeningitis virus (LCMV), leading to the hypothesis that slowly replicating viruses might evade immune surveillance to allow persistent infection.(10) In addition, MNV-1 and CR3 display different carbohydrate-binding properties in macrophages and differences in tropism for the colon.(46, 47) Thus, it is possible that infection of macrophages, the precise tissue sites of replication, or the effectiveness of immune surveillance contribute to the persistence phenotype of CR3 or the enhanced clearance of MNV-1. Future studies are required to determine the mechanism of MNV persistence.

Our results demonstrate that M cells facilitate the initial steps of productive MNV infection in mice. Viral titers were significantly reduced within the GI tract following depletion of M cells in animals infected with either of two MNV strains (Figure 3.4). M cells are not likely susceptible to MNV replication, as M-like cells do not become infected in an *in vitro* model of the FAE.(20) Our *in vivo* findings (Figure 3.6) are consistent with the *in vitro* data. Unfortunately, despite using multiple assays

(immunofluorescence, immunohistochemistry, and flow cytometry), we were unable to detect viral replication in PPs of wild-type Balb/c mice. This finding most likely reflects the very low number of infected cells in wild-type mice, as has been observed previously.(34) Together, these data point to M cells as a conduit for MNV transport across the mucosa but not as a site for replication as is seen with some viruses.(12) However, residual MNV was still detectable within the GI tract of anti-RANKL-treated mice. One reason for this occurrence could be the incomplete depletion of M cells, as weak GP2 expression was detected in PPs from depleted mice (see Figures 3.2h and Figure 3.3). In addition, we cannot exclude the presence of villous M cells following M cell depletion. We focused on PPs to quantify M cell depletion because the majority of M cells are located in PPs, and villous M cells are rare.(28) The effect of RANKL depletion on villous M cells has not been examined, although villous M cells have been reported to be induced by RANKL.(28)

In addition, the likelihood of incomplete M cell depletion in our studies suggests that once residual virus has crossed the intestinal epithelium and undergone the first round of replication, progeny virus will be capable of infecting new cells for additional rounds of replication. Thus, differences in viral titers in M-cell- and control-depleted mice likely will diminish with increasing rounds of replication. A second possibility is that MNV may use multiple mechanisms to cross the epithelial barrier. Since MNV infects DCs, sentinel DCs that insert dendritic processes between intestinal epithelial cells(37) or M cell-specific transcellular pores(32) may provide an alternate route of MNV entry (Figure 3.8). It is unlikely that the DC pathway is up-regulated only under these specific experimental conditions. PP DCs and macrophages express negligible levels of

Tnfrsf11a, the gene encoding RANK, and mice treated with anti-RANKL antibody have normal numbers and distribution of DCs and macrophages in the intestine and spleen.(15, 50) In addition, while RANKL can stimulate the activity of DCs to activate T cells,(2) the timeframe of our experiments (less than 24 h) is too short for antiviral T cell activity, which is not detectable until 7-8 d postinfection.(9, 49) The incomplete block to MNV replication observed in our study is in contrast to another study in which M cells were depleted using the same anti-RANKL antibody approach. This study shows that prion disease progression in the brain following peroral prion inoculation is abolished following M cell depletion.(15) Mice completely lacking M cells will be required to determine whether M cells are the only route used by MNV to infect mice.

Depletion of M cells substantially reduced reovirus titers in the intestine of infected mice (Figure 3.5), indicating that M cells also are required for the initiation of a productive infection with reovirus. After proteolytic conversion of reovirus T1L virions to infectious subvirion particles (ISVPs) in the small intestine of mice,(1, 7) reovirus binds to α2,3-linked sialic acid on the apical surface of M cells via the attachment protein σ1.(8, 23, 55) By electron microscopy, reovirus particles are observed in M cells within vesicles, suggesting that virions are endocytosed into these cells. In suckling mice, viral particles also are observed in M cells within cytoplasmic inclusions, which are a hallmark of reovirus replication.(8) Interestingly, our studies using PPs from isotype-treated adult mice immunostained with the M cell-specific marker GP2 and an anti-reovirus antibody showed that the majority of reovirus-positive cells were enterocytes adjacent to M cell positive cells, while only the occasional cell stained positive for both markers (Figure 3.7). No reovirus staining was observed in anti-RANKL-treated

animals, consistent with the absence of reovirus plaque-forming units in the small intestine of these mice (see Figure 3.5). Similar GP2 and reovirus staining patterns were seen by immunohistochemistry (data not shown). Previous studies indicate that reovirus virions prefererenttially adhere to and are taken up from the basolateral surfaceof epithelial cells cultivated from the murine small intestine.(8) Our data are consistent with those earlier findings and further support the model that reovirus infection is initiated by the uptake of virions into and transport across M cells followed by basolateral infection of enterocytes, in which reovirus replicates.(3) Conversely, it is highly unlikely that reovirus infects enterocytes from the apical side to initiate a productive infection of the host. Reovirus also is capable of infecting human airway epithelial cells via the basolateral route,(16) suggesting common themes of reovirus infection of polarized epithelia.

Reovirus titers in the GI tract following M cell depletion were reduced to a substantially greater extent compared with titers of MNV in M-cell depleted mice (compare Figure 3.4 and Figure 3.5). While these findings might reflect differences in replication kinetics, we favor an alternate explanation. Reovirus does not replicate in DCs(17) and, thus, we think it is dependent on M cells for transport across the epithelial barrier. In contrast, MNV replicates in DCs,(54) which can extend dendrites across the epithelial barrier, providing an alternative entry route for the virus to access the host (Figure 3.8).

Our findings demonstrate that M cells are an essential gateway for MNV and reovirus infection and serve an important role in the initiation of productive infection in addition to their function in development of immune responses.(31) The question of

whether M cells are used universally by all enteric viruses during pathogenesis or only by specific enteric viruses remains to be determined. Nonetheless, the induction of mucosal immunity via targeting M cells is an area of intense research(25) and identifying surface molecules involved in MNV and reovirus uptake by M cells may reveal new strategies for the development of mucosal vaccines. Moreover, knowledge that M cells are used as entry portals by at least some enteric virus infections opens up potential therapeutic approaches for the use of non-infectious viral particles as drug-delivery vehicles to prevent or treat infectious diseases.

## 2.6 References


1. **Amerongen, H. M., G. A. Wilson, B. N. Fields, and M. R. Neutra.** 1994. Proteolytic processing of reovirus is required for adherence to intestinal M cells. Journal of virology **68:**8428-8432.
2. **Anderson, D. M., E. Maraskovsky, W. L. Billingsley, W. C. Dougall, M. E. Tometsko, E. R. Roux, M. C. Teepe, R. F. DuBose, D. Cosman, and L. Galibert.** 1997. A homologue of the TNF receptor and its ligand enhance T-cell growth and dendritic-cell function. Nature **390:**175-179.
3. **Antar, A. A., J. L. Konopka, J. A. Campbell, R. A. Henry, A. L. Perdigoto, B. D. Carter, A. Pozzi, T. W. Abel, and T. S. Dermody.** 2009. Junctional adhesion molecule-A is required for hematogenous dissemination of reovirus. Cell host & microbe **5:**59-71.
4. **Autenrieth, I. B., and R. Firsching.** 1996. Penetration of M cells and destruction of Peyer's patches by Yersinia enterocolitica: an ultrastructural and histological study. Journal of medical microbiology **44:**285-294.
5. **Baker, E. S., S. R. Luckner, K. L. Krause, P. R. Lambden, I. N. Clarke, and V. K. Ward.** 2012. Inherent structural disorder and dimerisation of murine norovirus NS1-2 protein. PLoS ONE **7:**e30534.
6. **Barton, E. S., J. L. Connolly, J. C. Forrest, J. D. Chappell, and T. S. Dermody.** 2001. Utilization of sialic acid as a coreceptor enhances reovirus attachment by multistep adhesion strengthening. The Journal of biological chemistry **276:**2200-2211.
7. **Bass, D. M., D. Bodkin, R. Dambrauskas, J. S. Trier, B. N. Fields, and J. L. Wolf.** 1990. Intraluminal proteolytic activation plays an important role in replication of type 1 reovirus in the intestines of neonatal mice. Journal of virology **64:**1830-1833.

8. **Bass, D. M., J. S. Trier, R. Dambrauskas, and J. L. Wolf.** 1988. Reovirus type I infection of small intestinal epithelium in suckling mice and its effect on M cells. Laboratory investigation; a journal of technical methods and pathology **58:**226-235.
9. **Bharhani, M. S., J. S. Grewal, M. J. Pilgrim, C. Enocksen, R. Peppler, L. London, and S. D. London.** 2005. Reovirus serotype 1/strain Lang-stimulated activation of antigen-specific T lymphocytes in Peyer's patches and distal gut-mucosal sites: activation status and cytotoxic mechanisms. J Immunol **174:**3580-3589.
10. **Bocharov, G., B. Ludewig, A. Bertoletti, P. Klenerman, T. Junt, P. Krebs, T. Luzyanina, C. Fraser, and R. M. Anderson.** 2004. Underwhelming the immune response: effect of slow virus growth on CD8+-T-lymphocyte responses. Journal of virology **78:**2247-2254.
11. **Boehme, K. W., M. Ikizler, T. Kobayashi, and T. S. Dermody.** 2011. Reverse genetics for mammalian reovirus. Methods **55:**109-113.
12. **Buller, C. R., and R. A. Moxley.** 1988. Natural infection of porcine ileal dome M cells with rotavirus and enteric adenovirus. Veterinary pathology **25:**516-517.
13. **Clark, M. A., M. A. Jepson, N. L. Simmons, T. A. Booth, and B. H. Hirst.** 1993. Differential expression of lectin-binding sites defines mouse intestinal M-cells. J Histochem Cytochem **41:**1679-1687.
14. **Corr, S. C., C. C. Gahan, and C. Hill.** 2008. M-cells: origin, morphology and role in mucosal immunity and microbial pathogenesis. FEMS Immunol Med Microbiol **52:**2-12.
15. **Donaldson, D. S., A. Kobayashi, H. Ohno, H. Yagita, I. R. Williams, and N. A. Mabbott.** 2012. M cell-depletion blocks oral prion disease pathogenesis. Mucosal Immunol **5:**216-225.
16. **Excoffon, K. J., K. M. Guglielmi, J. D. Wetzel, N. D. Gansemer, J. A. Campbell, T. S. Dermody, and J. Zabner.** 2008. Reovirus preferentially infects the basolateral surface and is released from the apical surface of polarized human respiratory epithelial cells. The Journal of infectious diseases **197:**1189-1197.
17. **Fleeton, M. N., N. Contractor, F. Leon, J. D. Wetzel, T. S. Dermody, and B. L. Kelsall.** 2004. Peyer's patch dendritic cells process viral antigen from apoptotic epithelial cells in the intestine of reovirus-infected mice. The Journal of experimental medicine **200:**235-245.
18. **Forrest, J. C., and T. S. Dermody.** 2003. Reovirus receptors and pathogenesis. Journal of virology **77:**9109-9115.
19. **Gonzalez-Hernandez, M. B., J. Bragazzi Cunha, and C. E. Wobus.** 2012. Plaque assay for murine norovirus. J Vis Exp**:**e4297.
20. **Gonzalez-Hernandez, M. B., T. Liu, L. P. Blanco, H. Auble, H. C. Payne, and C. E. Wobus.** 2013. Murine Norovirus Transcytosis across an In Vitro Polarized Murine Intestinal Epithelial Monolayer Is Mediated by M-Like Cells. Journal of virology **87:**12685-12693.
21. **Hansman, G. S., X. J. Jiang, and K. Y. Green.** 2010. Caliciviruses Molecular and Cellular Virology, 1 ed, vol. 1. Caister Academic Press, Norfolk, UK.

22. **Hase, K., K. Kawano, T. Nochi, G. S. Pontes, S. Fukuda, M. Ebisawa, K. Kadokura, T. Tobe, Y. Fujimura, S. Kawano, A. Yabashi, S. Waguri, G. Nakato, S. Kimura, T. Murakami, M. Iimura, K. Hamura, S. Fukuoka, A. W. Lowe, K. Itoh, H. Kiyono, and H. Ohno.** 2009. Uptake through glycoprotein 2 of FimH(+) bacteria by M cells initiates mucosal immune response. Nature **462:**226-230.
23. **Helander, A., K. J. Silvey, N. J. Mantis, A. B. Hutchings, K. Chandran, W. T. Lucas, M. L. Nibert, and M. R. Neutra.** 2003. The viral sigma1 protein and glycoconjugates containing alpha2-3-linked sialic acid are involved in type 1 reovirus adherence to M cell apical surfaces. Journal of virology **77:**7964-7977.
24. **Jensen, V. B., J. T. Harty, and B. D. Jones.** 1998. Interactions of the invasive pathogens Salmonella typhimurium, Listeria monocytogenes, and Shigella flexneri with M cells and murine Peyer's patches. Infection and immunity **66:**3758-3766.
25. **Jepson, M. A., M. A. Clark, and B. H. Hirst.** 2004. M cell targeting by lectins: a strategy for mucosal vaccination and drug delivery. Advanced drug delivery reviews **56:**511-525.
26. **Jones, B. D., N. Ghori, and S. Falkow.** 1994. Salmonella typhimurium initiates murine infection by penetrating and destroying the specialized epithelial M cells of the Peyer's patches. The Journal of experimental medicine **180:**15-23.
27. **Karst, S. M., C. E. Wobus, M. Lay, J. Davidson, and H. W. Virgin.** 2003. STAT1-dependent innate immunity to a Norwalk-like virus. Science (New York, N.Y **299:**1575-1578.
28. **Knoop, K. A., N. Kumar, B. R. Butler, S. K. Sakthivel, R. T. Taylor, T. Nochi, H. Akiba, H. Yagita, H. Kiyono, and I. R. Williams.** 2009. RANKL is necessary and sufficient to initiate development of antigen-sampling M cells in the intestinal epithelium. J Immunol **183:**5738-5747.
29. **Knoop, K. A., M. J. Miller, and R. D. Newberry.** 2013. Transepithelial antigen delivery in the small intestine: different paths, different outcomes. Current opinion in gastroenterology **29:**112-118.
30. **Kobayashi, T., L. S. Ooms, M. Ikizler, J. D. Chappell, and T. S. Dermody.** 2010. An improved reverse genetics system for mammalian orthoreoviruses. Virology **398:**194-200.
31. **Kraehenbuhl, J. P., and M. R. Neutra.** 2000. Epithelial M cells: differentiation and function. Annu Rev Cell Dev Biol **16:**301-332.
32. **Lelouard, H., M. Fallet, B. de Bovis, S. Meresse, and J. P. Gorvel.** 2012. Peyer's patch dendritic cells sample antigens by extending dendrites through M cell-specific transcellular pores. Gastroenterology **142:**592-601 e593.
33. **Mantis, N. J., M. C. Cheung, K. R. Chintalacharuvu, J. Rey, B. Corthesy, and M. R. Neutra.** 2002. Selective adherence of IgA to murine Peyer's patch M cells: evidence for a novel IgA receptor. J Immunol **169:**1844-1851.
34. **Mumphrey, S. M., H. Changotra, T. N. Moore, E. R. Heimann-Nichols, C. E. Wobus, M. J. Reilly, M. Moghadamfalahi, D. Shukla, and S. M. Karst.** 2007. Murine norovirus 1 infection is associated with histopathological changes in immunocompetent hosts, but clinical disease is prevented by STAT1-dependent interferon responses. Journal of virology **81:**3251-3263.

35. **Neutra, M. R., N. J. Mantis, A. Frey, and P. J. Giannasca.** 1999. The composition and function of M cell apical membranes: implications for microbial pathogenesis. Seminars in immunology **11:**171-181.
36. **Nice, T. J., D. W. Strong, B. T. McCune, C. S. Pohl, and H. W. Virgin.** 2013. A single-amino-acid change in murine norovirus NS1/2 is sufficient for colonic tropism and persistence. Journal of virology **87:**327-334.
37. **Niess, J. H., S. Brand, X. Gu, L. Landsman, S. Jung, B. A. McCormick, J. M. Vyas, M. Boes, H. L. Ploegh, J. G. Fox, D. R. Littman, and H. C. Reinecker.** 2005. CX3CR1-mediated dendritic cell access to the intestinal lumen and bacterial clearance. Science (New York, N.Y **307:**254-258.
38. **Perry, J. W., and C. E. Wobus.** 2010. Endocytosis of murine norovirus 1 into murine macrophages is dependent on dynamin II and cholesterol. Journal of virology **84:**6163-6176.
39. **Rol, N., L. Favre, J. Benyacoub, and B. Corthesy.** 2012. The role of secretory immunoglobulin A in the natural sensing of commensal bacteria by mouse Peyer's patch dendritic cells. The Journal of biological chemistry **287:**40074-40082.
40. **Sansonetti, P. J., J. Arondel, J. R. Cantey, M. C. Prevost, and M. Huerre.** 1996. Infection of rabbit Peyer's patches by Shigella flexneri: effect of adhesive or invasive bacterial phenotypes on follicle-associated epithelium. Infection and immunity **64:**2752-2764.
41. **Sato, T., R. G. Vries, H. J. Snippert, M. van de Wetering, N. Barker, D. E. Stange, J. H. van Es, A. Abo, P. Kujala, P. J. Peters, and H. Clevers.** 2009. Single Lgr5 stem cells build crypt-villus structures in vitro without a mesenchymal niche. Nature **459:**262-265.
42. **Schiff, L. A., M. L. Nibert, and K. L. Tyler.** 2007. Orthoreoviruses and their replication, p. 1853-1915. *In* D. M. Knipe and P. M. Howley (ed.), Fields virology, 5 ed, vol. 2. Lippincott Wiliams & Wilkins, Philadelphia, PA.
43. **Sicinski, P., J. Rowinski, J. B. Warchol, Z. Jarzabek, W. Gut, B. Szczygiel, K. Bielecki, and G. Koch.** 1990. Poliovirus type 1 enters the human host through intestinal M cells. Gastroenterology **98:**56-58.
44. **Smith, D. B., N. McFadden, R. J. Blundell, A. Meredith, and P. Simmonds.** 2012. Diversity of murine norovirus in wild-rodent populations: species-specific associations suggest an ancient divergence. The Journal of general virology **93:**259-266.
45. **Starkey, W. G., D. C. Candy, D. Thornber, J. Collins, A. J. Spencer, M. P. Osborne, and J. Stephen.** 1990. An in vitro model to study aspects of the pathophysiology of murine rotavirus-induced diarrhoea. Journal of pediatric gastroenterology and nutrition **10:**361-370.
46. **Taube, S., J. W. Perry, E. McGreevy, K. Yetming, C. Perkins, K. Henderson, and C. E. Wobus.** 2012. Murine noroviruses bind glycolipid and glycoprotein attachment receptors in a strain-dependent manner. Journal of virology **86:**5584-5593.
47. **Taube, S., J. W. Perry, K. Yetming, S. P. Patel, H. Auble, L. Shu, H. F. Nawar, C. H. Lee, T. D. Connell, J. A. Shayman, and C. E. Wobus.** 2009. Ganglioside-

linked terminal sialic acid moieties on murine macrophages function as attachment receptors for murine noroviruses. Journal of virology **83:**4092-4101.

48. **Thackray, L. B., C. E. Wobus, K. A. Chachu, B. Liu, E. R. Alegre, K. S. Henderson, S. T. Kelley, and H. W. t. Virgin.** 2007. Murine noroviruses comprising a single genogroup exhibit biological diversity despite limited sequence divergence. Journal of virology **81:**10460-10473.
49. **Tomov, V. T., L. C. Osborne, D. V. Dolfi, G. F. Sonnenberg, L. A. Monticelli, K. Mansfield, H. W. Virgin, D. Artis, and E. J. Wherry.** 2013. Persistent enteric murine norovirus infection is associated with functionally suboptimal virus-specific CD8 T cell responses. Journal of virology **87:**7015-7031.
50. **Totsuka, T., T. Kanai, Y. Nemoto, T. Tomita, R. Okamoto, K. Tsuchiya, T. Nakamura, N. Sakamoto, H. Akiba, K. Okumura, H. Yagita, and M. Watanabe.** 2009. RANK-RANKL signaling pathway is critically involved in the function of CD4+CD25+ regulatory T cells in chronic colitis. J Immunol **182:**6079-6087.
51. **Tyler, K. L., D. A. McPhee, and B. N. Fields.** 1986. Distinct pathways of viral spread in the host determined by reovirus S1 gene segment. Science (New York, N.Y **233:**770-774.
52. **Ward, J. M., C. E. Wobus, L. B. Thackray, C. R. Erexson, L. J. Faucette, G. Belliot, E. L. Barron, S. V. Sosnovtsev, and K. Y. Green.** 2006. Pathology of immunodeficient mice with naturally occurring murine norovirus infection. Toxicol Pathol **34:**708-715.
53. **Wetzel, J. D., J. D. Chappell, A. B. Fogo, and T. S. Dermody.** 1997. Efficiency of viral entry determines the capacity of murine erythroleukemia cells to support persistent infections by mammalian reoviruses. Journal of virology **71:**299-306.
54. **Wobus, C. E., S. M. Karst, L. B. Thackray, K. O. Chang, S. V. Sosnovtsev, G. Belliot, A. Krug, J. M. Mackenzie, K. Y. Green, and H. W. Virgin.** 2004. Replication of Norovirus in cell culture reveals a tropism for dendritic cells and macrophages. PLoS Biol **2:**e432.
55. **Wolf, J. L., R. S. Kauffman, R. Finberg, R. Dambrauskas, B. N. Fields, and J. S. Trier.** 1983. Determinants of reovirus interaction with the intestinal M cells and absorptive cells of murine intestine. Gastroenterology **85:**291-300.
56. **Wolf, J. L., D. H. Rubin, R. Finberg, R. S. Kauffman, A. H. Sharpe, J. S. Trier, and B. N. Fields.** 1981. Intestinal M cells: a pathway for entry of reovirus into the host. Science (New York, N.Y **212:**471-472.

# CHAPTER 4

## Murine Norovirus Infection is Reduced in Rag2 Gamma Chain and RANK$^{fl/fl}$ Villin-Cre (M-less) Deficient Mice After Oral Administration

The work presented in this chapter is preliminary and it is currently in progress.

### 4.1 Abstract

In chapter 3, we described how infection of two divergent murine norovirus (MNV) strains were reduced in mice conditionally depleted of Microfold (M) cells. However, residual MNV was still detectable within the gastrointestinal (GI) tract of mice. The presence of this low level of MNV replication suggests two things: 1) there was incomplete depletion of M cells, or 2) that additional mechanisms for viral entry exist (*i.e.,* transepithelial dendritic cells, villous M cells or immature M cells). To explore some of these possibilities, this chapter describes my preliminary studies investigating two different mouse models lacking M cells in Peyer's patches (PPs) (*i.e.*, Rag2-/-γc-/- mice) or along the whole small intestine (M-less mice). We show that oral infection with MNV is blocked to greater extents in the small and large intestine of mice that completely lack M cells in the PP when compared to the conditional M cell depletion strategy. However, in the large intestine (*i.e*, cecum) of Rag2-/-γc-/- mice, virus replicated to low quantities in a strain-dependent manner.

Studies are currently looking at the potential entry via DCs, immature M cells and whether differences in carbohydrates present in the small and large intestine are responsible for the virus-strain dependent binding.

## 4.2 Introduction

Questions looking at the importance of M cells in the pathogenesis of enteric infections *in vivo*, would be best understood with the existence of small animal models that can be manipulated genetically to lack these cells. This chapter describes my preliminary studies investigating two different mouse models lacking M cells in Peyer's patches (PPs) or along the whole small intestine.

Mice that are genetically modified to lack the recombination activating gene 2 (Rag2) and the interleukin-2 (IL-2) receptor (common cytokine receptor) gamma chain (γc) are commonly used as a transplantation model for stem cells studies. Along with T-lymphocytes, B-lymphocytes, and Natural Killer (NK) cells, these mice have a deficiency in cell signaling pathways via the γc for IL-2, -4, -7, -9, and -15 cytokines (1, 2, 6). These cytokines are mainly involved in differentiation, function and survival of lymphocytes, and this deficiency greatly compromises development of mouse lymphatic compartments. In particular, Rag2-/-γc-/- mice lack gut-associated lymphoid tissues (GALT) such as PPs, mainly due to the deficiency in IL-7 receptor signaling that is critical for PPs development (1, 4, 8). Interestingly, a study showed that PPs are the critical tissue site for CD4+ T-cell priming in *Helicobacter pylori* infection and a deficiency in PPs abolishes this step (8). In addition, Rag2-/-γc-/- mice in a Balb/c background, recently discovered to be susceptible to human noroviruses (HuNoVs)

replication following intraperitoneal (i.p.) infection, are not susceptible to HuNoV by oral infection (9). This could also be due to the fact that they do not possess PPs (1, 4, 5, 8, 9). Hence, Rag2-/-γc-/- mice can be used as a model to study the importance of PPs and PP M cells in oral infection of enteric pathogens such as HuNoV and murine norovirus (MNV).

We show that MNV oral infection of two distinct MNV strains (MNV-1 and CR3) is completely blocked in the small intestine of Rag2-/-γc-/- mice when compared to normal wild-type controls and to mice that were i.p. infected with each MNV strain. Low levels of residual MNV titers were observed in the large intestine (*i.e.*, cecum) of CR3 and MNV-1 infected Rag2-/-γc-/- mice when compared to wild-type mice. This suggests that at least in the cecum, other routes of entry such as transepithelial dendritic cells, immature or villous M cells may play a role for MNV. Additionally, since both CR3 and MNV-1 have different requirements on binding to carbohydrates (10, 11), it is possible that carbohydrates present in the cecum, but not in the small intestine, account for the virus-strain dependent tropism. Interestingly, when Rag2-/-γc-/- mice were orally infected with the S99 MNV strain, which has similar carbohydrate binding properties as MNV-1 but causes a persistent infection as CR3, viral titers were similar to those of MNV-1. This suggests that carbohydrates may be playing a role in the virus-strain dependent tissue tropism. Interestingly, positive staining for villous M cells was observed in Rag2-/-γc-/- mice, that suggests another alternate route for MNV entry. However, when virus was given orally to M-less mice ($RANK^{fl/fl}$-Villin-Cre), which are a much more specific villous and PPs M-cell knockout mouse model, no viral titers were observed in both small and large intestine. Taken together, our data suggests that M

cells are absolutely required for efficient MNV entry into the intestine. Future studies will use light-sensitive MNV strains to distinguish input from replicated viruses that could account for the low residual viral titers observed in several cases.

### 4.3 Materials and Methods

**Mice.** Six- to eight-week-old mice were used for MNV studies. Wild-type BALB/c mice were purchased from Jackson Laboratory (Bar Harbor, ME), Rag2-/-γc-/- mice on a Balb/c background were obtained from Dr. Irvine Weissman, Stanford University, and bred and maintained in a specific pathogen free mouse facility at University of Michigan. C57BL/6 mice carrying a floxed RANK allele ($RANK^{fl/fl}$) were obtained from Dr. Ifor R. Williams at Emory University. Villin-Cre mice on a C57BL/6 background (Taconic Farms) were purchased from Taconic Farms and used to establish a breeding colony of $RANK^{fl/fl}$ by Villin-Cre. Villin-Cre x $RANK^{fl/fl}$ mice, referred herein as M-less mice, which lack all M cells in the mouse intestine were obtained and $RANK^{fl/fl}$ littermates were used as controls.

**Virus stocks and plaque assays.** The plaque-purified MNV-1 clone (GV/MNV1/2002/USA) MNV-1.CW3, the fecal isolates CR3 (GV/*CR3*/2005/USA) and S99 (GV/S99/Berlin/2006/DE) were used at passage 6 for all experiments (7, 12). Viral titers were quantified by plaque assay as described (3).

**Infection of mice with MNV.** Balb/c and Rag2-/-γc-/- mice were inoculated with $10^5$ PFU of MNV-1 or CR3 perorally (p.o.) or intraperitoneally (i.p.). Tissue samples were collected 24 hpi and processed as described (3). M-less mice were inoculated perorally

with $10^5$ PFU of MNV-1 or CR3 and tissue samples (stomach (ST), jejunum/duodenum (J/D), proximal ileum (PI), distal ileum (DI), cecum (CE), colon (CO) and one fecal pellet (FE) to measure viral shedding) were collected respectively at 12 hpi, from MNV-1 infected mice, as described in chapter 3. Viral titers were determined by plaque assay for each mouse model.

**Immunostaining of cryosections.** Cecum and ileum were harvested from Balb/c and Rag2-/-γc-/- mice, fixed with 4% paraformaldehyde in PBS for 15 min and frozen in cryo-molds for cryosectioning. Sections were then blocked with 10% (v/v) of FBS and 1% (v/v) of normal goat serum (NGS; Gibco) in PBS for 30 to 60 min at room temperature (RT). Afterwards, sections were incubated with lectins for 60 min at RT: rhodamin-conjugated *Ulex europeaus* agglutinin I (UEA-1, 5 µg/mL), FITC-conjugated Peanut agglutinin (PA, 10 µg/mL), rhodamin-conjugated Concanavalin A (ConA, 10 µg/mL), Alexa647-conjugated Wheat-germ agglutinin (WGA, 1:300 dilution), FITC-conjugated *Aleuria aurantia* (Ale, 10 µg/mL), FITC-conjugated *Sambucus nigra* (SN, 10 µg/mL), biotinylated *Maackia amurensis* II (MAL II, 10 µg/mL), and FITC-conjugated *Phaseolus vulgaris erythroagglutinin* (PHA-E, 10 µg/mL) (all from Vector Laboratories, Burlingame, CA). An alexa594-conjugated-streptavidin was incubated for 60 min at RT only for detection of the biotinylated-MAL II lectin. Sections were washed three times with PBS and mounted with ProLong Gold antifade reagent containing DAPI (Invitrogen, Grand Island, NY). Images were captured using an Olympus BX60 upright microscope.

To visualize the presence of villous M cells, cryosections from the ileum of Balb/c and Rag2-/-γc-/- mice were blocked in a similar fashion as mentioned above. The M cell marker GP2 was used for staining of sections with 3 µg/mL of primary rat anti-mouse

glycoprotein 2/GP2 (MBL, Woburn, MA) antibody for 60 min at RT and followed by three consecutive washes with PBS. A rat IgG2a antibody was also used as a GP2 isotype control to determine background levels. Sections were then incubated with an Alexa-488 secondary anti-rat antibody, washed three times with PBS and mounted with ProLong Gold antifade reagent containing DAPI (Invitrogen, Grand Island, NY). Images were captured using an Olympus BX60 upright microscope. Immunofluorescence images were quantified from 3 to 6 individual PPs using the scoring system of intensities by the Metamorph Premier v6.3 image analysis software (Molecular Devices; Downington, PA).

**Statistical analysis.** Data are presented as mean ± standard error of the mean (SEM). Statistical analysis was performed using Prism software version 5.01 (GraphPad Software, CA). The two-tailed Student's *t* test was used to determine statistical significance.

### 4.4 Results

**Oral infection with MNV-1 and CR3 is significantly reduced in Rag2-/-γc-/- mice.**

To determine whether PPs M cells are essential to initiate a productive MNV infection *in vivo*, Rag2-/-γc-/- on a Balb/c background were inoculated perorally (p.o.) with the MNV strains MNV-1 or CR3, and sections of the gastrointestinal (GI) tract were harvested 24 hours post-infection (hpi). As a control, Balb/c wild-type mice were infected and treated similarly. MNV-1 and CR3 viral titers were not detected or detected at very low levels in the small intestine (stomach, ST; jejunum-duodenum, JD; proximal ileum, PI; distal ileum, DI) of Rag2-/-γc-/- mice when compared to wild-type controls

(Figures 4.1A and 4.2A). In the large intestine of MNV-1 infected Rag2-/-γc-/- mice, viral titers were also reduced and this reduction was particularly significant in the ascending colon (AC) (Figure 4.1A). On the contrary, viral titers were significantly reduced in the cecum (CE), ascending colon (AC) and feces (FE) of CR3 infected Rag2-/-γc-/- mice (Figure 4.2A). Interestingly, viral titers in the cecum of CR3 infected Rag2-/-γc-/- mice was significantly higher (*p=0. 0.0366) than viral titers in the cecum of MNV-1 infected Rag2-/-γc-/- mice (compare Figures 4.1A and 4.2A, and data not shown). In order to verify that MNV was capable of efficiently infecting Rag2-/-γc-/- mice, mice were inoculated i.p. to circumvent the intestinal epithelial barrier with either MNV-1 or CR3 and compared to wild-type Balb/c mice. MNV-1 viral titers were not significantly different between wild-type Balb/c and Rag2-/-γc-/- mice in the small or large intestine, and no viral shedding was detected (Figure 4.1B). Interestingly, CR3 viral titers were significantly higher in Rag2-/-γc-/- mice when compared to control wild-type mice for both small and large intestines as well as in the feces (Figure 4.2B). This suggests that cell types (i.e., NK, T- or B-lymphocyte) or cytokines lacking in these mice may be required for controlling systemic infection. Taken together, our data suggests that PPs M cells are required for efficient oral infection of the small intestine with MNV-1 and CR3 and that MNV entry in the small intestine is mediated by PP M cells.

**The cecum does not show differences in carbohydrate binding.**

The previously observed significant difference on the level of MNV and CR3 infection in the cecum of Rag2-/-γc-/- mice, could suggest a potential difference in carbohydrate binding within this site that could account for the MNV strain dependent

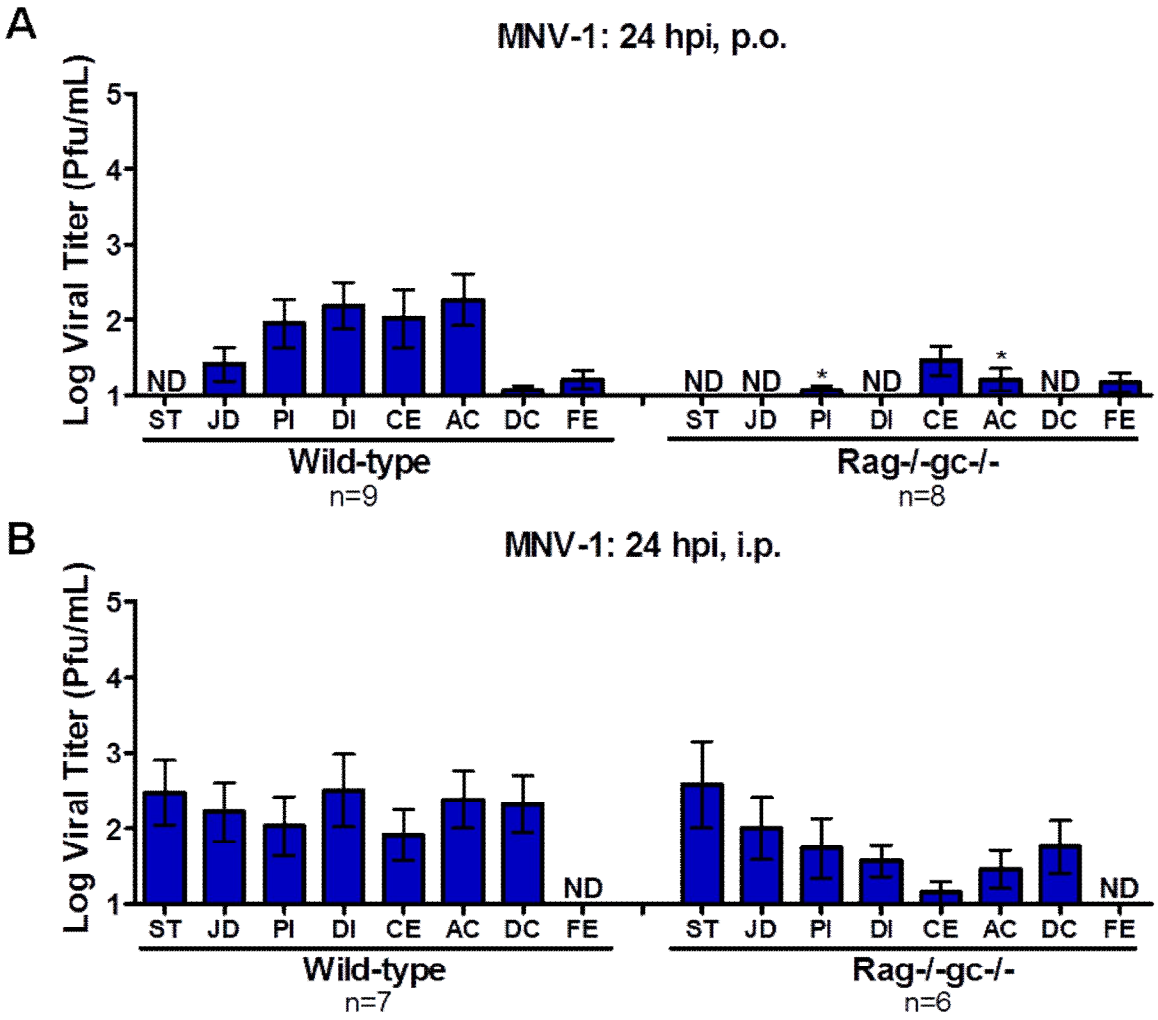


**Figure 4.1. Oral infection with MNV-1 is significantly reduced in Rag-/-gc-/- mice**. (A) Control wild-type BALB/c and Rag-/-gc-/- mice (7-to-8 weeks old) were inoculated by oral gavage with $10^5$ PFU of MNV-1. The GI tract was dissected 24h later, and viral titers determined by plaque assay. (B) Mice in each group were inoculated intraperitoneally (i.p.) with $10^5$ PFU of MNV-1 and treated similar as in (A). Data are expressed as mean ± SEM for at least three independent experiments. Significance was done comparing Rag-/-gc-/- mice to wild-type controls in each route of infection. *, $P < 0.05$; ND = not detectable; n= number of mice; ST = stomach; J/D = jejunum/duodenum; PI = proximal ileum; DI = distal ileum; CE = cecum; AC = ascending colon; DC = descending colon; FE = feces.

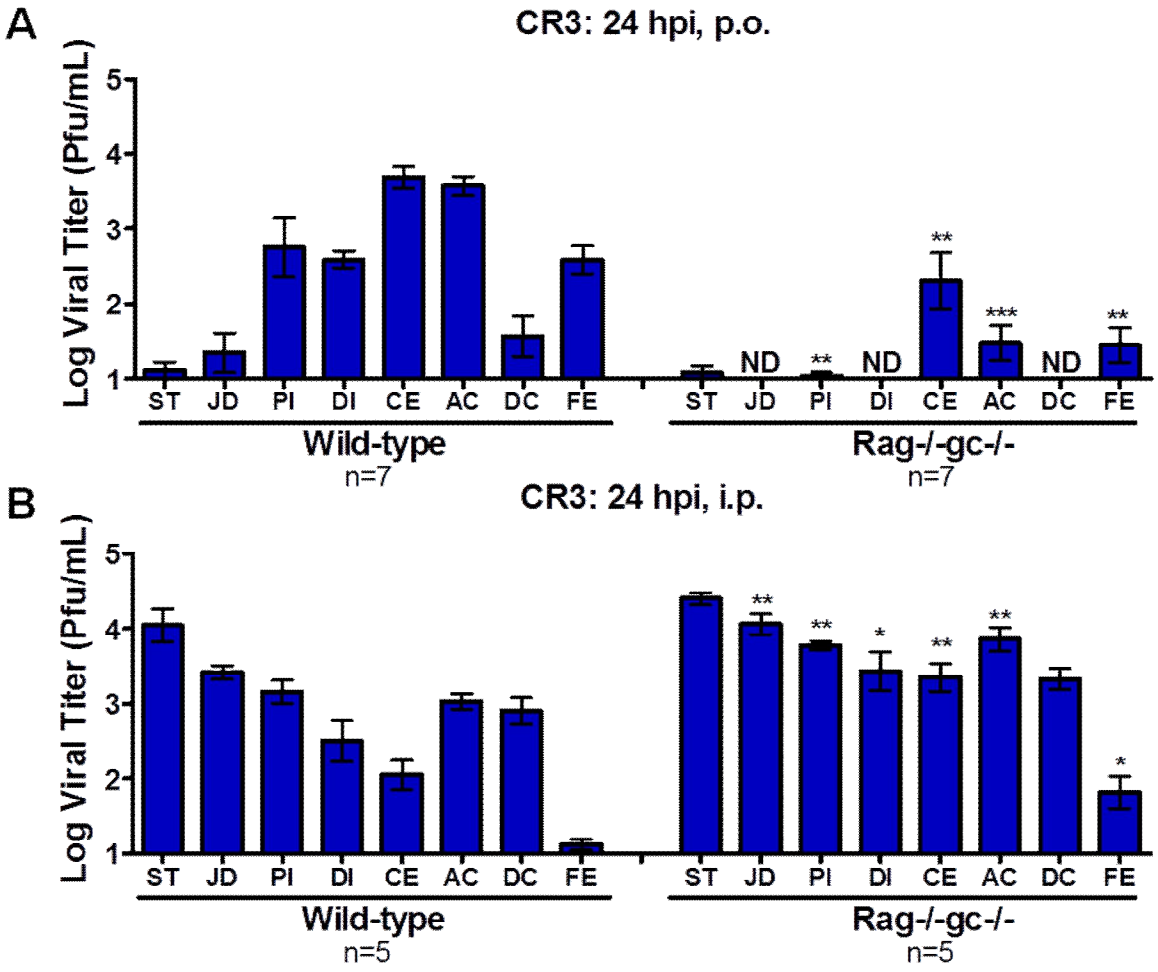


**Figure 4.2. Oral infection with CR3 is significantly reduced in Rag-/-gc-/- mice but is increased after intraperitoneal infection.** (A) Control wild-type BALB/c and Rag-/-gc-/- mice (7-to-8 weeks old) were inoculated by oral gavage with $10^5$ PFU of CR3. The GI tract was dissected 24h later, and viral titers determined by plaque assay. (B) Mice in each group were inoculated intraperitoneally (i.p.) with $10^5$ PFU of CR3 and treated similar as in (A). Data are expressed as mean ± SEM for at least three independent experiments. *, $P < 0.05$; **, $P < 0.01$; ***, $P < 0.001$; ND = not detectable; n= number of mice; ST = stomach; J/D = jejunum/duodenum; PI = proximal ileum; DI = distal ileum; CE = cecum; AC = ascending colon; DC = descending colon; FE = feces.

tissue tropism. Similar MNV strain dependent tissue tropism in cecum was previously observed in mice with a C57BL/6 background (10). Therefore, we wanted to test if carbohydrates located in the cecum and not in the small intestine might play a role in MNV strain-dependent binding. It has been previously shown that MNV-1 binding to murine macrophages is dependent on terminal sialic acid residues of the ganglioside GD1a, N- linked, or O-linked glycoproteins, while CR3 binding only requires N-linked glycoproteins (10, 11). Hence, it could be possible that similar patterns can take place in our *in vivo* model. Sections of cecum and ileum from both Rag2-/-γc-/- mice and wild-type Balb/c controls were incubated with the lectins shown in Table 4.1. If our hypothesis was correct, we would expect one or more lectins to show a high fluorescent staining pattern throughout the epithelial lining of the cecum, but not the ileum of mice. However, no differences in lectin binding to carbohydrates that are preferentially located in the cecum were observed (Figure 4.3). Moreover, only the PA and the PHA-E were observed to preferentially bind to carbohydrates present in the ileum but not the cecum (Figure 4.3). Hence, these data suggests that the tested carbohydrates do not play a role for CR3's preference on binding to the cecum for efficient replication. Taken together, with our current approach we were unable to find specific carbohydrates required for the MNV strain-dependent binding to the cecum.

**Oral infection with the persistent MNV strain (S99) is significantly reduced in Rag2-/-γc-/- mice, to a similar fashion as MNV-1.**

To test the hypothesis that carbohydrates may play a role in MNV-strain dependent tissue tropism, we infected wild-type mice and Rag2-/-γc-/- with the S99 MNV persistent strain. As mentioned in Chapter 2, the S99 MNV strain was previously

## Table 4.1: Tested lectins with their respective sugar specificity

| Lectin name | Abbreviation | Preferred sugar specificity |
|---|---|---|
| *Ulex europeaus* agglutinin I | UEA-1 | αFucose |
| Peanut agglutinin | PA | Galactose-β3-*N*-Acetylgalactosamine [Galβ3GalNAc] |
| Concanavalin A | ConA | αMannose and αGlucose |
| Wheat-germ agglutinin | WGA | *N*-Acetylglucosamine [GlcNAc] |
| *Aleuria aurantia* | Ale | Fucose-α6-*N*-Acetylglucosamine [Fucα6GlcNAc] |
| *Sambucus nigra* | SN | *N*-Acetyl-neuraminic Acid α6-galactose-*N*-Acetylgalactosamine [Neu5Acα6Gal/GalNAc |
| *Maackia amurensis* II | MAL II | *N*-Acetyl-neuraminic Acid α3-galactose-β4-*N*-Acetylgalactosamine [Neu5Acα3Galβ4GalNAc] |
| *Phaseolus vulgaris erythroagglutinin* | PHA-E, | GlcNAcβ4, GlcNAcβ4Manα3 |

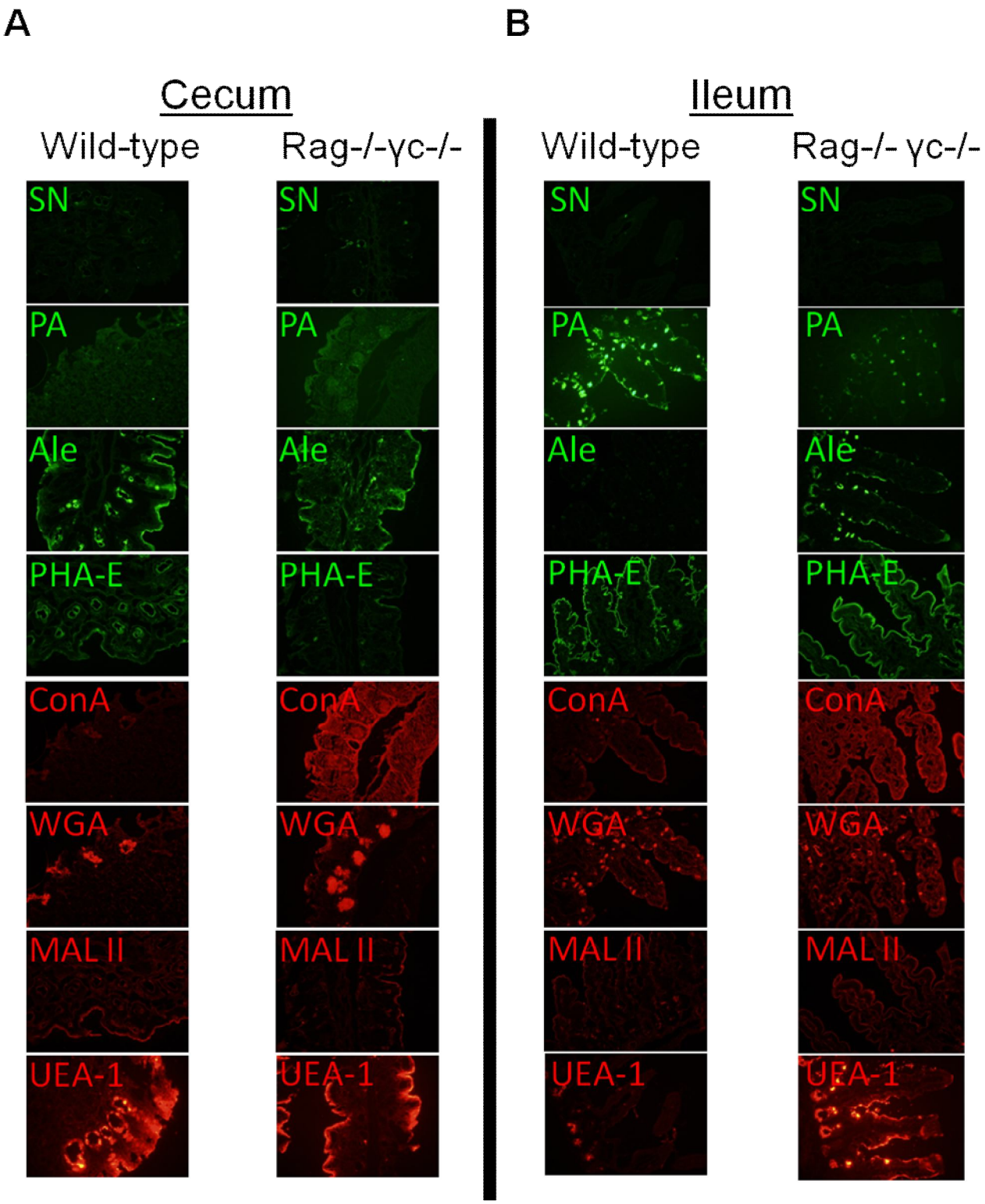
A
B
Cecum
Ileum
Wild-type
Rag-/-γc-/-
Wild-type
Rag-/- γc-/-
SN
PA
Ale
PHA-E
ConA
WGA
MAL II
UEA-1

**Figure 4.3. Cryosection staining of cecum and ileum shows no differences in carbohydrate presence.** (A and B) Representative fluorescent microscopic images of sections from cecum and ileum of wild-type and Rag2-/-γc-/- with different carbohydrate lectins. In green: Peanut agglutinin (PA), *Aleuria aurantia* (Ale), *Sambucus nigra* (SN), and *Phaseolus vulgaris erythroagglutinin* (PHA-E). In red: (Concanavalin A (ConA), Wheat-germ agglutinin (WGA), *Maackia amurensis* II (MAL II) and *Ulex europeaus* agglutinin I (UEA-1).

found to persist in mice (7) and, in macrophages, it can bind to similar carbohydrates as MNV-1, such as: terminal sialic acid residues of the ganglioside GD1a, N-linked, or O-linked glycoproteins (10, 11), Hence, we hypothesized that Rag2-/-γc-/- mice orally infected with the S99 MNV strain would have a similar phenotype of low viral titers in the cecum like MNV-1 but less than CR3. No significant differences were observed between Rag2-/-γc-/- mice and wild-type controls after i.p. infection with S99. Similar to what was observed in i.p. MNV-1 infected wild-type and Rag2-/-γc-/- mice, no viral titers were detected in the feces of S99 i.p. infected mice (compare Figures 4.4B with 4.1B). This could suggest that even though infection can occur when circumventing the intestinal epithelial barrier, both MNV-1 and S99 require PP M cells for efficient viral shedding. On the other hand, after oral (p.o.) infection with S99, viral titers were not detected or significantly reduced in the small intestine (stomach, ST; jejunum-duodenum, JD; proximal ileum, PI; distal ileum, DI) of Rag2-/-γc-/- mice when compared to wild-type controls (Figures 4.4A). In addition, the large intestine, particularly the cecum and ascending colon, as well as the feces of Rag2-/-γc-/- mice showed significant reduction in S99 viral titers when compared to wild-type controls. Interestingly, the levels of S99 viral titers along the GI tract of Rag2-/-γc-/- mice after oral infection were very similar to MNV-1 (compare Rag2-/-γc-/- mice from Figures 4.4A and 4.1A). This could suggest that carbohydrates may indeed play a role in the virus strain preference for binding to the cecum. On a side note, we observed that the levels of S99 infected control wild-type mice were similar to that of CR3 infected control wild-type mice (compare wild-type controls from Figures 4.4A and 4.2A), but this was not surprising since both virus strains share a similar persistent phenotype in normal wild-type mice. Taken together, our

preliminary results suggest that carbohydrate differences in the cecum play a role in MNV strain-dependent tissue tropism. However, further studies will need to be performed to distinguish input from replicated viruses for each MNV strain.

Current studies are also looking at the possibility that the viral capsid defines the difference in tissue tropism. In order to do this, we will use chimeric viruses by swapping the viral capsid from the CR3 strain to the MNV-1 strain, and infecting mice orally to visualize differences in viral titers within the large intestine, which may help define the distinct virus strain tropism for the cecum.

**Villous M cells are still present in intestinal ileum of Rag2-/-γc-/- mice and may account for the residual MNV viral titers.**

Although viral titers were significantly reduced in several compartments of the small and large intestine of Rag2-/-γc-/- mice orally infected with each MNV strain when compared to wild-type controls, there was still some residual virus present. While current studies are verifying if this residual virus is replicated versus input virus, it may be possible that other mechanisms for virus entry, such as villous M cells, are taking place. To test if villous M cells are present in Rag2-/-γc-/- mice, we took sections of intestinal ileum from both wild-type and Rag2-/-γc-/- mice and performed immunostaining with the M cell marker GP2/glycoprotein 2. A representative image shows the expected GP2 positive staining lining pattern within the intestinal epithelium of villa (Figure 4.5A). Interestingly, we observed positive GP2 staining that although seemed to be reduced when compared to the wild-type control (compare Figures 4.5A and 4.5B), did not show any significant difference with the numbers of sections used for quantification (Figure 4.5C). This result suggests that although Rag2-/-γc-/- mice lack

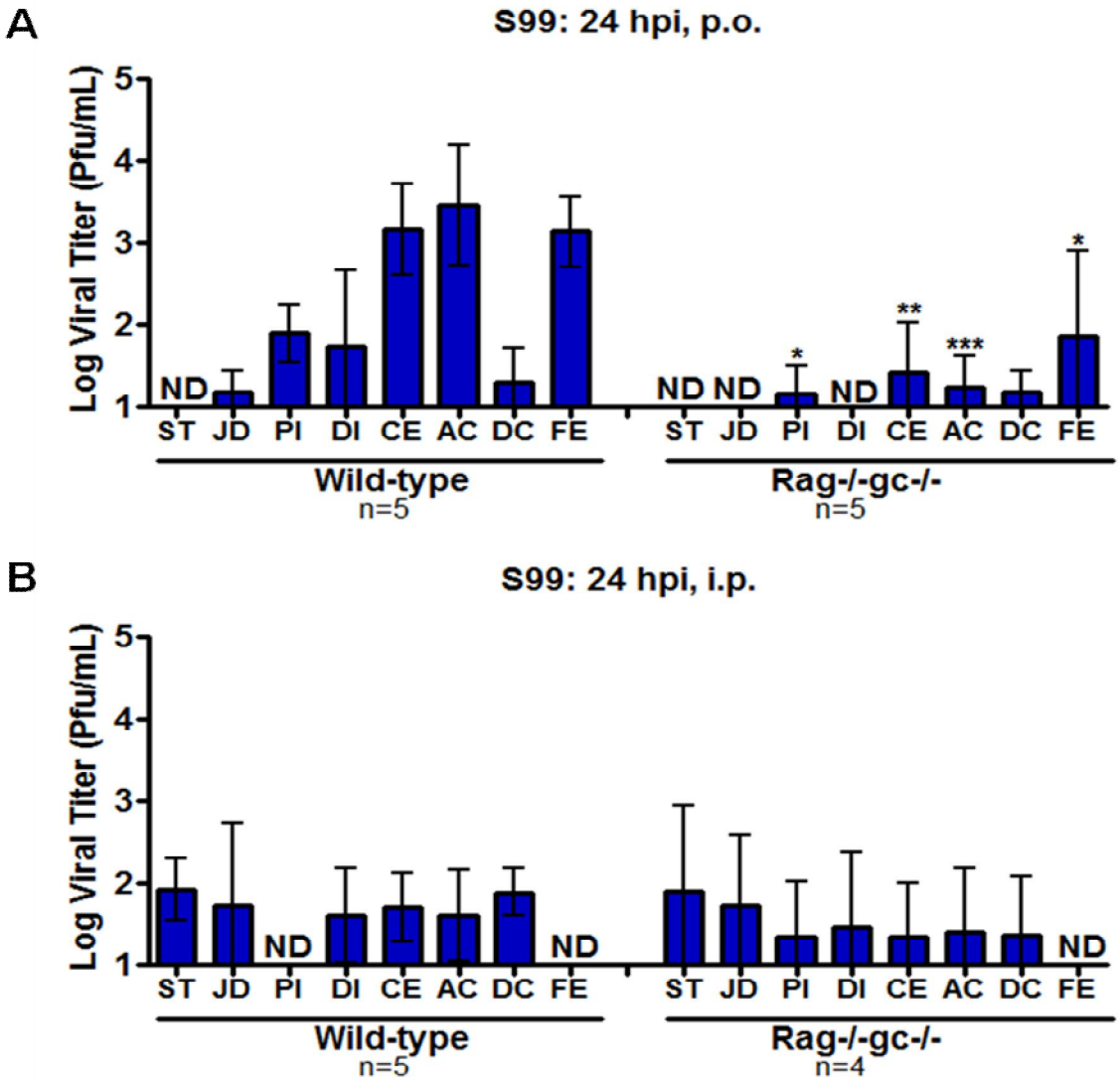


**Figure 4.4. Oral infection with S99 is significantly reduced in Rag-/-gc-/- mice.** (A) Control wild-type BALB/c and Rag-/-gc-/- mice (7-to-8 weeks old) were inoculated by oral gavage with $10^5$ PFU of S99. The GI tract was dissected 24h later, and viral titers determined by plaque assay. (B) Mice in each group were inoculated intraperitoneally (i.p.) with $10^5$ PFU of S99 and treated similar as in (A). Data are expressed as mean ± SEM for at least three independent experiments. *, $P < 0.05$; **, $P < 0.01$; ***, $P < 0.001$; ND = not detectable; n= number of mice; ST = stomach; J/D = jejunum/duodenum; PI = proximal ileum; DI = distal ileum; CE = cecum; AC = ascending colon; DC = descending colon; FE = feces.

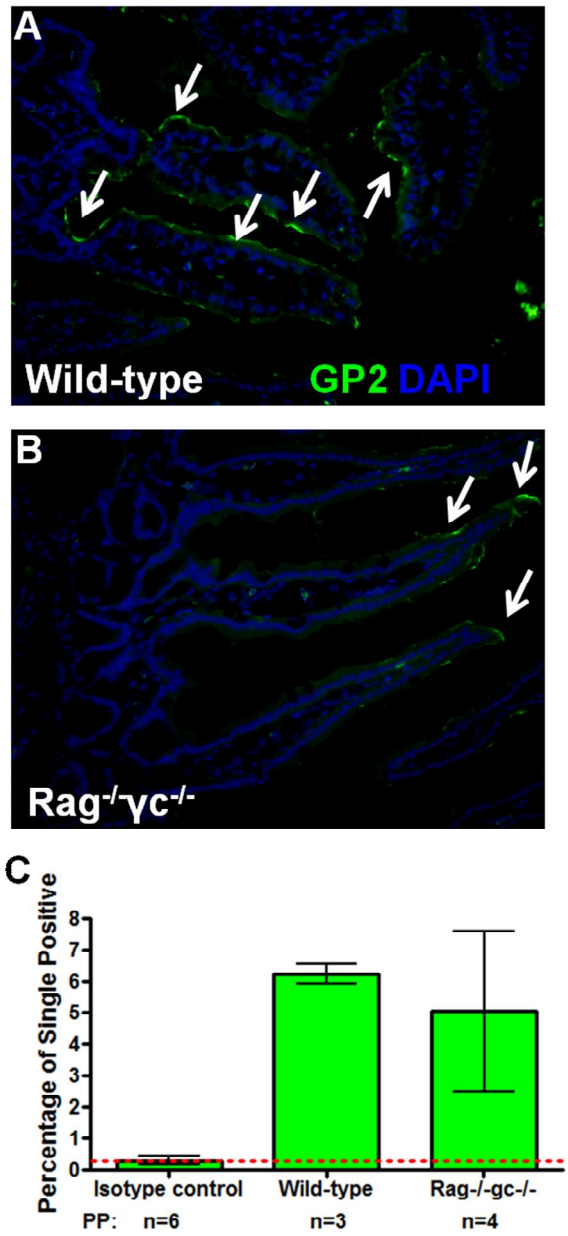


**Figure 4.5. Villous M cell positive staining in Rag-/-γc-/- mice.** (A and B) Representative fluorescent microscopic images of sections from ileum of wild-type and Rag2-/-γc-/- mice with the M cell marker (GP2). (C) Quantification of GP2 positive staining for images taken at a 10x magnification from sections of 3 to 4 mice. n= number of mice; PP= sections taken close to Peyer patches (PP) of wild-type mice or sections taken from a similar region were an imaginary PP would be located in Rag2-/-γc-/- mice.

PP M cells, they still contain villous M cells that may be responsible for a second route of MNV entry to the host. However, there is still some debate regarding the existence of villous M cells (personal communication with Dr. Ifor R Williams and Dr. Tatyana V. Golovkina). Hence, further studies will look at more sections of Rag2-/-γc-/- mice to quantify the presence of GP2 positive cells along with the binding and uptake of fluorescently labeled beads as a specificity control for M cell positive staining.

**Preliminary results suggest MNV oral infection is reduced in complete M-less mice.**

To determine whether alternate routes besides M cells exist for MNV entry into the intestine, we took advantage of a recently developed mouse model from Ifor R. Williams (Emory) that is completely deficient of M cells in the villi and PPs, Villin-Cre x Rank fl/fl mice (M-less). MNV-1 was given p.o. in both M-less mice and $RANK^{fl/fl}$ control littermates, and GI compartments were harvested 12 hpi. $RANK^{fl/fl}$ control mice showed MNV titers in the cecum (CE) and feces (FE) (Figure 4.6). On the other hand, M-less mice showed almost complete reduction of MNV-1 viral titers close to non-detectable levels (Figure 4.6), suggesting that M cells may be the only route for MNV-1 oral infection. Current studies are looking at later time-points as well as verifying differences between input and replicated virus, by using neutral red light-sensitive MNV strains.

## 4.5 Discussion

Since studies are still at their preliminary state, no conclusions can be made as of yet. However, a few observations based on the preliminary work presented in this

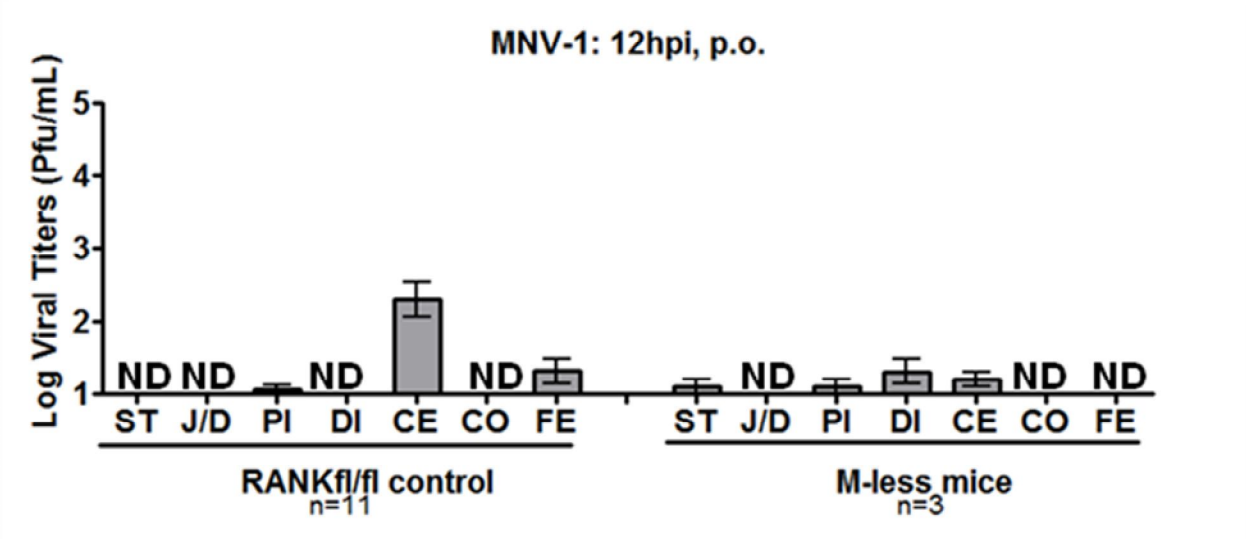


**Figure 4.6. Oral infection with MNV-1 is reduced in M-less mice.** Control RANK$^{fl/fl}$ mice were inoculated with $10^5$ PFU of MNV-1. The GI tract was dissected 12 h later, and viral titers determined by plaque assay. Data are expressed as mean ± SEM for at least three independent experiments. ND = not detectable; n= number of mice; ST = stomach; J/D = jejunum/duodenum; PI = proximal ileum; DI = distal ileum; CE = cecum; CO = colon; FE = feces.

chapter have been described more thoroughly in Chapter 5. Interestingly, although more thorough characterization of other potential routes for MNV entry are still work in progress, it may be the case that the initiating factor for efficient MNV infections in mice is solely based on M cells. Nevertheless, Chapter 5 discusses this and other points regarding the requirement for a productive MNV infection.

## 4.6 References


1. **Cao, X., E. W. Shores, J. Hu-Li, M. R. Anver, B. L. Kelsall, S. M. Russell, J. Drago, M. Noguchi, A. Grinberg, E. T. Bloom, and et al.** 1995. Defective lymphoid development in mice lacking expression of the common cytokine receptor gamma chain. Immunity **2:**223-238.
2. **Goldman, J. P., M. P. Blundell, L. Lopes, C. Kinnon, J. P. Di Santo, and A. J. Thrasher.** 1998. Enhanced human cell engraftment in mice deficient in RAG2 and the common cytokine receptor gamma chain. Br J Haematol **103:**335-342.
3. **Gonzalez-Hernandez, M. B., J. Bragazzi Cunha, and C. E. Wobus.** 2012. Plaque assay for murine norovirus. J Vis Exp**:**e4297.
4. **Honda, K., H. Nakano, H. Yoshida, S. Nishikawa, P. Rennert, K. Ikuta, M. Tamechika, K. Yamaguchi, T. Fukumoto, T. Chiba, and S. I. Nishikawa.** 2001. Molecular basis for hematopoietic/mesenchymal interaction during initiation of Peyer's patch organogenesis. The Journal of experimental medicine **193:**621-630.
5. **Luther, S. A., K. M. Ansel, and J. G. Cyster.** 2003. Overlapping roles of CXCL13, interleukin 7 receptor alpha, and CCR7 ligands in lymph node development. The Journal of experimental medicine **197:**1191-1198.
6. **Mazurier, F., A. Fontanellas, S. Salesse, L. Taine, S. Landriau, F. Moreau-Gaudry, J. Reiffers, B. Peault, J. P. Di Santo, and H. de Verneuil.** 1999. A novel immunodeficient mouse model--RAG2 x common cytokine receptor gamma chain double mutants--requiring exogenous cytokine administration for human hematopoietic stem cell engraftment. J Interferon Cytokine Res **19:**533-541.
7. **Muller, B., U. Klemm, A. Mas Marques, and E. Schreier.** 2007. Genetic diversity and recombination of murine noroviruses in immunocompromised mice. Archives of virology **152:**1709-1719.
8. **Nagai, S., H. Mimuro, T. Yamada, Y. Baba, K. Moro, T. Nochi, H. Kiyono, T. Suzuki, C. Sasakawa, and S. Koyasu.** 2007. Role of Peyer's patches in the induction of Helicobacter pylori-induced gastritis. Proceedings of the National Academy of Sciences of the United States of America **104:**8971-8976.

9. **Taube, S., A. O. Kolawole, M. Hohne, J. E. Wilkinson, S. A. Handley, J. W. Perry, L. B. Thackray, R. Akkina, and C. E. Wobus.** 2013. A mouse model for human norovirus. MBio **4**.
10. **Taube, S., J. W. Perry, E. McGreevy, K. Yetming, C. Perkins, K. Henderson, and C. E. Wobus.** 2012. Murine Noroviruses (MNV) bind glycolipid and glycoprotein attachment receptors in a strain- dependent manner. Journal of virology **doi:10.1128/JVI.06854-11**.
11. **Taube, S., J. W. Perry, K. Yetming, S. P. Patel, H. Auble, L. Shu, H. F. Nawar, C. H. Lee, T. D. Connell, J. A. Shayman, and C. E. Wobus.** 2009. Ganglioside-linked terminal sialic acid moieties on murine macrophages function as attachment receptors for murine noroviruses. Journal of virology **83:**4092-4101.
12. **Thackray, L. B., C. E. Wobus, K. A. Chachu, B. Liu, E. R. Alegre, K. S. Henderson, S. T. Kelley, and H. W. Virgin.** 2007. Murine noroviruses comprising a single genogroup exhibit biological diversity despite limited sequence divergence. Journal of virology **81:**10460-10473.

# CHAPTER 5

## Discussion and Future Directions

### 5.1 Conclusions

For many enteric viruses, breaching the intestinal epithelial barrier is an initial event that must take place to productively infect the host. Since no tissue culture model exists for human norovirus (HuNoV) and no studies can be efficiently performed to study HuNoV pathogenesis in its natural host, murine norovirus (MNV) can be used as a model to evaluate norovirus pathogenesis in its host. The main focus of this dissertation was to elucidate how MNV crosses the intestinal epithelium to initiate infection. MNV does not directly infect enterocytes (18), hence, Figure 5.1 shows a representation of several potential routes for MNV entry across the intestinal epithelium. Transepithelial dendritic cells (DCs), which are DCs that can extrude dendritic processes through epithelial cells (39) or Microfold (M)-cell transcellular pores (29), could play a role in MNV entry. However, this thesis shows evidence, for the first time, that M cells are responsible for initial MNV entry across the intestinal epithelium. Particularly, Chapter 2 describes an *in vitro* approach taken to understand how MNV becomes transported across the intestinal epithelium and points to M-like cells as the main target cell. The importance of M cells for the pathogenesis of MNV and another

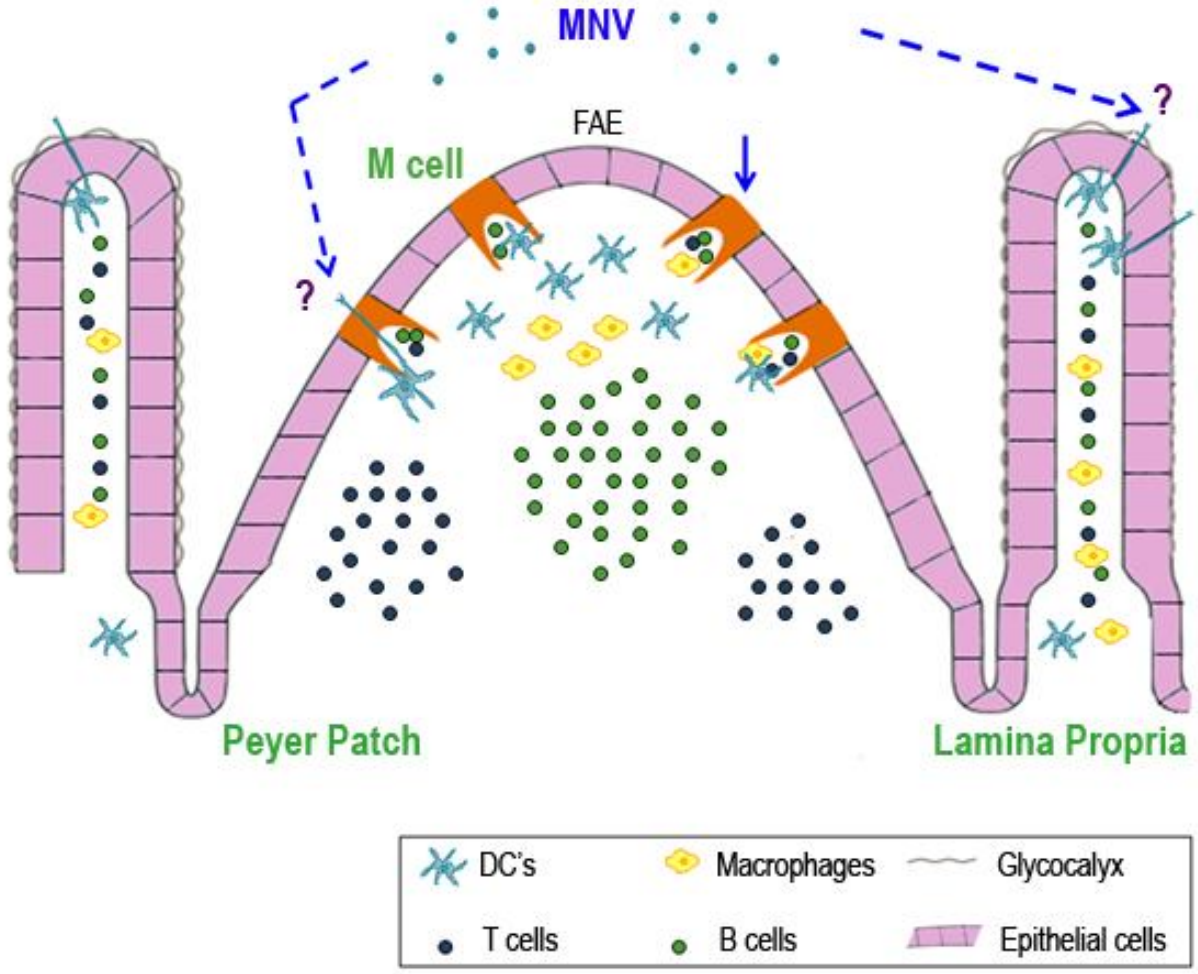


**Figure 5.1. Schematic representation of potential mechanisms of MNV entry across the intestinal epithelium.** MNV (light blue circles) in the intestinal lumen initially interact with M cells within the follicle-associated epithelium (FAE) overlying Peyer's patches (blue arrow) to establish a productive infection. However, the partial reduction in MNV infection suggests that other mechanisms like trans-epithelial dendritic cells or dendritic cells via M cell specific transcellular pores (dashed blue arrows with question marks), may provide an alternative route of entry for MNV.

enteric virus (*i.e.,* reovirus) *in vivo*, using a conditional depletion strategy, is examined in Chapter 3. Additionally, defining the unique requirement of M cells for productive MNV entry and infection using knockout mouse models is further explained in Chapter 4. Knowing that M cells are the essential requirement for MNV to traverse the intestinal epithelium and initiate a productive infection, allows for an understanding of how HuNoV may initiate infection. In addition, knowledge that M cells are used as a portal for norovirus entry, as well as for some other enteric viruses, aids in the future development of mucosal anti-viral treatments that can prevent disease.

In Chapter 2, we described a transwell model of a polarized trans-immortalized murine intestinal epithelial cell line ($mIC_{cl2}$) as an *in vitro* follicle-associated epithelium (FAE) model system. We demonstrate that MNV does not disrupt the epithelial integrity of the polarized $mIC_{cl2}$ monolayer (Chapter 2, Figure 2.1). In addition, with a time-course study and with the use of a neutral red light-sensitive virus that distinguishes replicated from input virus, we were able to demonstrate that MNV does not replicate in the $mIC_{cl2}$ monolayer (Chapter 2, Figure 2.2). We also showed that two distinct MNV strains significantly increased their traffic across the polarized monolayer, via a transcytosis mechanism, when $mIC_{cl2}$ cells were cultured in M-like cell inducing conditions (*i.e.*, co-cultured with B myeloma cells), and transcytosis was mediated by the interaction of MNV with M-like cells in the monolayer (Chapter 2, Table 2.1, Figures 2.2, 2.3 and 2.4). Moreover, we demonstrated that the addition of B myeloma cells to the $mIC_{cl2}$ cultures only increased the transcytotic activity but not the number of M-like cells (Chapter 2, Figures 2.4 through 2.6). These data indicates that, *in vitro*, M-like cells are essential for

MNV transport across the intestinal epithelium and, thus, suggest that M cells are likely to be a portal for MNV entry *in vivo*.

Similar to our study, others have looked at pathogen-interactions with the intestinal epithelium using *in vitro* FAE models with intestinal epithelial cells lines such as HT29 or Caco-2 cells. One study in particular, showed that spores from *Bacillus anthracis*, the causative agent of anthrax, were transcytosed across Caco-2/Raji B cell cocultures, suggesting that M-like cells are an entry portal for spores (53). In addition, studies looking at *Vibrio cholera* and its toxin, and poliovirus suggest that M-like cells play a role in the transcytosis mechanism for each enteric pathogen (7, 8, 40). Another study demonstrated that *Salmonella typhimurium* can be transported across polarized Caco-2 monolayers cocultured with dendritic cells (DCs) via direct interaction with the DC's, which extrude dendritic processes through the epithelial tight junctions (46). Additionally, human T-cell leukemia virus type 1 (HTLV-1) can transcytose across a polarized Caco-2 cell monolayer without disrupting the epithelial integrity to productively infect underlying dendritic cells (31). Also, human immunodeficiency virus type 1 (HIV-1) can infect and transcytose across polarized Caco-2 cells that express both the virus' chemokine receptors CCR5 and CXCR4, and a glycosphingolipid galactosylceramide (15, 17). The establishment of these intestinal epithelial cell lines as *in vitro* FAE models have greatly aided in the understanding of molecular events important in host-pathogen interactions. Hence, these models could help reveal critical targets important for therapeutic development against enteric pathogens.

Interestingly, in our case, we demonstrated that MNV transport across the murine intestinal epithelial monolayer occurs in a saturable manner, suggesting the presence of

an MNV receptor (Chapter 2, Figure 2.2). Knowledge that a receptor is responsible for aiding in the transportation of MNV across the epithelium, suggests the use of the *in vitro* intestinal epithelial model as a pharmacological system for the test of potential inhibitory molecules that could interfere with MNV binding and transport. In fact, unpublished data looking at sialic acid cleavage and glycosphingolipid depletion with inhibitors (*i.e.*, neuraminidase from *Vibrio cholera* and D-threonine-P4), suggest that MNV requires carbohydrates such as terminal sialic acids and gangliosides at the apical surface for efficient transcytosis. This carbohydrate-dependent transcytosis requirement, in turn, indicates that MNV enters through a receptor-mediated endocytosis mechanism for successful internalization and transport across the cell. In fact, it has been shown that certain proteins, viruses and bacteria are internalized into M cells via clathrin-mediated endocytosis (38), macropinocytosis (9, 21, 41) or actin-dependent phagocytosis mechanisms (38, 43) before moving across to the other side of the polarized monolayer. We have preliminary data that suggest that MNV transcytosis is dependent on cholesterol and dynamin II, which are two molecules important for endocytosis (unpublished results). A similar requirement of carbohydrates, cholesterol and dynamin II in MNV binding and entry has been shown for macrophages (44, 51, 52). Further characterization of MNV receptors and internalization mechanisms within the intestinal epithelium may reveal potential molecules required for MNV entry and infection.

As previously mentioned throughout this thesis, M cells are specialized intestinal epithelial cells that possess an important role in sampling microorganisms and transporting them across for the initiation of an immune response. However, several

enteric bacterial pathogens such as *Listeria monocytogenes, Salmonella typhimurium, Shigella flexneri*, and *Yersinia enterocolitica* take advantage of these M cells to successfully invade, disseminate and establish infections in its hosts (4, 23, 24, 47, 57). In addition, only a few enteric viruses have been suggested to exploit M cells for productive infections. Previous poliovirus and reovirus studies, have shown that these viruses can selectively adhere to M cells *in vivo* (2, 5, 33, 42, 49, 56). Additionally, HIV-1 also has been shown to adhere to M cells and to be transported to the M cell pocket (1). However, whether other enteric viruses including noroviruses take advantage of M cells for efficient infection, is not known.

We have demonstrated that MNV is transcytosed via M-like cells *in vitro* (Chapter 2), and to investigate whether this holds true in the native host, studies were performed in Balb/c mice using a conditional antibody M cell depletion strategy. In Chapter 3, we demonstrated that two divergent MNV strains with different replication kinetics have reduced viral loads in mice that were depleted of M cells (Chapter 3, Figures 3.1 and 3.4). We showed that, similar to *in vitro* M-like cells (Chapter 2), M cells are not susceptible to MNV replication (Chapter 3, Figure 3.6). Additionally, we demonstrated that reovirus, which replicates in epithelial cells, also had reduced viral loads in M cell-depleted mice (Chapter 3, Figure 3.5). Taken together, these results suggested that M cells are essential for initiating entry and pathogenesis of two distinct enteric viruses: MNV and reovirus.

Interestingly, the MNV studies using the antibody M cell depletion strategy, showed that residual virus was still present in several compartments of the gastrointestinal (GI) tract of mice (Chapter 3, Figure 3.4). It is possible that an

incomplete depletion of M cells may be the cause for the residual virus, since: 1) we observed weak expression of an M cell marker (Chapter 3, Figures 3.2 and 3.3) and, 2) it has been previously shown that less than 2 percent of M cells are still present when using this depletion strategy (26). However, other mechanisms such as villous M cells, or dendritic cells (DCs) that protrude dendrites between epithelial cells (13, 39, 54) or M-cell transcellular pores (29), could also act as alternate routes for MNV entry. Studies, both *in vitro* and *in* vivo, have shown that upon a bacterial or viral stimuli (*i.e.*, *Salmonella* and HIV R5 tropic virus), extensions of DCs processes between epithelial cells are induced (12, 13, 46), suggesting that transepithelial DCs are a mechanism of pathogen uptake. Interestingly, Chieppa *et.al.* (13) demonstrated that the number of transepithelial DC extensions in mice varies along the small intestine, in which higher numbers are found in the proximal jejunum but only few are found in the terminal ileum. However, in the presence of *Salmonella* organisms, the numbers in the terminal ileum increased (13), suggesting that transepithelial DCs play a role in *Salmonella* uptake. A separate study, suggests that absence of transepithelial DCs does not impair pathogen entry to the lamina propria, after persistence in the entry of *Aspergillus fumigatus* conidia, was observed in mice deficient of the DCs (54). The authors suggest that other mechanisms such as villous M cells play a role in antigen uptake. Interestingly, the authors also proposed that transepithelial dendrites are dependent on mouse strain. This was suggested since a lack of these cells was observed in the terminal ileum of mice with a Balb/c background when compared to mice with a C57BL/6 background, in a steady state or after exposure of either *Aspergillus fumigatus* or *Salmonella* (54). Hence, it may be that the primary route for pathogen uptake (*e.g.* transepithelial DCs,

villous M cells, etc.) could depend on the mouse' genetic background, although future studies need to determine if this is the case.

The likelihood that MNV uses transepithelial DCs as an alternate route of entry in the intestine of mice is possible. However, although we do not discard this possibility, we hypothesize that even though villous M cells are rare (27), they would be an alternate mechanism for MNV transport across the epithelium. Nevertheless, current studies are looking at whether this or other possible routes (such as DCs), are in fact playing a role for MNV entry.

If other mechanisms of MNV entry across the intestinal epithelium are playing a role for efficient infection, M cells need to be ruled out completely. Since the administration of an M cell depletion antibody does not fully eliminate M cells (26), a more direct approach using mice genetically deficient of M cells would be beneficial. Using mice with this deficiency, will help determine if there is an essential and unique requirement for M cells in MNV pathogenesis. To elucidate if the residual viral titers observed on Chapter 3 were due to incomplete depletion of M cells, Chapter 4 describes our recent attempts in identifying if M cells are the sole route for MNV entry.

Mice that have a deficiency in the recombination activating gene 2 (Rag2) and the interleukin-2 (IL-2) receptor (common cytokine receptor) gamma chain (γc) (*i.e.*, Rag2-/-γc-/-), do not contain Peyer's patches (PPs) and cecal patches most likely due to the lack of IL-7 receptor signaling critical for their development (11, 22, 32, 35). Our lab has shown, for the first time, that these mice can be used as a small animal model for human norovirus (HuNoV) replication when the virus is given intraperitoneally (i.p.) (50). However, these mice are not susceptible to HuNoV replication if given orally (p.o.) (50).

In the case of MNV, we showed that Rag2-/-γc-/- mice had very little to no detectable viral loads in the small intestine when virus was given orally (Chapter 4, Figures 4.1 and 4.2). This result suggests that PP M cells are required for MNV infection. In contrast, the large intestine, and particularly the cecum, still showed significant viral titers following oral infection with the CR3 strain, when compared to the MNV-1 strain (Chapter 4, compare Figures 4.1 to 4.2). This result was surprising to us since no cecal patches are present in Rag2-/-γc-/- mice. Currently, studies are in the process of verifying if virus is truly replicating by using neutral red light-sensitive MNV virus strains as described in Chapters 2 and 3. However, if the replication holds true, one suggestion for the differences in viral replication in the cecum, is that MNV strains could have differences in tissue tropism based on distinct carbohydrate moieties that are present. The reason for this hypothesis is because in macrophages, CR3 and MNV-1 have different carbohydrate binding requirements (such as terminal sialic-acids, ganglioside GD1a, N-linked and O-linked glycoproteins) (51, 52). Moreover, this could suggest that since MNV-1 binding is dependent on many more carbohydrates than CR3 (51), after oral inoculation with MNV-1, the virus preferentially binds more rapidly than CR3 in the small intestine to initiate replication. Also, if CR3 binds to different carbohydrates that are present in high quantities in the cecum but not the small intestine, it may indicate why this region could be the initial site for CR3 replication. However, differential lectin-binding to carbohydrates present in the cecum but not in the small intestine were not observed with the lectins tested (Chapter 4, Figure 4.3). Although our data is still preliminary, this suggest that our hypothesis in which MNV tropism for the cecum is dependent on carbohydrate moieties present in this region, is not accurate in its

entirety. Nevertheless, further examination into other distinct carbohydrates within the small and large intestine will provide a better understanding for the MNV strain dependent tissue tropism.

Additional possibilities for the difference in MNV strain-dependent tissue tropism, could be that immature M cells and/or dendritic cells present in cecum are playing a role in MNV entry. Visualization of these cells directly interacting with MNV will provide a better understanding for their role in MNV entry. Unfortunately, acquiring a sensitive enough signal to visualize MNV-positive staining in normal wild-type mice has not yet been achieved (34), and in our hands, it has proven to be difficult as well (Chapter 3 and data not shown). Further characterization of the interaction of MNV with immature M cells and DCs present in the cecum of Rag2-/-γc-/- and control mice, will help understand their role as alternate routes for MNV entry.

Although Rag2-/-γc-/- lack PP M cells, it is also possible that villous M cells may still be present and, thus, could be responsible for the residual MNV entry and infection. In fact, our preliminary results show that the levels of an M cell marker (GP2) in the small intestinal villa of Rag2-/-γc-/- mice compared to wild-type, are not significantly different (Chapter 4, Figure 4.5). However, current studies are looking at different regions of the small intestine and large intestine of Rag2-/-γc-/- mice to verify any difference in the levels of GP2 positive M cells.

In humans, it is known that the microbiota (also known as commensal bacteria or bacterial flora) patterns differ depending on the GI site such as the small intestine, colon and rectum (6, 14, 16, 19, 30, 45). Studies with mice have shown that viruses such as, poliovirus, reovirus and mouse mammary tumor virus (MMTV), rely on commensal

bacteria for efficient replication and transmission (25, 28). Interestingly, although some HuNoV infected patients have alterations in the microbiota with a loss of some and an increase of other bacterial species (37), MNV infection in mice does not affect the distribution of the microbiota (36). However, it is possible that the microbiota could help in MNV entry, as well as explain the MNV strain-dependent tissue tropism. Additional experimentation looking at the role of microbiota in MNV entry and strain-dependent tissue tropism, will be beneficial for future understanding of interactions between MNV and commensal bacteria.

Besides our Rag2-/-γc-/- MNV infection studies, preliminary results using a newly develop genetic mouse model with a deficiency in all M cells from the intestine (M-less mice), suggest that M cells may be the only route for MNV-1 entry after oral infection (Chapter 4, Figure 4.6). However, further studies still need to be performed to verify these findings. While MNV infection was almost completely blocked in M-less mice, small amounts of virus were still present in several compartments of the GI tract (Chapter 4, Figure 4.6). Nonetheless, because the viral titers were close to the limit of detection, this could likely represent input virus and not virus that underwent several rounds of replication. Current studies are examining these mice with neutral red light-sensitive MNV strains to help distinguish input versus replicated virus, as performed in Chapter 3.

Finally, to understand if another enteric virus requires M cells to cause pathogenesis in mice, this dissertation also looked at reovirus infection in mice conditionally depleted of M cells. Reoviruses can cause disease in children but not in adults (48), and a study with reovirus T1L has shown that, in newborn mice, reovirus

replicates in intestinal enterocytes at the villus tips (3). Other studies have shown that reovirus binding to M cells, at the apical surface, is mediated by the viral attachment protein σ1 (20, 55). In addition, internalized virus particles have been observed replicating in M cells (5). Interestingly, in our case, we observed that the majority of reovirus-positive cells were enterocytes adjacent to M cells in a representative image of normal control mice infected with reovirus T1L (Chapter 3, Figure 3.7), while only one M cell showed positive staining for reovirus. No reovirus staining was observed in mice depleted of M cells (Chapter 3, Figure 3.7). This is consistent with the viral loads below the limit of detection observed in the small intestine of M cell depleted mice (Chapter 3, Figure 3.5). These results support a model which suggests that once virions are transported across by M cells, they can directly interact with the reovirus junctional adhesion molecule A (JAM-A) receptor located in the basolateral surface of enterocyte cells (3, 10) for efficient reovirus entry and replication in the epithelium. Future studies will look at other enteric viruses (*e.g.* rotavirus, tulane virus) using M-less mice to verify if M cells are also essential for the pathogenesis of these viruses in mice.

Taken together, the research presented in this thesis has added significant information to the norovirus literature by showing, for the first time, that M cells are the initiating factor for productive MNV infection in the mouse intestine. In addition, it has provided new information regarding the requirement of M cells for the pathogenesis of another enteric virus (*i.e.* reovirus) in mice. Knowledge that M cells are required for MNV infection, has provided the basis for future studies to look into M cell surface molecules involved in MNV uptake that could be critical targets for the development of

anti-viral treatments. Future studies in our lab will further address the role of carbohydrates and other potential receptor molecules in MNV uptake.

## 5.2 Future Directions

- **Identification of carbohydrate determinants for MNV binding and transcytosis across the intestinal epithelium *in vitro.***
- **Characterization of the mechanisms of MNV internalization *in vitro* for efficient entry and transcytosis across the intestinal epithelium.**
- **Characterization of MNV strain-dependent tissue tropism using chimeric versions of MNV strains with differences in persistence.**
- **Elucidation of the extent of MNV infection in M-less mice.**
- **Characterization of MNV infection in antibiotic-treated mice for the importance of commensal bacteria in MNV pathogenesis.**
- **Characterization of the importance of M cells for the pathogenesis of other enteric viruses.**

## 5.3 References


1. **Amerongen, H. M., R. Weltzin, C. M. Farnet, P. Michetti, W. A. Haseltine, and M. R. Neutra.** 1991. Transepithelial transport of HIV-1 by intestinal M cells: a mechanism for transmission of AIDS. J Acquir Immune Defic Syndr **4:**760-765.
2. **Amerongen, H. M., G. A. Wilson, B. N. Fields, and M. R. Neutra.** 1994. Proteolytic processing of reovirus is required for adherence to intestinal M cells. Journal of virology **68:**8428-8432.
3. **Antar, A. A., J. L. Konopka, J. A. Campbell, R. A. Henry, A. L. Perdigoto, B. D. Carter, A. Pozzi, T. W. Abel, and T. S. Dermody.** 2009. Junctional adhesion molecule-A is required for hematogenous dissemination of reovirus. Cell host & microbe **5:**59-71.

4. **Autenrieth, I. B., and R. Firsching.** 1996. Penetration of M cells and destruction of Peyer's patches by Yersinia enterocolitica: an ultrastructural and histological study. Journal of medical microbiology **44:**285-294.
5. **Bass, D. M., J. S. Trier, R. Dambrauskas, and J. L. Wolf.** 1988. Reovirus type I infection of small intestinal epithelium in suckling mice and its effect on M cells. Laboratory investigation; a journal of technical methods and pathology **58:**226-235.
6. **Bentley, D. W., R. L. Nichols, R. E. Condon, and S. L. Gorbach.** 1972. The microflora of the human ileum and intrabdominal colon: results of direct needle aspiration at surgery and evaluation of the technique. The Journal of laboratory and clinical medicine **79:**421-429.
7. **Blanco, L. P., and V. J. Dirita.** 2006. Antibodies enhance interaction of Vibrio cholerae with intestinal M-like cells. Infection and immunity **74:**6957-6964.
8. **Blanco, L. P., and V. J. DiRita.** 2006. Bacterial-associated cholera toxin and GM1 binding are required for transcytosis of classical biotype Vibrio cholerae through an in vitro M cell model system. Cellular microbiology **8:**982-998.
9. **Bockman, D. E., and M. D. Cooper.** 1973. Pinocytosis by epithelium associated with lymphoid follicles in the bursa of Fabricius, appendix, and Peyer's patches. An electron microscopic study. The American journal of anatomy **136:**455-477.
10. **Campbell, J. A., P. Schelling, J. D. Wetzel, E. M. Johnson, J. C. Forrest, G. A. Wilson, M. Aurrand-Lions, B. A. Imhof, T. Stehle, and T. S. Dermody.** 2005. Junctional adhesion molecule a serves as a receptor for prototype and field-isolate strains of mammalian reovirus. Journal of virology **79:**7967-7978.
11. **Cao, X., E. W. Shores, J. Hu-Li, M. R. Anver, B. L. Kelsall, S. M. Russell, J. Drago, M. Noguchi, A. Grinberg, E. T. Bloom, and et al.** 1995. Defective lymphoid development in mice lacking expression of the common cytokine receptor gamma chain. Immunity **2:**223-238.
12. **Cavarelli, M., C. Foglieni, M. Rescigno, and G. Scarlatti.** 2013. R5 HIV-1 envelope attracts dendritic cells to cross the human intestinal epithelium and sample luminal virions via engagement of the CCR5. EMBO molecular medicine **5:**776-794.
13. **Chieppa, M., M. Rescigno, A. Y. Huang, and R. N. Germain.** 2006. Dynamic imaging of dendritic cell extension into the small bowel lumen in response to epithelial cell TLR engagement. The Journal of experimental medicine **203:**2841-2852.
14. **Evans, D. F.** 1998. Physicochemical environment of the colon. European journal of cancer prevention : the official journal of the European Cancer Prevention Organisation (ECP) **7 Suppl 2:**S79-80.
15. **Fantini, J., D. G. Cook, N. Nathanson, S. L. Spitalnik, and F. Gonzalez-Scarano.** 1993. Infection of colonic epithelial cell lines by type 1 human immunodeficiency virus is associated with cell surface expression of galactosylceramide, a potential alternative gp120 receptor. Proceedings of the National Academy of Sciences of the United States of America **90:**2700-2704.

16. **Flourie, B., C. Florent, J. P. Jouany, P. Thivend, F. Etanchaud, and J. C. Rambaud.** 1986. Colonic metabolism of wheat starch in healthy humans. Effects on fecal outputs and clinical symptoms. Gastroenterology **90:**111-119.
17. **Furuta, Y., K. Eriksson, B. Svennerholm, P. Fredman, P. Horal, S. Jeansson, A. Vahlne, J. Holmgren, and C. Czerkinsky.** 1994. Infection of vaginal and colonic epithelial cells by the human immunodeficiency virus type 1 is neutralized by antibodies raised against conserved epitopes in the envelope glycoprotein gp120. Proceedings of the National Academy of Sciences of the United States of America **91:**12559-12563.
18. **Gonzalez-Hernandez, M. B., T. Liu, L. P. Blanco, H. Auble, H. C. Payne, and C. E. Wobus.** 2013. Murine Norovirus Transcytosis across an In Vitro Polarized Murine Intestinal Epithelial Monolayer Is Mediated by M-Like Cells. Journal of virology **87:**12685-12693.
19. **Gorbach, S. L., A. G. Plaut, L. Nahas, L. Weinstein, G. Spanknebel, and R. Levitan.** 1967. Studies of intestinal microflora. II. Microorganisms of the small intestine and their relations to oral and fecal flora. Gastroenterology **53:**856-867.
20. **Helander, A., K. J. Silvey, N. J. Mantis, A. B. Hutchings, K. Chandran, W. T. Lucas, M. L. Nibert, and M. R. Neutra.** 2003. The viral sigma1 protein and glycoconjugates containing alpha2-3-linked sialic acid are involved in type 1 reovirus adherence to M cell apical surfaces. Journal of virology **77:**7964-7977.
21. **Heppner, F. L., A. D. Christ, M. A. Klein, M. Prinz, M. Fried, J. P. Kraehenbuhl, and A. Aguzzi.** 2001. Transepithelial prion transport by M cells. Nature medicine **7:**976-977.
22. **Honda, K., H. Nakano, H. Yoshida, S. Nishikawa, P. Rennert, K. Ikuta, M. Tamechika, K. Yamaguchi, T. Fukumoto, T. Chiba, and S. I. Nishikawa.** 2001. Molecular basis for hematopoietic/mesenchymal interaction during initiation of Peyer's patch organogenesis. The Journal of experimental medicine **193:**621-630.
23. **Jensen, V. B., J. T. Harty, and B. D. Jones.** 1998. Interactions of the invasive pathogens Salmonella typhimurium, Listeria monocytogenes, and Shigella flexneri with M cells and murine Peyer's patches. Infection and immunity **66:**3758-3766.
24. **Jones, B. D., N. Ghori, and S. Falkow.** 1994. Salmonella typhimurium initiates murine infection by penetrating and destroying the specialized epithelial M cells of the Peyer's patches. The Journal of experimental medicine **180:**15-23.
25. **Kane, M., L. K. Case, K. Kopaskie, A. Kozlova, C. MacDearmid, A. V. Chervonsky, and T. V. Golovkina.** 2011. Successful transmission of a retrovirus depends on the commensal microbiota. Science (New York, N.Y **334:**245-249.
26. **Knoop, K. A., N. Kumar, B. R. Butler, S. K. Sakthivel, R. T. Taylor, T. Nochi, H. Akiba, H. Yagita, H. Kiyono, and I. R. Williams.** 2009. RANKL is necessary and sufficient to initiate development of antigen-sampling M cells in the intestinal epithelium. J Immunol **183:**5738-5747.

27. **Knoop, K. A., M. J. Miller, and R. D. Newberry.** 2013. Transepithelial antigen delivery in the small intestine: different paths, different outcomes. Current opinion in gastroenterology **29:**112-118.
28. **Kuss, S. K., G. T. Best, C. A. Etheredge, A. J. Pruijssers, J. M. Frierson, L. V. Hooper, T. S. Dermody, and J. K. Pfeiffer.** 2011. Intestinal microbiota promote enteric virus replication and systemic pathogenesis. Science (New York, N.Y **334:**249-252.
29. **Lelouard, H., M. Fallet, B. de Bovis, S. Meresse, and J. P. Gorvel.** 2012. Peyer's patch dendritic cells sample antigens by extending dendrites through M cell-specific transcellular pores. Gastroenterology **142:**592-601 e593.
30. **Marteau, P., P. Pochart, J. Doré, C. Béra-Maillet, A. Bernalier, and G. Corthier.** 2001. Comparative Study of Bacterial Groups within the Human Cecal and Fecal Microbiota. Applied and environmental microbiology **67:**4939-4942.
31. **Martin-Latil, S., N. F. Gnädig, A. Mallet, M. Desdouits, F. Guivel-Benhassine, P. Jeannin, M.-C. Prevost, O. Schwartz, A. Gessain, S. Ozden, and P.-E. Ceccaldi.** 2012. Transcytosis of HTLV-1 across a tight human epithelial barrier and infection of subepithelial dendritic cells. Blood **120:**572-580.
32. **Meier, D., C. Bornmann, S. Chappaz, S. Schmutz, L. A. Otten, R. Ceredig, H. Acha-Orbea, and D. Finke.** 2007. Ectopic lymphoid-organ development occurs through interleukin 7-mediated enhanced survival of lymphoid-tissue-inducer cells. Immunity **26:**643-654.
33. **Morin, M. J., A. Warner, and B. N. Fields.** 1994. A pathway for entry of reoviruses into the host through M cells of the respiratory tract. The Journal of experimental medicine **180:**1523-1527.
34. **Mumphrey, S. M., H. Changotra, T. N. Moore, E. R. Heimann-Nichols, C. E. Wobus, M. J. Reilly, M. Moghadamfalahi, D. Shukla, and S. M. Karst.** 2007. Murine norovirus 1 infection is associated with histopathological changes in immunocompetent hosts, but clinical disease is prevented by STAT1-dependent interferon responses. Journal of virology **81:**3251-3263.
35. **Nagai, S., H. Mimuro, T. Yamada, Y. Baba, K. Moro, T. Nochi, H. Kiyono, T. Suzuki, C. Sasakawa, and S. Koyasu.** 2007. Role of Peyer's patches in the induction of Helicobacter pylori-induced gastritis. Proceedings of the National Academy of Sciences of the United States of America **104:**8971-8976.
36. **Nelson, A. M., M. D. Elftman, A. K. Pinto, M. Baldridge, P. Hooper, J. Kuczynski, J. F. Petrosino, V. B. Young, and C. E. Wobus.** 2013. Murine norovirus infection does not cause major disruptions in the murine intestinal microbiota. . Microbiome **1:**7.
37. **Nelson, A. M., S. T. Walk, S. Taube, M. Taniuchi, E. R. Houpt, C. E. Wobus, and V. B. Young.** 2012. Disruption of the Human Gut Microbiota following Norovirus Infection. PLoS ONE **7:**e48224.
38. **Neutra, M. R., P. Sansonetti, and J.P. Kraehenbuhl.** 2003. Role of intestinal M cells in microbial pathogenesis, p. 23-42. *In* G. A. Hecht (ed.), Microbial Pathogenesis and the Intestinal Epithelial Cell. ASM Press, Washington, DC.
39. **Niess, J. H., S. Brand, X. Gu, L. Landsman, S. Jung, B. A. McCormick, J. M. Vyas, M. Boes, H. L. Ploegh, J. G. Fox, D. R. Littman, and H. C. Reinecker.**

2005. CX3CR1-mediated dendritic cell access to the intestinal lumen and bacterial clearance. Science (New York, N.Y **307:**254-258.

40. **Ouzilou, L., E. Caliot, I. Pelletier, M. C. Prevost, E. Pringault, and F. Colbere-Garapin.** 2002. Poliovirus transcytosis through M-like cells. The Journal of general virology **83:**2177-2182.
41. **Owen, R. L.** 1999. Uptake and transport of intestinal macromolecules and microorganisms by M cells in Peyer's patches--a personal and historical perspective. Seminars in immunology **11:**157-163.
42. **Owen, R. L., D. M. Bass, and A. J. Piazza.** 1990. Colonic lymphoid patches. A portal of entry in mice for type I reovirus administered anally. Gastroenterology **98:**A468.
43. **Owen, R. L., N. F. Pierce, R. T. Apple, and W. C. Cray, Jr.** 1986. M cell transport of Vibrio cholerae from the intestinal lumen into Peyer's patches: a mechanism for antigen sampling and for microbial transepithelial migration. The Journal of infectious diseases **153:**1108-1118.
44. **Perry, J. W., and C. E. Wobus.** 2010. Endocytosis of murine norovirus 1 into murine macrophages is dependent on dynamin II and cholesterol. Journal of virology **84:**6163-6176.
45. **Pochart, P., F. Lemann, B. Flourie, P. Pellier, I. Goderel, and J. C. Rambaud.** 1993. Pyxigraphic sampling to enumerate methanogens and anaerobes in the right colon of healthy humans. Gastroenterology **105:**1281-1285.
46. **Rescigno, M., M. Urbano, B. Valzasina, M. Francolini, G. Rotta, R. Bonasio, F. Granucci, J. P. Kraehenbuhl, and P. Ricciardi-Castagnoli.** 2001. Dendritic cells express tight junction proteins and penetrate gut epithelial monolayers to sample bacteria. Nature immunology **2:**361-367.
47. **Sansonetti, P. J., J. Arondel, J. R. Cantey, M. C. Prevost, and M. Huerre.** 1996. Infection of rabbit Peyer's patches by Shigella flexneri: effect of adhesive or invasive bacterial phenotypes on follicle-associated epithelium. Infection and immunity **64:**2752-2764.
48. **Schiff, L. A., M. L. Nibert, and K. L. Tyler.** 2007. Orthoreoviruses and their replication, p. 1853-1915. *In* D. M. Knipe and P. M. Howley (ed.), Fields virology, 5 ed, vol. 2. Lippincott Wiliams & Wilkins, Philadelphia, PA.
49. **Sicinski, P., J. Rowinski, J. B. Warchol, Z. Jarzabek, W. Gut, B. Szczygiel, K. Bielecki, and G. Koch.** 1990. Poliovirus type 1 enters the human host through intestinal M cells. Gastroenterology **98:**56-58.
50. **Taube, S., A. O. Kolawole, M. Hohne, J. E. Wilkinson, S. A. Handley, J. W. Perry, L. B. Thackray, R. Akkina, and C. E. Wobus.** 2013. A mouse model for human norovirus. MBio **4**.
51. **Taube, S., J. W. Perry, E. McGreevy, K. Yetming, C. Perkins, K. Henderson, and C. E. Wobus.** 2012. Murine noroviruses bind glycolipid and glycoprotein attachment receptors in a strain-dependent manner. Journal of virology **86:**5584-5593.
52. **Taube, S., J. W. Perry, K. Yetming, S. P. Patel, H. Auble, L. Shu, H. F. Nawar, C. H. Lee, T. D. Connell, J. A. Shayman, and C. E. Wobus.** 2009. Ganglioside-

linked terminal sialic acid moieties on murine macrophages function as attachment receptors for murine noroviruses. Journal of virology **83:**4092-4101.

53. **Tonry, J. H., S. G. Popov, A. Narayanan, F. Kashanchi, R. M. Hakami, C. Carpenter, C. Bailey, and M. C. Chung.** 2013. In vivo murine and in vitro M-like cell models of gastrointestinal anthrax. Microbes and infection / Institut Pasteur **15:**37-44.
54. **Vallon-Eberhard, A., L. Landsman, N. Yogev, B. Verrier, and S. Jung.** 2006. Transepithelial pathogen uptake into the small intestinal lamina propria. J Immunol **176:**2465-2469.
55. **Wolf, J. L., R. S. Kauffman, R. Finberg, R. Dambrauskas, B. N. Fields, and J. S. Trier.** 1983. Determinants of reovirus interaction with the intestinal M cells and absorptive cells of murine intestine. Gastroenterology **85:**291-300.
56. **Wolf, J. L., D. H. Rubin, R. Finberg, R. S. Kauffman, A. H. Sharpe, J. S. Trier, and B. N. Fields.** 1981. Intestinal M cells: a pathway for entry of reovirus into the host. Science (New York, N.Y **212:**471-472.
57. **Zhang, T., J. Yu, Y. Zhang, L. Li, Y. Chen, D. Li, F. Liu, C. Y. Zhang, H. Gu, and K. Zen.** 2014. Salmonella enterica serovar Enteritidis modulates intestinal epithelial miR-128 levels to decrease macrophage recruitment via M-CSF. The Journal of infectious diseases.

# APPENDIX 1

## Neutral Red Assay for Murine Norovirus Replication and Detection in a Mouse Protocol

This protocol was published in bio-protocol.org:

http://www.bio-protocol.org/wenzhang.aspx?id=415

**Abstract:**

Neutral red (NR) is a dye that must be actively imported into the cell, and, therefore, the dye has been used for decades to selectively stain living cells. In addition, NR can also be incorporated into virus particles, although the mechanism behind this is poorly understood. Once encapsulated into the virion, NR, a light sensitive dye, can be photoactivated to inactivate the virus. The proposed mechanism explaining this observation is that activation of NR allows the dye to cross-link viral genome to viral capsid and thus preventing viral uncoating and infection. To study the early events of murine norovirus (MNV)-host interaction, light-sensitive NR-containing MNV is used to distinguish between input virus (i.e., NR-containing virus) and replicated virus (i.e., NR-free virus). This protocol describes the incorporation of NR into MNV capsids and the use of these virions for detection of viral replication in a mouse and in tissue culture by standard plaque assay. The same technique is also used for study of poliovirus

replication (1-3). Thus, there is the potential that this technique can be used for additional non-enveloped viruses. However, this has to be tested on a case-by-case basis as unpublished data on feline calicivirus suggests not all viruses may be able to stably incorporate NR into their capsid (J. Parker, personal communication).

**Materials and Reagents:**

1. Neutral red 0.33% solution (Sigma, N2889)
2. DMEM/ High glucose (Hyclone, SH30243.02)
3. 2x MEM (Gibco,11935)
4. 100x Penicillin and streptomycin (Hyclone, SV30010)
5. 100x Non-essential amino acids (Hyclone, SH30238.01)
6. 1 M Hepes (Hyclone, SH30237.01)
7. 200 mM (100x) L-glutamine (Hyclone, SH30034.01)
8. Fetal Bovine Serum (Gibco, 10437 or Hyclone, SH30070.02)
9. RAW 264.7 cell line (ATCC TIB-71)
10. Murine norovirus (MNV-1; GV/MNV1/2002/USA)
11. Sea Plaque Agarose (Lonza, 50100)
12. Aluminum foil
13. 1.0 mm Zirconia/Silica beads (BioSpec Products, 11079110z)
14. Mice (6-8 week old Balb/cJ)

**Equipment:**

1. 175 $cm^2$ flask (Corning, 3292)
2. Model 35 Speed Rocker (Labnet, S2035)
3. Tissue culture incubator (Sanyo, MCO-36M)
4. Magna Lyser Bead beater (Roche, 03358968001)
5. Photographic safe red light

**Procedure:**

1. Neutral red virus preparation

   a. Seed RAW 264.7 cells in a total of 30 mL of DMEM-10 media at a density of $4x10^7$ cells in a 175 $cm^2$ flask and incubate in a tissue culture incubator at 37$^oC$ and 5% $CO_2$ overnight.

   b. To obtain a virus stock, infect cells the next day with MNV by adding MNV at a multiplicity of infection (MOI) of 0.05 and incubate for 1 hour in a tissue culture incubator at 37$^oC$ and 5% $CO_2$.

   c. After the hour, add neutral red at 0.001% v/v from a 0.33% stock solution to the cells.

   d. Wrap the entire flask with aluminum foil including the filter cap of the flask.

   e. Incubate in a tissue culture incubator at 37$^oC$ and 5% $CO_2$ for 48 hours.

   f. After the 48 hours, generate a freeze/thaw lysate. Freeze cells by moving the entire flask (including cells and media) covered with aluminum foil to -80$^oC$ for at least 60 min. Then thaw flask contents at room temperature or in a tissue culture incubator at 37$^oC$ until all ice has melted. Repeat freeze/thaw a second time. This will be your virus stock.

      Note: after the second freeze/thaw cycle, virus stock should be aliquoted (in a darkened room) into single-use aliquots (e.g., 1 mL) and stored at -80$^oC$ since light-sensitivity of virus stock decreases after repeated freeze/thaw cycles.

   g. Block out all light in your tissue culture room to make a dark room and equip with a safe red light used in photography dark rooms.

   h. Perform plaque assay to determine viral titer of your virus stock as previously described in detail (2) and as described briefly below. The day before the plaque assay seed $2x10^6$ Raw 264.7 cells in DMEM-10/ well in six well plates.

   i. On the day of the plaque assay, perform 10-fold serial dilutions of your virus stock in DMEM-5. Make sure to adjust the volume for duplicate plaque assays, i.e., you will need a total volume of 2.5 mL for each dilution.

j. Next, take the six well plates with cells seeded on the day before, aspirate the media and infect cells in the dark in duplicate wells for each dilution with 0.5 mL/well, wrap in aluminum foil and rock for 1 hour at room temperature with a speed rocker at ~18 oscillations per min.

   Note: the 1 hour incubation was determined experimentally to ensure efficient entry and uncoating of MNV. However, the length of time necessary for other viruses may vary.

k. Turn on the lights and leave the remaining 10-fold viral dilutions in the light for at least 10 minutes.

l. Repeat step 1-j. but keep plates exposed to light (i.e., do not wrap plates in aluminum foil)

m. After the hour, finish the plaque assay for both sets of plates with or without aluminum foil in the light by adding 2 mL/well of a 1:1 ratio of molten media (1:1 ratio of SeaPlaque agarose and 2x MEM). To allow agarose to solidify incubate plates at room temperature for 10 min. Then, move plates to a tissue culture incubator and incubate at 37$^{o}$C, 5% CO2 for 48 hours.

n. After 48 hours stain cells with a neutral red solution overlay (0.01% neutral red in 1x PBS), for 1-3 hours prior to aspirating the solution and counting plaques as described previously in detail (2).

   Note: To calculate viral titers and obtain plaque forming units per milliliter (PFU/mL), add the number of plaques in both wells at a single dilution and multiply by the dilution factor (i.e., 1 mL if 2 wells are infected with 0.5 mL). Appendix Figure 1.1 shows an example of a 6 well plate with plaques. To calculate the viral titer in the example: 11 + 9 = 20 plaques; 20 x $10^2$ dilution factor = 2x$10^3$ PFU/mL. Two- to three-log reductions are typically observed in viral titers comparing total virus titers (i.e. obtained in dark) and light-insensitive (i.e. obtained in light) infections. Depending on the viral strain, log reductions may differ.

2. Tissue culture infection with neutral red virus

   a. Seed 2x$10^6$ Raw 264.7 cells in six well plates the day before.

b. The next day, block out all light in your tissue culture room to make a dark room and equip with a safe red light used in photography dark rooms.

c. Infect with MNV containing NR at an MOI of 0.001 for 1 hour.

   Note: pre-treatments with inhibitors of viral entry or uncoating can be performed before incubating with virus. Post-treatments with the same inhibitors are performed as a control after the 1 hour incubation with virus as described (5).

d. Flash with light for various lengths of times between 0 to 60 min at the end of the infection time.

   Note: For MNV, times between 0 and 60 minutes are typically used and at least 10 min has been sufficient to inactivate any leftover input virus (5).

e. Overlay with 2 mL of a 1:1 ratio of molten media (1:1 ratio of SeaPlaque agarose and 2x MEM), as you would do for plaque assays and as described (2, 4).

f. Incubate for 48-72 hours in a tissue culture incubator at $37^{o}$C and 5% $CO_2$.

g. Count plaques by adding the number of plaques in both wells at a single dilution and multiplying by the dilution factor, as described above and previously (2, 4).

3. Mouse infection with neutral red virus

a. Inoculate mice perorally by pipetting virus directly into the mouth or by oral gavage with NR-MNV in a darkened room with a safe red light.

   Note: we infected six- to eight-week old Balb/c mice perorally with NR-MNV at $10^5$ pfu. Depending on the experiment, the length of infection will vary. We typically infect mice for 12 – 72 hours. At the experimental endpoint (i.e. 12 hours post-infection), sacrifice mice in a darkened room with a safe red light and harvest different regions of the gastrointestinal tract, each 1 cm in lengths. Place each tissue piece in an individual 2 mL centrifuge screw cap tube containing 0.4 - 0.5 g of silica beads and 1 mL of DMEM-10.

b. Homogenize tissues in the dark with a bead beater for 60 min at 6000 rpm, as described (2).

c. Freeze (at -80$^{o}$C) and thaw tissues (at 37$^{0}$C) once before performing parallel plaque assays in the dark and following light exposure as described above.

d. Count plaques 48 hours later.

Note: MNV-1 is known to undergo the first round of replication in ~12 hours. Therefore, samples collected 3 hours post-infection should only show input virus (i.e., virus containing NR and sensitive to light).

**Recipes:**

1. DMEM-10

   DMEM/High glucose (1 liter)
   10% low-endotoxin Fetal Bovine Serum
   1% Hepes
   1% Penicillin and streptomycin
   1% Non-essential amino acids
   1% L-glutamine

2. DMEM-5

   DMEM/High glucose (1 liter)
   5% low-endotoxin Fetal Bovine Serum
   1% Hepes
   1% Penicillin and streptomycin
   1% Non-essential amino acids
   1% L-glutamine

3. 2x MEM media (500 mL)

   10% low-endotoxin Fetal Bovine Serum
   1% Hepes
   1% Penicillin and streptomycin
   2% L-glutamine
   Equilibrate to 37 $^{o}$C

4. SeaPlaque agarose

   1.5 g SeaPlaque agarose

   50 mL water

   Autoclave solution

   Equilibrate to 42 $^{o}$C

5. 1:1 ratio of molten media

   Mix 50 mL of 2x MEM and 50 mL of SeaPlaque agarose a 1:1 before adding to the cells

**References:**


1. **Brandenburg, B., L. Y. Lee, M. Lakadamyali, M. J. Rust, X. Zhuang, and J. M. Hogle.** 2007. Imaging Poliovirus Entry in Live Cells. PLoS Biol **5:**e183.
2. **Gonzalez-Hernandez, M. B., J. Bragazzi Cunha, and C. E. Wobus.** 2012. Plaque Assay for Murine Norovirus. J Vis Exp**:**e4297.
3. **Kuss, S. K., C. A. Etheredge, and J. K. Pfeiffer.** 2008. Multiple Host Barriers Restrict Poliovirus Trafficking in Mice. PLoS Pathog **4:**e1000082.
4. **Perry, J. W., M. Ahmed, K.-O. Chang, N. J. Donato, H. D. Showalter, and C. E. Wobus.** 2012. Antiviral Activity of a Small Molecule Deubiquitinase Inhibitor Occurs via Induction of the Unfolded Protein Response. PLoS Pathog **8:**e1002783.
5. **Perry, J. W., and C. E. Wobus.** 2010. Endocytosis of murine norovirus 1 into murine macrophages is dependent on dynamin II and cholesterol. J Virol **84:**6163-76.

$10^{-1}$ $10^{-2}$ $10^{-3}$

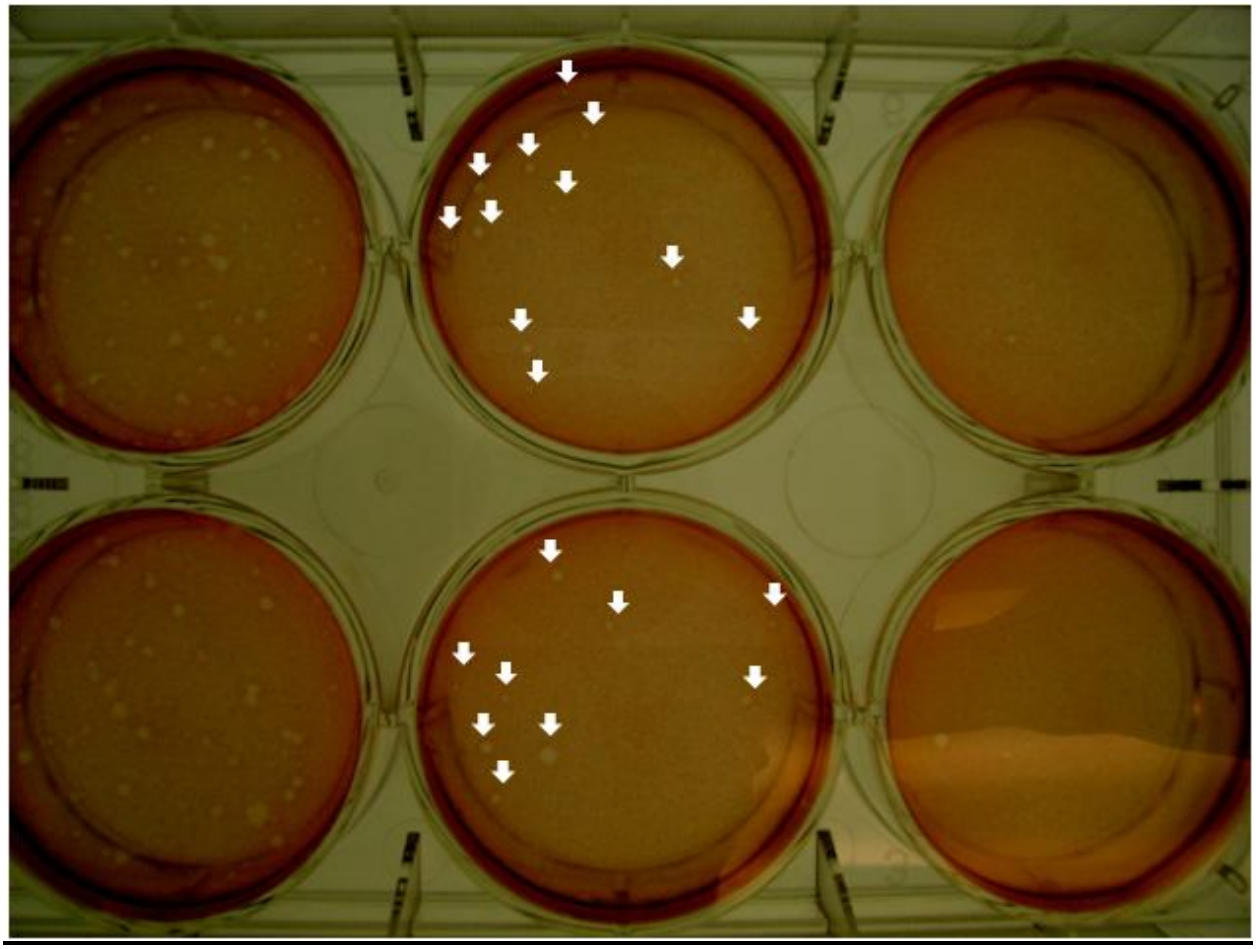

**Answer: 11+9= 20 x $10^2$ = 2 x $10^3$ PFU/mL**

**Appendix Figure 1.1: Example of plaque formation in cell monolayers after MNV-1 infection.** Representative image of a plaque assay plate after 48 hours of MNV-1 infection. Plaques are observed after staining with a neutral red solution overlay for 1-3 hours. The image shows duplicate wells of three 10-fold viral dilutions: $10^{-1}$, $10^{-2}$ and $10^{-3}$ dilutions. Arrows indicate the formation of plaques and the viral titer of the sample is indicated below.

# APPENDIX 2

## Plaque Assay for Murine Norovirus Protocol

This protocol was published by:

Journal of Visualized Experiments (JOVE) Volume (66): 4297 doi:10.3791/4297; 2012.

**Short Abstract:**

Here we describe a method to quantify infectious particles of murine norovirus (MNV), which is the only norovirus that efficiently replicates in cell culture. The plaque assay takes advantage of MNV's tropism for murine macrophages and can be adapted for use with biological or environmental samples containing MNV.

**Long Abstract:**

Murine norovirus (MNV) is the only member of the *Norovirus* genus that efficiently grows in tissue culture (10, 11). Cell lysis and cytopathic effect (CPE) are observed during MNV-1 infection of murine dendritic cells or macrophages (10). This property of MNV-1 can be used to quantify the number of infectious particles in a given sample by performing a plaque assay (10). The plaque assay relies on the ability of MNV-1 to lyse cells and to form holes in a confluent cell monolayer, which are called plaques (3).

Multiple techniques can be used to detect viral infections in tissue culture, harvested tissue, clinical, and environmental samples, but not all measure the number of infectious particles (e.g. qRT-PCR). One way to quantify infectious viral particles is to perform a plaque assay (3), which will be described in detail below. A variation on the MNV plaque assay is the fluorescent focus assay, where MNV antigen is immunostained in cell monolayers (9). This assay can be faster, since viral antigen expression precedes plaque formation. It is also useful for titrating viruses unable to form plaques. However, the fluorescent focus assay requires additional resources beyond those of the plaque assay, such as antibodies and a microscope to count focus-forming units. Infectious MNV can also be quantified by determining the 50% Tissue Culture Infective Dose ($TCID_{50}$) (3). This assay measures the amount of virus required to produce CPE in 50% of inoculated tissue culture cells by endpoint titration (7). However, its limit of detection is higher compared to a plaque assay (9).

In this article, we describe a plaque assay protocol that can be used to effectively determine the number of infectious MNV particles present in biological or environmental samples (2, 9, 10). This method is based on the preparation of 10-fold serial dilutions of MNV-containing samples, which are used to inoculate a monolayer of permissive cells (RAW 264.7 murine macrophage cells). Virus is allowed to attach to the cell monolayer for a given period of time and then aspirated before covering cells with a mixture of agarose and cell culture media. The agar enables the spread of viral progeny to neighboring cells while limiting spread to distantly located cells. Consequently, infected cells are lysed and form holes in the monolayer known as plaques. Upon sufficient spread of virus, plaques become visible following staining of cells with dyes, like neutral red, methylene blue, or crystal violet. At low dilutions, each plaque originates from one infectious viral particle and its progeny, which spread to neighboring cells. Thus, counting the number of plaques allows one to calculate plaque-forming units (PFU) present in the undiluted sample (3).

**Protocol Text:**

**1) Culturing of the macrophage cell line RAW 264.7**

1.1) Maintain RAW 264.7 cells (ATCC, catalog # TIB-71) in DMEM-10 media, which consists of high glucose DMEM with 10% (v/v) low-endotoxin fetal bovine serum (< 10 EU/mL), 10 mM HEPES, 100 U/mL penicillin, 100 μg/mL streptomycin, 1 mM non-essential amino acids, 2 mM L-glutamine. Cells are typically maintained in 175 $cm^2$ tissue culture flasks containing 35 mL of media per flask and incubated at 37°C and 5% $CO_2$ in a tissue culture incubator. However, any size flask can be used with a volume of media that is appropriate for the size of the flask.

1.2) To split cells: aspirate off the old media, add 10 mL of fresh DMEM-10 media to the cells, and then scrape the cells from the bottom of the flask by using a cell scraper. Next, resuspend the cells into a homogenous solution by drawing up cells into a 10 mL pipette and forcefully squeezing the cells through the pipette tip pressed against the bottom of the flask. Repeat this action at least 3 times so the cells no longer clump together. Verify by light microscopy that a single cell suspension was generated. Then transfer 1 mL (1:10 dilution or ~$1x10^7$ cells) - 2 mL (1:5 dilution or ~$2x10^7$ cells) of the cell suspension to a new 175$cm^2$ flask, and bring the final volume of media up to 35 mL.

1.3) Split cells when they are nearly confluent (~$1x10^8$ cells total/175 $cm^2$ flasks): every three days if starting with a 1:10 dilution, or every two days if starting with a 1:5 dilution. Use light microscopy to check cell morphology before splitting cells. Most of the cells should look round and not activated. Activated cells have granules and/or extended, spindly morphology with appendages. Do not let cells overgrow as those cells do not typically form plaques. Keep track of the passage number and frequently start over by thawing a lower passage aliquot of cells. (We use passage 30 as a cut-off).

**2) Infect RAW 264.7 cells with MNV inoculum**

2.1) Seed RAW 264.7 cells into 6-well plates (3.5 cm diameter) at a density of $1x10^6$ viable cells/mL in DMEM-10 media, and add 2 mL of this suspension to each well. It is important to distribute cells evenly in wells either by rocking plates by hand at least 10

times or by using a rocking apparatus for ~10 min. Do not swirl the plates as this will cause the cells to cluster in the center of the well. Place plates into a tissue culture incubator (at 37$^{o}$C and 5% $CO_2$). Allow cells to attach overnight or for at least 4 hrs at 37ºC. Cells should be 60 - 80% confluent for the plaque assay and distributed evenly throughout the well.

2.2) The next day, prepare the virus inoculum, which can be from MNV-infected cells in tissue culture or from homogenized tissues or fecal samples of MNV-infected mice. When using tissue samples, pea-sized pieces of tissue are homogenized in 2 mL screw-cap tubes containing sterile silica beads in 1 mL of DMEM-10 using a tissue homogenizer (e.g. bead beater). For fecal samples, no more than 3 fecal pellets should be homogenized in 1 mL media. All samples are then frozen (at -80$^{o}$C) and thawed once before performing the plaque assay.

2.3) Prepare 10-fold dilutions of the virus inoculum in complete DMEM-5 medium, which consists of DMEM/High glucose, 5% (v/v) low-endotoxin fetal bovine serum (< 10 EU/mL), 10 mM HEPES, 100 U/mL penicillin, 100 μg/mL streptomycin, 1 mM non-essential amino acids, 2 mM L-glutamine.

2.4) Ten-fold serial dilutions are prepared in 24-well plates: A repeater pipette is used to dispense 1.35 mL media into multiple wells, the $10^{-1}$ dilution is made by mixing 1.35 mL of media and 0.15 mL of virus-containing sample, and then 0.15 mL of the $10^{-1}$ dilution is added to 1.35 mL of media to make the $10^{-2}$ dilution and so on. It is important to change tips each time you make a new dilution. A multichannel pipette can be used to make the dilutions of multiple samples at a time with two tips fitting into one well of a 24-well plate transferring a total volume of 0.15 mL per well (see Appendix Figure 2.3A).

2.5) A typical dilution range for tissue homogenates and fecal contents is $10^{-1}$ to $10^{-3}$. However, plaques from these samples tend to be smaller compared to those from tissue culture samples. Furthermore, in some cases a 1:100 dilution of fecal samples is needed to sufficiently dilute out any toxic components of the feces that may disrupt the

cell monolayer, thus hindering the ability to count plaques. The dilution range of tissue culture lysates depends on the time point of interest during the viral life cycle. Dilutions that go up to $10^{-8}$ may be needed at the peak of infection.

2.6) After the serial dilutions are prepared, label the 6-well plates containing RAW 264.7 monolayers (from section 2.1) with the sample name and dilutions being plated. One plate at a time, remove all media by flicking it out or aspirating it. Immediately afterwards add 0.5 mL of a diluted sample to a well, then repeat with a duplicate well, before proceeding to the next dilution. Once all 3 dilutions are added to one plate, tilt plate back and forth by hand to ensure all cells have been covered. Handle one plate at a time to ensure that cells will not dry out.

2.7) After adding 0.5 mL of the dilutions to each well, stack plates upright and incubate them for 1 hour at room temperature. Because the volume added to each well is not sufficient to cover the monolayer completely, the plates need to be gently tilted back and forth by hand every 10-15 min or placed on a rocking apparatus (~18 oscillations per minute). This prevents cells from drying out.

**3) Low melting point agarose (SeaPlaque) overlay preparation**

Note: it is advisable to have several bottles with autoclaved SeaPlaque agarose prepared ahead of time. Agarose can be re-melted in a microwave before use.

3.1) Calculate the amount of overlay required for the total volume of plates before the 1 hr incubation is complete. The volume needed is 2 mL/well or 12 mL/6-well plate. Prepare agarose (see section 3.2) and media (see section 3.3) separately.

3.2) To prepare the agarose, suspend 3 g of SeaPlaque agarose in a total volume of 100 mL of distilled water (3% w/v) in a glass bottle. Autoclave for 20-30 min. (If agarose was already prepared before-hand, re-melt agarose in microwave.) It is important to equilibrate SeaPlaque agarose to 42°C in a water bath before use because if the

agarose is too hot, it will kill the cells. Make sure water level is equal to or above the level of the agarose to avoid undesired solidification.

3.3) To prepare the media: make 100 mL of 2x MEM media, which consists of 2x MEM, 10% (v/v) low-endotoxin fetal bovine serum (< 10 EU/mL), 10 mM HEPES, 100 U/mL penicillin, 100 μg/mL streptomycin, 4 mM L-glutamine. Equilibrate media to 37°C in a water bath.

3.4) Mix both the SeaPlaque agarose and the 2x MEM media together in a sterile bottle at a 1:1 ratio immediately before overlaying the infected cell monolayers. If more than 200 mL overlay is needed, split volume into multiple bottles and keep in 37$^{o}$C water bath until ready to use.

3.5) At the end of the 1 hour incubation (see section 2.7), aspirate the inoculum off of each well. Slowly add 2 mL of overlay to the edge of each well by placing the pipette tip against the wall of each well. Up to 5 plates can be handled simultaneously without cells drying out.

3.6) Allow the overlay to solidify for approximately 10 minutes at room temperature before placing plates upright into the tissue culture incubator. Incubate plates for 48 hours at 37$^{o}$C in 5% $CO_2$.

3.7) After the incubation period, plaques are faintly visible to the naked eye, so check unstained plates for presence of plaques. If no plaques are visible, incubate for an additional 4 hrs and check again. However, the maximum incubation time should not exceed 72 hrs.

**4) Visualization of plaques by neutral red staining**

4.1) To visualize plaques, the neutral red staining solution is prepared by adding 3 mL of neutral red (0.33% w/v in DPBS; Sigma, catalog # N2889) to every 100 mL of 1X

PBS (tissue culture grade, $Mg^{2+}$-, $Ca^{2+}$-free; Gibco, catalog # 10010). Calculate the volume of neutral red staining solution needed for the experiment. Twelve mL neutral red staining solution are required for each 6-well plate. Equilibrate the neutral red staining solution to 37$^{o}$C in a water bath, and then add 2 mL to each well. Although some plaque assay protocols require the agarose plug to be removed from the wells, in this protocol the neutral red staining solution is added directly onto the overlay.

4.2) After a one hour incubation at 37$^{o}$C, check if plaques are visible with neutral red staining solution still in wells. If plaques are not readily apparent, allow the staining to continue for another hour. Continue incubating until plaques are visible. (Note: Staining for more than 3 hours is not optimal and if no plaques are visible in the positive control sample after 3 hours of staining, the plaque assay did not work properly.) After the staining is complete, aspirate the neutral red staining solution, ensuring the agarose plug is not disturbed, and then proceed to counting the plaques.

4.3) Count plaques by placing plate upside down on a light box and marking a dot on counted plaques to avoid duplicate counts. Choose the dilution to count plaques in wells where plaques are clearly separated (i.e. no visual evidence of plaques fusing together). If possible, count plaques at two dilutions. It is important to note that plaque size may vary between MNV strains, virus inoculum, and depends on the condition of the RAW 264.7 cells during the plaque assay.

4.4) If no plaques are visible in a well, either there was no virus was present in the sample or the amount of virus was under the limit of detection of the plaque assay. In this case, the wells stain red with a similar color as other plaque-containing wells. Alternatively, no plaques are also observed when there are too many viral particles present in a given dilution. This leads to lysis of the entire monolayer and wells appear orange/yellow in color.

4.5) Calculate viral titers. Add the number of plaques in both wells at a single dilution and multiply by the dilution factor (i.e. 1 mL if 2 wells are infected with 0.5 mL). This will

yield the amount of plaque forming units (PFU) in your inoculum volume of 1 mL. For example, in Appendix Figure 2.4 at the $10^{-2}$ dilution, one well (marked "II") has 14 plaques and the other well (marked "V") has 17 plaques. Thus, the viral titer will be $14x10^2 + 17x10^2 = 3{,}100$ ($3.1x10^3$) PFU/mL.

**Representative Results:**

Infectious MNV-1 particles can be quantified using a plaque assay as outlined schematically in Appendix Figure 2.1. Appendix Figure 2.2A shows a well with a monolayer of RAW 264.7 cells just prior to infection, while Appendix Figure 2.2B shows three visible plaques indicated by roman numbers I, II and III in a well. Individual steps of the assay are depicted in Appendix Figures 2.3A through F. Appendix Figure 2.3A shows the preparation of the 10-fold dilution series of a virus-containing sample. Appendix Figure 2.3B shows the transfer of dilutions to duplicate wells of a 6-well plate. Appendix Figure 2.3C shows the rocking apparatus used to incubate RAW 264.7 cells with the inoculum at room temperature for 1 hour. Appendix Figure 2.3D shows cells being overlaid with the SeaPlaque:MEM mixture. Appendix Figure 2.3E shows a plate at room temperature to allow the overlay to solidify, while Appendix Figure 2.3F shows cells being stained with a 0.01% neutral red solution 48 hrs later. After staining cells for 1-3 hours and aspirating the neutral red staining solution, plaques are visible and can be counted (Appendix Figure 2.4).

**Discussion:**

The plaque assay method for MNV-1 presented here is a way of quantifying infectious MNV particles. By following the assay steps illustrated in Appendix Figure 2.3, one can obtain reproducible viral titers. The limit of detection of the assay depends on the starting dilution used. When starting with a 1:10 dilution of sample as described above, the limit of detection of the plaque assay is 10 pfu (*i.e.,* 1 plaque visible at the $10^{-1}$ dilution). Since each plaque represents a single virus, the plaque assay can also be used to purify clonal populations of MNV by picking isolated plaques and propagating

them as described previously (10). In addition, plaque purifications can also be used to separate an individual virus population from mixed virus populations. A limitation of using a plaque assay for the detection of MNV infection is that not all MNV strains form plaques (9). However, it may be possible to overcome the inability of some MNV strains, isolated from animals, to form plaques by serially passaging these viruses in tissue culture (1). An alternative to the plaque assay is to measure infectious particles via the $TCID_{50}$ technique (3, 9). This assay quantifies the amount of virus required to produce CPE in 50% of inoculated tissue culture cells following endpoint dilutions and takes 1 week to complete for MNV (9). In addition to being slower than a plaque assay, the $TCID_{50}$ assay is also not as sensitive (limit of detection = 200 $TCID_{50}$/mL) due to the toxicity of tissue samples to RAW 264.7 cells (9).

Although critical steps within the protocol have been described throughout the protocol, the following section provides a summary to facilitate trouble-shooting. The most critical step in the protocol is to ensure that RAW 264.7 cells remain viable throughout the assay to support virus replication. This can be monitored at each stage of the assay via light microscopy. Cell viability is ensured in two ways. First, care should be taken not to let cells dry out while handling plates. Thus, plates are inoculated one at a time, rocked during the infection period, and should remain closed whenever they are not being handled. Second, solutions added onto cells should be equilibrated to ~37$^{o}$C. Furthermore, it is vital for the overall health of the RAW 264.7 cells to maintain them in media containing low endotoxin serum (< 10 EU/mL), which limits activation of cells. In addition, we have observed a higher failure rate of the plaque assay when using cells from passage 30 or higher. Although this will likely vary from lab to lab, it is important to include a positive control (*e.g.,* a sample with a known viral titer) to ensure reproducible titers, especially when using higher passage RAW 264.7 cells. To limit use of higher passage cells, it is advisable to freeze vials of early passage cells upon receipt of RAW 264.7 cells and start a new culture from the frozen vials frequently. Starting over with low passage cell cultures will also be helpful when cells exhibit altered characteristics, such as failure to adhere, changes in cell morphology (e.g. from round to spindly and spread out), or when mycoplasma contamination has been detected.

Another important point to pay attention to is to ensure that pipette tips are changed between samples and during dilutions. This will ensure accurate serial dilutions and prevent cross-contamination between samples. The one place in the protocol where the same pipette tip can be used again is when serial dilutions of the same sample are added to wells. In that case, one should start from the most diluted inoculum to the least, and vigorously pipette up and down when drawing up a new dilution.

The plaque assay protocol is amendable to several modifications. One modification that can be made when there are not enough cells for inoculating wells in duplicate is to inoculate only a single well for each dilution. However, since the inoculum volume is 0.5 mL, the number of plaques then needs to be multiplied by a factor of 2 to normalize to pfu/mL. The plaque assay can also be adapted for use with any other adherent cell line that is able to support replication of MNV, and this has been described for the murine microglial BV-2 cell line (5). Other modifications that can be implemented are adaptations that have been described for plaque assay protocols developed for other viruses. In case of MNV, the following modifications have already been implemented successfully; the use of methyl cellulose instead of Sea Plaque agarose (4), and staining of cells with crystal violet or methylene blue instead of neutral red (6, 8).

Overall, this protocol can easily be adapted as needed to quantify other plaque-forming viruses or used for other viruses that cause lytic infections in RAW 264.7 cells, making it a useful tool to quantify infectious viral particles in general.

**Acknowledgements:** We thank members of the Wobus laboratory for critical comments and suggestions. Work in the laboratory of CEW was funded by start-up funds from the University of Michigan, a career development grant from the NIH/NIAID Regional Center of Excellence for Bio-defense and Emerging Infectious Diseases Research (RCE) Program, Region V 'Great Lakes' RCE (NIH award 1-U54-AI-057153) and NIH R01 AI080611. M.B.G.-H. was funded by the Experimental Immunology (NIH T32 A1007413-16) and the Molecular Mechanisms in Microbial Pathogenesis (NIH T32

A1007528) training grants to the University of Michigan. J.B.C. was funded by Coordenação de Aperfeiçoamento de Pessoal de Nível Superior (CAPES), Brasilia, Brazil.

**Disclosures:** The authors have nothing to disclose.

**Table of specific reagents and equipment:**

| **Name of the reagent** | **Company** | **Catalogue number** |
|---|---|---|
| DMEM/ High glucose | Hyclone | SH30243.02 |
| 2x MEM | Gibco | 11935 |
| 100x Penicillin and streptomycin | Hyclone | SV30010 |
| 10 mM Non-essential amino acids | Hyclone | SH30238.01 |
| 1M HEPES | Hyclone | SH30237.01 |
| 200 mM (100x) L-glutamine | Hyclone | SH30034.01 |
| Fetal Bovine Serum | Gibco, Hyclone | 10437, SH30070.02 |
| Sea Plaque Agarose | Lonza | 50100 |
| Neutral Red 0.33% | Sigma | N2889 |
| 1x PBS | Gibco | 10010 |
| 1.0 mm Zirconia/Silica beads | BioSpec Products | 11079110z |
| Model 35 Speed Rocker | Labnet | S2035 |
| Magna Lyser Instrument | Roche | 03358968001 |
| Raw 264.7 cell line | ATCC | TIB-71 |
| Tissue culture incubator | Sanyo | MCO-18AIC |

**References:**


1. **Barron, E. L., S. V. Sosnovtsev, K. Bok, V. Prikhodko, C. Sandoval-Jaime, C. R. Rhodes, K. Hasenkrug, A. B. Carmody, J. M. Ward, K. Perdue, and K. Y. Green.** 2011. Diversity of murine norovirus strains isolated from asymptomatic mice of different genetic backgrounds within a single U.S. research institute. PLoS ONE **6:**e21435.
2. **Chachu, K. A., D. W. Strong, A. D. LoBue, C. E. Wobus, R. S. Baric, and H. W. Virgin IV.** 2008. Antibody is critical for the clearance of murine norovirus infection. Journal of virology **82:**6610-6617.
3. **Condit, R. C.** 2007. Principles of Virology, p. 25-58. *In* D. M. Knipe, Howley, P. M. (ed.), Fields Virology, 5 ed, vol. 1. Lippincott Williams & Wilkins, Philadelphia.
4. **Cooper, P. D.** 1961. The plaque assay of animal viruses. Adv Virus Res **8:**319-378.
5. **Cox, C., S. Cao, and Y. Lu.** 2009. Enhanced detection and study of murine norovirus-1 using a more efficient microglial cell line. Virology journal **6:**196.
6. **Hyde, J. L., S. V. Sosnovtsev, K. Y. Green, C. Wobus, H. W. Virgin, and J. M. Mackenzie.** 2009. Mouse norovirus replication is associated with virus-induced vesicle clusters originating from membranes derived from the secretory pathway. Journal of virology **83:**9709-9719.
7. **Reed, L. J., Muench, H.** 1932. A simple method for estimating 50% endpoints. American Journal of Hygiene **27:**493–497.
8. **Simmonds, P., I. Karakasiliotis, D. Bailey, Y. Chaudhry, D. J. Evans, and I. G. Goodfellow.** 2008. Bioinformatic and functional analysis of RNA secondary structure elements among different genera of human and animal caliciviruses. Nucleic acids research **36:**2530-2546.
9. **Thackray, L. B., C. E. Wobus, K. A. Chachu, B. Liu, E. R. Alegre, K. S. Henderson, S. T. Kelley, and H. W. Virgin IV.** 2007. Murine noroviruses comprising a single genogroup exhibit biological diversity despite limited sequence divergence. Journal of virology **81:**10460-10473.
10. **Wobus, C. E., S. M. Karst, L. B. Thackray, K. O. Chang, S. V. Sosnovtsev, G. Belliot, A. Krug, J. M. Mackenzie, K. Y. Green, and H. W. Virgin.** 2004. Replication of Norovirus in cell culture reveals a tropism for dendritic cells and macrophages. PLoS Biol **2:**e432.
11. **Wobus, C. E., L. B. Thackray, and H. W. Virgin IV.** 2006. Murine norovirus: a model system to study norovirus biology and pathogenesis. Journal of virology **80:**5104-5112.

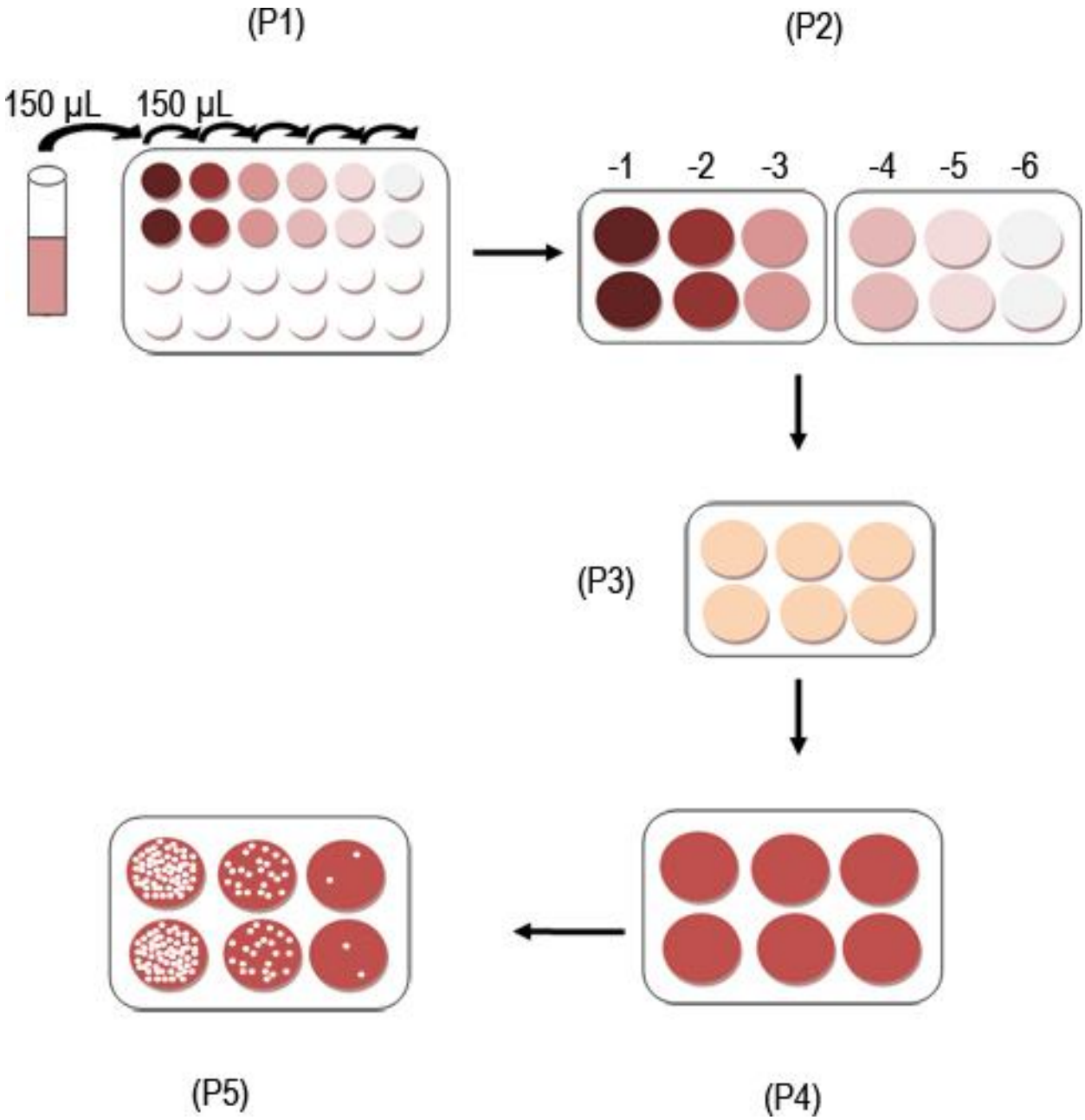


**Appendix Figure 2.1: Schematic of the MNV plaque assay protocol.**

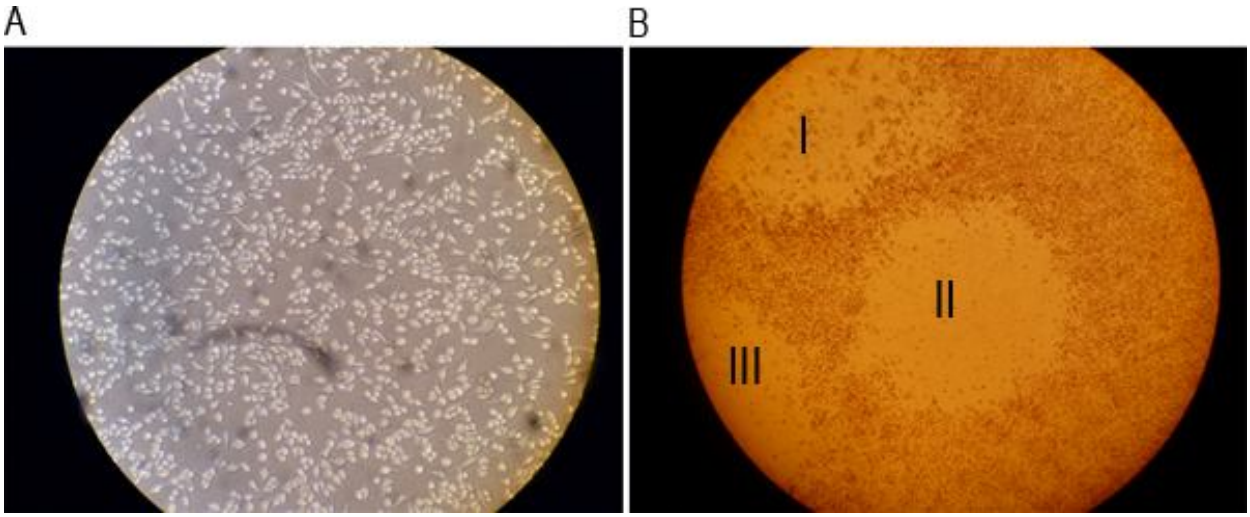


**Appendix Figure 2.2: Representative images of a well of a monolayer before infection and after formation of plaques.** A) RAW 264.7 cells were cultured overnight and imaged under a light microscope at 20x magnification. B) Cells were stained with a 0.01% neutral red solution after 48 hrs of infection and visualized under a light microscope at 4x magnification. Roman numbers I, II, and III indicate three visible plaques.

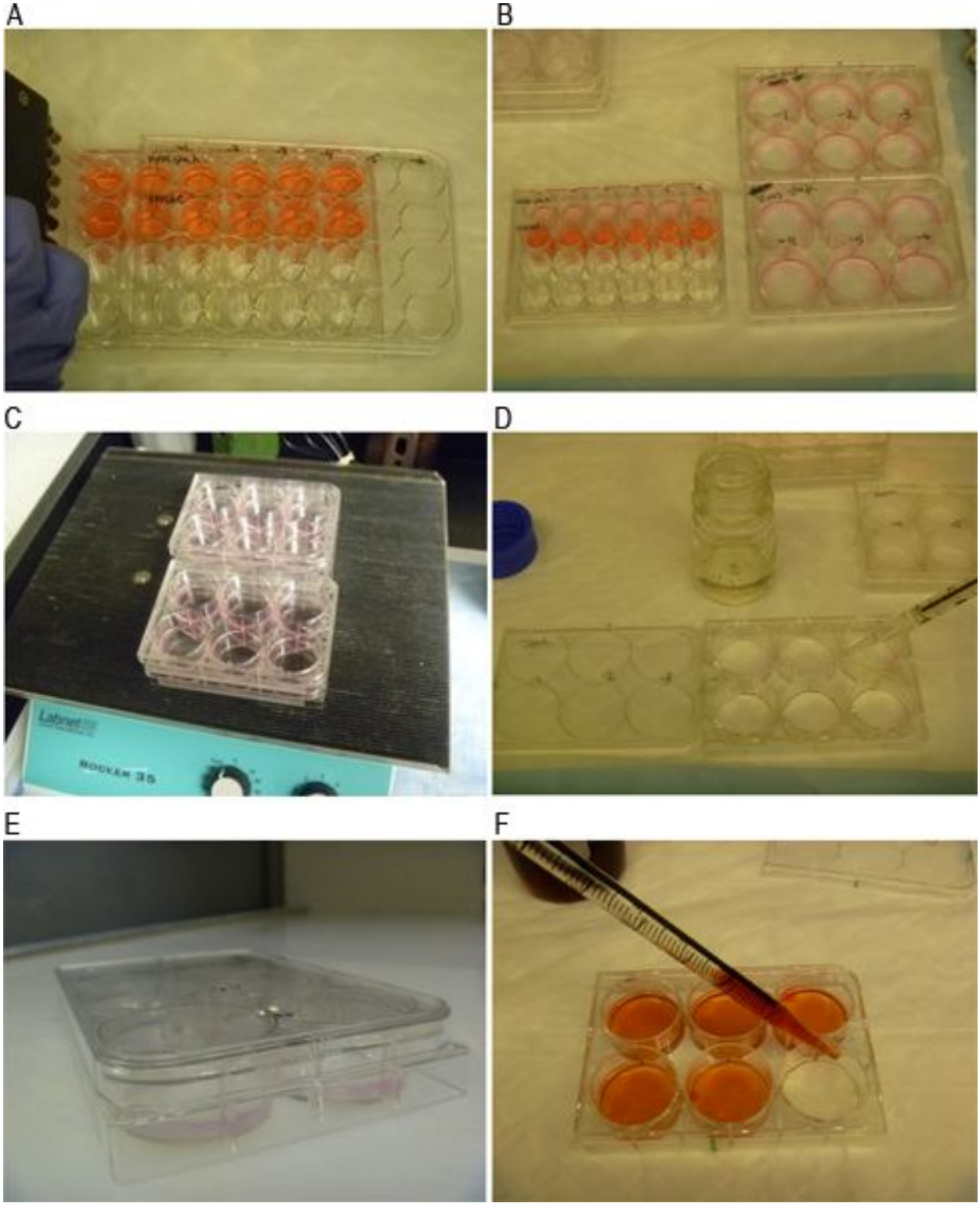
A
B
C
D
E
F

**Appendix Figure 2.3: Representative images of the different plaque assay steps.** A) MNV-1 inoculum is prepared in 10-fold dilutions. B) Inoculum is added to cell monolayers in duplicate wells. C) Cells and inoculum are incubated by rocking for 1 hour at room temperature. D) Cells are overlaid with a 1:1 mixture of SeaPlaque agarose and 2x MEM media. E) Plates are incubated for 10 min at room temperature to allow the overlay to solidify. F) Staining of cells with the neutral red staining solution 48 hrs post-infection.

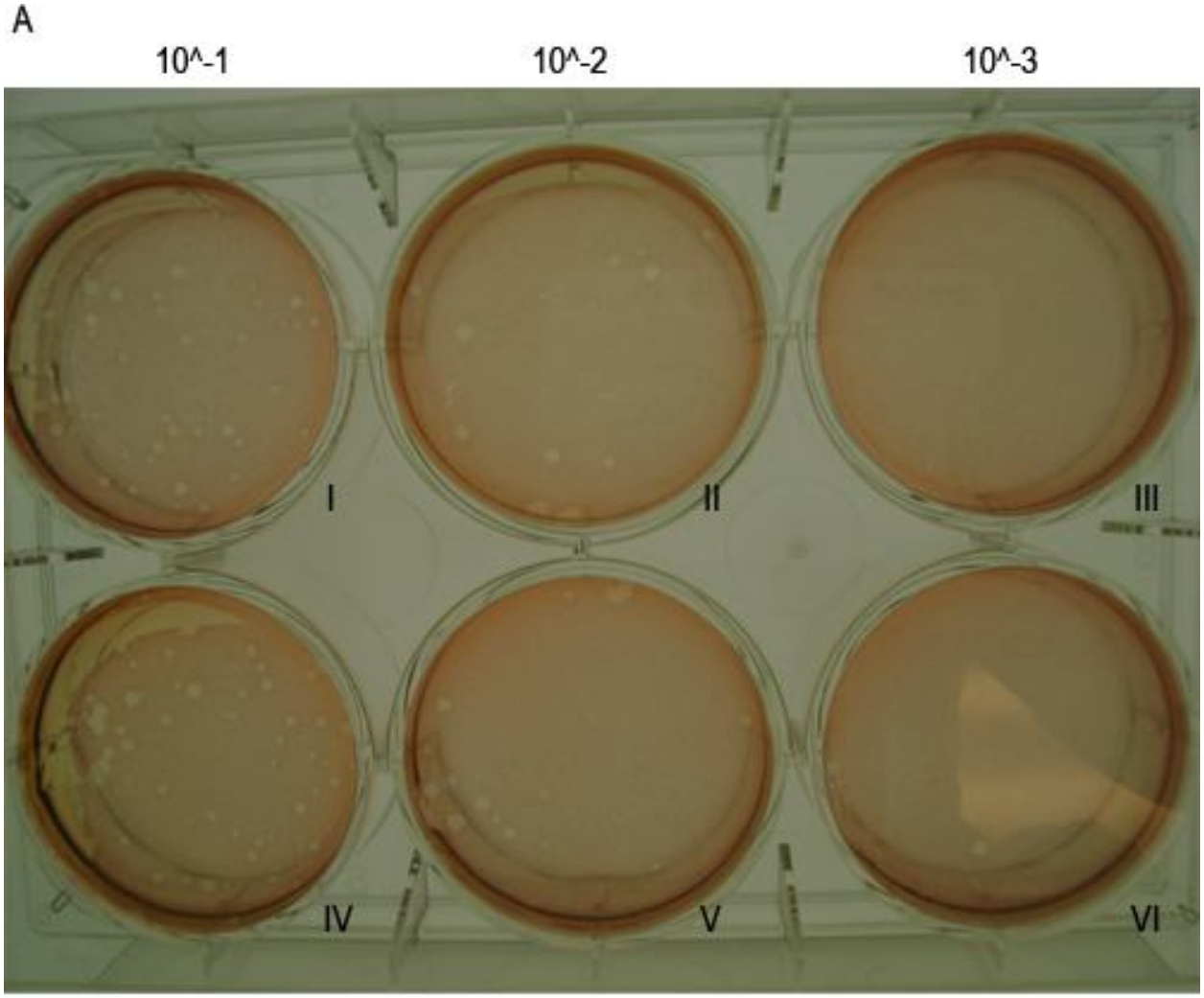


**Appendix Figure 2.4: MNV-1 forms plaques in cell monolayers.** Shown here is a representative plaque assay plate, showing plaques stained with neutral red staining solution after 48 hrs of incubation. The plate shows duplicate wells of three 10-fold dilutions. Wells labeled with roman numbers I and IV correspond to the $10^{-1}$ dilution; II and V correspond to the $10^{-2}$ dilution; III and VI correspond to the $10^{-3}$ dilution. The viral titer of the sample is indicated below (see Section 4.5 for details of the calculation).